

NUREG-0661

---

# **Safety Evaluation Report**

Mark I Containment

Long-Term Program

Resolution of Generic Technical Activity A-7

---

July 1980

Office of Nuclear Reactor Regulation  
U.S. Nuclear Regulatory Commission



8008060 369

Available from

GPO Sales Program  
Division of Technical Information and Document Control  
U. S. Nuclear Regulatory Commission  
Washington, D. C. 20555

Printed copy price: \$6.50

and

National Technical Information Service  
Springfield, Virginia 22161

---

# **Safety Evaluation Report**

Mark I Containment

Long-Term Program

Resolution of Generic Technical Activity A-7

---

Manuscript Completed: March 1980  
Date Published: July 1980

Office of Nuclear Reactor Regulation  
U.S. Nuclear Regulatory Commission



## ABSTRACT

This Safety Evaluation Report prepared by the staff of the Office of Nuclear Reactor Regulation discusses suppression pool hydrodynamic loads in boiling water reactor (BWR) facilities with the Mark I pressure-suppression containment design. The report finishes the NRC's Generic Technical Activity A-7 (Mark I Containment Long-Term Program), which has been designated an "Unresolved Safety Issue" pursuant to Section 210 of the Energy Reorganization Act of 1974. The report describes the generic techniques for the definition of suppression pool hydrodynamic loads in a Mark I system and the related structural acceptance criteria.

On the basis of a review of the experimental and analytical programs conducted by the Mark I Owners Group, the staff has concluded that, with one exception, the proposed suppression pool hydrodynamic load definition procedures (as modified by the staff's requirements in Appendix A of this report) will provide conservative estimates of these loading conditions. The exception is the lack of an acceptable specification for the downcomer "condensation oscillation" loads. In addition, requirements for confirmatory analyses and testing have been identified. The resolution of these issues will be described in a supplement to this report.

The staff also has concluded that the proposed structural acceptance criteria are consistent with the requirements of the applicable codes and standards. In conjunction with the general structural analysis techniques, these criteria will provide an acceptable basis for establishing the margins of safety in the Mark I containment design.

## CONTENTS

|  | <u>Page</u> |
|--|-------------|
| ABSTRACT . . . . .   | iii         |
| ACKNOWLEDGMENTS . . . . .                                    | xi          |
| NOMENCLATURE . . . . .                                       | xiii        |
| <br>   |             |
| 1. INTRODUCTION . . . . .                                    | 1           |
| 1.1 Problem Definition . . . . .                             | 1           |
| 1.2 Short-Term Program Summary . . . . .                     | 5           |
| 1.3 Long-Term Program Description . . . . .                  | 5           |
| <br>   |             |
| 2. BACKGROUND . . . . .                                      | 8           |
| 2.1 Mark I Containment System Description . . . . .          | 8           |
| 2.2 LOCA-Related Hydrodynamic Phenomena . . . . .            | 11          |
| 2.2.1 Pool Swell Phenomena . . . . .                         | 11          |
| 2.2.2 LOCA Steam Condensation Phenomena . . . . .            | 14          |
| 2.3 Safety-Relief Valve Discharge Phenomena . . . . .        | 16          |
| 2.4 Long-Term Program Task Descriptions . . . . .            | 17          |
| <br>   |             |
| 3. HYDRODYNAMIC LOAD EVALUATION . . . . .                    | 23          |
| 3.1 Introduction . . . . .                                   | 23          |
| 3.2 Containment Response Models . . . . .                    | 23          |
| 3.2.1 Postulated Pipe Breaks . . . . .                       | 24          |
| 3.2.2 Event Combinations and Timing . . . . .                | 26          |
| 3.2.3 Containment Mass and Energy Release . . . . .          | 28          |
| 3.3 Vent System Pressurization and Thrust Loads . . . . .    | 29          |
| 3.4 Torus Pool Swell Pressure Loads . . . . .                | 31          |
| 3.4.1 Net Torus Vertical Pressure Load . . . . .             | 34          |
| 3.4.2 Torus Pressure Load Distribution . . . . .             | 40          |
| 3.5 Pool Swell Impact and Drag Loads. . . . .                | 41          |
| 3.5.1 Vent System Impact and Drag. . . . .                   | 42          |
| 3.5.2 Vent Header Deflector Impact and Drag. . . . .         | 45          |
| 3.5.3 Impact and Drag on Other Internal Structures . . . . . | 50          |
| 3.6 Pool Swell Froth Impingement Loads. . . . .              | 67          |
| 3.7 Pool Fallback Loads . . . . .                            | 74          |
| 3.8 Condensation Oscillation Loads. . . . .                  | 76          |

## CONTENTS (Continued)

|  | <u>Page</u> |
|--|-------------|
| 3.8.1 Condensation Oscillation Torus Shell<br>Pressure Loads . . . . .   | 82          |
| 3.8.2 Condensation Oscillation Downcomer Loads . . . . .                 | 85          |
| 3.8.3 Condensation Oscillation Vent System<br>Pressure Loads . . . . .   | 88          |
| 3.9 Chugging Loads. . . . .  | 89          |
| 3.9.1 Chugging Loads on the Torus Shell. . . . .                         | 89          |
| 3.9.2 Chugging Downcomer Loads . . . . .                                 | 93          |
| 3.9.3 Chugging Vent System Pressure Loads. . . . .                       | 97          |
| 3.10 Safety-Relief Valve Discharge Loads . . . . .                       | 97          |
| 3.10.1 SRV Discharge Line Pressure Transient . . . . .                   | 99          |
| 3.10.2 SRV Air-Clearing Torus Pressure Loads . . . . .                   | 100         |
| 3.10.3 SRV Reflood Transient . . . . .                                   | 119         |
| 3.10.4 SRV Quencher Thrust Loads . . . . .                               | 121         |
| 3.10.5 SRV Temperature Transients. . . . .                               | 122         |
| 3.10.6 SRV Discharge Event Cases . . . . .                               | 123         |
| 3.10.7 Suppression Pool Temperature Limit. . . . .                       | 124         |
| 3.11 Submerged Structure Drag Loads. . . . .                             | 127         |
| 3.11.1 LOCA Water-Jet Loads. . . . .                                     | 128         |
| 3.11.2 LOCA Pool Swell Bubble-Drag Loads . . . . .                       | 129         |
| 3.11.3 LOCA Condensation Oscillation Drag Loads. . . . .                 | 133         |
| 3.11.4 LOCA Chugging Drag Loads. . . . .                                 | 135         |
| 3.11.5 SRV Water-Jet Loads . . . . .                                     | 136         |
| 3.11.6 SRV Bubble-Drag Loads . . . . .                                   | 136         |
| 3.12 Secondary Loads and Other Considerations. . . . .                   | 137         |
| 3.12.1 Seismic Slosh . . . . .   | 138         |
| 3.12.2 Post-Pool Swell Waves . . . . .                                   | 139         |
| 3.12.3 Asymmetric Vent System Flow . . . . .                             | 139         |
| 3.12.4 Downcomer Air-Clearing Loads. . . . .                             | 141         |
| 3.12.5 Sonic and Compression Wave Loads. . . . .                         | 141         |
| 3.12.6 Downcomer Submergence and Pool Thermal<br>Stratification. . . . . | 142         |
| 3.12.7 Differential Pressure Control . . . . .                           | 143         |
| 3.12.8 SRV Steam Discharge Loads . . . . .                               | 146         |
| 4. STRUCTURAL AND MECHANICAL ANALYSES AND ACCEPTANCE CRITERIA. . .       | 147         |
| 4.1 Introduction. . . . .  | 147         |
| 4.2 Classification of Structures. . . . .                                | 149         |

CONTENTS (Continued)

|   | <u>Page</u> |
|---|-------------|
| 4.2.1 Pressure Suppression System. . . . .  | 149         |
| 4.2.2 Attached Piping System . . . . .  | 149         |
| 4.2.3 Internal Structures. . . . .  | 150         |
| 4.3 Service Limits and Associated Load Combinations . . . . .   | 150         |
| 4.3.1 Service Limits . . . . .  | 151         |
| 4.3.2 Applicable Code Sections . . . . .  | 156         |
| 4.3.3 Service Level Assignments. . . . .  | 157         |
| 4.3.4 Operability and Functionality Requirements . . . . .  | 163         |
| 4.4 Analysis Techniques . . . . .   | 166         |
| 4.4.1 General Guidelines . . . . .  | 166         |
| 4.4.2 Damping. . . . .  | 167         |
| 4.4.3 Combination of Structural Responses. . . . .  | 167         |
| 5. CONCLUSIONS. . . . .   | 169         |
| 6. REFERENCES . . . . .   | 172         |
| APPENDIX A - NRC ACCEPTANCE CRITERIA FOR THE MARK I CONTAINMENT<br>LONG-TERM PROGRAM. . . . .             | A-1         |
| APPENDIX B - LETTER TO THE CHAIRMAN, USNRC, FROM THE ADVISORY<br>COMMITTEE ON REACTOR SAFEGUARDS. . . . . | B-1         |

## LIST OF FIGURES

|        |  | <u>Page</u> |
|--------|--|-------------|
| 2.1-1  | Mark I Containment System . . . . .  | 9           |
| 2.1-2  | Mark I Suppression Chamber . . . . .   | 10          |
| 2.2-1  | LOCA Sequence of Primary Events . . . . .  | 12          |
| 2.3-1  | Mark I T-Quencher Discharge Device . . . . .   | 18          |
| 3.2-1  | Typical Mark I DBA Pressure Response . . . . .   | 25          |
| 3.2-2  | Mark I Event Combinations . . . . .  | 27          |
| 3.4-1  | Mark I Torus Vertical Pressure Transient . . . . .   | 35          |
| 3.5-1  | Mark I Vent-Header Deflector Designs . . . . .   | 46          |
| 3.5-2  | Typical Cylindrical Target Impact Pressure Transient . . . . .                                     | 53          |
| 3.5-3  | Cylindrical Target Impact Transient Approximation . . . . .  | 55          |
| 3.5-4  | Cylindrical Target Drag Coefficient Following Impact . . . . .                                     | 57          |
| 3.5-5  | Typical Flat Target Impact Pressure Transient . . . . .  | 60          |
| 3.6-1  | Froth Impingement Zone - Region I . . . . .  | 68          |
| 3.6-2  | Froth Impingement Zone - Region II . . . . .   | 69          |
| 3.6-3  | Vent-Header Impact Wave Formation . . . . .  | 71          |
| 3.7-1  | Pool Fallback Load Directional Range . . . . .   | 77          |
| 3.8-1  | Mark I Full-Scale Test Facility . . . . .  | 79          |
| 3.8-2  | Condensation Oscillation Torus Shell Pressure Transient . . . . .                                  | 80          |
| 3.8-3  | Condensation Oscillation Amplitude - Frequency Spectrum . . . . .                                  | 84          |
| 3.8-4  | Downcomer Condensation Oscillation Load Histogram . . . . .  | 87          |
| 3.9-1  | Chugging Torus Shell Pressure Transient . . . . .  | 90          |
| 3.9-2  | Chugging Asymmetric Torus Shell Pressure . . . . .   | 92          |
| 3.9-3  | Multiple Downcomer Chugging Load Probability Distribution . . . . .                                | 95          |
| 3.10-1 | Mark I T-Quencher Discharge Device . . . . .   | 98          |
| 3.10-2 | Typical T-Quencher Shell Pressure Transient . . . . .  | 113         |
| 3.11-1 | Comparison of Drag Forces in Accelerating Flows . . . . .  | 131         |
| 3.11-2 | Comparison of Drag Forces in Oscillating Flows . . . . .   | 132         |
| 4.3-1  | Event Combinations and Service Levels for Class MC<br>Components and Internal Structures . . . . . | 152         |
| 4.3-2  | Event Combinations and Service Levels for Class 2 and 3<br>Piping . . . . .                        | 153         |
| 4.3-3  | Event Combinations and Load Factors for Concrete<br>Structurals . . . . .                          | 154         |



LIST OF TABLES

|  | <u>Page</u> |
|--|-------------|
| 1.1-1 Domestic BWR/Mark I Facilities . . . . .                     | 2           |
| 2.4-1 Mark I Long-Term Program Task . . . . .                      | 19          |
| 3.4-1 Mark I Pool Swell Test Programs . . . . .                    | 34          |
| 3.8-1 FSTF Test Matrix . . . . .                                   | 81          |
| 3.10-1 Comparison of Mark I SRV Parameters . . . . .               | 103         |
| 3.10-2 Comparison of Quencher Geometries and Test Conditions . . . | 105         |
| 3.10-3 Comparison of Mark I T-Quencher Load Trends . . . . .       | 107         |
| 4.3-1 Structural Criteria Symbol Definition . . . . .              | 158         |

## ACKNOWLEDGMENTS

### A-7 REVIEW TEAM

The following individuals participated in the Mark I Containment Long-Term Program Safety Evaluation and contributed substantially to this Report:

- C. I. Grimes, USNRC, Division of Operating Reactors (A-7 Task Manager)
- J. R. Fair, USNRC, Division of Operating Reactors
- K. R. Wichman, USNRC, Division of Operating Reactors
- T. M. Su, USNRC, Division of Systems Safety (A-39 Task Manager)
- J. D. Ranlet, Brookhaven National Laboratory
- G. Maise, Brookhaven National Laboratory
- R. L. Kosson, Brookhaven National Laboratory (Grumman Aerospace Corporation)
- C. Economos, Brookhaven National Laboratory
- C. Brennen, California Institute of Technology
- A. A. Sonin, Massachusetts Institute of Technology
- G. Bienkowski, Princeton University

## NOMENCLATURE

|       |  |
|-------|--|
| ADS   | automatic depressurization system        |
| ASME  | American Society of Mechanical Engineers |
| BWR   | boiling water reactor                    |
| CDF   | cumulative distribution function         |
| DBA   | design-basis accident                    |
| DLF   | dynamic load factor                      |
| ECCS  | emergency core-cooling system            |
| EPRI  | Electric Power Research Institute        |
| FSAR  | Final Safety Analysis Report             |
| FSI   | fluid-structure interaction              |
| FSTF  | Full-Scale Test Facility                 |
| GE    | General Electric Company                 |
| HEM   | homogeneous equilibrium model            |
| HPCI  | high-pressure coolant injection          |
| IBA   | intermediate-break accident              |
| KWU   | Kraftwerk Union AG, West Germany         |
| LCO   | limiting conditions for operation        |
| LDR   | Load Definition Report                   |
| LLL   | Lawrence Livermore Laboratory            |
| LOCA  | loss-of-coolant accident                 |
| LTP   | long-term program                        |
| MVA   | multiple-valve actuation                 |
| NRC   | Nuclear Regulatory Commission            |
| PAP   | Program Action Plan                      |
| PSTF  | Pressure-Suppression Test Facility       |
| PUA   | plant-unique analysis                    |
| PUAAG | plant-unique analysis-applications guide |
| QSTF  | Quarter-Scale Test Facility              |
| RHR   | residual-heat-removal system             |
| RSEL  | resultant-static-evaluation load         |
| SBA   | small break accident                     |
| SER   | Safety Evaluation Report                 |
| SRSS  | square root of the sum of the squares    |
| SRV   | safety-relief valve                      |
| SRVDL | safety-relief valve discharge line       |
| STP   | short-term program                       |
| SVA   | single-valve actuation                   |
| TAP   | Task Action Plan                         |

## MARK I CONTAINMENT LONG-TERM PROGRAM SAFETY EVALUATION REPORT

### 1. INTRODUCTION

Pursuant to Section 210 of the Energy Reorganization Act of 1974, the capability of the boiling water reactor (BWR) Mark I containment suppression chamber to withstand suppression pool hydrodynamic loads which were not considered in the original design of the structures was designated an "Unresolved Safety Issue" (Task Action Plan A-7). This report describes the generic suppression pool hydrodynamic load definition and structural assessment techniques that are to be used to design plant modifications necessary to restore the margins of safety in the containment structures of the BWR/Mark I facilities. The staff has reviewed the experimental and analytical programs, and has concluded that the assessment procedures, as modified by the requirements set forth in Appendix A ("NRC Acceptance Criteria for the Mark I Containment Long-Term Program"), will provide a conservative evaluation of the structural response to suppression pool hydrodynamic loading events. The designation of the requirements in Appendix A constitutes the resolution of TAP A-7.

#### 1.1 Problem Definition

The first generations of General Electric (GE) BWR nuclear steam supply systems are housed in a containment structure designated as the Mark I containment system. A total of 25 BWR facilities with the Mark I containment system have been or are being built in the United States; of these, 22 are licensed for power operation. A listing of the domestic BWR/Mark I facilities is provided in Table 1.1-1. The original design of the Mark I containment system considered postulated accident loads previously associated with containment design. These included pressure and temperature loads associated with a loss-of-coolant accident (LOCA), seismic loads, dead loads, jet-impingement loads, hydrostatic loads due to water in the suppression chamber, overload pressure test loads, and construction loads.

Table 1.1.1 Listing of Domestic BWR Facilities with the Mark I Containment System

| Plants Licensed for Power Operation | Licensee                          |
|-------------------------------------|-----------------------------------|
| Browns Ferry Units 1, 2, and 3      | Tennessee Valley Authority        |
| Brunswick Units 1 and 2             | Carolina Power and Light          |
| Cooper Station                      | Nebraska Public Power District    |
| Dresden Units 2 and 3               | Commonwealth Edison Company       |
| Duane Arnold                        | Iowa Electric Light and Power     |
| FitzPatrick                         | Power Authority State of New York |
| Hatch Units 1 and 2                 | Georgia Power Company             |
| Millstone Unit 1                    | Northeast Nuclear Energy Company  |
| Monticello                          | Northern States Power Company     |
| Nine Mile Point Unit 1              | Niagara Mohawk Power Corporation  |
| Oyster Creek                        | Jersey Central Power and Light    |
| Peach Bottom Units 2 and 3          | Philadelphia Electric Company     |
| Pilgrim Unit 1                      | Boston Edison Company             |
| Quad Cities Units 1 and 2           | Commonwealth Edison Company       |
| Vermont Yankee                      | Yankee Atomic Electric Company    |
| Plants Under Construction           | Applicant                         |
| Fermi Unit 2                        | Detroit Edison Company            |
| Hope Creek Units 1 and 2            | Public Service Electric and Gas   |

However, since the establishment of the original design criteria, additional loading conditions which arise in the functioning of the pressure-suppression concept utilized in the Mark I containment system design have been identified.

In the course of performing large-scale testing of an advanced design pressure-suppression containment (Mark III), and during in-plant testing of Mark I containments, new suppression pool hydrodynamic loads which had not explicitly been included in the original Mark I containment design basis were identified. These additional loads result from dynamic effects of drywell air and steam being rapidly forced into the suppression pool (torus) during a postulated LOCA and from suppression pool response to safety-relief valve (SRV) operation generally associated with plant transient operating conditions. Because these hydrodynamic loads had not been considered in the original design of the Mark I containment, the staff determined that a detailed reevaluation of the Mark I containment system was required.

To better understand the reasons for reevaluating the Mark I containment design, the historical development of the original Mark I containment design basis must be reviewed. The Mark I containment design was based on experimental information obtained from testing performed on a pressure-suppression concept for the Humboldt Bay Power Plant and from testing performed for the Bodega Bay Plant concept. The purpose of these initial tests, performed from 1958 through 1962, was to demonstrate the viability of the pressure-suppression concept for reactor containment design. The tests were designed to simulate LOCAs with breaks in piping sized up to approximately twice the cross-sectional break area of the design-basis LOCA.

The tests were instrumented to obtain quantitative information for establishing containment design pressures. The data from these tests were the primary experimental bases for the design and the initial staff approval of the Mark I containment system.

During the large-scale testing of the Mark III containment system design, in the period 1972 through 1974, new suppression pool hydrodynamic loads were identified for the postulated LOCAs. GE tested the Mark III containment concept

in its Pressure Suppression Test Facility (PSTF) (Ref. 1). These tests were initiated for the Mark III concept because of configurational differences between the previous containment concepts and the Mark III design. More sophisticated instrumentation was available for the Mark III tests, as were computerized methods for data reduction. It was from the PSTF testing that the short-term dynamic effects of drywell air being forced into the pool in the initial stage of the postulated LOCA were first identified. This air injection into the suppression pool water results in a pool swell event of short duration. In this event, a slug of water rises and impacts the underside of structural components within the suppression chamber.

In addition to the information obtained from the PSTF data, other LOCA-related dynamic load information was obtained from foreign testing programs (Ref. 2) for similar pressure-suppression containments. It was from these foreign tests that oscillatory condensation loads during the later stages of a postulated LOCA were identified.

Also, experience at operating plants indicated that SRV discharges to the suppression pool would cause oscillatory hydrodynamic loads on the suppression chamber. Both the LOCA and SRV discharge are characterized by an initial short-period injection of air into the suppression pool, followed by a longer period of steam discharge into the suppression pool.

Consequently, in February and April 1975, the NRC transmitted letters to all utilities owning BWR facilities with the Mark I containment system design, requesting that the owners quantify the hydrodynamic loads and assess the effect of these loads on the containment structure. The February 1975 letters reflected NRC concerns about the dynamic loads from SRV discharges, while the April 1975 letters indicated the need to evaluate the containment response to the newly identified dynamic loads associated with a postulated design-basis LOCA.

As a result of these letters from the NRC, and recognizing that the additional evaluation effort would be very similar for all Mark I BWR plants, the affected utilities formed an "ad hoc" Mark I Owners Group, and GE was designated as the

Group's lead technical organization. The objectives of the Group were to determine the magnitude and significance of these dynamic loads as quickly as possible and to identify courses of action needed to resolve any outstanding safety concerns. The Mark I Owners Group proposed to divide this task into two programs: a short-term program (STP) to be completed in early 1977 and a long-term program (LTP) to be completed in 1979.

### 1.2 Short-Term Program Summary

The objectives of the STP were to verify that each Mark I containment system would maintain its integrity and functional capability when subjected to the most probable loads induced by a postulated design-basis LOCA, and to verify that licensed Mark I BWR facilities could continue to operate safely, without endangering the health and safety of the public, while a methodical, comprehensive LTP was being conducted.

The STP structural acceptance criteria used to evaluate the design of the torus and related structures were based on providing adequate margins of safety, i.e., a safety-to-failure factor of 2, to justify continued operation of the plant before the more detailed results of the LTP were available.

The basis for the staff's conclusions relative to the STP are described in the "Mark I Containment Short-Term Program Safety Evaluation Report," NUREG-0408, dated December 1977. The staff concluded that a sufficient margin of safety had been demonstrated to assure the functional performance of the containment system and, therefore, any undue risk to the health and safety of the public was precluded. Subsequently, the staff granted the operating Mark I facilities exemptions relating to the structural factor of safety requirements of 10 CFR 50.55(a). These exemptions were granted for an interim period of approximately 2 years, while the more comprehensive LTP was being conducted.

### 1.3 Long-Term Program Description

The objectives of the LTP were to establish design-basis (conservative) loads that are appropriate for the anticipated life of each Mark I BWR facility (40 years), and to restore the originally intended design-safety margins for each Mark I containment system.



During July and August 1976, the Mark I Owners Group made several presentations to the NRC staff regarding the proposed content and schedule for completion of the LTP. Much of this information was subsequently documented in the "Mark I Containment Program, Program Action Plan" submitted to the NRC staff on October 29, 1976 (Ref. 3). As a result of NRC staff comments and questions on this document, the Mark I Owners Group revised several of the proposed LTP tasks and objectives. These revisions were discussed with the NRC staff in meetings held in February 1977 and are documented in Revision 1 to the "Mark I Containment Program, Program Action Plan" which was submitted on February 11, 1977 (Ref. 4). During the course of the LTP, additional revisions were made to the Program Action Plan (Refs. 5, 6) to reflect task scope and schedule changes which evolved from the initial results of specific tasks.

The principal thrust of the LTP has been the development of generic methods for the definition of suppression pool hydrodynamic loading events and the associated structural assessment techniques for the Mark I configuration. The generic analysis techniques are intended to be used to perform a plant-unique analysis (PUA) for each Mark I facility. This analysis would demonstrate that the proposed configuration of the plant has restored the original design-safety margin.

The generic aspects of the Mark I Owners Group LTP were completed with the submittal of the "Mark I Containment Program Load Definition Report" (Ref. 7) hereafter referred to as the LDR, and the "Mark I Containment Program Structural Acceptance Guide" (Ref. 8), hereafter referred to as the PUAAG; as well as supporting reports on the LTP experimental and analytical tasks.

The purpose of this report is to present the staff's evaluation of the generic load definition and structural assessment techniques that have been proposed by the Mark I Owners Group in the reports mentioned above. The requirements which have resulted from the staff evaluation (Appendix A) will be used by each BWR/Mark I licensee to perform plant-unique analyses. These analyses will serve to identify those plant modifications that are needed to restore the margins of safety in the containment design.

Section 2 of this report presents a general description of the Mark I containment system and the phenomena associated with suppression pool hydrodynamic loading events. A more detailed description of the hydrodynamic phenomena is presented in Section 3, along with the staff's evaluation of the load definition techniques proposed in the LDR. Section 4 presents the staff's evaluation of the general structural analysis techniques and acceptance criteria that are to be used for the plant-unique analyses.

## 2. BACKGROUND

### 2.1 Mark I Containment System Description

The Mark I containment system is designed to condense the steam released during a postulated LOCA, to limit the release of the fission products associated with the accident, and to serve as a source of water for the emergency core cooling system (ECCS).

The Mark I containment system (Figures 2.1-1 and 2.1-2) consists of (1) a drywell which encloses the reactor vessel, the reactor coolant recirculation system, and other branch connections of the reactor coolant system; (2) a toroidal shaped pressure-suppression chamber (torus) containing a large volume of water; (3) a vent system connecting the drywell to the water space of the torus; (4) containment isolation valves; (5) containment cooling systems; and (6) other service equipment.

The drywell is a steel pressure vessel, supported in concrete, with a spherical lower section and a cylindrical upper section. For all but one of the Mark I facility designs, the suppression chamber is a steel pressure vessel in the shape of a torus, located below the drywell and encircling it. The steel suppression chamber is mounted on supports which transmit operational, accident, and seismic loads to the concrete foundation of the reactor building. The remaining Mark I design utilizes a steel-lined, reinforced concrete suppression chamber, also in the shape of a torus.

The drywell and suppression chamber volumes are interconnected by a vent system. Main vents connect the drywell to a vent header, which is located in the airspace of the suppression chamber. A bellows in each main vent allows for possible movement of the suppression chamber relative to the drywell (e.g., thermal expansion). Projecting downward from the vent header are downcomer pipes, which are nominally 24 inches in diameter and terminate 3 to 4 feet below the surface of the pool. Typically there are 8 to 10 main vents and 48 to 120 downcomers.

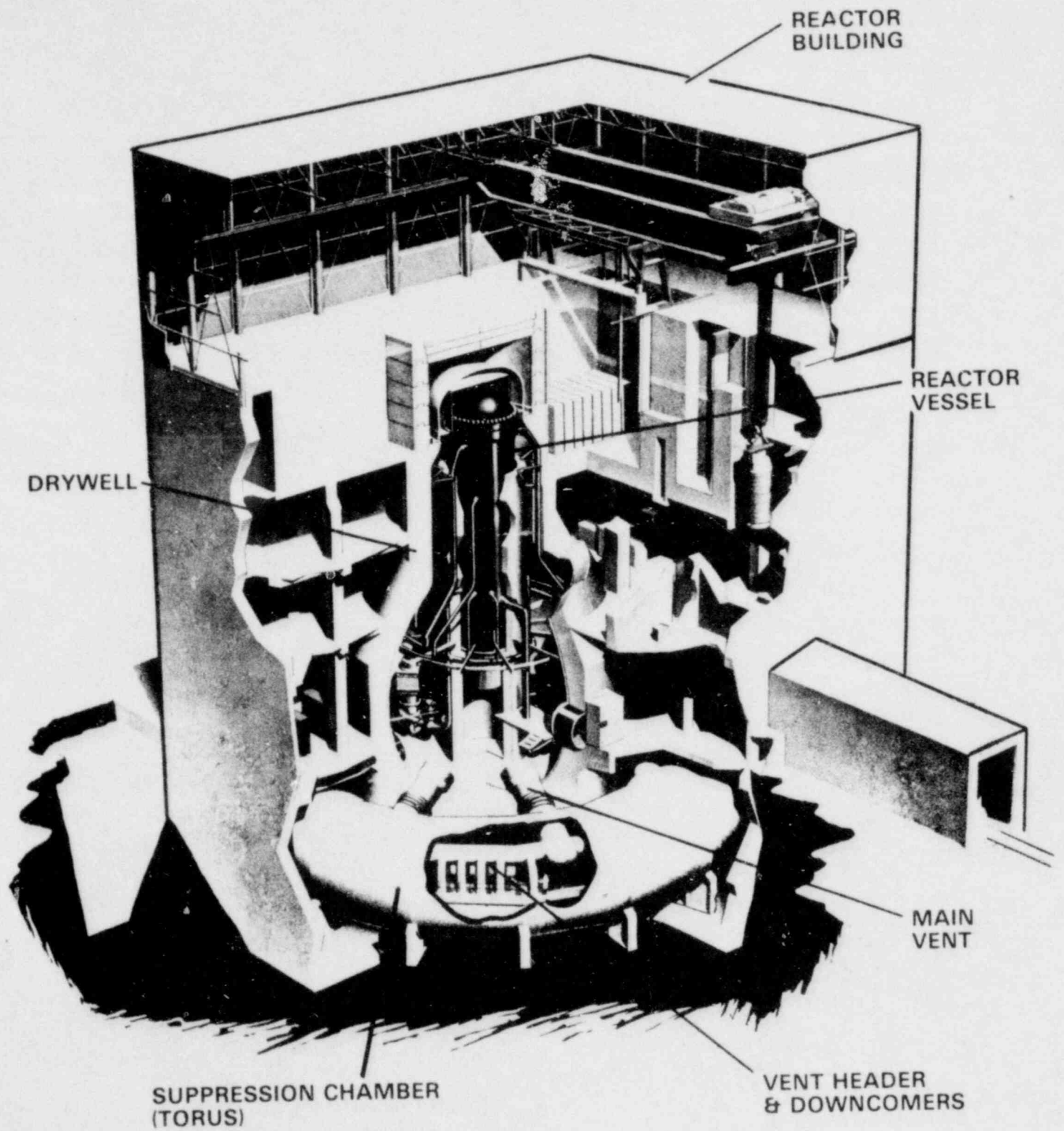


Figure 2.1-1 Mark I containment system.

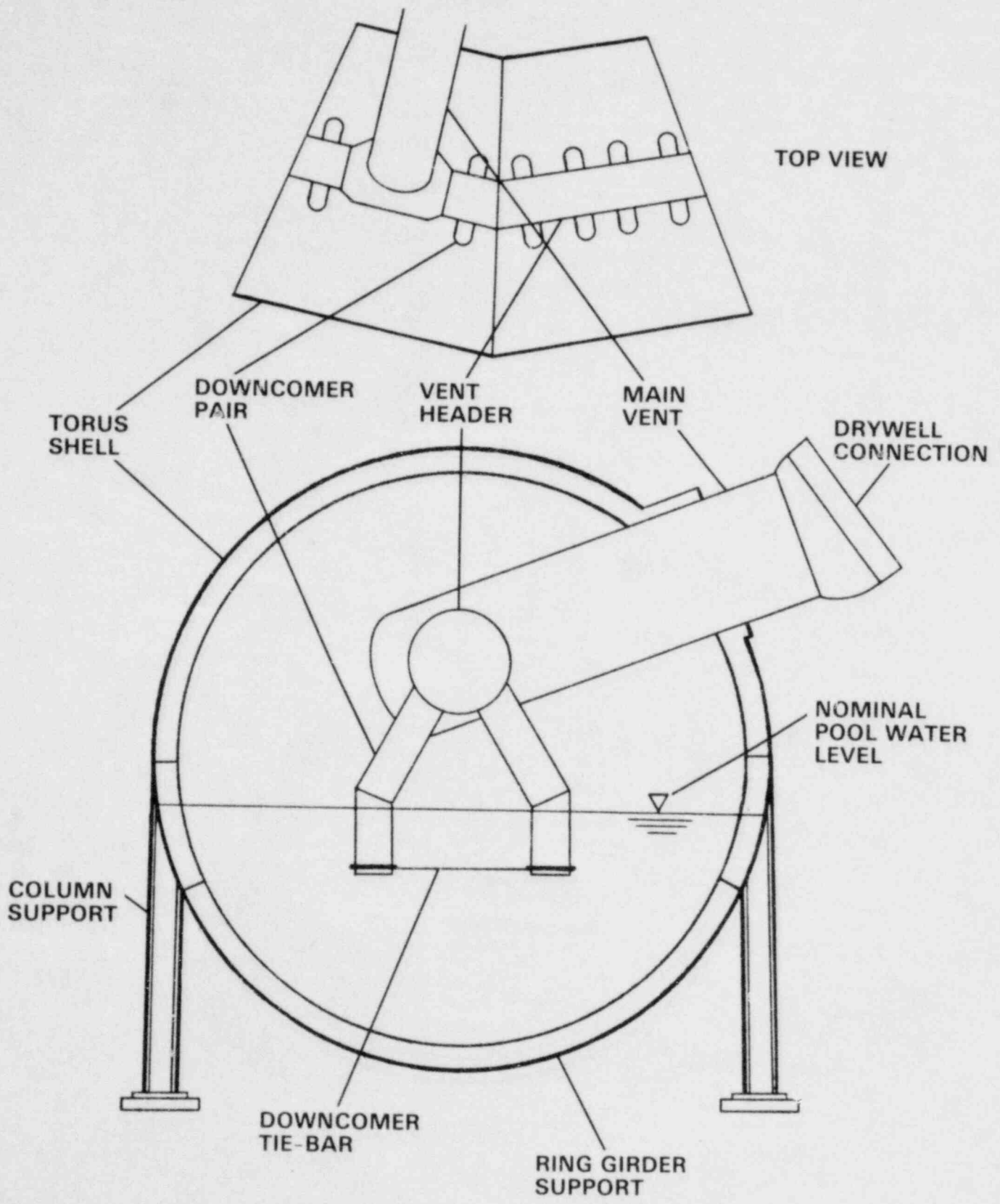


Figure 2.1-2 Mark I suppression chamber.

In the event of a postulated LOCA, reactor water and steam would expand into the drywell atmosphere. As a result of the increasing drywell pressure, a mixture of drywell atmosphere, steam, and water would be forced through the vent system into the pool of water which is stored in the suppression chamber. The steam vapor would condense in the suppression pool, thereby reducing the drywell pressure. Noncondensable gases and fission products would be collected and contained in the suppression chamber. Initially, the drywell atmosphere is transferred to the suppression chamber and pressurizes the chamber. At the end of the blowdown, when ECCS water spills out of the break and rapidly reduces the drywell pressure, the suppression chamber is vented to the drywell through installed vacuum breakers to equalize the pressure between the two vessels. The ECCS cools the reactor core and transports the heat to the water in the suppression chamber. Cooling systems are provided to remove heat from the water in the suppression chamber, thus providing a continuous path for the removal of decay heat from the primary system.

## 2.2 LOCA-Related Hydrodynamic Phenomena

The following sections contain a qualitative description of the various phenomena that could occur during the course of a postulated design basis LOCA in a BWR with the Mark I containment system, as well as a description of the hydrodynamic loads which these phenomena could impose upon the suppression chamber and related structure. Figure 2.2-1 shows the sequence of events after a postulated LOCA and the potential loading conditions associated with these events.

### 2.2.1 Pool Swell Phenomena

With the instantaneous rupture of a steam or recirculation line, a shock wave exits the broken primary system pipe and expands into the drywell atmosphere. At the break exit point, the wave amplitude theoretically is equal to reactor operating pressure (1000 psia); however, there would be rapid attenuation as the wave front expands spherically outward into the drywell. Further attenuation would occur as the wave enters the drywell vent system and progresses into the suppression pool.

PHENOMENON

POTENTIAL DYNAMIC LOADING CONDITION

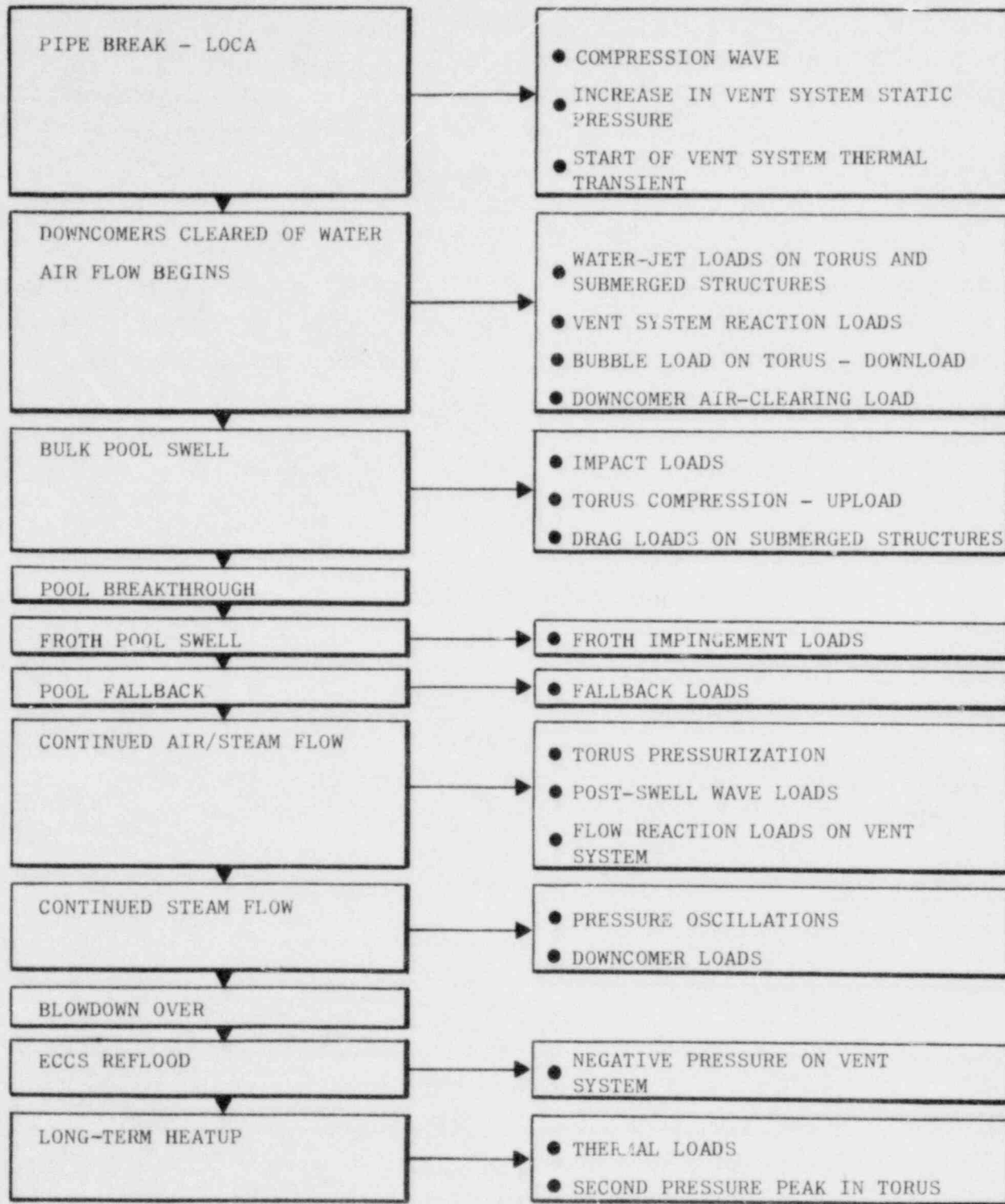


Figure 2.2-1 LOCA sequence of primary events.

Because there would be a very rapid drywell pressure increase associated with the postulated LOCA, a compression wave would propagate into the water initially standing in the downcomers. Before this water is cleared from the downcomers, this compression wave would propagate through the suppression pool and result in a dynamic loading on the suppression chamber (torus). The compression wave could also result in a dynamic loading condition on any structures within the suppression pool.

Immediately following the postulated LOCA, the pressure and temperature of the drywell atmosphere would increase. These increases also would occur in the vent system and would lead to mechanical and thermal loadings on the vents, vent header, and downcomers.

With the drywell pressure increase, the water initially standing in the downcomers accelerates into the pool, and the downcomers clear of water. During this water-clearing process, a water jet forms in the suppression pool, and causes a potential water-jet-impingement load on the structures within the suppression pool and on the torus section beneath the downcomers.

Immediately following downcomer clearing, a bubble of air starts to form at the exit of the downcomers. As the bubble forms, its pressure is nearly equal to the drywell pressure at the time of downcomer clearing. The bubble pressure is transmitted through the suppression pool water and results in a downward load on the torus.

When the air/steam flow from the drywell becomes established in the vent system, the initial bubble expands and subsequently decompresses as a result of over-expansion. During the early stages of this process, the pool will swell in bulk mode (i.e., a ligament of solid water is being accelerated upward by the air bubble). During this phase of pool swell, structures close to the pool surface experience impact loads as the rising pool surface strikes the lower surfaces of the structures. This is followed by drag loads as the pool surface continues to rise past the structures. In addition to these impact and drag loads above the pool, there will also be drag loads as the bubble formation causes water flow past submerged structures and equipment.



As the water slug continues to rise (pool swell), the bubble pressure falls below the torus airspace pressure. However, the momentum of the water slug causes it to continue to rise, this compresses the air volume above the pool and results in a net upward pressure loading on the torus. The thickness of the water slug will decrease as it rises. Aided by impact of the vent header, it will begin to break up and evolve into a two-phase "froth" of air and water. The froth will continue to rise as a result of its own momentum, and it will impinge on structures above the pool breakthrough elevation.

When the drywell air flow rate through the vent system decreases and the air/water mixture in the suppression pool experiences gravity-induced phase separation, the pool liquid upward movement stops, and the "fallback" process starts. During this process, structures in the torus may experience a downward loading, and the submerged portion of the torus could be subjected to a pressure increase. Following "fallback," waves may develop on the suppression pool surface, thereby presenting a potential source of dynamic loads on the downcomers, torus, and any other structures close to the water surface.

The pool swell transient typically lasts on the order of 3 to 5 seconds. Because of the configuration of the drywell and the volume of the vent system, this period is dominated by the flow of the drywell atmosphere\* through the vent system. Steam flow will follow, beginning near the end of the pool swell transient, with a relatively high concentration of noncondensable gas. Throughout these periods, there is a significant pressure differential between the drywell and the torus. This, together with flow-induced reaction forces, leads to structural loads on the vent system.

### 2.2.2 LOCA Steam Condensation Phenomena

As the flow of steam through the vent system continues, pressure oscillations will occur in the event system and the suppression pool. Experimental data suggest that the amplitude and frequency of these pressure oscillations are

\*The drywell atmosphere for most operating BWR facilities is inerted (i.e., nitrogen rich). However, pool swell experimental studies conducted for this program used air as the flowing medium, because of its availability and the thermohydraulic similarities of air and nitrogen. In addition, the terms drywell atmosphere and drywell air are often used interchangeably.

primarily functions of the mass flow rate through the vent system, the concentration of noncondensibles in the mass flow, the downcomer submergence, and the suppression pool temperature. The pressure oscillations will cause loadings on the vent system, the torus shell, and the structures submerged in the pool.

Early in the transient, when the mass flow rate is relatively high, the pressure oscillations appear as a sinusoidal function whose amplitude varies with time. These oscillations are referred to as "condensation oscillations."

When the mass flow rate through the vent system decreases, the pool will begin to reenter the downcomers intermittently. This period, termed "chugging," is characterized by fairly irregular pressure pulses.

The ECCS is designed so that shortly after a postulated LOCA, the ECCS will automatically start to pump condensate water and/or suppression pool water into the reactor pressure vessel. This water floods the reactor core and subsequently cascades into the drywell through the postulated break. The time at which this will occur depends upon break size and location. Because the drywell will be full of steam when the vessel floods, the sudden introduction of water causes steam condensation and drywell depressurization. As the drywell pressure falls below the torus pressure, the vacuum relief system allows air from the torus to enter the drywell. Eventually, enough air will return to equalize the drywell and torus pressures; however, during this drywell depressurization transient, there will be a period of negative pressure on the vent system within the torus volume. When the mass flow from the break is small, the pressure oscillations will essentially be terminated.

Following vessel flooding, suppression pool water is continuously recirculated through the core by the ECCS pumps. The energy associated with the core decay heat will result in a slow heatup of the suppression pool. To control suppression pool temperature, operators will activate the suppression pool cooling mode of the residual-heat-removal (RHR) system. After several hours, the RHR heat exchangers will terminate the increase in the suppression pool temperature. An increase in the pressure in the drywell and torus is associated with this post-LOCA suppression pool temperature increase; however, the resultant maximums will not exceed the pressures that occur during the short-term blowdown phase of the accident.

### 2.3 Safety-Relief Valve Discharge Phenomena

BWR plants are equipped with safety-relief valves (SRVs) to control primary system pressure transients. The SRVs are mounted on the main steam lines inside the drywell, with discharge pipes routed down the main vents into the suppression pool. When an SRV is actuated, steam released from the primary system will be discharged into the suppression pool where it will condense.

Small variations in primary system pressure can be controlled by changing the system power level. However, more rapid pressure transients (e.g., turbine trip) require a positive-acting relief system. For these transients, the SRVs actuate to divert part or all of the generated steam to the suppression pool. The number of SRVs in any particular plant is dependent upon the configuration and rated power of the primary system. The SRVs will either self-actuate at a preset pressure (nominally 1100 psia) or actuate by an external signal (e.g., manual actuation). A specified number of the SRVs is used for the automatic depressurization system (ADS), which is designed to reduce the reactor system pressure to permit the low-pressure emergency core spray and/or the low-pressure coolant injection systems to function. The ADS performs this function by automatically actuating the specified SRVs, following the receipt of specific signals from the reactor protection system.

Upon actuation of an SRV, the air column within the partially submerged discharge line is compressed by the high-pressure steam and accelerates the water leg into the suppression pool. The water jets thus formed create pressure and velocity transients which cause drag or jet impingement loads on submerged structures.

Following water clearing, the compressed air is accelerated into the suppression pool and forms a high-pressure air bubble. This bubble expands and contracts a number of times before it rises to the suppression pool surface. The associated transients again create drag loads on submerged structures, as well as pressure loads on the submerged boundaries. These loads are referred to as SRV air-clearing loads.

Following the air-clearing phase, essentially pure steam is injected into the pool. Experiments indicate that the steam jet/water interface which exists at the discharge line exit is relatively stationary, as long as the local pool temperature is low. Thus, condensation proceeds in a stable manner, and no significant loads are experienced. Continued steam blowdown into the pool will increase the local pool temperature. The condensation rates at the turbulent steam/water interface are eventually reduced to levels below those needed to readily condense the discharge steam. At this "threshold" level, the condensation process becomes unstable; i.e., steam bubbles are formed and shed from the pipe exit, and the bubbles oscillate and collapse. This results in severe pressure oscillations, which are imposed on the pool boundaries. To preclude unstable condensation, limits are established for the allowable suppression pool temperature and are restricted to those values in the plant Technical Specifications. These restrictions are referred to as the pool temperature limits.

The magnitude of the SRV discharge-related loads is a function of the type of discharge device used. In the past, straight-pipe, elbows, and "ramshead" discharge devices have been used. Current practice calls for the installation of "quencher" SRV discharge devices, which are perforated pipe sections. The quencher device has been found to reduce substantially the hydrodynamic discharge loads in comparison to those observed for the other discharge devices. The T-quencher discharge device developed specifically for the Mark I torus configuration is shown in Figure 2.3-1.

#### 2.4 Long-Term Program Task Descriptions

In order to assure the timely completion of the LTP and provide an adequate basis for the evaluation of suppression pool hydrodynamic loads, the Mark I Owners Group divided the program into a series of subtasks. The task descriptions and organization were presented to the staff in the "Mark I Containment Program, Program Action Plan" (Refs. 3, 4, 5, 6), as discussed in Section 1.3. A list of the LTP tasks is presented in Table 2.4-1.

The individual program tasks provided not only experimental and analytical bases for the development of suppression pool hydrodynamic loads, but also provided

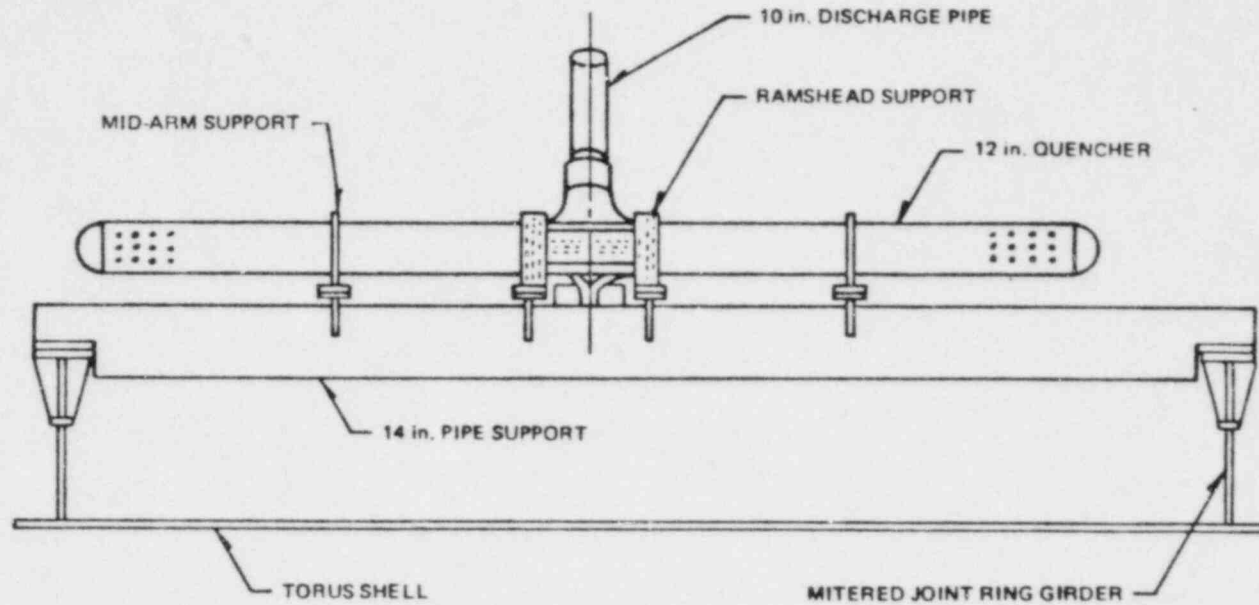


Figure 2.3-1 Mark I T-quencher discharge device.

Table 2.4-1 Mark I Long-Term Program Tasks

| Task Number | Task Description                     |
|-------------|--------------------------------------|
| 1.0         | Program Action Plan                  |
| 2.0         | Preliminary Load Evaluation          |
| 3.0         | Structural Acceptance Criteria       |
| 4.0         | Generic Structural Evaluation        |
| 5.0         | Hydrodynamic Load Evaluation         |
| 5.1         | Monticello In-Plant SRV Tests        |
| 5.1.1       | SRV Ramshead Tests                   |
| 5.1.2       | SRV T-Quencher Tests                 |
| 5.2         | 4T Condensation Tests                |
| 5.3         | Flexible Cylinder Tests              |
| 5.3.1       | Hydrodynamic Impact Tests            |
| 5.3.2       | Cylinder Drop Tests                  |
| 5.3.3       | Pool Swell Impact Tests              |
| 5.4         | Seismic Slosh Tests                  |
| 5.5         | 1/4-Scale 2-D Pool Swell Tests       |
| 5.5.1       | Scaling Law Verification             |
| 5.5.2       | Downflow Oscillation Evaluation      |
| 5.5.3       | LDR Plant-Unique Tests               |
| 5.6         | 3-D Pool Swell Tests                 |
| 5.6.1       | 1/12-Scale 3-D Tests                 |
| 5.6.2       | 1/30-Scale 3-D Tests                 |
| 5.7         | Initially Deleted                    |
| 5.8         | 1/12-Scale 2-D Tests                 |
| 5.9         | Pool Swell Model Development         |
| 5.10        | Miscellaneous Monitoring             |
| 5.11        | Full-Scale Test Facility             |
| 5.12        | Multivent Chugging Tests (Cancelled) |
| 5.13        | Chugging Analytical Evaluation       |
| 5.14        | Submerged Structures Evaluation      |

Table 2.4-1 (Continued)

| Task Number | Task Description   |
|-------------|--|
| 5.15        | Structural Hydrodynamic Interaction                      |
| 5.15.1      | Interaction Analytical Evaluation                        |
| 5.15.2      | Interaction Test Support                                 |
| 5.16        | Mark I Submergence Tests                                 |
| 5.16.1      | Chugging Submergence Tests                               |
| 5.16.2      | Chugging Mitigation Tests                                |
| 5.17        | Condensation Oscillation Evaluation                      |
| 5.18        | Multivalent Interaction Test (Cancelled)                 |
| 6.0         | Load Mitigation Development                              |
| 6.1         | Chugging Mitigation                                      |
| 6.1.1       | Chugging Parametric Sensitivity                          |
| 6.1.2       | Chugging Mitigation Tests (Cancelled)                    |
| 6.2         | SRV Mitigation   |
| 6.2.1       | T-Quencher Development                                   |
| 6.2.2       | Discharge Line Mitigation (Cancelled)                    |
| 6.3         | Pool Swell Mitigation                                    |
| 6.3.1       | Pool Swell Screening Tests                               |
| 6.3.2       | 1/4-Scale Mitigation Tests (Cancelled)                   |
| 6.3.3       | Vent Header Impact Mitigation (Cancelled)                |
| 6.4         | Mitigation Requirements Assessment                       |
| 6.5         | LOCA Mitigator Application Criteria (Cancelled)          |
| 6.6         | $\Delta P$ and Reduced Submergence Functional Assessment |
| 7.0         | Generic Load Definition Report                           |
| 7.1         | SRV Loads Analytical Models                              |
| 7.1.1       | SRV Discharge Load Models                                |
| 7.1.2       | SRV Discharge Pipe Load Models                           |
| 7.1.3       | Multiple/Consecutive SRV Actuation Evaluation            |
| 7.2         | SRV Loads Applications Guide                             |
| 7.3         | LOCA Loads   |
| 7.3.1       | Drywell Pressurization Model                             |
| 7.3.2       | LOCA Load Calculational Techniques                       |
| 7.4         | Load Combination Criteria and Methods                    |

Table 2.4-1 (Continued)

| Task Number | Task Description                     |
|-------------|--------------------------------------|
| 7.4.1       | Timing Bar Charts                    |
| 7.4.2       | SRSS Load Combinations               |
| 7.5         | SRV Discharge Steam Mixing Model     |
| 7.6         | Load Definition Report - Preparation |



scoping studies which were used by the Mark I Owners Group to direct the course of the program. Consequently, throughout the course of the LTP, task scopes were modified or tasks were cancelled on the basis of the results of the Mark I Owners Group's "decision points." These decision points principally involved selecting options relative to structural modifications or load mitigation. Periodic meetings were held between the staff and the Mark I Owners Group to discuss preliminary task results and decision point conclusions.

Most of the LTP tasks were directed toward the development of experimental and analytical information which could be used to develop generic suppression pool hydrodynamic load definition and assessment procedures. Other tasks provided information concerning potential structural modifications and hydrodynamic load mitigation techniques which could be used to implement the program in the plant-unique analyses. Through the decision points, four load mitigation techniques were developed generically for application to the Mark I plants: (1) differential pressure control for LOCA loads, which is described in Section 3.12.7; (2) reduced submergence for LOCA loads, described in Section 3.12.6; (3) the vent-header deflectors for the LOCA vent header impact loads, described in Section 3.5.2; and (4) the T-quencher discharge device for SRV loads, described in Section 3.10. When each Mark I licensee performs the LTP plant-unique analysis, the licensee's engineering group will select the optimum combination of structural modifications and/or load mitigation techniques by which the originally intended design-safety margin for the containment structure will be restored.

The applicable results of the LTP tasks were submitted to the staff in a series of reports and are summarized in the LDR and the PUAAG. Specific reports are referenced in the text of this evaluation.

### 3. HYDRODYNAMIC LOAD EVALUATION

#### 3.1 Introduction

The sections below present the staff's evaluation of the definition procedures for suppression pool hydrodynamic loads which were proposed by the Mark I Owners Group for use in the LTP plant-unique analyses. In certain cases, the staff has concluded that the load definition procedures as proposed are unacceptable. For these cases, modifications and/or clarifications to the load definition techniques have been specified to ensure that a method acceptable to the NRC will be used in the plant-unique analyses. These requirements are presented in Appendix A and were originally transmitted to each Mark I licensee in October 1979 to begin implementation of this program. The bases for these requirements are also presented in the following evaluation.

This evaluation and the plant-unique assessments are intended to address only those events or event combinations which involve suppression pool hydrodynamic loads. This evaluation includes certain loads in the event combinations which were reviewed and approved by the staff in the Final Safety Analysis Report (FSAR) for each plant. However, these loads are discussed in this evaluation because improved analysis techniques have evolved since the time the FSAR was reviewed. Unless otherwise specified, any loading condition or structural analysis technique not addressed by this evaluation will be in accordance with the plant's approved FSAR.

#### 3.2 Containment Response Models

The drywell and suppression chamber transient-pressure-and-temperature response to a LOCA are calculated by the GE Pressure-Suppression Containment Analytical Model (Ref. 9). This analytical model calculates the thermodynamic response of the drywell, vent system, and suppression chamber volumes to the mass and energy released from the primary system following a postulated LOCA.

For the design-basis accident (DBA) analysis, the drywell is assumed to be at a maximum operating temperature of 135°F and a relative humidity of 20 percent,

the suppression chamber is assumed to be at the arithmetic mean of the maximum and minimum operating pool temperatures, with a relative humidity of 100 percent, and the pool level is assumed to be at the maximum submergence of the downcomers (minimum torus airspace volume). Condensation in the drywell is conservatively neglected, and the vent system flow loss characteristics are maximized. The mass and energy release into the containment from the primary system is calculated independently, as described in Section 3.2.3. A typical calculated DBA containment pressure response is shown in Figure 3.2-1.

The assumed initial conditions will result in a conservative estimate of the drywell pressure and pressurization rate following a postulated LOCA. Because the analysis assumes an average torus temperature which is conservative for vent system loads (see Section 3.3), the torus pressure is stepped-up 1.0 psi before 30 seconds and 2.0 psi after 30 seconds to estimate the torus pressure response for maximum pool temperature.

These analysis techniques have provided conservative estimates of the containment response to a LOCA, in comparison with the results of the staff's CONTEMPT-LT computer code. On this basis, the staff has concluded that the containment pressure and temperature analysis techniques are acceptable.

### 3.2.1 Postulated Pipe Breaks

The DBA for the Mark I containment design is the instantaneous guillotine rupture of the largest pipe in the primary system (the recirculating line). This LOCA leads to a specific combination of dynamic, quasi-static, and static loads in time. However, the DBA does not represent the limiting case for all structural elements. Consequently, a spectrum of postulated pipe breaks must be investigated to determine the worst loading condition for each structural element. For the LTP, an intermediate break accident (IBA) and a small break accident (SBA) have been specified, in addition to the DBA.

The IBA is a 0.1 square foot instantaneous liquid-line break in the primary system. This break size will not result in rapid reactor depressurization and, consequently, will not result in significant pool swell loads. However, this break size is large enough that the high pressure coolant injection (HPCI) cannot

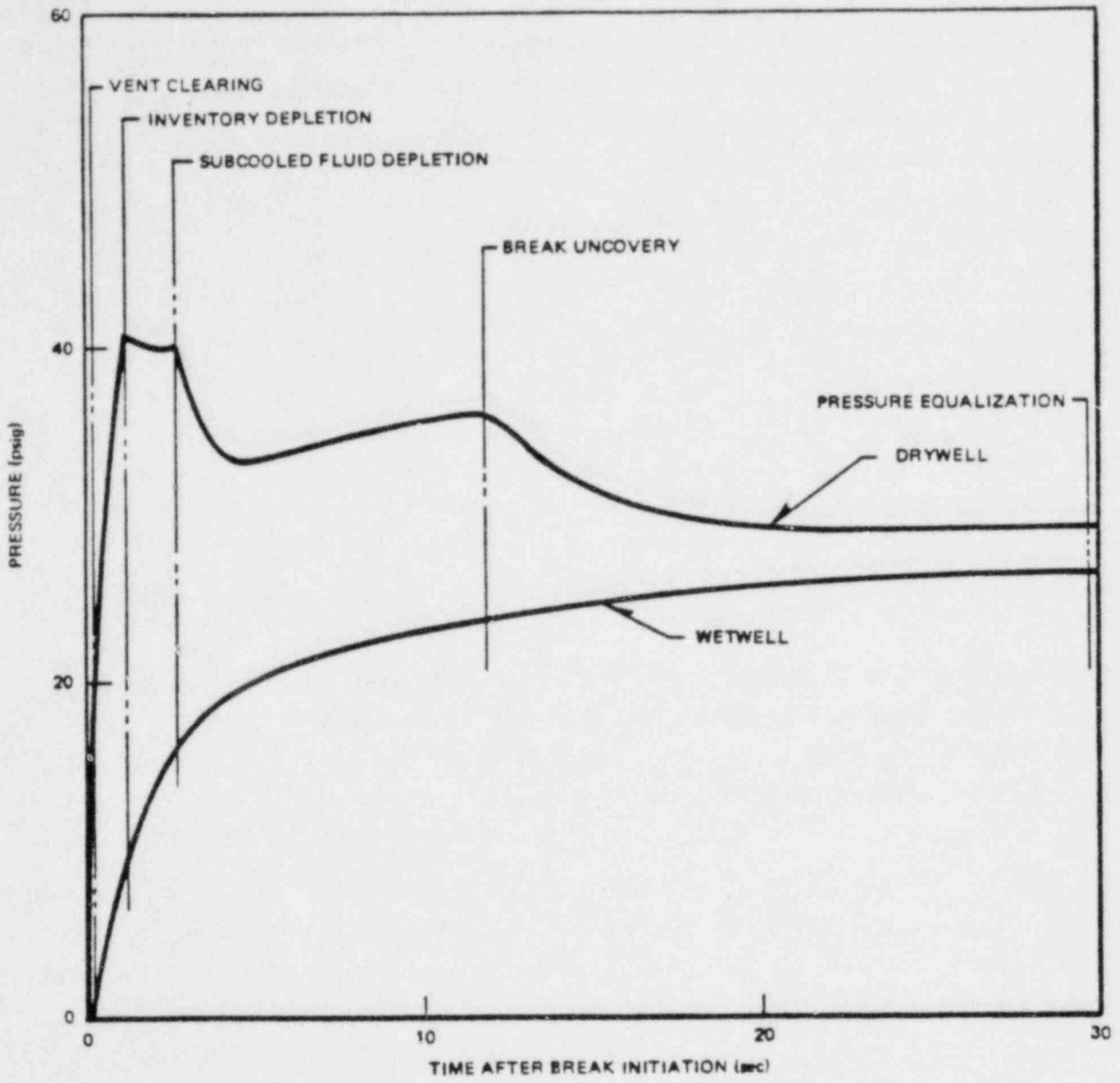


Figure 3.2-1 Typical Mark I DBA pressure response.

maintain the reactor vessel water level. Therefore, this LOCA will result in a combination of condensation loads and multiple SRV discharge loads.

The SBA is a 0.01 square-foot instantaneous steam-line break in the primary system. The fluid loss rate for this break size is large enough to depressurize the reactor vessel and small enough so that HPCI operation can maintain the reactor vessel water level. Therefore, this LOCA will result in a long-duration combination (relative to the DBA and IBA) of chugging and multiple SRV discharge loads.

### 3.2.2 Event Combinations and Timing

Not all of the suppression pool hydrodynamic loads discussed in this evaluation can occur at the same time. In addition, the load magnitudes and timing will vary, depending on the accident scenario under consideration. Therefore, it is necessary to construct a series of event combinations which can be used to describe the circumstances under which individual loads might combine.

The event combinations proposed for the LTP are shown in Figure 3.2-2. The combinations of loading conditions have been determined from typical plant primary system and containment response analyses, with considerations for automatic actuation, manual actuation, and single active failures of the various systems in each event.

The magnitude and timing for each loading condition are discussed in the individual load evaluations in the following sections. In general, the timing and duration of the loads are determined as follows:

- (1) Containment response (pressure, temperature, and reaction) is determined from the containment response analysis.
- (2) Pool swell-related loads are determined from the small-scale tests described in Sections 3.4 through 3.7.
- (3) LOCA condensation loads are bounded on the basis of a typical plant containment response analysis, based on vent system flow.

| Earthquake Type                | SRV |   | SRV + EQ |   | SBA IBA |   | SBA + EQ IBA + EQ |   |   |    | SBA+SRV IBA+SRV |    | SBA+SRV+EQ IBA+SRV+EQ |    |    |    | DBA |    | DBA + EQ |    |    |    | DBA+SRV |    | DBA+SRV+EQ |    |    |  |
|--------------------------------|-----|---|----------|---|---------|---|-------------------|---|---|----|-----------------|----|-----------------------|----|----|----|-----|----|----------|----|----|----|---------|----|------------|----|----|--|
|                                | 1   | 2 | 3        | 4 | 5       | 6 | 7                 | 8 | 9 | 10 | 11              | 12 | 13                    | 14 | 15 | 16 | 17  | 18 | 19       | 20 | 21 | 22 | 23      | 24 | 25         | 26 | 27 |  |
| Normal                         | X   | X | X        | X | X       | X | X                 | X | X | X  | X               | X  | X                     | X  | X  | X  | X   | X  | X        | X  | X  | X  | X       | X  | X          | X  | X  |  |
| Earthquake                     |     | X | X        |   |         | X | X                 | X | X |    |                 | X  | X                     | X  | X  |    |     | X  | X        | X  | X  |    |         | X  | X          | X  | X  |  |
| SRV Discharge                  | X   | X | X        |   |         |   |                   |   |   | X  | X               | X  | X                     | X  |    |    |     |    |          |    |    | X  | X       | X  | X          | X  | X  |  |
| LOCA Thermal                   |     |   |          | X | X       | X | X                 | X | X | X  | X               | X  | X                     | X  | X  | X  | X   | X  | X        | X  | X  | X  | X       | X  | X          | X  | X  |  |
| LOCA Reactions                 |     |   |          | X | X       | X | X                 | X | X | X  | X               | X  | X                     | X  | X  | X  | X   | X  | X        | X  | X  | X  | X       | X  | X          | X  | X  |  |
| LOCA Quasi-Static Pressure     |     |   |          | X | X       | X | X                 | X | X | X  | X               | X  | X                     | X  | X  | X  | X   | X  | X        | X  | X  | X  | X       | X  | X          | X  | X  |  |
| LOCA Pool Swell                |     |   |          |   |         |   |                   |   |   |    |                 |    |                       |    | X  |    | X   | X  |          |    |    | X  |         | X  | X          |    |    |  |
| LOCA Condensation Oscillations |     |   |          |   | X       |   |                   | X | X |    | X               |    |                       | X  | X  |    | X   |    |          | X  | X  |    | X       |    |            | X  | X  |  |
| LOCA Chugging                  |     |   |          |   | X       |   |                   | X | X |    | X               |    |                       | X  | X  |    | X   |    |          | X  | X  |    | X       |    |            | X  | X  |  |

EQ = Earthquake Event

O = Operating-Basis Earthquake

S = Safe-Shutdown Earthquake

SRV = Safety-Relief Valve Discharge Event

SBA = Small-Break Accident

IBA = Intermediate-Break Accident

DBA = Design-Basis Accident

Figure 3.2-2 Mark I event combinations.

(4) SRV discharge loads are based on a plant-unique primary system analysis.

However, the duration of the SBA condensation loads proposed by the Mark I Owners Group is assumed to be terminated by manual actuation of the ADS 10 minutes after the postulated pipe break. Each licensee or applicant must assure the limited duration of the SBA condensation loads by specifying procedures and primary system parameters that the operator will use to terminate the event (Appendix A, Section 2.1). Longer durations may be assumed for the SBA condensation loads where specific plant procedures dictate such a change. However, the staff assessment of the effects of pool thermal stratification (Section 3.12.6) and asymmetric vent system flow (Section 3.12.3) was predicated on a 10-minute duration for the SBA condensation period. Those licensees or applicants that select a longer period must assure that their procedures are adequate to preclude adverse consequences from these effects.

The staff review of the proposed event combinations for the Mark I LTP indicates that the load combinations, in conjunction with the postulated accident scenarios and the proposed load definition techniques and, as modified by the acceptance criteria in Appendix A, will provide a conservative assessment of the accident and normal transient loading conditions which could be imposed on the suppression chamber structures. On this basis, the proposed event combinations are acceptable. An additional evaluation concerning the application of the event combinations to determine the design service levels is presented in Section 4.3.

### 3.2.3 Containment Mass and Energy Release

The primary-system-break flowrates are a principal input to the containment response analysis. For the design-basis accident (DBA), the proposed mass and energy release rates from the primary system are to be calculated with the homogeneous equilibrium model (HEM) (Ref. 10) applied in a nonmechanistic reactor system, which does not take credit for pressure reduction in the piping during the early portion of blowdown, and with conservatively assumed liquid flow during most of the remainder of the blowdown (Refs. 9, 11). The staff has compared the mass and energy release rate predictions of the GE model to those of a conservative RELAP-4 analysis, and has concluded that the GE model will provide a

conservative estimate of the maximum mass and energy release rates for a postulated double-ended recirculation line break in BWRs with a Mark I containment system. On this basis, the staff has further concluded that application of the HEM model for the DBA containment response analysis is acceptable. A detailed evaluation of the HEM model has been issued by the staff (Ref. 12) and is contained in a revision to the GE topical report (Ref. 13).

The staff has determined that the application of HEM to calculate the mass and energy release rates from the primary system will not necessarily provide conservatively high release rates for the IBA and the SBA due to the potential break configurations. However, the purpose of the IBA and SBA is to provide a spectrum of event combinations where the primary loading conditions are steam condensation and SRV discharge loads. The primary loading condition affected by the HEM model is the containment pressure and temperature response. For the IBA and SBA, the containment response is of secondary importance to the loading condition, and the primary loading conditions are calculated independently of the results of the containment response analysis. On this basis, application of the HEM model for the IBA and SBA event combinations is acceptable.

### 3.3 Vent System Pressurization and Thrust Loads

Reaction loads occur on the vent system (main vent, vent header, and downcomers) following a LOCA because of pressure imbalances between the increasing pressure in the event system and in the surrounding torus airspace and because of forces resulting from changes in flow direction. The load definition procedures proposed in Section 4.2 of the LDR are derived from the pressure and flow transients calculated by the GE containment response analysis. These loads are calculated only for the DBA, which provides a more rapid pressurization rate and higher mass flow rate than either the IBA or SBA. Horizontal and vertical force components are calculated at each location of a change in flow direction.

Two different sets of equations to calculate the vent system loads are provided in the LDR. The first set, intended for use up to and including the time of downcomer clearing, assumes the entire vent system (excluding the portion of the downcomers containing water) is at drywell pressure.



In order to determine the downcomer clearing time, the GE containment response model incorporates a conservative virtual mass, equivalent to an extended downcomer length of 2.25 feet for a 2-foot diameter downcomer. This was based on the Bodega Bay test facility (Ref. 9) which has a relatively small ratio of pool area to vent area. Hydrodynamic theory indicates the virtual mass should decrease with an increasing pool area to vent area ratio. A large virtual mass is conservative, since it leads to a later clearing time, with a correspondingly larger instantaneous difference between drywell and torus pressures. Comparisons of the predicted downcomer clearing time with measured values for the Humboldt Bay test facility show that the predicted clearing times are conservative (i.e., later), although the differences are small.

The second set of equations is applied starting at 200 milliseconds after downcomer clearing, the set accounts for unbalanced pressure area terms and forces arising from changes in the direction of the flow momentum vector. The instantaneous vent system flow rate is calculated by the GE containment response analysis assuming homogeneous flow from the drywell. The instantaneous pressures in the main vent, ring header, and downcomers are calculated assuming a conservative distribution of the flow resistance in the vent system. The 200-millisecond interval after downcomer clearing is intended to be a relatively early estimate of the time of bubble breakthrough. While the LDR considers this conservative, the method of analysis does not include any water inertia effects after vent clearing, so that the assumed bubble breakthrough time serves only as an initial time for applying the steady-flow equations.

Between downcomer clearing and bubble breakthrough, the LDR proposed method of calculation assumes a linear variation in vent system thrust loads. Based on a review of the scaled pool swell data (Ref. 14), this procedure appears adequate for cases with zero initial drywell-torus pressure differential, since measured downcomer internal pressures drop rapidly after downcomer clearing. This method for coupling the two sets of equations does not appear adequate, however, for plants with a large initial drywell-torus pressure differential. For these cases, downcomer clearing occurs at earlier times and at lower drywell pressure values than for plants with zero pressure differential, and the difference between vent system internal pressure and torus airspace pressure can increase after

vent clearing. This effect has been observed in several of the scaled pool swell tests (Ref. 14). Also, it should be noted that when the drop in internal pressure after downcomer clearing occurs, it starts at the downcomer end of the vent system. We would expect the vent header and main vent to approach steady-state values at even later times. The delayed drop in vent system internal pressures can result in peak thrust loads on the vent system which exceed those at the time of downcomer clearing and subsequent bubble breakthrough. Consequently, the staff has required (Appendix A, Section 2.2) that the downcomer clearing transition time for plants that use an initial drywell-torus pressure differential be calculated assuming zero pressure differential. For those plants with an initial pressure differential, the criteria discussed above regarding the time of downcomer clearing will assure a conservative transition to the steady-flow regime.

Based on the assessment above, the staff has concluded that the proposed method, as modified by the acceptance criteria in Appendix A, will provide a conservative estimate of the vent system pressurization and thrust loads and is, therefore, acceptable.

#### 3.4 Torus Pool Swell Pressure Loads

In the event of a postulated design-basis accident (DBA), as described in Section 2.2.1, the drywell and vent system would be pressurized, causing the water leg initially in the downcomers to be accelerated downward into the suppression pool. Immediately following downcomer clearing, air bubbles form at the exit of the downcomers. As these bubbles form, their presence is felt on the submerged portion of the torus walls as an increase in pressure. Consequently, the torus will experience a dynamic net downward load as the bubble pressure (which at the time of the downcomer clearing is approximately equal to drywell pressure) is transmitted through the suppression pool. At that time, the torus airspace has not yet sensed the effects of the transient. The air bubbles continue to expand and decompress, causing a ligament of solid water above the bubbles to be accelerated upward. As the water slug continues to rise, the wetwell airspace volume above the water in the torus is compressed, resulting in a dynamic net upward load on the torus. The pool swell continues until there is a breakup of the water ligament, and direct communication between the bubble and airspace is achieved.

From the testing done during the STP, the phenomena described above have been shown to be sensitive to various plant parameters, such as downcomer submergence and drywell-to-torus differential pressure (Section 3.12.7). Consequently, the Mark I Owners Group devised a testing program for the LTP whereby the pool swell loads could be assessed on a plant-specific basis. The Quarter-Scale Test Facility (QSTF) was used for this task. The QSTF was designed so that the torus sector width, drywell volume, downcomer system configuration, vent system resistance, vent header deflector, and other test conditions could be varied on a plant-specific basis (Ref. 14). The data obtained from the QSTF plant-unique tests serve as the principal source for the pool swell load specifications for the LTP. Although the QSTF is nominally one-quarter scale, the plant-specific scaling factor will vary slightly based on a fixed torus diameter, with all other geometrical parameters scaled accordingly.

The scaling relationships for the pool swell tests were developed during the STP based on the method of similitude. This technique involved the formulation of the governing conservation equations, boundary conditions, and initial conditions for each of three regions, i.e., an air bubble in a pool, the pool water, and a trapped air space above the pool. The equations and boundary conditions are then nondimensionalized, which results in similarity parameters appearing as coefficients. The significant scaling parameters, selected on the basis of their relative order of magnitude, are retained from the analysis. The following scaling relationships evolved for typical Mark I conditions:

$$p_f = p_s (L_f/L_s)$$

$$t_f = t_s (L_f/L_s)^{1/2}$$

$$(\dot{m}h)_f = (\dot{m}h)_s (L_f/L_s)^{7/2}$$

where the subscripts f and s refer to the full-scale and small-scale systems, respectively, and

p = pressure

t = time

$\dot{m}$  = mass flow rate into the bubble

h = enthalpy of the mass flow

L = characteristic dimension (e.g., torus diameter).

These general scaling relationships for pool swell were confirmed by comparisons of the 1/12-scale test results from the STP and QSTF test results for matched test conditions (Ref. 15) within the uncertainty limits of the test data. In addition, independent research studies performed for the NRC by the Massachusetts Institute of Technology (Ref. 16), the Lawrence Livermore Laboratory (Ref. 17), and the University of California at Los Angeles (Ref. 18) have also confirmed these general pool swell scaling relationships. However, during our review of the pool swell data base, we found that errors can be introduced by the method used to establish the enthalpy flow into the bubble ( $\dot{m}h$ ).

The enthalpy flow scaling is an approximation, because exact scaling of the flow into the bubble cannot be practically achieved in the small-scale models. The method commonly used to scale the enthalpy flow involves the use of orifices to increase the flow resistance. Through comparisons of data from the various pool swell tests (Table 3.4-1), the relative location of the orifices and the techniques used to establish the 3-D downcomer orifice size distribution were found to have a significant effect on the net torus vertical pressure load. This effect has been considered in the QSTF plant-unique tests, and the uncertainties associated with enthalpy flow scaling have been included in our review of those tests (described in Section 3.4.1).

Another uncertainty associated with flow scaling concerns the effects of compressibility of the flowing medium. Acoustic waves travel back and forth through the vent system during the downcomer clearing process. These waves cannot be accurately scaled, and their presence is further masked in the scaled pool swell tests by the flow orifices. The effect of these waves is to cause an increase or decrease in the pressure at the downcomer exit at the time of downcomer clearing. Based on preliminary calculations performed by EPRI and GE, the staff has determined that these effects are small in comparison to other uncertainties identified in Section 3.4.1. On this basis, the staff has concluded that implementation of the LTP should continue while the Mark I Owners Group continues its assessment of compressibility effects. As described in Appendix A, Section 2.5, the staff has required that the Mark I Owners Group complete this assessment and justify the adequacy of the affected load specifications. The staff will report the results of its evaluation in a supplement to this report.

Table 3.4-1 Mark I Pool Swell Test Programs

| Facility  | Scale  | Sector  | Number of Tests |
|-----------|--------|---------|-----------------|
| GE (STP)  | 1/12   | 2-D     | 110             |
| GE (LTP)  | 1/4*   | 2-D     | 324             |
| EPRI/SRI  | 1/11.7 | 3-D     | 68              |
| Livermore | 1/5    | 2-D/3-D | 27              |

\*Scale varies slightly for plant-unique tests.

#### 3.4.1 Net Torus Vertical Pressure Load

The net torus vertical pressure load is equal in magnitude to the net dynamic force acting on the torus divided by the projected torus cross-sectional area. A typical vertical load pressure transient is shown in Figure 3.4-1.

As previously discussed, the net torus vertical load specifications proposed by the Mark I Owners Group for the LTP are derived from a series of QSTF plant-specific tests (Ref. 14) (with a minimum of four test runs per plant design). The Mark I Owners Group further proposed that the mean (average) loads from these tests should be used for the LTP structural assessment.

The testing procedures adopted in the plant-unique test program incorporated methods to ensure that a conservative loading condition was obtained. The more significant items include:

- (1) The calculated drywell pressure history was used as a lower bound for the test drywell pressurization history.
- (2) QSTF tests were performed at the minimum plant operating  $\Delta p$  and maximum downcomer submergence for the plant.

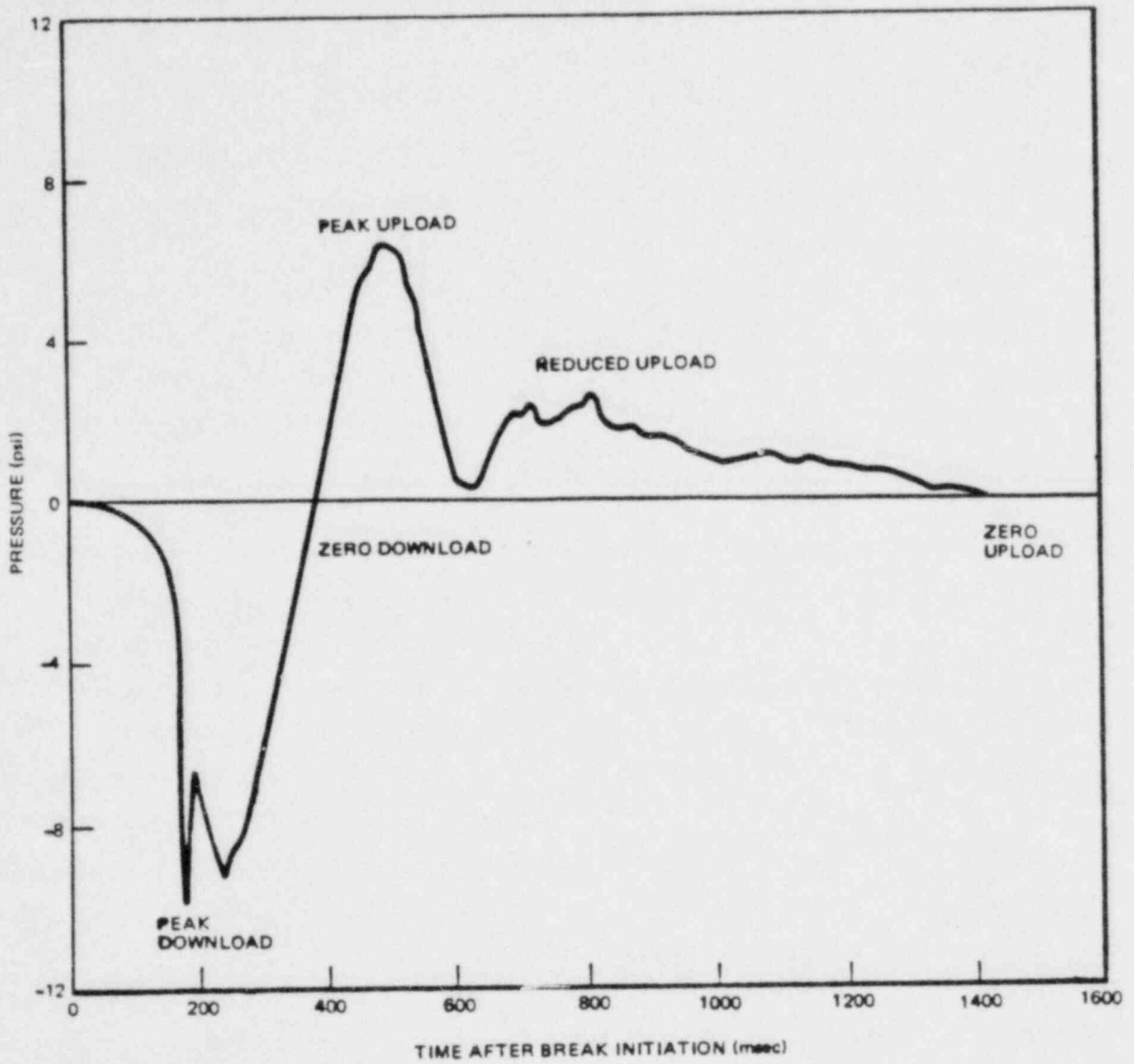


Figure 3.4-1 Mark I torus vertical pressure transient.

- (3) The vent flow resistance was decreased to account for the fact that the initial air temperature in the drywell for the QSTF tests was 70° F, whereas the maximum plant drywell operating temperature is 135° F.

A margin of conservatism which will vary on a plant-specific basis is inherent in the above items, especially in the test drywell pressurization history.

On the basis of the staff review, the proposed load definition methods presented in Section 4.3.1 of the LDR are unacceptable in their present form. The areas in which the staff finds the procedures deficient concern the use of the mean values for the load specification and the data base used to assess the potential for three-dimensional pool swell effects.

Based on a number of conservatisms inherent in the load definition, the direct use of the mean values determined in the QSTF has been deemed appropriate in the LDR. Although that there are conservatisms in the load definition, the use of the mean loading function without taking into account the statistical variance of the measurements is not acceptable. This conclusion was reached because the conservatisms are plant-specific and they have not been quantified. Therefore, the acceptance criteria (Appendix A, Section 2.3) includes margins to be applied to the net vertical pressure loads, which are expressed in terms of pounds-force at the scaled test condition. These margins were derived from a statistical analysis of the QSTF data base (Ref. 19), and they represent an estimate of the standard deviation in the peak loads. For the downward pressure loads, the variance was found to be a function of the load magnitude and has been expressed as a quadratic function of the peak downward load (i.e., 0.00002 times the square of the QSTF mean peak downward load). For the upward pressure loads, the variance was found to be approximately linear with load magnitude; therefore, a constant percentage margin has been specified (i.e., 6.5 percent). An additional margin on the upward load has been specified for the reasons described below.

The QSTF is a two-dimensional (2-D) test facility; i.e., it consists of a single pair of downcomers with a cell width equal to the average downcomer spacing.

However, in the actual plant the downcomers are irregularly spaced along the axis of the torus. In order to assess three-dimensional (3-D) pool swell effects, the Mark I Owners Group sponsored a separate testing program, which was conducted by the Electric Power Research Institute (EPRI). The EPRI test facility was a 1/12-scale, straight cylinder equivalent of a 90° torus sector, containing 2 main vents and 12 downcomer pairs prototypically spaced (Ref. 20). The Mark I Owners Group assessed 3-D effects by directly comparing QSTF data and EPRI data for similar test conditions (Ref. 21). The QSTF test series and the EPRI facility both modelled the Browns Ferry plant geometry, and the comparisons were made at conditions of full  $\Delta p$  and 3-foot, 4-inch submergence. On the basis of its review, the staff has concluded the QSTF/EPRI data comparison does not adequately assess the potential for 3-D effects. This conclusion was based principally on the following observations:

- (1) The EPRI tests used in the comparison were conducted at higher values of flow resistance than were the QSTF tests. As a result, the EPRI uploads are lower than would have been obtained if the flow resistances were properly matched.
- (2) The Browns Ferry geometry is not prototypical of the majority of Mark I plants. In fact, the 45° downcomer configuration has been found to cause early breakthrough, thereby reducing maximum torus airspace compression.
- (3) The data used for the comparison were obtained using orifices located in the downcomers. From its studies, the staff has concluded that an exaggerated pool surface curvature resulted from the use of downcomer orifices in these tests.
- (4) The use of full  $\Delta p$  and reduced submergence as test conditions for the QSTF/EPRI comparison tends to minimize pool swell effects. Thus, the staff would not expect to bound a 3-D effect at these conditions.

To establish bounds on the potential for the 3-D pool swell effects, the staff turned to a confirmatory data base provided by the Lawrence Livermore Laboratory (LLL) ( Ref. 17). The LLL test program was conducted for the NRC to provide



confirmatory pool swell test data. The test facility consisted of 1/5-scale 90° (3-D) and 7.5° (2-D) torus sectors, modeled after the Peach Bottom plant geometry. The test data from this facility have generally confirmed the basic hydrodynamic phenomena observed in the testing programs conducted by the Mark I Owners Group; however, the peak upward pressure loads in the 3-D sector were consistently higher than those in the 2-D sector.

Based on its review of the LLL test data, the staff has found that a part of the difference is the result of a mismatch in the modeling of the 3-D and 2-D sectors. The mismatch resulted from differences in the sizing and location of the flow-scaling orifices in the two LLL sectors. The staff concluded that the location of the flow scaling orifices in the main vents, coupled with the effects of the tested geometry and initial conditions, provided a conservative assessment of the potential 3-D pool swell effects. However, the staff has performed an analysis of the LLL facility geometry in order to extract the differences that result from the mismatch in flow scaling.

A one-dimensional transient pool swell analysis was performed for both the Livermore 2-D and 3-D sectors. The system as modeled consisted of drywell volume, vent line volumes upstream and downstream of the orifice, header volume, downcomer volume, liquid slug, and torus airspace volume. Maximum values of upload pressure were determined by computer analysis for both the 3-D and 2-D sectors for initial drywell pressurization rates ranging from 40 to 80 psi per second. The results of these calculations have demonstrated that the LLL sectors were mismatched as a result of differences in vent system capacitance (volume) and flow resistance. The effect on peak upload pressures varied from 3 percent to 9 percent over the range of pressurization rates considered in the study. After adjusting the LLL experimentally observed upload ratios to account for these findings, the staff was able to estimate a margin to bound the uncertainties arising from the comparison of all the two-dimensional and three-dimensional upload test data. For completeness, it should be stated here that similar download comparisons were made and were found to exhibit excellent agreement. Therefore, no additional margin is necessary to account for the possibility of a 3-D/2-D effect on the torus downloads obtained in the QSTF.

Based on this assessment, the staff has concluded that a margin of 15 percent applied to upward vertical pressure loads derived from a 2-D testing program will provide a conservative estimate of the upward loads resulting from a design-basis LOCA. This margin, coupled with the margins for uncertainty previously described, forms the requirements presented in Appendix A, Section 2.3.

As previously discussed, the QSTF tests were conservatively performed; the degree of conservatism could be established on a plant-specific basis. To avoid penalizing specific plants whose tests were overly conservative, the staff requirements permit the margins specified above to be reduced or omitted where offsetting conservatisms in the tested conditions can be quantified. These conservatisms are to be established using sensitivity parameters from the generic series of QSTF tests (Ref. 22). Conservatisms will be retained in the load specification by using minimum parameter deviations from the nominal plant conditions.

For those plants that propose  $\Delta p$  operation for the LTP, an additional structural analysis is required assuming a loss of the  $\Delta p$ , as described in Sections 3.12.7 and 4.3.3. For this analysis, the staff has concluded that a single plant-specific QSTF test run is sufficient for the purpose of the analysis, provided that the downward and upward loads are increased by the margins established for the base-case analysis at the normal plant operating conditions.

During the STP, an issue relating to the net torus vertical pressure loads was identified which concerned an anomaly in the downward load observed in the 1/12-scale test results. The peak downward loads from the January 1976 1/12-scale test series were approximately 33 percent higher than those from the December 1975 test series for similar test conditions. To ascertain the cause of this anomaly, the Mark I Owners Group conducted an additional 1/12-scale test program as part of the LTP (Ref. 23). From these tests, they determined that the load increase was caused by a flexing of the test facility sidewalls. A similar testing program was conducted with the QSTF (Ref. 24), from which a method of reinforcing the sidewalls of the test facility was devised.

This reinforcing was used in all of the QSTF plant-unique tests for the LTP. The staff concurs with the Mark I Owners Group assessment and corrective action and concludes that this issue has been adequately resolved.

In summary, the staff has concluded that the application of the QSTF plant-specific tests, as described in Section 4.3.1 of the LDR and as modified by the margins set forth in Appendix A, Section 2.3, will provide conservative estimates of the net torus vertical pressure loads resulting from a design-basis LOCA.

#### 3.4.2 Torus Pressure Load Distribution

The spatial distribution of the pressure on the torus shell during pool swell, as proposed in Section 4.3.2 of the LDR, consists of the following elements:

- (1) An average submerged-pressure history on the torus shell derived from the QSTF plant-specific tests.
- (2) A table of multipliers which account for the variation of the average submerged transient pressure at different positions on the shell, derived from the EPRI 1/12-scale 3-dimensional tests for axial variation and QSTF tests for circumferential variation.
- (3) A pressure transient in the torus airspace region, derived from the QSTF plant-specific tests.

The average submerged-pressure transient is defined as the net force applied to the submerged portion of the torus divided by the torus horizontal cross-sectional area. The average submerged-pressure history and torus airspace-pressure history are derived from the torus shell pressure transients measured in the QSTF plant-specific test series. In all of the transients, the initial conditions have been extracted so that only the dynamic portion of the transients is presented. Therefore, care must be taken to assure that the appropriate plant-specific values of initial torus airspace pressure and hydrostatic head are incorporated into the pressure definition. The transients which correspond to normal plant operating conditions represent means (averages) of the multiple QSTF tests performed at this condition.

In order to account for the spatial variation of the average submerged pressure, multipliers are specified at pertinent times throughout the pool swell transient at various longitudinal and azimuthal locations on the torus. The multipliers presented in Table 4.3.2-1 of the LDR are given as a function of time and a nondimensional position on the torus shell. Since the downcomer spacing is approximately the same in all Mark I plants, it has been assumed in the LDR that the multipliers are applicable to all plants. The variations in the torus circumferential or azimuthal direction is based on an arithmetic mean of 44 tests performed in QSTF. The multipliers are specified at 11 angular positions around the torus circumference, ranging from bottom dead center to 90° above bottom dead center, with symmetry being assumed. The longitudinal pressure multipliers were obtained in a similar manner from the pressure measurements in a unit cell of the EPRI 1/12-scale model (Ref. 20). The unit cell extends from the main vent centerline plane to the adjacent nonvent bay midplane. The arithmetic mean of 24 EPRI tests was used to obtain the multipliers for each location at the times of interest during the pool swell. At points on the torus shell between those where the multipliers are defined, linear interpolation has been proposed.

As a result of its review of the applicable pool swell test data, the staff has found that the proposed methods should provide a reasonable definition of the distribution. However, to incorporate a margin for uncertainty, the staff requirements (Appendix A, Section 2.4) specify that the local pressure distribution is to be increased by the pressure-equivalent margins specified for the net torus vertical pressure load, so that the margin on the downward load is applied to the average submerged pressure transient and the margin on the upward load is applied to the torus airspace transient. The staff has concluded that this technique will provide a reasonably conservative torus local pressure definition, especially since the torus structural response is more sensitive to the total applied load, rather than the load distribution.

### 3.5 Pool Swell Impact and Drag Loads

Impact loads are a consequence of pool swell. As the suppression pool surface rises, any structures or components located above the pool (but lower than the

maximum elevation of the pool surface achieved during pool swell) will be subjected to water impact loads followed by a drag load until the upward motion of the pool stops. The principal structures which experience impact and drag loads during pool swell in a Mark I containment system are the vent system, the vent header deflector (if installed), and miscellaneous structural elements (e.g., pipes, beams, and gratings). In general, the load definition techniques proposed in the LDR are based on data from the QSTF plant-specific test series. The specific load definition techniques for each of the principal structural groups described above are presented in the evaluations below.

The impact and drag loading transient consists of an initial impact spike, which is caused by water striking and wetting the lower surface of the structure, followed by a transition to a drag force, which is composed of a "steady-flow drag" component and an "unsteady-flow drag" component. (The latter is a result of the acceleration or deceleration of the flow field around the structure.) The specific loading transient is a function of the geometry of the affected structure and the velocity and curvature of the pool surface at the time of impact.

### 3.5.1 Vent System Impact and Drag

#### 3.5.1.1 Vent header

The LDR specification of the vent header impact load is based directly on QSTF data. The load definition consists of:

- (1) the experimental data of local vent header pressure in each of the Mark I plants obtained from the QSTF plant-unique tests;
- (2) the specification, for each Mark I plant, of the pressure inside the vent header relative to that in the torus airspace at the time of water impact on the vent header, determined from the QSTF plant-unique tests; and
- (3) the plant-unique header impact timing, i.e., longitudinal and circumferential time delays, based on the EPRI three-dimensional pool swell tests and the QSTF generic test series, respectively.

The load specification is presented in terms of the differential pressure acting on the shell of the vent header, as measured in the QSTF plant-unique tests. The staff has concluded that the QSTF tests will provide a reasonably conservative estimate of this loading function and are, therefore, acceptable. However, the longitudinal impact timing defined in the LDR may not be sufficiently conservative.

The longitudinal variation in the vent header impact load proposed in the LDR is based on an average of the header impact timing observed in the EPRI main-vent-orifice and downcomer-orifice three-dimensional pool swell tests. The orifices were introduced to provide the proper flow scaling (as described in Section 3.4). The longitudinal header impact timing observed in the main-vent-orifice and downcomer-orifice tests were substantially different. In addition, the downcomer orifices in the EPRI tests were varied in size from downcomer to downcomer to match the full-scale flow distribution which would result from steady-flow conditions with a uniform backpressure.

Additional EPRI tests were conducted with split orifices; i.e., with half the resistance in the main vent and half in the downcomers. A similar downcomer orifice size distribution was used. The header impact timing observed in these tests was very close to that observed in the downcomer-orifice tests. From these data, the Mark I Owners Group concluded that the average of the impact timing from the main-vent-orifice and downcomer-orifice tests will provide a conservative assessment of the loading condition, because the main vent orifices allowed the flow through the downcomers to equalize, causing an atypically flat pool surface.

Based on its review of the test data, the staff has determined that the assumptions used to establish the downcomer orifice size distribution may not have resulted in a sufficiently prototypical flow distribution during the transient flow conditions that actually prevailed. From analyses of the flow resistance distribution in the downcomer-orifice and split-orifice tests (as compared to the resistance distribution in a full-scale plant), the staff has concluded that the flow distribution achieved in the main-vent-orifice tests may have been closer to the prototypical conditions. Nevertheless, the main-vent-orifice tests were certainly conservative with respect to the longitudinal header impact timing

(i.e., longitudinal variation of the pool surface velocity as compared to the average).

Consequently, the staff has required that the longitudinal variation in the impact loads be derived from the EPRI "main vent orifice" tests, as described in Appendix A, Section 2.1. The use of these test data in a manner consistent with that proposed by the Mark I Owners Group will provide sufficiently conservative loads to offset any uncertainty associated with flow distribution effects on the pool swell longitudinal variation.

#### 3.5.1.2 Downcomers

The LDR specifies the impact load on the projected surface of the downcomers as 8 psid to be applied uniformly over the bottom 50° of the angled portion of the downcomer, starting when the rising pool reaches the lower end of the angled portion and ending at the time of maximum pool swell height. The pressure is to be applied perpendicular to the local downcomer surface. This specification is based on plant-specific measurements in the QSTF facility and bounds the loads observed for all plants.

The staff finds the proposed load specification acceptable, with the proviso that the structural analysis of the downcomer shall be dynamic, accounting for the approximate virtual mass of the water near the submerged parts of the downcomer, or a dynamic load factor of 2 shall be applied.

#### 3.5.1.3 Main Vent

The impact load specification for the main vent proposed in the LDR is based on the impact and drag load specification for general cylindrical structures, as described in Section 3.5.3. In general, this approach is acceptable. However, the staff has developed specific requirements for the main vent impact loads (Appendix A, Section 2.6.3) which will ensure a sufficient level of detail in the loading transient and will provide consistency with the impact loads for other cylindrical structures. The staff has concluded that the proposed procedures, as modified by the criteria in Appendix A, will provide a conservative estimate of the transient impact load on the main vent.

### 3.5.2 Vent Header Deflector Impact and Drag

In some Mark I containment systems, deflectors will be installed below the vent header to shield the header from the rising pool surface and reduce the impact load on the header itself. Four deflector designs are under consideration; they are identified as Types 1 to 4 in Figure 3.5-1. Two methods to define the impact and drag loads on the deflector were proposed in the LDR and are evaluated separately below. When a vent header deflector is used, there is still an impact and drag loading condition on the vent header. The header impact and drag loads for either of the deflector load definition techniques described below are defined by the methods described in Section 3.5.1.

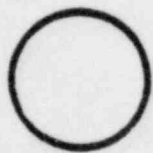
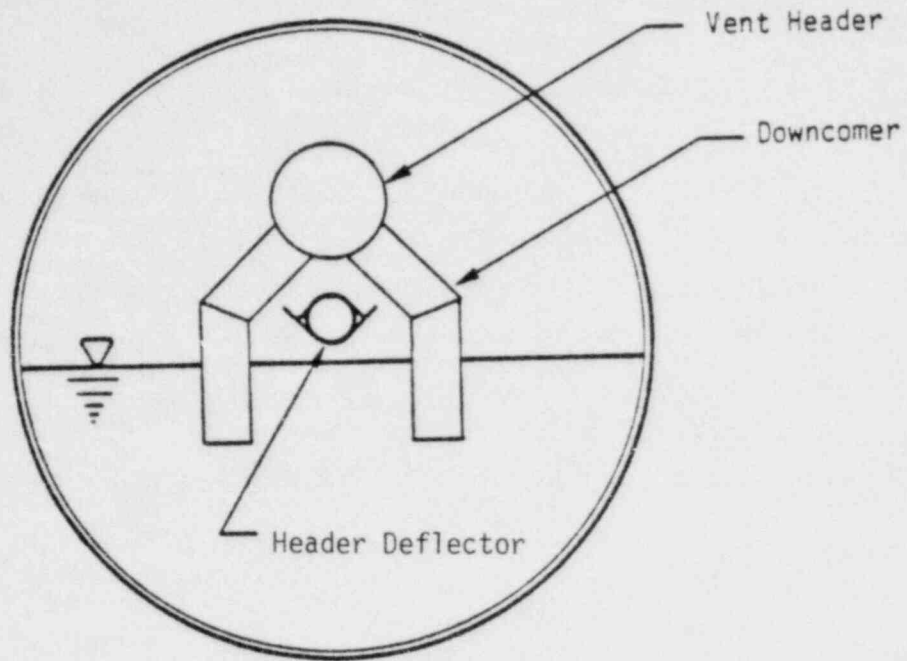
#### 3.5.2.1 Alternative A

The LDR has proposed that specific Mark I plants may choose to use scaled-up deflector impact and drag force histories from the QSTF plant-unique tests. This technique is applicable only where deflector force transients were measured in the QSTF plant-specific tests.

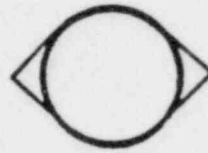
On the basis of its review of the scaling relationships (discussed in Section 3.4) and the QSTF plant-unique test series, the staff has concluded that this approach will provide a conservative estimate of the deflector force transients, with the following corrections and clarifications:

- (1) The QSTF deflector load measurement does not always respond fast enough to resolve the initial impact pressure spike for the deflector Types 1-3. Consequently, the loading transient must be adjusted to include the empirical vertical force history of the spike shown in Figure 2.10-1 of Appendix A. This empirical force history has been derived from impact tests of cylinders conducted by EPRI (Ref. 35). Based on our review of impact forces on wedges, we conclude that this adjustment is not necessary for the Type 4 deflector.
- (2) The QSTF plant-unique loads must be adjusted to account for the effects of impact time delays and pool swell velocity and acceleration differences

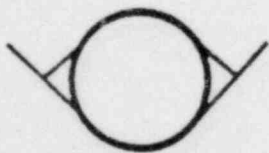




Type 1 - Pipe



Type 2 - Pipe with angles



Type 3 - Pipe with tees



Type 4 - Wedge

Figure 3.5-1 Mark I vent-header deflector designs.

which result from the uneven spacing of the downcomer pairs. The longitudinal variation in the deflector force transient (i.e., sweep time) must

be based on the EPRI main-vent-orifice tests, for the reasons described in Section 3.5.1.

- (3) In applying the load to the deflector, the inertia due to the added mass of water impacting the deflector must be accounted for in the structural assessment of the deflector and its supports.

These corrections and clarifications are set forth as requirements in Section 2.10.1 of Appendix A.

#### 3.5.2.2 Alternative B

For those Mark I plants for which the vent header deflector has not been tested via plant-specific QSTF simulations, the LDR specifies that a semi-empirical approach can be taken, where the load is a superposition of (1) an impact transient, (2) a "steady" drag, and (3) an acceleration drag (Ref. 26). The LDR specifies certain empirical expressions for each of the three contributions. Both the local, instantaneous pool velocity and pool acceleration are needed to evaluate the empirical expressions for the load and are to be inferred from plant-specific QSTF tests.

The staff finds the proposed semi-empirical load definition technique unacceptable because the "steady" drag contribution for the cylindrical (Type 1) deflector is not conservative with respect to the applicable test data and because an appropriate force transient for the wedge-shaped parts of deflector Types 2-4 has not been specified. The Mark I Owners Group has concluded that the proposed specification is validated by the fact that it conservatively predicts the vent header deflector loads for those cases that have been tested in the QSTF. The staff does not accept this claim because (1) comparisons have been done only for some cases, (2) the degree of the conservatism in the comparisons varies from case to case, and (3) the source of the conservatism is not clear. Because all of the essential ingredients in the proposed analysis technique have not

been established to be correct or conservative, the staff is not confident that the model will yield acceptable results in all cases.

Consequently, the staff has specified requirements (Appendix A, Section 2.10.2) that modify the proposed load definition technique to assure that a conservative estimate of the deflector force transient will be achieved in all cases. These requirements principally involve a redefinition of the drag coefficient expressed as a dimensionless force-time history (as shown in Figures 2.10-2 through 2.10-5 in Appendix A). These figures have been modified from those originally transmitted to the Mark I Owners Group, based on a clarification of the geometries of the deflector designs and a reinterpretation of the data base for the drag coefficient following impact for cylindrical structures. For deflector designs that do not exactly match those shown in Figures 2.10-3 through 2.10-5 in Appendix A, but which differ slightly in either the wedge angle or the ratio  $w/d$ , the impact and steady drag correlation should be based on Wagner's force history for a wedge (Ref. 27) and on the final steady-state drag, following the basic method described above.

The initial impact transient for the cylindrical portions of deflector Types 1-3 (as shown in Figures 2.10-2 through 2.10-4 of Appendix A) has been derived from EPRI impact data (Ref. 25). The steady drag component for a cylinder (Appendix A, Figure 2.10-2b) is based on the estimated values at which the EPRI impact load measurements leveled out. In Appendix A, Figure 2.10-2b, only the large-cylinder EPRI data have been used, because the small-cylinder data were less complete.

Also, the assumption is made that the drag is largely independent of Reynolds number (at supercritical Reynolds numbers); hence, the dimensionless drag depends only on Froude number. This correlation further recognizes that, in the limit of large Froude number, the drag for this case, with an open wake at torus air-space pressure, must approach the value it would have in a cavitating flow with a cavitation number of zero,  $C_D = 0.5$  (Ref. 28).

Figure 2.10-5 of Appendix A shows the impact transient for the Type 4 deflector, which is a simple wedge with a  $45^\circ$  deadrise angle. The impact transients of wedges have been studied extensively in order to understand the loads on seaplane

floats during landing. The first analysis was presented by Von Karman in 1929 (Ref. 29). Von Karman used a simple estimate for the virtual mass of the water during impact and obtained a relation which, for the case of constant-velocity vertical penetration, may be expressed as

$$F = \pi \rho V^2 (\cot \beta)^x$$

where

$F$  = instantaneous vertically upward force (lbf)

$\rho$  = water density (slug/ft<sup>3</sup>)

$V$  = water velocity (ft/sec)

$\beta$  = angle of wedge surfaces with respect to horizontal (deadrise angle)

and

$$x = V t \cot \beta$$

is the instantaneous elevation of the water surface, far from the wedge, relative to the wedge tip, with  $t$  the time from the instant of first impact on the wedge tip.

Soon thereafter, Wagner (Ref. 30) developed his first rough approximation for  $F$ , which differed from the equation for  $F$  above only in that it was higher by a factor of  $(\pi/2)^2$ . By 1932, however, Wagner had published a much more careful and elaborate analysis (Ref. 27), and on this basis he suggested the formula

$$F = \frac{\pi^3}{4} \rho V^2 \left[ \frac{\pi}{2\beta} - 1 \right]^2 \left[ \frac{2 \tan \beta}{\pi} \right]^2 (\cot \beta)^x$$

where  $x$  is given as above and  $\beta$  is in radians. This relation, which is not an analytic solution for  $F$ , was merely suggested by Wagner as a correlation equation which accurately predicted both his analytical solutions for  $\beta \rightarrow 0$  and  $\beta \rightarrow \pi/2$ , as well as his numerical solution for one point in between, at  $\beta = 18^\circ$ . Note that at  $\beta = 45^\circ$ , the case of interest in our present context, both Von Karman's and Wagner's relations for  $F$  yield exactly the same results.

Wagner's expression has received confirmation in the almost five decades since its publication, both from experiments (provided  $\beta$  is not too close to 0), as

well as from other theoretical studies (Refs. 31,32,33,34,35). Consequently, the force-time histories shown in Figures 2.10-3 through 2.10-5 of Appendix A are based on the assumption that Wagner's expression applies to the  $45^\circ$  deadrise angle wedges, with  $x$  measured from the point of the wedge tip (projected or actual) up to the time the undisturbed water surface would reach the top of the wedge. In Figures 2.10-3 and 2.10-4 in Appendix A, which apply to deflectors with a circular leading edge, the cylinder impact transient of Figure 2.10-1, based on the EPRI data previously described, has been added. Furthermore, it has been assumed that after the water level passes the elevation of the top of the wedge, the force drops, in a time corresponding to half the time it takes the water to envelop the wedge, to a steady-drag value which corresponds to the case of a  $45^\circ$  half-angle wedge in a flow with cavitation number equal to zero (Ref. 30). The latter flow field is the same, at least at large Froude numbers, as when there is an open wake cavity. The force transients shown in Figures 2.10-3 through 2.10-5 should be accurate (in the absence of pool acceleration) at the earlier times, but they are merely conservative estimates near the times when the water level approaches and passes the level of the top of the wedge shape. The total impulse of the impact transient is expected to be conservative, since it exceeds, somewhat, the impulse associated with an impact on a flat beam of the same width as the wedge.

For deflector designs that do not exactly match those shown in Figures 2.10-3 through 2.10-5 in Appendix A but differ slightly in either the wedge angle or the ratio  $w/d$ , the impact and steady drag correlation should be based on Wagner's force history for a wedge (Ref. 27) and on the final steady-state drag, following the basic method described above.

The staff has concluded that the force-time histories specified in Section 2.10 of Appendix A, coupled with the proposed method for defining the pool velocity from the QSTF tests, will assure a conservative estimate of the deflector impact and drag load transients.

### 3.5.3 Impact and Drag on Other Internal Structures

"Other structures," in the present context, are defined as all structures above the initial suppression pool water level, exclusive of the vent system. Typically,

these structures are cylindrical pipes or structural beams with a flat surface toward the pool. In addition, gratings may be located above the pool. The LDR presents impact load definition techniques for (1) cylindrical pipes, (2) elongated structures whose cross-section is not circular (e.g., I-beams), and (3) gratings. The water impact loads on these commonly encountered structural shapes are discussed separately in the following sections.

### 3.5.3.1 Cylindrical Structures

The LDR specifies the impact loading on cylinders in the following manner:

(1) the impact velocity at the elevation in question is obtained from QSTF tests (Ref. 14) with adjustment for longitudinal position along the torus derived from the EPRI 3-D test results (Ref. 20); (2) the impulse of impact is calculated from

$$I = 0.2 M_h V_n / g_c$$

where  $I$  is the impact impulse (lbf-sec),  $M_h$  is the hydrodynamic mass of the cylinder under fully submerged conditions (lbm),  $V_n$  is the impact velocity (ft/sec), and  $g_c$  is the gravitational constant (lbm-ft/lbf-sec<sup>2</sup>); (3) the duration of impact is taken equal to the time required for the pool to submerge a 50° included angle of the cylinder; (4) the impact load transient is assumed to be parabolic in time; and (5) the drag following impact is based on a standard drag coefficient.

As a result of its review of the proposed analysis techniques, the staff has concluded that, although the approach is generally reasonable, the specific assumptions made are not consistent with applicable test data. The deficiencies that have been identified are the following: (1) the parabolic pulse shape is not realistic for cylinders, as evidenced by more recent impact data (Ref. 25); (2) the empirical factor of 0.2 in the impulse equation is based on limited data (Ref. 36) and does not bound the data from other cylinder impact tests (Refs. 25,37); and (3) the "standard" fully submerged drag coefficient is not appropriate for cylinder drag immediately after impact.

The staff's acceptance criteria, as defined in Section 2.7.1 of Appendix A, make extensive use of the recently generated data for rigid cylinder impact (Ref. 35). We believe that this data base is the best available for cylinder impact under Mark I LOCA conditions. This judgment is based on the detailed nature of the measurements and on the range of test conditions used: impact velocities from 7.6 to 24.2 ft/sec and diameters of 8.25 and 17 inches.

Test data developed by EPRI (Ref. 25) generally exhibit an impact pressure transient like that shown in Figure 3.5-2. With the shape of the impact pulse so defined, there are three parameters that characterize the impact pressure transient: (1) maximum pressure, (2) pulse duration, and (3) impulse.

In reality, only two of these are independent; the third is readily calculated from the other two. In reviewing the available data for cylinders, it was concluded that the maximum pressure and the impulse are the more reliably known parameters. This leaves the pulse duration as the derived quantity.

In developing the staff's criteria for impact loads on cylinders, we made use of an assessment of the rigid cylinder impact data, which found that the maximum pressure, over the whole range of test conditions, correlates well with the dynamic pressure as

$$P_{\max} = 7.0 \left[ \frac{\frac{1}{2}\rho V^2}{144g_c} \right]$$

where  $P_{\max}$  is the maximum pressure averaged over the projected area (psi),  $\rho$  is the density of water (lbm/ft<sup>3</sup>),  $V$  is the impact velocity (ft/sec), and  $g_c$  is the gravitational constant (lbm-ft/lbf-sec<sup>2</sup>).

To specify the impulse of impact, one can make use of the correlations for the hydrodynamic mass of impact. This was, in fact, done in the LDR where the product  $0.2 M_h$  is the hydrodynamic mass of impact ( $M_h$ , by itself, is the hydrodynamic mass associated with acceleration of a fully submerged cylinder). The factor of 0.2 was obtained from QSTF vent header impact data (Ref. 36). The staff has examined additional data bases for cylinder impact (Refs. 25,37) and finds that the factor, 0.2, is too low. To yield a realistically conservative

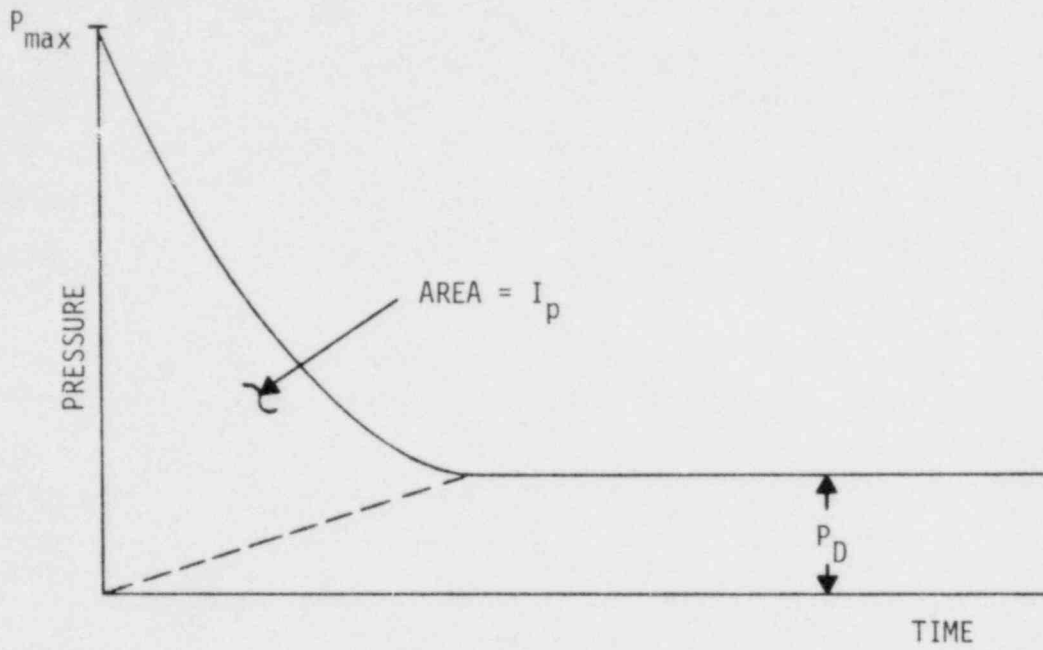


Figure 3.5-2 Typical cylindrical target impact pressure transient.



impulse value, the acceptance criteria specify that the hydrodynamic mass be obtained from a correlation derived for the Mark III containment design (Ref. 37), with a margin of 35 percent added to account for data scatter and to encompass other cylindrical impact data. Because the phenomena of pool swell impact are basically the same in the Mark I, Mark II, and Mark III containment designs, the PSTF (Mark III) impact data are also applicable to the Mark I design.

Once the hydrodynamic mass has been specified, the impulse of impact per unit area is readily determined by

$$I_{\rho} = \frac{M_H}{A} \left( \frac{V}{144 g_c} \right)$$

where  $I_{\rho}$  is the impulse per unit area (psi-sec),  $M_H / A$  is the hydrodynamic mass of impact per unit area (lbm/ft<sup>2</sup>), and  $V$  is the impact velocity (ft/sec).

The impulse, as defined here, does not include the drag contribution to the total force which is assumed to build up linearly from zero at the point of initial water contact to the steady-state value at the end of impact. Schematically, the value of impulse of impact (excluding drag) is equal to the area indicated in Figure 3.5-2.

To specify the pressure history fully, it is necessary to determine the duration of impact from the values of maximum pressure and impulse. Although it is possible to fit the shapes of the pulses by exponential curves and to calculate the corresponding pulse durations, a much simpler approach was used for the staff's acceptance criteria. The actual pulse was approximated by a triangular pulse of equal peak pressure and impulse. (This approximation will introduce a slight conservatism into the specification.) Figure 3.5-3 shows this step schematically. For a triangular shape the pulse duration is simply

$$\tau = 2 I_{\rho} / P_{\max}$$

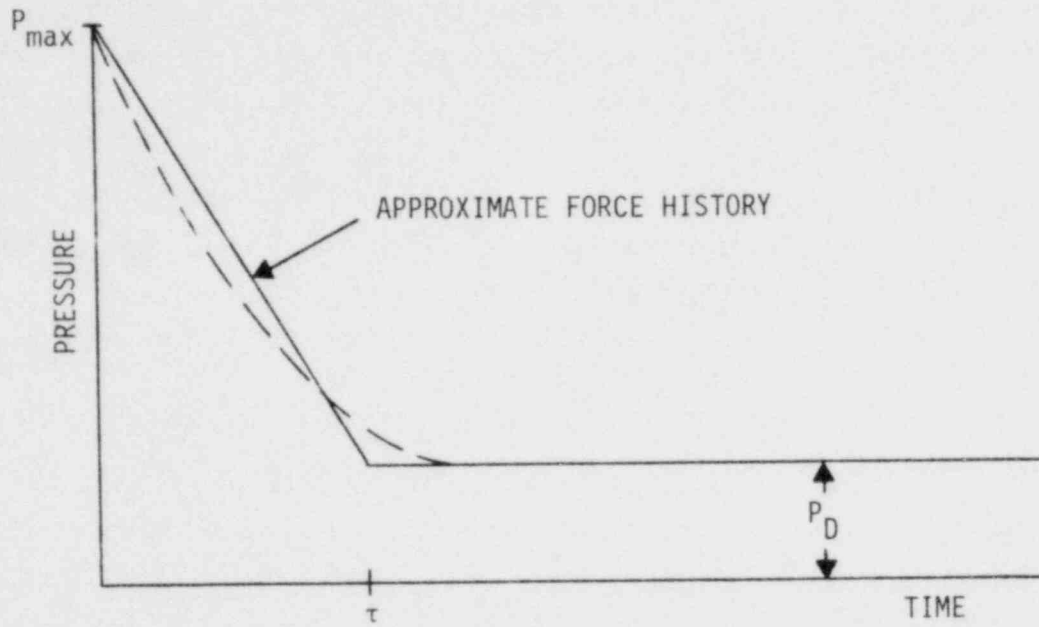


Figure 3.5-3 Cylindrical target impact transient approximation.

For the drag which follows the impact, it is not appropriate to use the standard drag coefficients as suggested in the LDR. After impact, an air cavity forms behind the cylinder, causing a departure from standard drag, which is based on fully submerged flow. The available data base for drag under these "open wake" conditions is relatively sketchy. This problem is similar to flow with a cavitating wake, and Hoerner (Ref. 28) presents some drag measurements on circular cylinders under these conditions. His Figure 15a presents the drag coefficients as a function of the cavitation number and Reynolds number. Although the data are not quantitatively applicable for the present purposes (the effective cavitation number is not known), the curves provide some information on trends. They show that, if the flow is laminar, ventilation of the wake can be expected to produce a reduction in the drag coefficient. If the flow is turbulent, however, ventilation of the wake can cause a substantial increase in the drag coefficient. In the case of fully cavitating flow (base pressure = ambient pressure), both laminar and turbulent cases indicate a drag coefficient of 0.5, independent of the Reynolds number.

In light of the above observations, the appropriate course of action is to rely on drag data obtained under conditions approximating the actual Mark I pool swell phenomena. The data base that best satisfies this requirement is the rigid cylinder impact data (Ref. 25). The staff established the drag coefficients based on the pressure histories presented for each test run. The pressures at which the pulses seemed to "level off" were taken to be the drag pressures following impact (shown schematically as  $P_D$  in Figure 3.5-2). The calculated drag coefficients corresponding to these are plotted in Figure 3.5-4 as a function of Froude number. Froude number was selected as the correlating parameter because the nature of the open wake behind the body depends primarily on inertia and gravity. (Only data with the larger, 17-inch cylinder are presented in Figure 3.5-4, since the smaller, 8.25-inch cylinder lacked sufficient instrumentation around the cylinder to provide accurate force measurements at later times.)

The acceptance criteria for drag following impact contain separate specifications for laminar and for turbulent flow. When the flow is laminar, a standard drag coefficient is used. With a ventilated wake, some reduction in  $C_D$  may be realized; however, since the rigid cylinder impact measurements were not in the laminar

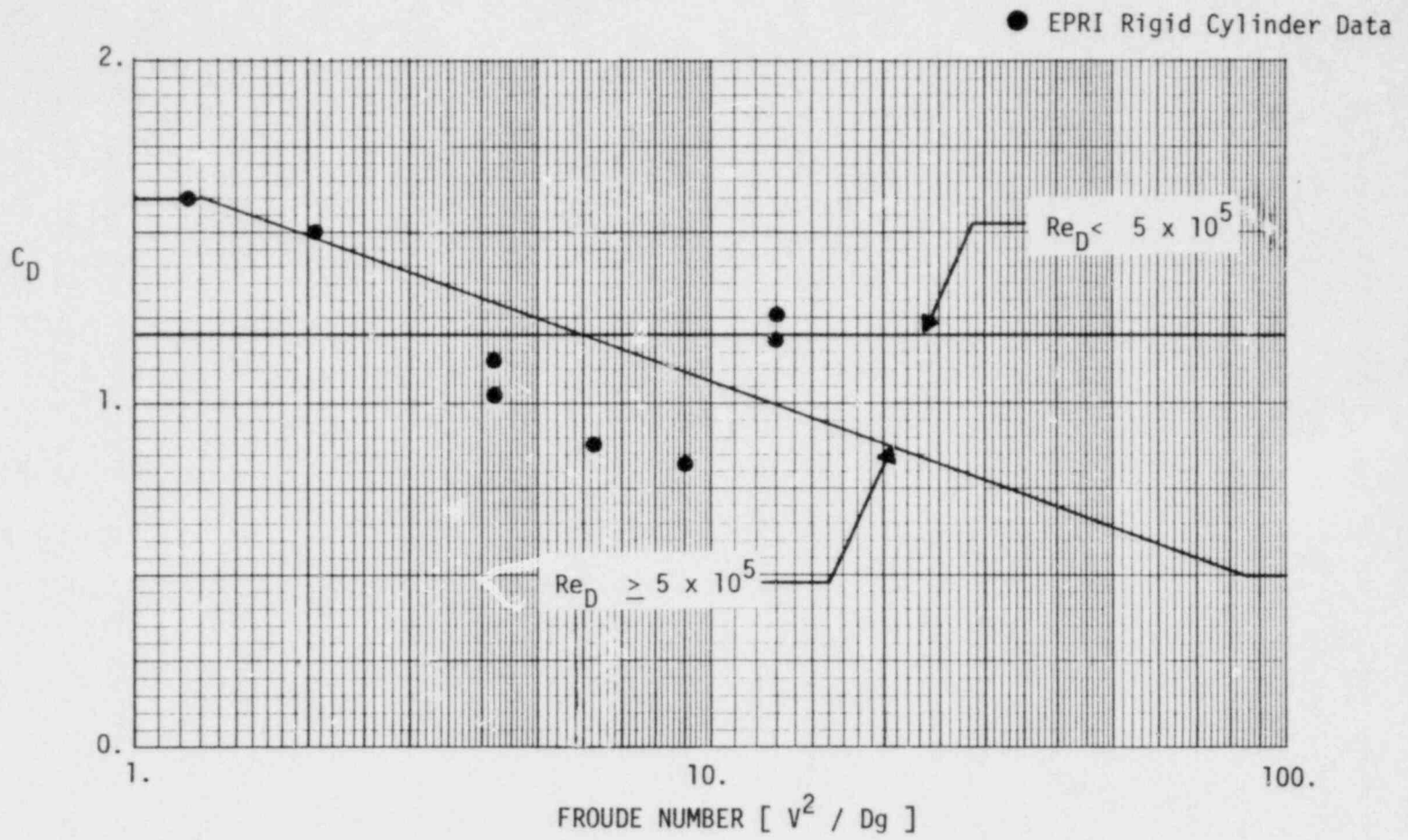


Figure 3.5-4 Cylindrical target drag coefficient following impact.

regime, it is not possible to quantify this reduction. Thus, a value of 1.2 will be used when Reynolds number is less than  $5 \times 10^5$ . When the flow is turbulent, a curve drawn through the measurements, as shown in Figure 3.5-4, has been specified for the drag coefficient. At Froude numbers greater than 85, a constant value has been specified, corresponding to the limiting case of a fully cavitating wake.

It should also be noted that the velocity in the drag computation is the maximum pool velocity rather than the velocity at the particular elevation of the structure in question. This specification is consistent with the LDR specification that the maximum pool velocity be used for viscous drag to compensate for neglecting the acceleration component in the total drag calculations.

The staff has concluded that the specifications outlined above and presented in Section 2.7.1 of Appendix A will provide conservative estimates of the impact and drag loads on circular structures.

#### 3.5.3.2 Elongated Noncircular Structures

The LDR treats all noncircular elongated structures alike. A circumscribing circle is drawn around the cross-section, and the structure is then treated as if it were circular.

This method is clearly an approximation. The staff has concluded that the method is unacceptable because it is not necessarily a conservative approximation, and it can lead to unrealistic results. A case in point is a structure in the form of a flat horizontal strip. The staff estimated that the LDR method for this case could underpredict the impulse by a factor of 3 and overpredict the pulse duration by a factor of 6.

Because of the difficulty in formulating criteria which are applicable to all noncircular shapes, the staff's acceptance criteria include a specification for flat structures only. As this configuration results in the most severe impact loading, all other noncircular structures (e.g., wedges) may be treated

as flat structures with the same projected width, or they must be evaluated on an individual basis.

The impact specification for flat structures is more complex than for cylinders. First, there is the potential for trapping air between the target and the pool. Secondly, although some experimental data are available, the detailed force histories over a wide range of velocities are not readily available for flat targets (as they were for cylinders). Consequently, the type of correlation for maximum pressure that was used for cylinders does not exist for flat targets. For this reason, the impulse and pulse duration have been used as the principal parameters to define the force history for flat structures. Maximum pressure then becomes the derived parameter.

The pulse shape is taken to be triangular (as shown in Figure 3.5-5). This shape is predicted from theoretical considerations (Refs. 27,29). The pressure impulse for flat targets is available from the correlations derived for the Mark III containment design (Ref. 37). A 35-percent margin was found to be necessary to account for scatter evident in those data.

The pulse durations for flat targets were derived from the studies of Chuang for the U.S. Navy (Ref. 35). His experimental investigation indicates that if the flat target is perfectly horizontal, a cushion of air is trapped between the target and pool, and the pulse duration is spread out in time. Chuang presents an approximate analytical method for calculating the pulse duration in the presence of this air cushion. In addition, he tested some wedges with small deadrise angles ( $1^\circ$ ,  $3^\circ$ ,  $6^\circ$ ,  $10^\circ$ , and  $15^\circ$ ) and noted that even a slight inclination in the target surface, with respect to the pool, was sufficient for the air to be pushed out of the way. Specifically, he noted that at  $1^\circ$  some air was still present, but at  $3^\circ$  the air had been pushed aside. Since the shortest pulse durations lead to the largest stresses, the staff has concluded that it would be prudent to identify the shortest reasonable pulse duration for the load specification. To do this, the pulse durations were determined for two different situations: perfectly horizontal targets with air cushions and targets inclined

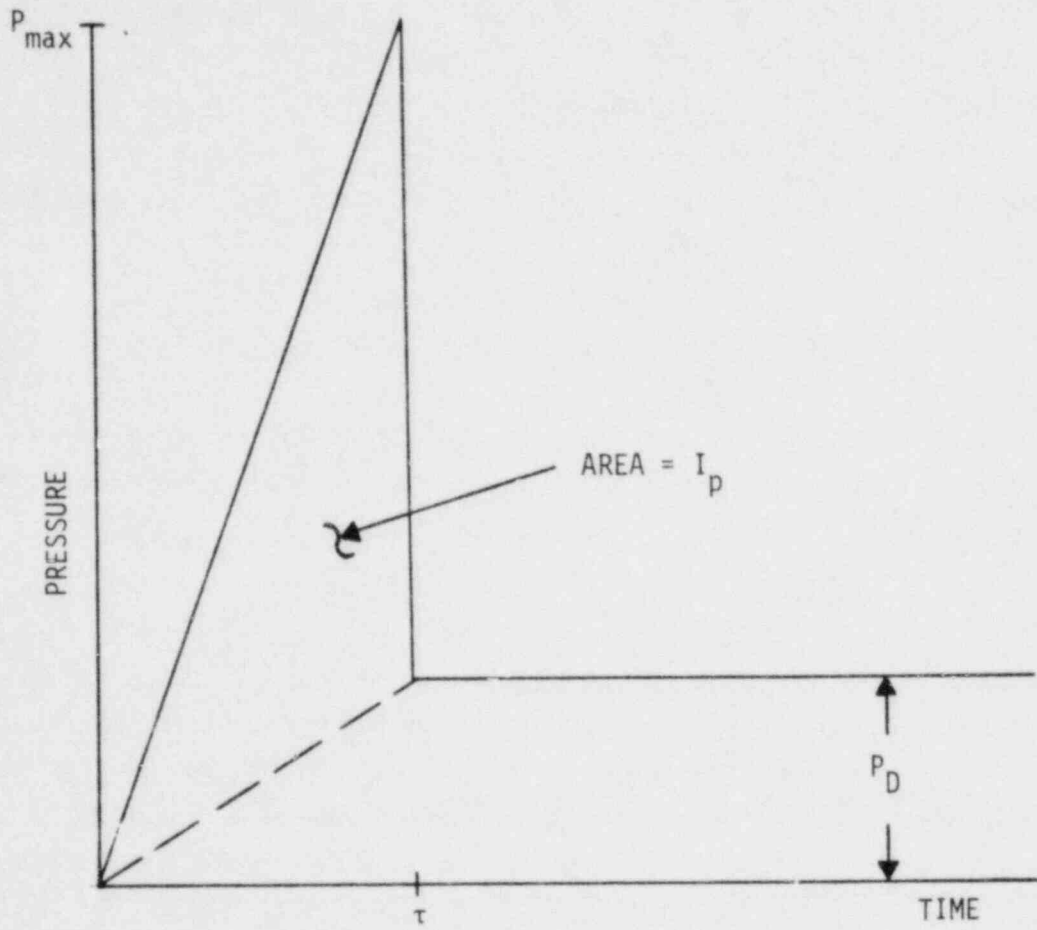


Figure 3.5-5 Typical flat target impact pressure transient.

at 1° without air cushions. Since the air cushion disappears at an inclination somewhere between 1° and 3°, the more conservative approach is to assume the lower inclination. Further, based on the range of Mark I configurations and the typical pool surface profile observed in experimental pool swell studies, we conclude that a 1° inclination of the target structure is reasonable.

The pulse durations with the air cushion were calculated by the analytical method suggested by Chuang (Ref. 35). For the 1° inclination, the pulse durations were determined in the following manner: From examination of the pressure traces for the individual transducers on wedge surfaces (Figure 8 of Chuang's report) it is apparent that during impact a high-pressure wave traverses the wedge from the keel to the edge. From these same pressure traces, one can calculate the (approximately constant) speed at which this wave travels, or, conversely, the time required to traverse a target of a certain width. This traverse time is essentially the pulse duration of impact. It was observed that, for small wedge angles, the traverse time was directly proportional to the wedge angle. Thus, one could readily establish the pulse durations for a 1° inclination at the particular velocity of impact (5.7 ft/sec) tested by Chuang. To generalize the pulse duration for higher velocities, it is noted from the theoretical treatment of this problem (Ref. 38) that the pulse travel times are inversely proportional to the pool velocity. Thus, we obtained the relation

$$\tau = 0.011 W/V$$

where the factor of 0.011 was established from Chuang's experiments, W is the width of the structure, and V is the impact velocity (with consistent units).

When, using the above equation, the pulse durations were compared to corresponding pulse durations for a horizontal target with an air cushion, it was found that, for pool velocities greater than 7 ft/sec, the pulse durations for the 1° inclined target were shorter. Therefore, the equation shown above was specified for impact velocities greater than 7 ft/sec. At impact velocities less than 7 ft/sec, the analysis for the air cushion leads to pulse durations approximated by the equation

$$\tau = 0.0016 W$$



where  $\tau$  is in seconds and  $W$  is in feet.

With the impulse data from the Mark III impact tests, the triangular shape for the pulse, and the pulse durations as specified in the preceding paragraph, the impact specification is complete. The remaining item, maximum amplitude of the pulse  $\rho_{\max}$  then automatically follows.

$$I\rho = \int_0^{\tau} \rho(t) dt = \frac{1}{2} \rho_{\max} \tau$$

$$\text{or } \rho_{\max} = 2I \rho / \tau$$

The drag force on flat targets following impact is based on a drag coefficient equal to 2.0. This value corresponds to the standard drag coefficient for a flat strip, and it bounds the Mark III drag data for flat geometries. As in the case of cylinders, an air wake will exist behind the flat structures immediately after impact. This will probably result in some reduction in the drag coefficient; however, in the absence of reliable data, a  $C_D$  of 2.0 has been specified as a conservative limit.

The staff has concluded that the specifications which are outlined above and presented in Section 2.7.2 of Appendix A will provide a conservative estimate of the impact and drag loads on flat-surfaced structures.

Other noncircular structures may be conservatively assessed as equivalent flat-surfaced structures by selecting the appropriate projected cross-sectional area. In those cases where the equivalent flat-surface impact is overly conservative, the impact and drag loads will have to be defined from applicable test data, using the methods outlined above. As previously discussed, this specification may result in impact and drag loads that are too conservative for certain structures. Such structures will have to be evaluated on a case-by-case basis.

### 3.5.3.3 Gratings

The LDR does not identify an impact load for gratings. This position is proposed on the grounds that none were detected during Mark III tests on a prototypical

grating target (Ref. 37). Thus, the only load identified for gratings during pool swell is a steady-state drag load.

The staff considers the proposed specification incomplete. However, the staff does concur that for gratings which are similar (in terms of percentage of solid area, bar thickness-to-length ratio, etc.) to that tested for the Mark III plants, the loads induced by impact are small. Nevertheless, for gratings of different design, impact loadings may be significant. In addition, even if only a constant drag is applied, a sudden application of this load will introduce a dynamic component which doubles the corresponding steady-state stresses.

To account for both the dynamic nature of the initial loading and for impact loads which may be significant for gratings different from those tested for Mark III, the staff will require that the drag load be increased by a multiplier given by

$$F_{SE}/D = 1 + \sqrt{1 + (0.0064 Wf)^2}$$

for  $Wf < 2000$  in/sec

where  $F_{SE}$  is the load to be applied to the grating (i.e., the static equivalent load),  $W$  is the width of the bars in the grating (inches),  $f$  is the natural frequency of the lowest mode (Hz), and  $D$  is the static drag load. In the structural assessment, it must be verified that the higher modes of response do not significantly contribute to the load. The detailed derivation of this multiplier is presented in Appendix C.4 of the staff's report on the Mark II Lead Plant Program (Ref. 39). This multiplier is to be applied to the steady-state force on the grating derived from the correlation shown in Section 2.7.3 of Appendix A.

The staff has concluded that this specification will provide a conservative estimate of the forces on gratings during pool swell.

#### 3.5.3.4 Fluid-Structure Interaction During Impact

In performing the structural dynamic analysis, one is faced with the question of fluid-structure interaction during impact. The pressure pulses, defined by

the load acceptance criteria, correspond to impact on rigid structures. This is due to the fact that the experimental data which were used as the basis for characterizing pulse durations (Refs. 25,35,37) were obtained with very rigid models. The real structures above the Mark I pools may be more flexible, with the result that the pressure pulse, during impact, will be modified by the motion of the target.

The motion of a slender uniformly loaded beam is given by the following equation (Ref. 40)

$$m \ddot{y} + EI = \frac{d^4 y}{dx^4} = p(t)$$

where

$m$  = mass of beam per unit length

$y$  = deflection from unloaded position

$p$  = force per unit length of beam ( $p$  has been used for pressure elsewhere in this report)

Consider the total force  $p$  as composed of the rigid body impact force,  $p_r$  and a perturbation,  $p_i$ , due to the fact that the body is deformable. Thus

$$p = p_r + p_i$$

If one neglects the damping and compressibility of water, the interaction force is simply equal to

$$p_i = -m_H \ddot{y}$$

where

$m_H$  = hydrodynamic mass of impact

The minus sign comes from the fact that as the interface moves in the positive direction (away from the water), the total force is reduced.

Combining the last three equations, the result is

$$m\ddot{y} + EI \frac{d^4 y}{dx^4} = p_r(t) - m_H \ddot{y}$$

or

$$(m + m_H) \ddot{y} + EI \frac{d^4 y}{dx^4} = p_r(t)$$

It is seen that the motion (and stresses) of a flexible beam can be calculated by driving it with a rigid beam forcing function. The mass of the beam, however, must be increased by the hydrodynamic mass of impact.

Consequently, the staff's criteria (Appendix A, Section 2.7.4) require that the mass of the impacted structure be increased by the hydrodynamic mass of impact, as derived from the Mark III impact tests (Ref. 37) in the structural analysis. This adjustment is not necessary for gratings, because its effect is negligible for these structures.

#### 3.5.3.4 Purely Impulsive Impact

When the loading is purely impulsive, the shape of the pressure history is unimportant; what matters is the area under the curve, i.e., the impulse. Thus, under these conditions, if the stress calculations have already been performed using the method proposed in the LDR, the calculated stresses may be used with some adjustments to provide acceptable loads with a minimum of additional effort.

The Mark I Owners Group has indicated it would like to use this approach for structures with natural frequencies less than 30 Hz to permit the use of existing analyses. The parameter that determines whether the load is purely impulsive is the ratio of pulse duration to the natural period of the structure. Theoretically, the loading is purely impulsive only when this ratio is zero. For practical purposes, however, the loading may be considered approximately impulsive when the ratio is less than 0.2. For a structure with a natural frequency of less than 30 Hz, this stipulates that the pulse duration,  $\tau$  is

$$\tau < 0.2/f = 0.0066 \text{ sec}$$

Using the proposed LDR method for pulse duration

$$\tau = 0.0468 D/V = 0.0066 \text{ sec}$$

gives

$$D/V \leq 0.141 \text{ sec}$$

as the condition when the loading can be considered impulsive. This criterion is shown in Figure 2.7-5 of Appendix A.

Although the pulse duration may be short enough for the load to be impulsive, that in itself is not sufficient. The equation proposed in the LDR for calculating the impulse contained an empirical constant of 0.2, which is too small. This must be increased by 35 percent to encompass a broader data base for cylinder impact (Refs. 25,37). Since, under impulsive loading, the stresses are proportional to impulse, the calculated stresses may simply be increased by a factor of 1.35.

The other correction (as indicated in Appendix A, Section 2.7.4) comes from the fact that drag, which follows impact, will contribute to the stresses under dynamic conditions. The amount of this correction can be obtained from the dynamic load factor (DLF) curves shown in Figure 2.7-5 of Appendix A. These corrections depend on the ratio of pulse duration to the natural period and the ratio of drag pressure to the peak impact pressure for a parabolic pulse. The DLF curves in Figure 2.7-6 of Appendix A were generated by calculating the response of a single-degree-of-freedom system to a parabolic force history without drag and, then, with drag forces of various magnitudes.

The staff has concluded that the adjustments to the proposed LDR impact and drag load specification for structures with a natural frequency less than 30 Hz will provide a reasonably conservative estimate of the purely impulsive impact loads.

### 3.6 Pool Swell Froth Impingement Loads

Froth is an air-water mixture which rises above the pool surface and may impinge on the torus walls and structures within the torus airspace. Subsequently, when the froth falls back, it creates froth fallback loads. There are two mechanisms by which froth may be generated:

- (1) As the rising pool strikes the bottom of the vent header and/or the vent header deflector, a froth spray is formed, which travels upward and to both sides of the vent header. For load definition purposes, this froth is assumed to be bounded by Region I, as shown in Figure 3.6-1.
- (2) A portion of the water above the expanding air bubble becomes detached from the bulk pool; this water is influenced by only its own inertia and gravity. The "bubble breakthrough" creates a froth which rises into the airspace beyond the maximum bulk pool swell height. This froth is assumed to be bounded by Region II, as shown in Figure 3.6-2.

The load specification proposed in Section 4.3.5 of the LDR is based on the transfer of all of the momentum of the froth to the impinged structure. The froth impingement pressure is then given as

$$p_f = (\rho_f V^2)/144g_c$$

where

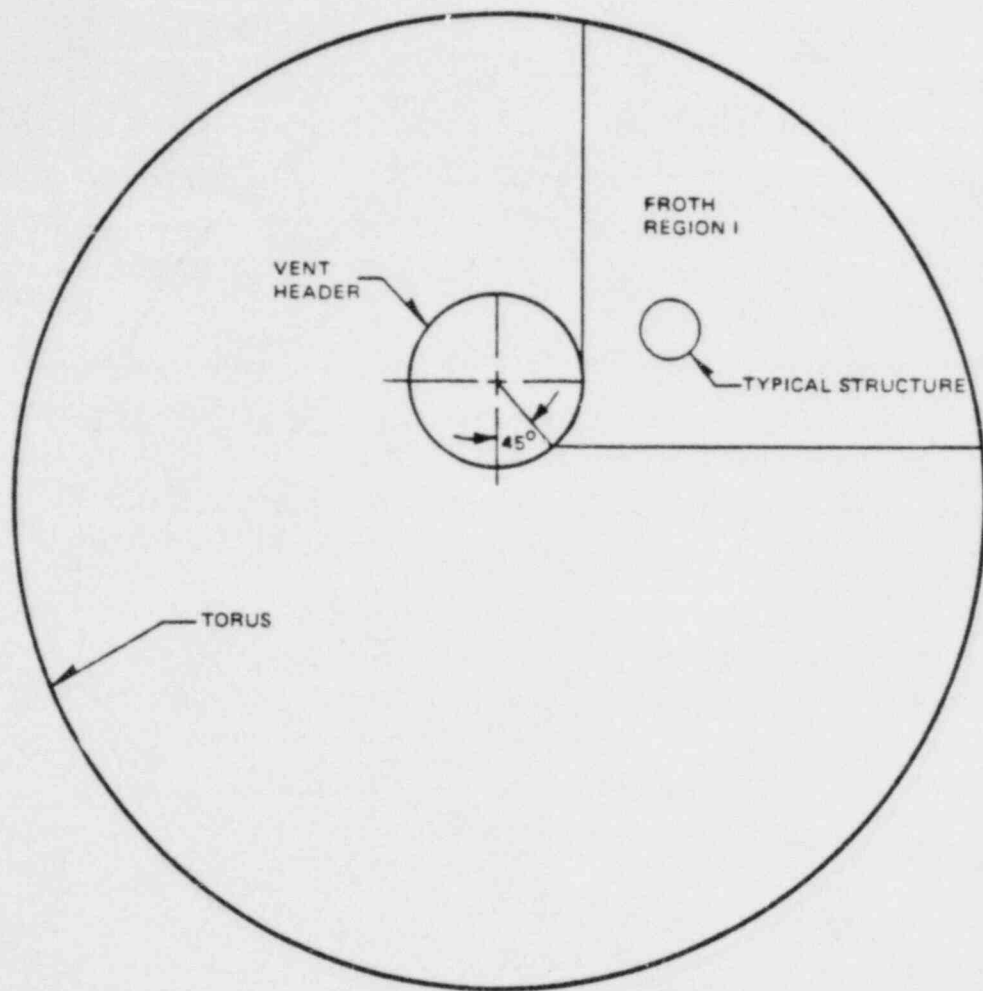
$p$  = froth impingement pressure (psi)

$\rho$  = froth density (lbm/ft<sup>3</sup>)

$V$  = froth impingement velocity (ft/sec)

$g_c$  = gravitational constant (lbm-ft/lbf-sec<sup>2</sup>)

The froth density and velocity are established from high-speed movies of the QSTF tests for Region I, Region II, and froth fallback. While the staff agrees with this approach in general, certain specific assumptions are not acceptable. These are described below.



Note: Region is symmetric on both sides of vent header.

Figure 3.6-1 Froth impingement zone - region I.

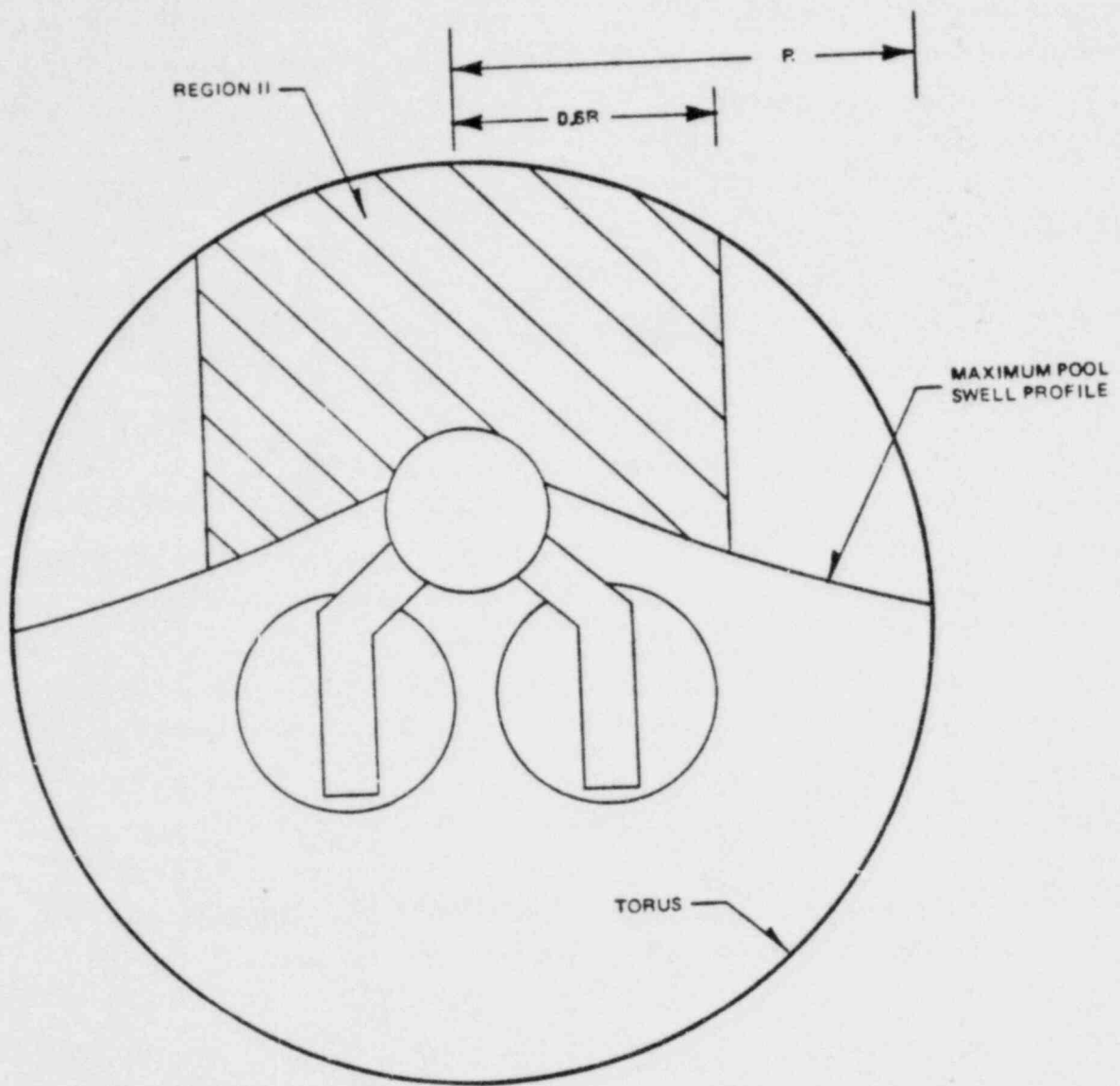


Figure 3.6-2 Froth impingement zone - region II.



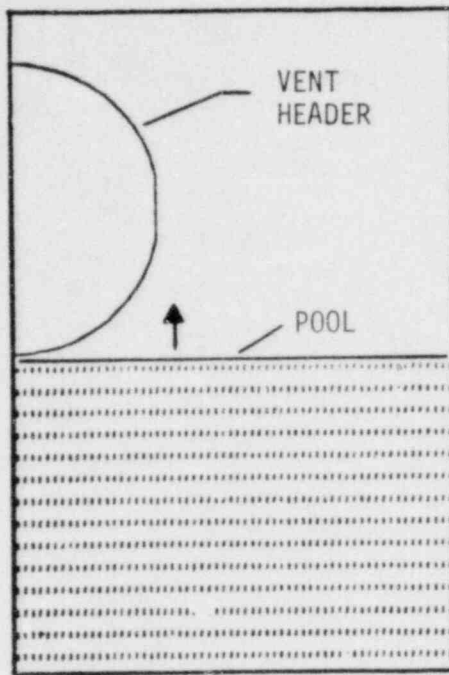
For Region I, the proposed load specification assumes that the froth density is 10-percent water density and the froth velocity is equal to the pool surface velocity just prior to vent header impact. The load duration is 0.080 seconds, applied in a direction defined by the 45° tangent at the bottom of the vent header with no allowance for gravity deceleration. Based on a review of selected QSTF movie frames and analytical results, the staff has concluded that the proposed specification does not adequately describe the loading condition.

The froth in Region I is a water spray formed by the displacement and acceleration of the pool surface by the vent header. Estimates of the initial departure velocity of the froth spray were made from the results of analyses performed by the Los Alamos Scientific Laboratory using the SOLA-SURF computer code (Ref. 41). These calculations provided fluid velocities within the wave formed during impact, as shown in Figure 3.6-3, but did not extend into the froth regime itself. The analyses indicated that the peak water velocity was more than twice the header impact velocity just prior to the formation of the froth. This estimate of the froth source velocity was confirmed by examination of the movie frames. The staff has concluded that a froth impingement velocity equal to 2.5 times the header impact velocity, corrected for gravitational deceleration to the point of impingement, is reasonably representative for the range of Mark I configurations. Further, the variation in header impact velocity and gravitational deceleration will tend to change the direction of the applied load. Consequently, the acceptance criteria also require (Appendix A, Section 2.8) that the load be applied in a direction most critical to the structure within the 90° sector which will bound the observed froth vectors.

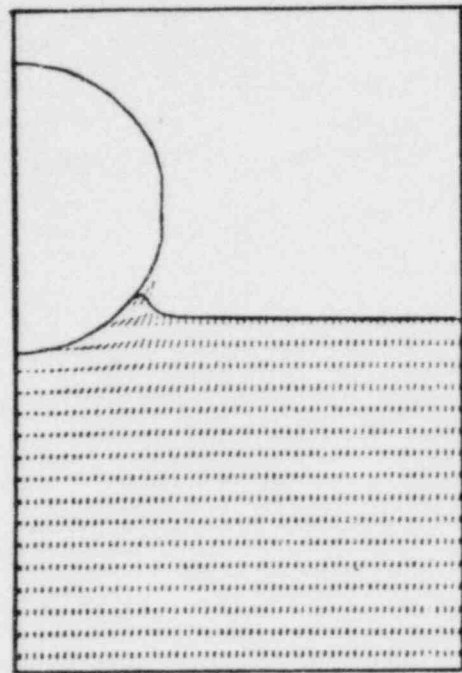
To determine a conservative estimate of the froth density, conservation of momentum and energy were evaluated. Treating the froth as a fluid with uniform initial velocity,  $V_f$ , directed at an angle,  $\theta$ , with the horizontal, and having a mass of froth,  $m_f$ , on either side of the vent header, the vertical momentum equation may be written

$$(m_h + m_{hf} + 2m_f) V_i = I_p + 2 m_f V_f \sin \theta$$

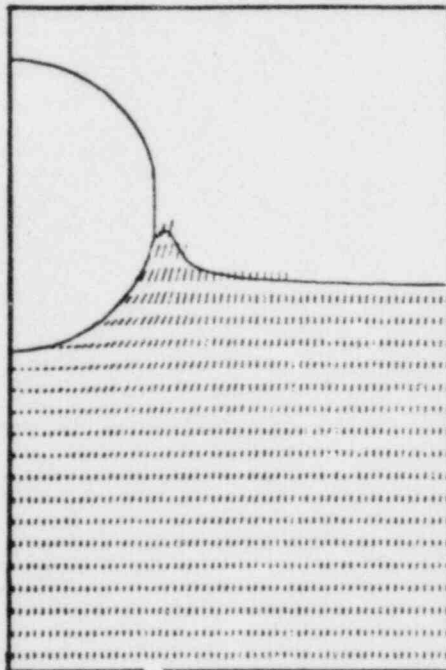
where



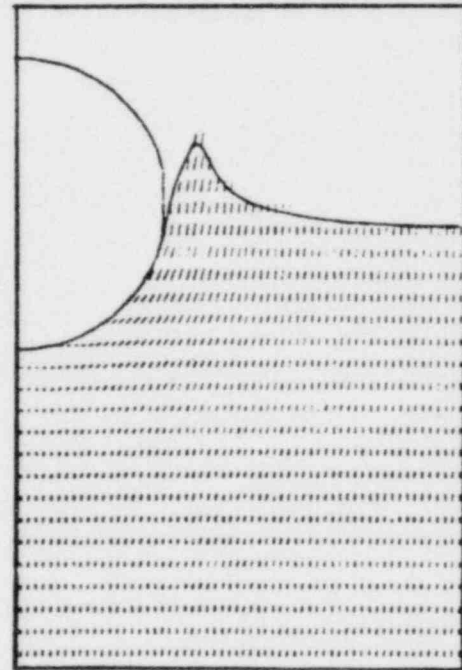
1.



2.



3.



4.

Figure 3.6-3 Vent-Header impact wave formation.

$m_h$  = hydrodynamic mass associated with cylinder impact

$m_{hf}$  = hydrodynamic mass associated with the froth

$I_p$  = impulse transferred to cylinder

$V_i$  = vent header impact velocity

Neglecting dissipative effects during the froth formation process, conservation of kinetic energy gives

$$(m_h + m_{hf} + 2m_f) \frac{V_i^2}{2} = 2m_f \frac{V_f^2}{2}$$

Setting  $m_h V_i = I_p$  (including drag), these two equations give

$$m_{hf} = m_h \frac{\left[ \frac{V_f}{V_i} \sin \theta - 1 \right]}{\left[ \left( \frac{V_f}{V_i} \right)^2 - \left( \frac{V_f}{V_i} \right) \sin \theta \right]}$$

and

$$m_f = \frac{(m_h + m_{hf})}{2} \left[ \frac{1}{\left( \frac{V_f}{V_i} \right)^2 - 1} \right]$$

To obtain some estimate of froth density,  $\rho_f$ , conservation of mass gives

$$m_f = \rho_f w_f L V_f \tau$$

where

$w_f$  = initial width of froth (estimated from movie frames)

$L$  = cylinder length

$\tau$  = duration of froth pulse

or

$$\rho = \frac{(m_f/L)}{w_f V_f \tau}$$

This approach was applied to typical plant conditions using data from the QSTF plant-unique tests (Ref. 14) to assess the variation in froth properties that should be expected as a result of variations in the wave width, density, and pulse time. Based on this assessment, the staff has concluded that, in combination with the source velocity previously specified and a rectangular pulse of 0.080 seconds, a froth density of 20-percent water density for structures with a cross-sectional dimension less than or equal to 1 foot and a proportionately lower density for larger structures will provide a conservative estimate of the froth impingement loads in Region I. This requirement (which is specified in Appendix A, Section 2.8) limits the impulse to that contained within an initial 1-foot wide wave as it spreads out with increasing distance from the vent header. It should be noted that this procedure does not allow for the effect of a vent header deflector on the Region I froth. The movie frames indicate significant froth formation as a result of impact with the vent header itself, even when deflectors are used. Because the effectiveness of the deflector as a froth mitigator is difficult to quantify generally, it is conservatively neglected.

To allow for plant-specific variations in the froth source velocity, departure angle, and froth density in Region I, and in consideration of the different vent system geometries and the presence of the vent header deflector, the criteria in Section 2.8 of Appendix A alternately allow the QSTF plant-specific movies to be used to define these parameters. The specified plant-specific load definition technique is based on the same conservation of momentum and energy approach that was used to define the generic froth load.

For Region II, the method proposed in the LDR assumes that the froth travels vertically to the target structure under the influence of gravity only, with a source velocity equal to the pool surface velocity at the time of maximum pool swell corrected for spatial variations in the surface velocity. However, strictly interpreted, the pool surface velocity at the time of maximum pool swell is zero. The froth formation during the later stages of the bubble expansion process is not a well-defined phenomenon. Froth which would not be affected by torus airspace pressurization could be formed before bubble breakthrough. Therefore, a more appropriate basis for establishing the froth velocity in Region II is a source velocity equal to the maximum pool surface velocity

directly beneath the target structure, corrected for subsequent deceleration from the elevation of the maximum velocity. (This requirement also is set forth in Appendix A, Section 2.8.)

The proposed froth density in Region II is assumed to be 100-percent water density for structures or sections of structures with a maximum cross-sectional dimension less than or equal to 1 foot, 25-percent water density for structures greater than 1 foot, and 10-percent water density for structures located within the projected region directly above the vent header. The load is to be applied in the direction most critical to the structure within the  $\pm 45^\circ$  sector of the upward vertical, as a rectangular pulse with a duration of 100 milliseconds. Based on a review of the pool swell test films, the staff has concluded that these assumptions, in conjunction with the froth velocity specification above, will provide a conservative estimate of the froth impingement loads in Region II and are, therefore, acceptable.

For froth fallback, the proposed method in the LDR assumes a fallback velocity based on freefall of the froth from the upper surface of the torus shell directly above the target structure. The froth density is assumed to be 25-percent water density, with the exception of the projected region directly above the vent header, which is 10-percent water density. The load is to be applied in the direction most critical to the structure within the  $\pm 45^\circ$  sector of the vertical downward, directly following the froth impingement load, with a duration of 1 second. The staff has concluded that these assumptions will provide a conservative estimate of the froth fallback loads following pool swell and are, therefore, acceptable.

### 3.7 Pool Fallback Loads

This section applies to structures within the torus (although not the torus itself) that are below the upper surface of the pool at its maximum height. Following the pool swell transient, the pool water falls back to its original level and, in the process, generates fallback loads. After the pool surface has reached its maximum height as a result of pool swell, it falls back under the influence of gravity and creates drag loads on structures inside the torus shell. These structures are between the maximum bulk pool swell height and

the downcomer exit level, or they may be immersed in an air bubble extending beneath the downcomer exit level. The fallback load starts as soon as the pool reaches its maximum height; it ends when the pool surface falls past the structure of concern or the pool velocity reaches zero.

For structures immersed in the pool, the drag force during fallback (as noted in the LDR) is the sum of standard drag (proportional to velocity squared) and acceleration drag (proportional to acceleration). For structures which are beneath the upper surface of the pool but are within the air bubble, there will be an initial load associated with resubmergence of the structure by either an irregular impact with the bubble-pool interface or a process akin to froth fallback. This initial load will be bounded by the standard drag if suitably conservative assumptions are made in calculating the standard drag.

The load calculation procedure, as proposed in the LDR, requires determination of the maximum pool swell height ( $y_m$ ) above the height of the top surface of the structure ( $y_s$ ). Freefall of the bulk fluid from this height produces both standard drag and acceleration drag, with the total drag given by the sum. The fluid acceleration and velocity are then

$$dU/dt = g \quad \text{and} \quad U = \sqrt{2g (y_m - y_s)}$$

It should be noted that this is a conservative calculation of the velocity,  $U$ , since it is unlikely that any appreciable amount of pool fluid will be in freefall through this entire distance. The maximum pool swell height is determined from the QSTF plant-unique tests.

The evaluation of the drag coefficient,  $C_D$ ; the acceleration volume,  $V_A$ ; and corrections to both for interference effects should employ the same procedures as outlined in Section 3.11.2.

The assumption in the LDR that fallback loads on structures below the downcomer exit level are negligible is reasonable, except for structures which come within the bubble boundaries. Structures that may be enveloped by the LOCA bubble

must be evaluated for potential fallback loads as a result of bubble collapse to ensure that such loads are not larger than the LOCA bubble-drag loads (see Section 3.11.2).

With respect to the direction of load application, the procedure outlined in the DR is acceptable. The fallback load is applied uniformly over the upper projected surface of the structure in the direction most critical to the behavior of the structure. Figure 3.7-1 indicates the possible directions of application to be considered. This range ( $\pm 45^\circ$  from the vertical) applies to both the radial and longitudinal plants of the torus. Based on a review of various pool swell test movies, the staff has found that the proposed direction of application is conservative.

### 3.8 Condensation Oscillation Loads

Condensation oscillation loads and chugging loads refer to the oscillatory pressure loads imparted to structures as a result of the unsteady, transient behavior of the condensation of the steam (released during a LOCA) occurring near the end of the downcomers. Because the nature of this unsteadiness has been found to be significantly different at high steam-flow rates than at low steam-flow rates, it is convenient to divide the phenomena into two types: (1) "condensation oscillations," which occur at relatively high vent-flow rates and are characterized by continuous periodic oscillations, with neighboring downcomers oscillating in phase, and (2) "chugging," which occurs at lower vent-flow rates and is characterized by a series of pulses typically a second or more apart. The classifications, condensation oscillation and chugging, are somewhat arbitrary since there is a continuous spectrum of unsteady condensation phenomena. However, they are convenient for the purposes of defining the nature of the various loading conditions.

The condensation phenomenon involves an unsteady, turbulent, two-phase flow. No reliable analytical methods exist which allow one to model such flows. Furthermore, because of the apparently random element in the condensation phenomena, no reliable and proven empirical engineering methods exist which would allow

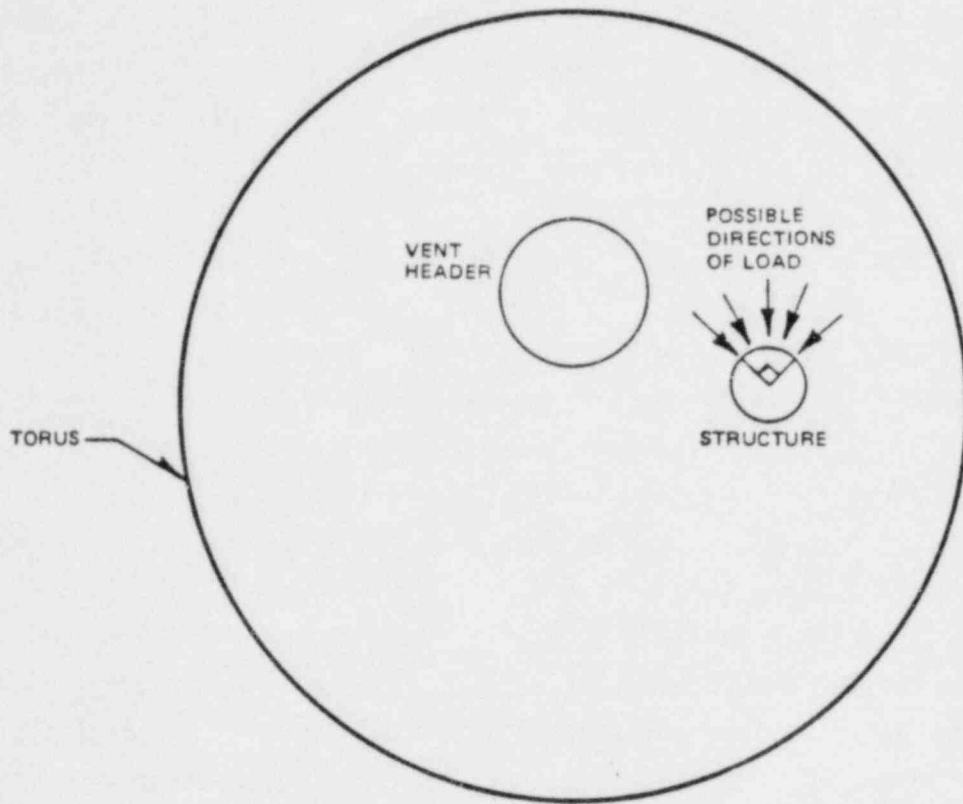


Figure 3.7-1 Pool fallback load directional range.



accurate assessment of either (1) the load magnitudes, (2) the parametric variation of the loads, or (3) the scaling of the loads. Consequently, load definition must rely on a data base taken from experiments which model as closely as possible the conditions in an actual plant. For this reason, condensation oscillation and chugging loads are based on the results of tests conducted in the Full-Scale Test Facility (FSTF), which was a full-scale, 22.5° sector of a typical Mark I torus connected to simulated drywell and pressure vessel volumes (Ref. 42).

The facility arrangement is depicted in Figure 3.8-1. A total of 10 tests were conducted, with parametric variations as shown in Table 3.8-1. The complete series of tests simulated blowdowns over a range from small breaks to the design-basis accident.

Previous condensation tests indicated that the magnitudes of the condensation loads were strongly dependent upon the concentration of air in the steam flowing through the vent system. The smaller the air concentration, the higher the loads, all other conditions being the same. Consequently, the simulated drywell volume in the FSTF was designed to expel the initial atmosphere to the torus volume as quickly as possible. In addition, air concentration in the vent flow was monitored during the course of each test.

The principal design parameters for the FSTF (e.g., vent-area-to-pool-area ratio and distance of the downcomer exit to the torus shell) were selected to produce conservative data from which the loads could be derived. Structurally, the FSTF torus sector was an exact replica of the Monticello plant. (Monticello is considered to be structurally "average" in relation to the range of the Mark I design characteristics.)

Earlier condensation tests which were not prototypical of Mark I identified more significant loading conditions during the chugging regime. However, during the course of the FSTF tests, the more significant loads for the Mark I configuration were found to occur during condensation oscillations, i.e., high vent-flow rate with low air content. (A typical shell pressure during the condensation oscillation regime is shown in Figure 3.8-2.)

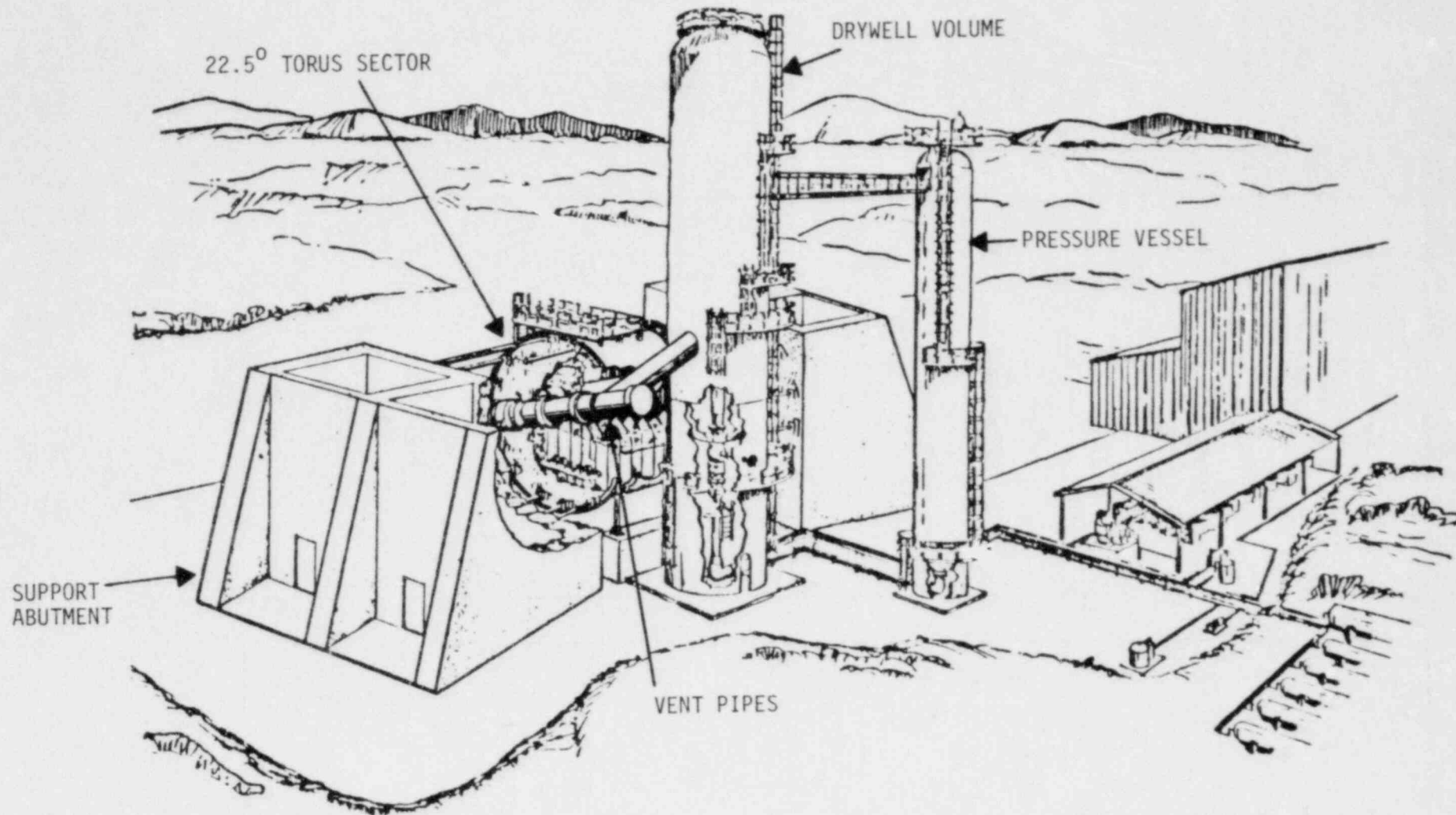


Figure 3.8-1 Mark I full-scale test facility.

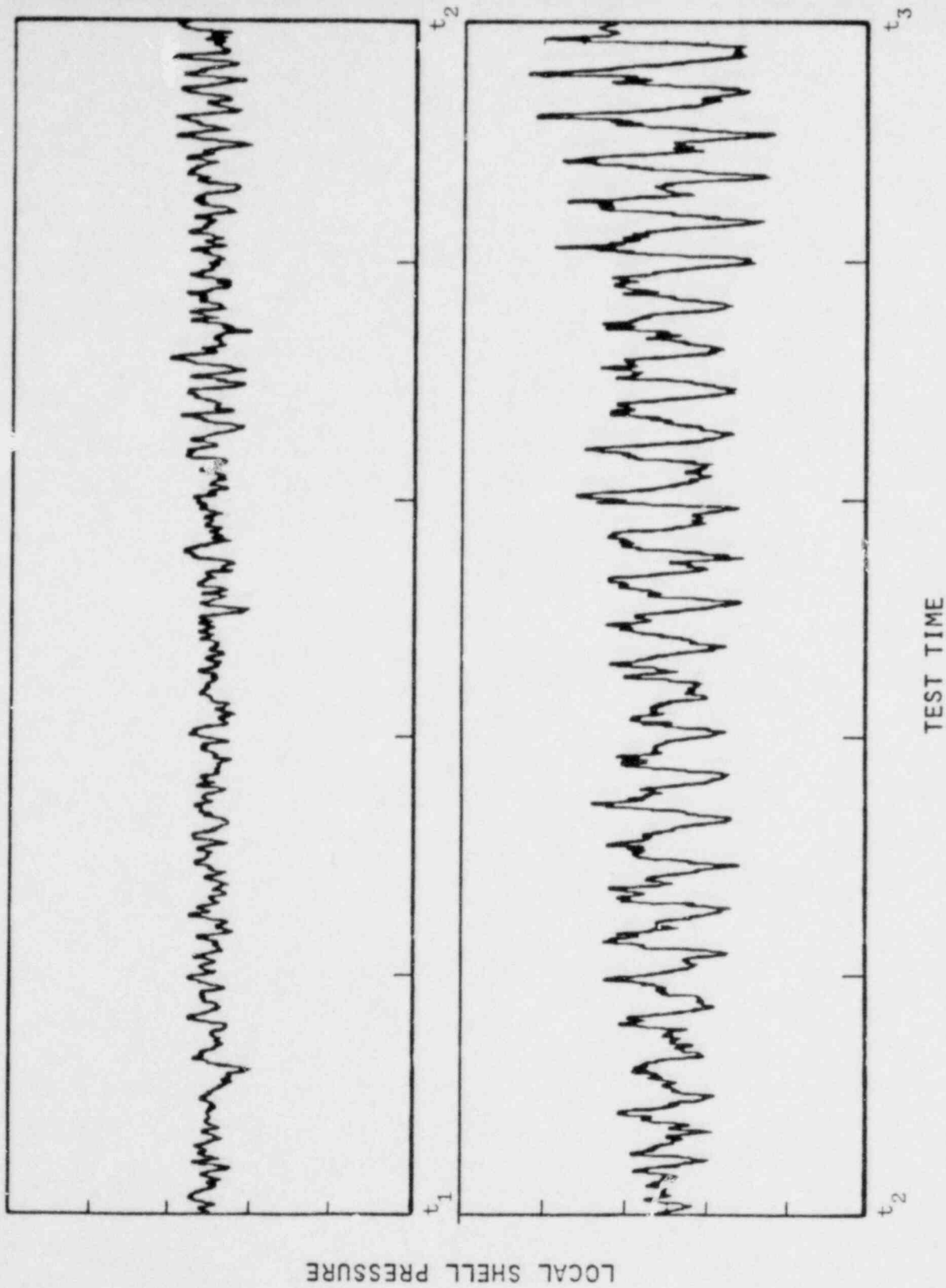


Figure 3.8-2 Condensation oscillation torus shell pressure transient.

Table 3.8-1 FSTF Test Matrix

| Test Number | Date Performed | Break Size | Break Type | Downcomer Submergence | Torus* Temperature | Torus* Pressure |
|-------------|----------------|------------|------------|-----------------------|--------------------|-----------------|
| M1          | 5/05/78        | Small      | Steam      | 3'4"                  | 70°F               | 0 psig          |
| M2          | 5/12/78        | Medium     | Steam      | 3'4"                  | 70°F               | 0 psig          |
| M3          | 5/25/78        | Small      | Liquid     | 3'4"                  | 70°F               | 0 psig          |
| M4          | 6/17/78        | Small      | Steam      | 3'4"                  | 70°F               | 5 psig          |
| M5          | 6/26/78        | Small      | Steam      | 3'4"                  | 120°F              | 0 psig          |
| M6          | 7/06/78        | Small      | Steam      | 1'6"                  | 120°F              | 0 psig          |
| M9          | 7/11/78        | Small      | Steam      | 4'6"                  | 70°F               | 0 psig          |
| M10**       | 7/27/78        | Small      | Steam      | 3'4"                  | 70°F               | 0 psig          |
| M7          | 8/10/78        | Large      | Steam      | 3'4"                  | 70°F               | 0 psig          |
| M8          | 8/22/78        | Large      | Liquid     | 3'4"                  | 70°F               | 0 psig          |

\*Initial torus conditions.

\*\*Air sensitivity test performed with vacuum breaker on vent system replaced by rupture discs.

The maximum condensation oscillation loads in the FSTF were found to occur for the large-break, liquid blowdown test. Only one such test was conducted (M8). Based on the periodic nature of the condensation oscillations and the stochastic nature of the complex condensation processes, the staff has concluded that test M8 constitutes only a single data point. Consequently, statistical variance or load magnitude uncertainty cannot be established with any useful accuracy from this single test run, even when magnitudes from test runs at much lower vent-flow rates are factored into the analysis. Thus, although the staff accepts the M8 test conditions as both conservative and prototypical for the Mark I design, the information is insufficient to establish a reasonable measure of the uncertainty in the loading functions and, hence, ensure margins of safety in the containment structure.

Nevertheless, the staff believes that the loads derived from M8 are probably conservative (although the degree of conservatism cannot be quantified) and, therefore, form a sufficient basis to proceed with the implementation of the Mark I long-term program. In letters dated October 2, 1979, each Mark I licensee was advised that additional FSTF tests would be required to establish the uncertainty in each of the condensation oscillation loads and to confirm the adequacy of the load specifications (Ref. 43). All of the following evaluations pertaining to condensation oscillation loads are predicated on the confirmatory testing and quantification of the uncertainties associated with the condensation oscillation load magnitudes. The resolution of this issue will be described in a supplement to this report.

The following sections present the staff's evaluation of the proposed condensation oscillation load definition techniques for (1) pressure loads on the torus shell, (2) condensation loads on the downcomers, and (3) oscillatory pressure loads within the vent system. The oscillatory drag loads on submerged structures are discussed separately in Section 3.11.

#### 3.8.1 Condensation Oscillation Torus Shell Pressure Loads

Condensation oscillations produce continuous, oscillatory pressures (Figure 3.8-2) acting on the torus shell over the wetted interior surface.

The FSTF was intended to be entirely prototypical so that loads measured in that facility could be applied directly in the plant-unique analyses. However, condensation oscillations and chugging loads transmitted to the structure by the water in the pool have been found to be affected by fluid-structure interaction (FSI) effects. Because there are variations in the structures of different plants, and, consequently, between the individual plants and the FSTF, some analysis and identification of these effects in both the FSTF and individual plants are necessary in order to define appropriate plant loads.

To assess this effect, the Mark I Owners Group developed a coupled fluid-structure analytical model simulating the FSTF structure and suppression pool (Ref. 44). In this model, an assumed oscillatory source applied at the end of each downcomer is varied until the wall pressures match the maximum amplitude pressures observed in the FSTF tests. The assumed source function is then applied to a similar model to derive an equivalent "rigid-wall" pressure transient. From these analyses, a global pressure load on the torus shell is generated by specifying:

- (1) A bottom-center pressure amplitude-frequency spectrum (as shown in Figure 3.8-3) derived from the FSTF tests, which represents the loading in the case of effectively rigid torus walls.
- (2) A distribution of load magnitude and frequency for the wall pressures in a torus cross-section. The distribution in magnitude is essentially hydrostatic and increases linearly with depth from zero at the pool surface to a maximum at the bottom center of the torus. This conforms with the FSTF measurements and is shown in Figure 3.8-3. The pressures are assumed to be inphase.
- (3) An axial distribution of phase for the loading described above, along the torus centerline. A symmetric global load is defined by zero phase distribution around the torus.
- (4) A time duration for the load.
- (5) A model which permits the incorporation of FSI effects in individual plants and utilizes as input the rigid wall loading described above, plus the added mass matrix for the water.
- (6) A plant-unique correction factor to account for different pool-to-vent area ratios.

The load specification proposed in the LDR was derived from selected periods of maximum-amplitude test data. Optional pressure amplitude-frequency spectra are included to ensure that the maximum pressure amplitude has been specified

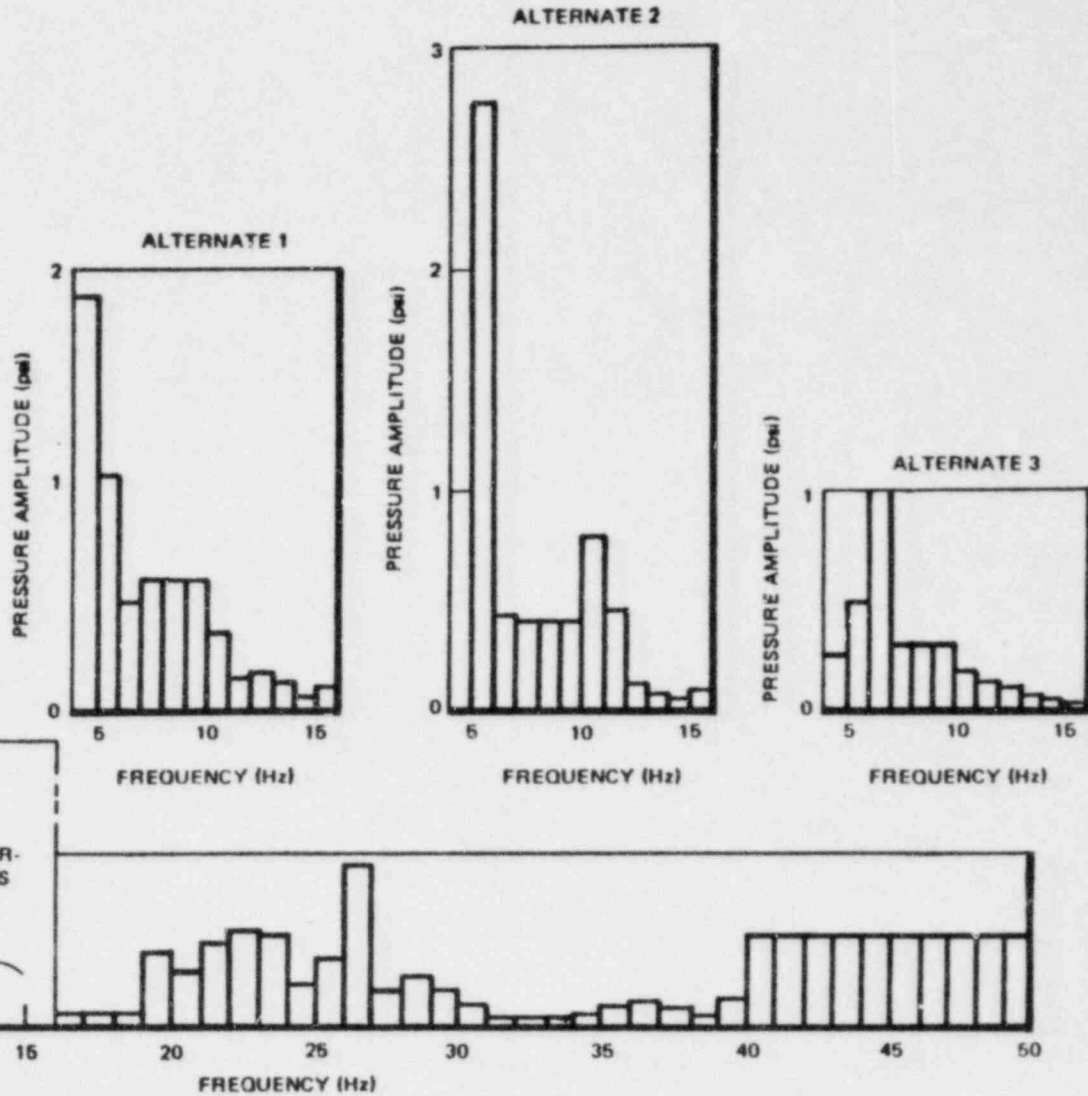
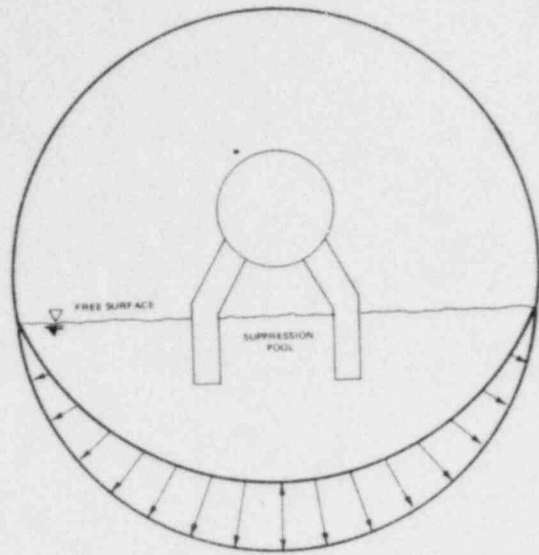


Figure 3.8-3 Condensation oscillation amplitude - frequency spectrum.

for those frequencies for which the structure might be sensitive. The FSI model used to derive the pressure amplitude-frequency spectra incorporates assumptions that are not necessarily conservative by themselves. However, the overall conservatism of this technique is demonstrated by comparisons of the predicted structural response using the load specification and the measured structural response in the FSTF (Ref. 45).

Only a symmetric global load has been specified. No appreciable asymmetric global load was detected in the FSTF tests during condensation oscillations; hence, it is assumed that the asymmetric chugging load definition would be bounding. This assumption will be verified by the confirmatory FSTF tests and will be addressed in a supplement to this report.

The onset and duration of the condensation oscillation period have been conservatively bounded from limiting containment response analyses, similar to those described in Section 3.2. The plant-unique pool-area-to-vent-area correction factor was derived from a potential flow analysis. This correction factor would be applied for both the gross torus response (since the condensation oscillations are assumed to be in phase) and the local shell pressures. This approach is reasonable and, in any case, the corrections are relatively small. For the IBA, the magnitude and frequency content of the condensation oscillation loads were found in the tests to be equivalent to the chugging load described in Section 3.9.1. Consequently, the chugging load specification is used for the IBA condensation oscillation. Based on its review of the condensation oscillation load specification, the FSTF test results, and the analytical assessment of the FSTF test results, the staff has concluded that the proposed method will provide a reasonably conservative estimate of the condensation oscillation loads on the torus shell, subject to the confirmation of the uncertainty in the loads (as described in Section 3.8) and provided that the load specification is used with a coupled fluid-structure analytical model (as described in Appendix A, Section 2.11.1).

### 3.8.2 Condensation Oscillation Downcomer Loads

The proposed load specification for the downcomers during the condensation oscillation regime is expressed by a resultant-static-equivalent load (RSEL),



which would be applied horizontally at the tip of the downcomers. This load specification is needed to assess the limiting stresses in the downcomer-vent header connection and to assess the overall loading on the vent system and its supports during condensation.

Spectra of RSELS are derived from a set of four equally spaced strain measurements located on the upper section of several downcomers in the FSTF (Ref. 46). These strain measurements are vectorially resolved into a single, directional load at the tip of the downcomer. A complete analysis of a particular data set will result in a histogram of the number of loads within a particular magnitude range that will occur within a particular range of directions (as shown in Figure 3.8-4).

Because the load specification has been derived from a specific downcomer configuration and for a specific period of time, scaling factors were devised which could be used to develop plant-specific loading conditions. The method used to derive the loading functions inherently includes specific response characteristics of the downcomer design in the FSTF. The plant-specific loading functions are defined as

$$P_{\max} = P_1 (DLF/DLF_1)$$

where

$P_{\max}$  = the plant-specific maximum RSEL

$P_1$  = the FSTF maximum RSEL

DLF = the plant-specific dynamic load factor

$DLF_1$  = the FSTF dynamic load factor

The dynamic load factor is a function of the type of loading (i.e., sinusoidal for condensation oscillations and triangular pulse for chugging), the natural frequency of the downcomer-vent header system, the damping of the downcomer-vent header system (including pool water), and the frequency of the forcing function. The duration of the loading condition is scaled directly by the period of time from which the loads were derived. In the proposed load specification, the loading function would be assumed to be in resonance; i.e., the frequency of the loads would be equal to the frequency of the structural system.

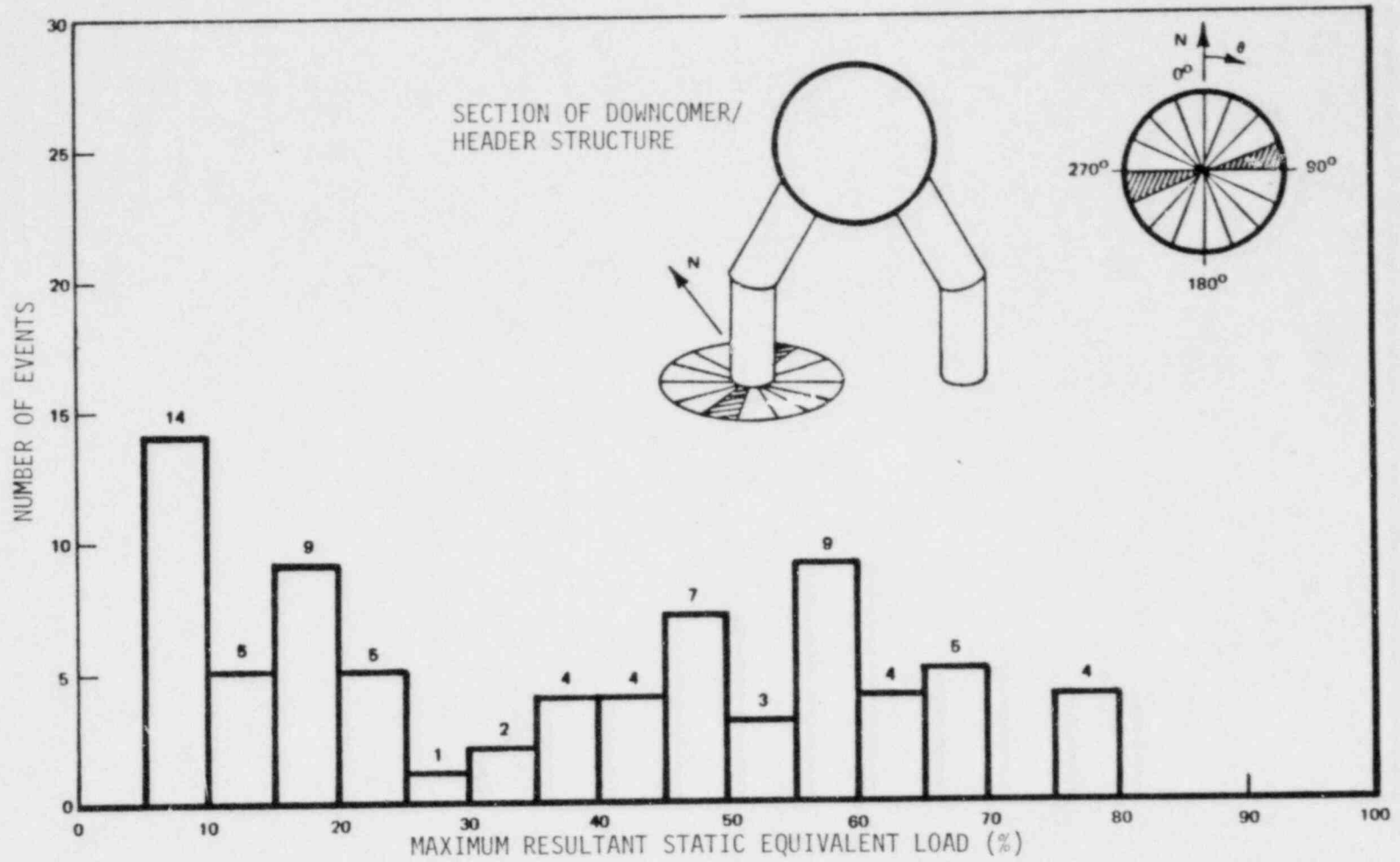


Figure 3.8-4 Downcomer condensation oscillation load histogram.

During the course of its review of the proposed downcomer lateral loads, the staff assessed the potential for dynamic amplification of the loads at resonant conditions. This assessment led to a more detailed comparison of the loading conditions observed in "tied" and "untied" downcomers in the FSTF. The "tied" downcomers contain a brace (tension or compression) between the ends of the downcomers. The strain measurements observed in the "tied" downcomers in the FSTF were significantly lower than those for the "untied" downcomers. Based on a detailed analysis of the downcomer-vent header system, the Mark I Owners Group concluded that the downcomer loads during condensation oscillations were primarily an in-phase vertical thrust load caused by the pressure oscillations inside the downcomer, with only a small lateral loading contribution.

Although this observation explained the differences in the test data, it also led the staff to conclude that the proposed lateral load specification would not adequately describe the dynamic loading components in the downcomer-vent header connection and in the tie-bar. Consequently, the staff is requiring that an improved load definition for the "tied" downcomers be developed from the FSTF data (as discussed in Appendix A, Section 2.11.2.2). The resolution of this issue will be described in a supplement to this report.

For the "untied" downcomers, however, the staff concluded that the specification of a lateral load equivalent, even for a vertical loading condition, would be acceptable, because the downcomer itself acts primarily as a lever, manifesting stresses in the downcomer-vent header connection. However, the staff is requiring (Appendix A, Section 2.11.2.1) that a more accurate determination of the FSTF downcomer response characteristics (i.e., natural frequency and damping) be developed to ensure a conservative dynamic load factor scaling. The staff has concluded that, with this correction, the proposed load specification will provide a conservative estimate of the condensation oscillation loads on "untied" downcomers.

### 3.8.3 Condensation Oscillation Vent System Pressure Loads

The condensation process produces an oscillatory pressure within the vent system. The peak positive and negative pressures from the FSTF data are specified as a continuous sinusoidal function for each of the components in the vent system

(i.e., downcomers, vent header, and main vents), for the duration of the condensation oscillation period. The staff has concluded that this specification will provide a conservative estimate of the oscillatory pressure transient within the vent system during the condensation oscillations.

### 3.9 Chugging Loads

"Chugging" refers to the unsteady condensation process which occurs late in the blowdown when the vent flow rates are low. Rapid condensation causes the pool water to reenter the downcomers. This is followed by a quiescent period until the steam-water interface is forced back out into the pool. Thus, chugging appears as intermittent events which occur at intervals of approximately 1 to 2 seconds.

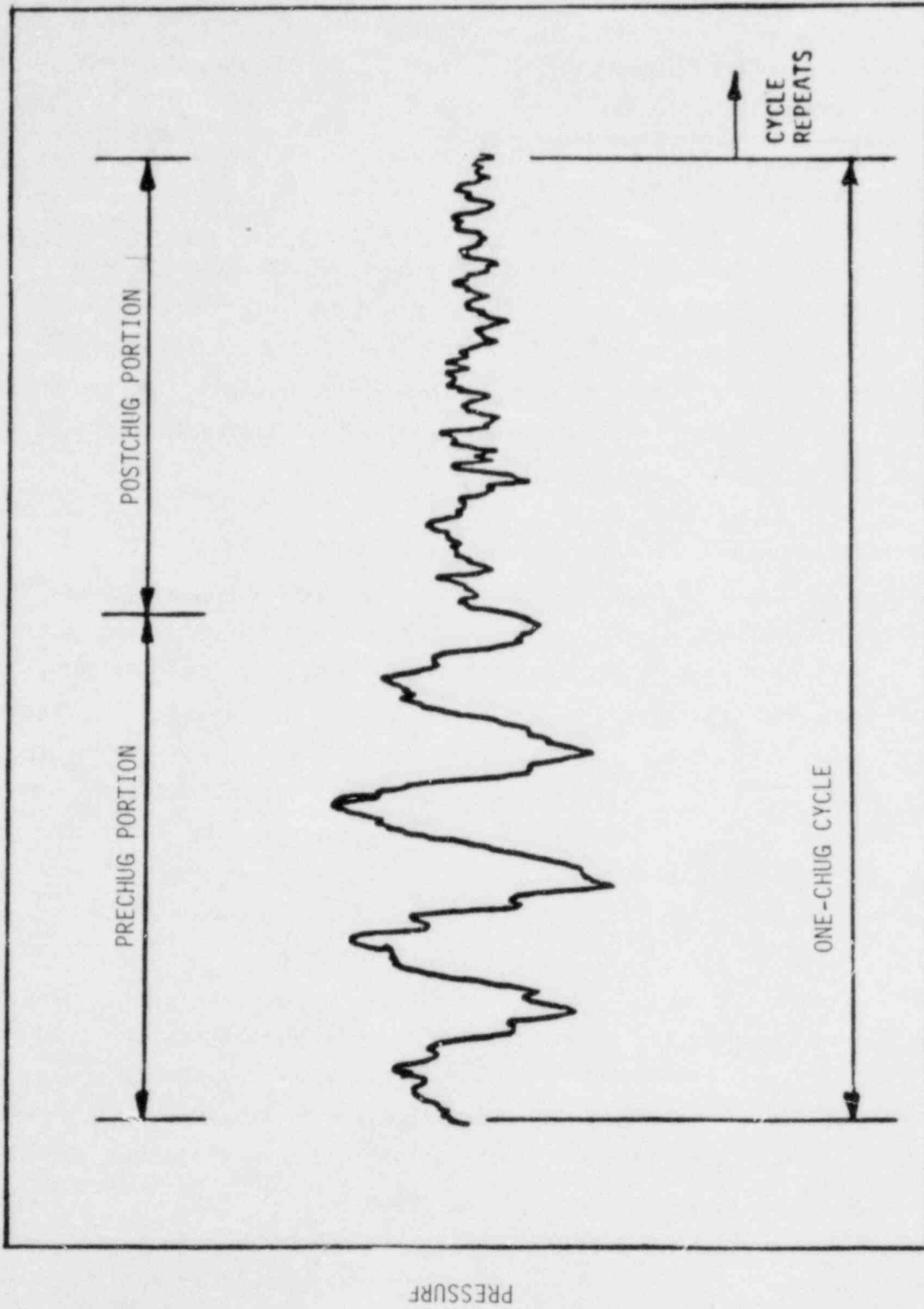
Significant chugging loads were observed in four of the FSTF tests (M1, M4, M9, and M10), as described in Section 3.8. Little or no chugging was observed in the other FSTF tests (M2, M3, M5, M6, M7, and M8). Consequently, the regime of chugging is much more clearly defined than the condensation oscillations, and the data base more extensive.

The duration of the chugging periods has been conservatively bounded from limiting containment response analysis, with the exception of the duration of the chugging period for the SBA (as described in Section 3.2.2).

#### 3.9.1 Chugging Loads on the Torus Shell

The intermittent pressure pulses on the torus shell during chugging appear as several cycles, followed by a decaying "ring out" (as shown in Figure 3.9-1). For the purpose of load definition, this phenomenon was separated into a "prechug" and a "postchug" period. The prechug describes the initial oscillations of the event, while the postchug describes the subsequent ring out.

Because the typical Mark I structural response was found not to be particularly sensitive to the amplitude-frequency spectra of the prechug observed in the FSTF, the prechug load specification was derived directly from the data of test M9. No effort was made to remove the potential contribution of fluid-structure interaction.



TIME

Figure 3.9-1 Chugging torus shell pressure transient.

The postchug period, however, contains a significant amount of structural response and, therefore, a number of structurally sensitive frequencies. Consequently, the same coupled fluid-structure analytical model that was used to analyze the condensation oscillation loads (Section 3.8.1) was also used to derive a "rigid-wall" amplitude-frequency spectra for the postchug loads. Eighteen maximum-amplitude chugging events from tests M1, M4, and M9 were used to develop the load specification. The conservatism of this technique has been confirmed, similar to the condensation oscillation loads, by comparing the predicted structural response of the FSTF with actual structural response data (Ref. 45). As in the case of condensation oscillations, these specifications are given in terms of a bottom-center pressure. The following discussion describes the distribution in load magnitude and phase.

In all but one of the FSTF tests, chugging events at the ends of the eight downcomers were not well synchronized. In M1 there were, however, periods of time during which the chugging was roughly synchronized to produce "pool chugs." However, the spatial distribution of the pressure oscillations on the torus walls in either case could not be represented by simple distributions as was done for the condensation oscillations. To simplify the load definition, the randomness in synchronization and in spatial distribution of the loads has been congealed into both symmetric and asymmetric shell-pressure specifications, which are conservatively based on the worst cases experienced in the FSTF. Both are somewhat arbitrarily based on a distribution of pressure in the cross-sectional plane identical to that used for condensation oscillations with an amplitude increasing linearly with pool depth. The symmetric load requires uniform application around the torus centerline. The asymmetric load requires the maximum to be applied at one axial location and decreasing magnitudes applied at axial locations further away (as shown in Figure 3.9-2). The latter distribution is not the bounding case that could be envisaged (which would correspond to having zero at the opposite side of the torus from the point at which the maximum amplitude is applied). However, the staff considers the distribution specified to be reasonable, since the worst case in which maximum chugging and zero chugging occur simultaneously in diametrically opposite parts of the torus is exceedingly unlikely, given the randomness in both magnitude and spatial distribution observed in all condensation test data.

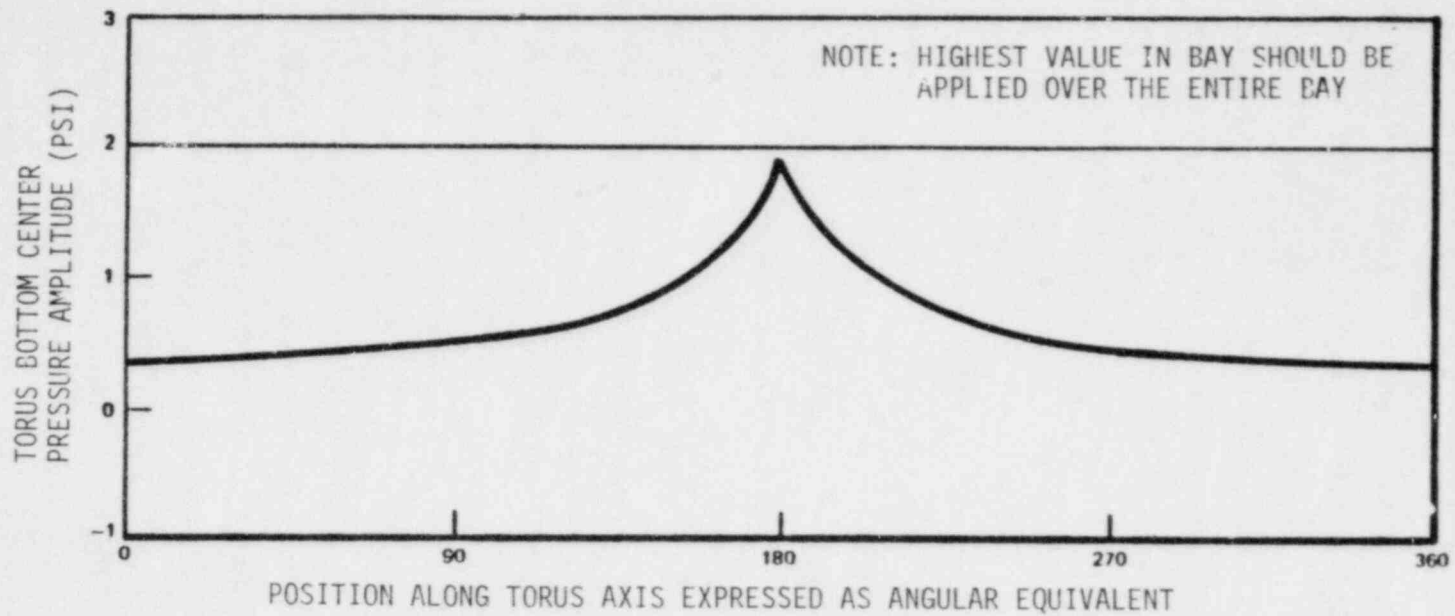


Figure 3.9-2 Chugging asymmetric torus shell pressure.

The staff has concluded that the proposed specifications for the prechug and postchug loads will provide a conservative estimate of the torus shell pressure transient during chugging, provided they are used with a coupled fluid-structure analytical model (as described in Appendix A, Section 2.12.1).

### 3.9.2 Chugging Downcomer Loads

During the chugging regime, water is intermittently pushed out and sucked back into the downcomers. As the water interface is pushed out of the downcomer mouth, the steam suddenly comes into contact with cold water and a condensation burst occurs, causing depressurization of the steam bubble. If the steam-water interface shape is asymmetric with respect to the downcomer centerline, the depressurization and subsequent collapse against the downcomer walls will cause a rapid lateral force transient. The downcomer lateral loads during chugging were derived from the FSTF data using the same technique described for the downcomer condensation oscillation loads (see Section 3.8.2). The staff review of the proposed chugging downcomer load has similarly been separated into the loads on "untied" and "tied" downcomers. However, the downcomer chugging loads were found to be less prone to dynamic amplification than the condensation oscillation downcomer loads, because the loading occurs in the form of somewhat randomly separated triangular pulses, as opposed to the sustained sinusoidal load of the condensation oscillations.

The proposed RSEL amplitude spectra, as applied to the untied downcomers, is acceptable with the following exceptions (as described in Appendix A, Section 2.12.2.1).

- (1) The load specification for comparison to the ASME Code primary stress limits shall be based on the maximum measured resultant static equivalent load (RSEL) in the FSTF, rather than the proposed upper 95-percent confidence limit.

This requirement was imposed because comparisons of the proposed load specification with the FSTF test data indicated that an actual load on the downcomer could exceed the statistically derived maximum load. The maximum RSEL observed in the entire data base is, however, sufficiently conservative to assure the integrity of the downcomer during chugging.



- (2) The fatigue usage analysis for each downcomer shall be based on a statistical loading with a 95-percent probability of nonexceedance.

The LDR did not specifically define a separate load for the downcomer fatigue analysis. However, as a corollary to position (1), above, the staff concluded that a statistically derived load is appropriate for the downcomer fatigue analysis (repeated loadings) due to the observed variation in the RSEL magnitudes.

- (3) The multiple downcomer loading to assess statistical directional dependence shall be based on a probability of exceedance of  $10^{-4}$  per LOCA.

This requirement relates to the potential for a number of downcomers experiencing a lateral load in the same direction at the same time, producing a net loading on the vent system and its supports. The load magnitude probability function shown in Figure 3.9-3 was derived from a statistical analysis of the RSEL/phase direction data from the FSTF. The staff concluded that the combined probability of a LOCA and the probability of a specific downcomer lateral load on any number of downcomers should be less than  $10^{-7}$  per reactor-year, and, in consideration of the small load increase associated with the lower RSEL probability levels, the staff concluded that a probability of exceedance of  $10^{-4}$  per LOCA would be adequately bounding.

The LDR proposed that the "tied" downcomers would be evaluated in the same manner as the "untied" downcomers, using "tied" downcomer data. However, the LDR does not adequately specify a procedure for deriving the strain in the tie bar between a downcomer pair. The staff's criteria (Appendix A, Section 2.12.2.2) stipulate that the stress in the tie bar shall be evaluated by assuming that one of the two tied downcomers is subjected to a dynamic load of triangular shape, with an amplitude of

$$F_{\max} = \text{RSEL}/\pi f t_d$$

where the RSEL is the maximum measured RSEL for an untied downcomer during chugging,  $f$  is the lowest natural frequency of vibration (Hz) of an untied downcomer for the specific plant, and the duration of the load,  $t_d$ , is assumed to be 3 milliseconds.

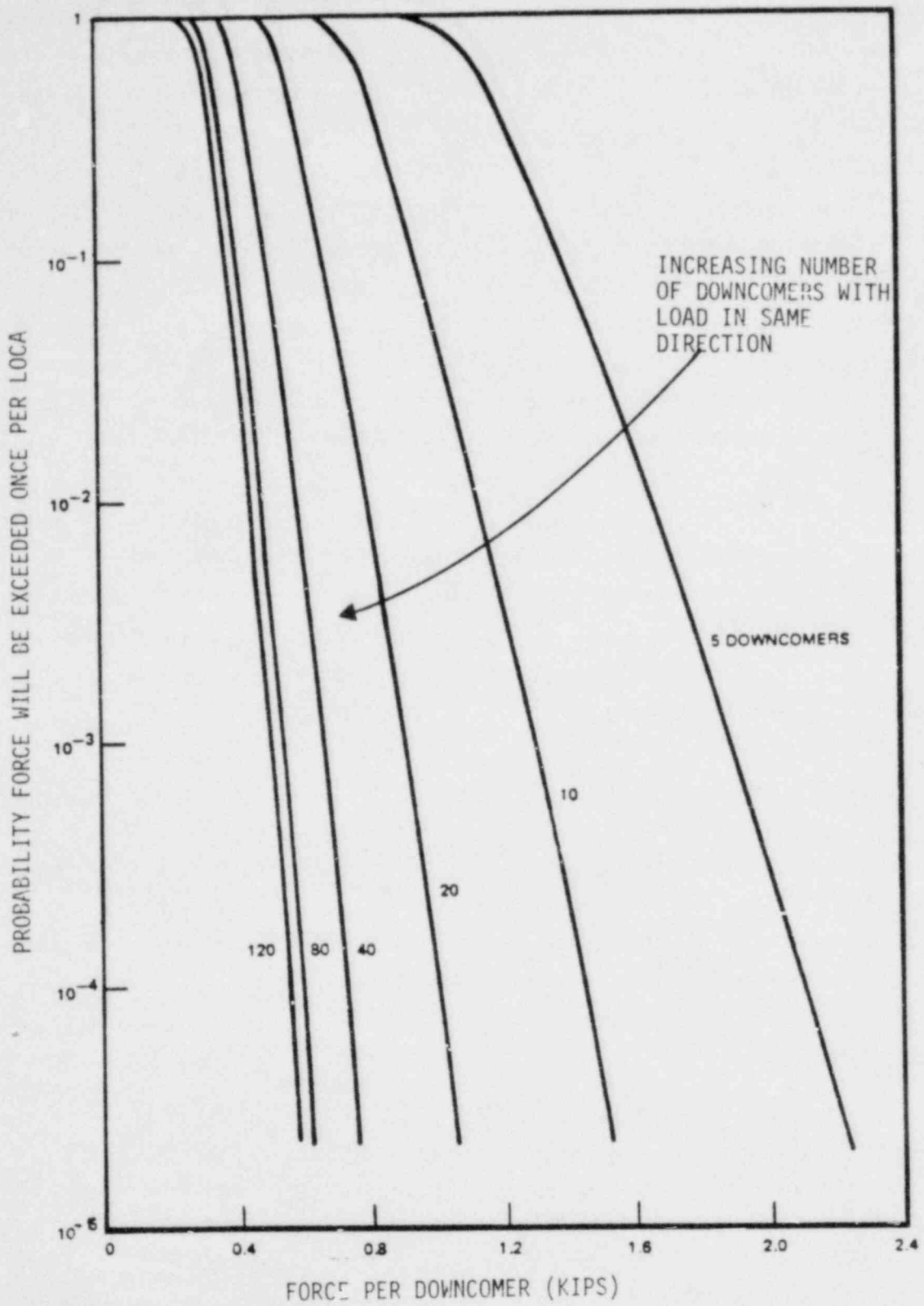


Figure 3.9-3 Multiple downcomer chugging load probability distribution.

The load direction shall be taken as that (in the horizontal plane) which results in the worst loading condition for the tie-bar and its attachments to the downcomers.

The criteria above were developed from the following arguments: First, based on the FSTF data, one may conclude that the presence of the tie bar does not significantly affect the lateral loading expected on either downcomer in the absence of a tie-bar. Because of the short duration of the chugging lateral loads, their somewhat random occurrence in time, and their random direction when they occur, the probability that the two tied downcomers are simultaneously loaded in a reinforcing manner is very small. Thus, the load on the tie-bar may be evaluated by assuming that only one downcomer is loaded. Because the duration of the chugging load is very small compared with the natural period of the downcomer oscillation, but large compared with the response time of the tie-bar (at least in tension), the loading on the downcomer must be specified as a dynamic force. Therefore, by definition, the actual peak dynamic load,  $F_{\max}$ , is related to the resultant static equivalent load (RSEL) and the dynamic load factor (DLF) by

$$F_{\max} = \text{RSEL}/\text{DLF}$$

The dynamic lateral load during chugging can be approximated as a triangular pulse with peak load  $F_{\max}$  and duration  $t_d$ . For such a load history, the DLF is given by

$$\text{DLF} = \frac{2}{t_d \omega} \left[ 2 \cos \left( \frac{\omega t_d}{2} \right) - \cos \omega t_d - 1 \right]$$

where  $\omega$  is the natural frequency (in radians per unit time) of the downcomer's lateral oscillation. In the application considered here,  $\omega t_d$  is small compared with unity, and, therefore, the DLF may be approximated as

$$\text{DLF} \approx \omega t_d / 2$$

Substituting the DLF approximation into the relation for  $F_{\max}$  results in the amplitude specification in the staff's criteria. The triangular force history

with this  $F_{\max}$  is to be applied on one of the two downcomers, and a dynamic calculation is to be performed for the tie-bar stress. The staff's criteria are conservative for the tie-bar stress, because that stipulate (1) that the lowest natural frequency of the downcomer be used in deriving the load, (2) that the value of  $t_d$  to be used is at the lowest end of the spectrum expected (based on a Mark II lateral load analysis) (Ref. 39), and (3) that the load direction be taken as that which results in the worst loading for the tie bar and its attachments.

The staff has concluded that the proposed load specification, as modified by its requirements, will provide a conservative estimate of the loads on the downcomers and the reaction loads in the downcomer tie-bar and vent system which occur during the chugging regime.

### 3.9.3 Chugging Vent System Pressure Loads

The oscillatory pressure loads on the components of the vent system are defined by dividing the pressure spectra into a low-frequency chug event frequency range, a range corresponding to the first main vent acoustic frequency, and a range corresponding to the first downcomer vent acoustic frequency. Worst-case measured amplitudes are defined for each from the FSTF data.

The staff has concluded that the proposed load specification will provide a conservative estimate of the oscillatory pressure loads within the vent system during chugging.

### 3.10 Safety-Relief Valve Discharge Loads

The phenomena associated with safety-relief valve (SRV) discharge to the suppression pool are described in Section 2.3. For the purpose of this evaluation, the staff has restricted its review to the load definition procedures proposed for the T-quencher discharge device shown in Figure 3.10-1 (Ref. 47). The load specifications described in the subsequent sections were derived specifically for this discharge device from full-scale tests in the Monticello plant (Ref. 47) and one-quarter-scale parametric tests (Ref. 48).

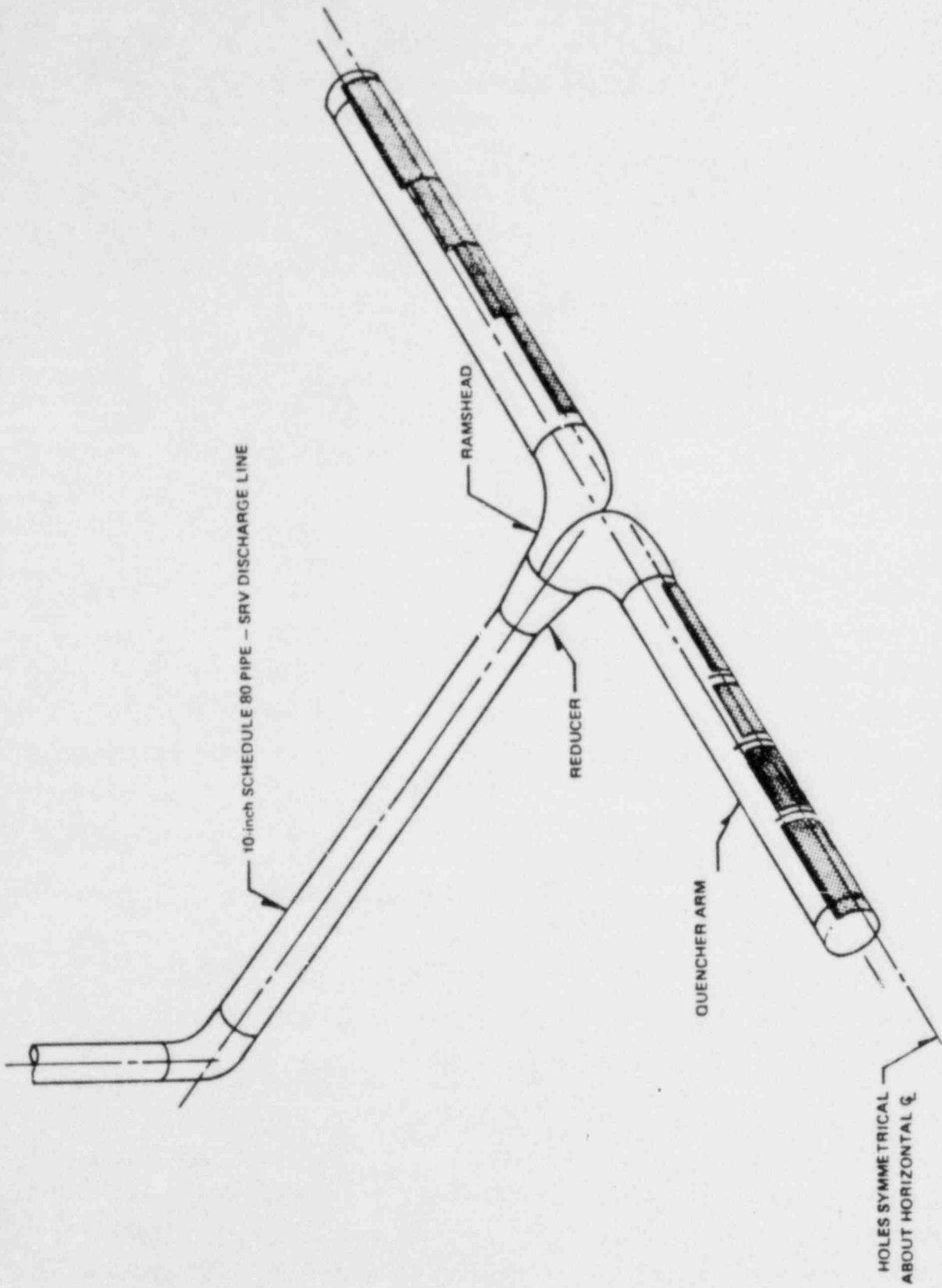


Figure 3.10-1 Mark I T-quencher shell discharge device.

Two of the Mark I licensees have proposed installing Y-quencher SRV discharge devices. As described below, quencher discharge devices generally behave in a similar manner, so that most of the proposed load definition procedures (i.e., SRV discharge line pressure, temperature, and reflood transients; quencher thrust loads; and SRV discharge event cases) are applicable with little or no change. However, the air-clearing loads on the torus are significantly affected by the geometry of the quencher. In addition, a number of Mark I licensees have indicated that the analysis techniques for the T-quencher air-clearing loads on the torus are overly conservative. Consequently, the staff has included requirements (Appendix A, Section 2.13.9) which permit plant-specific in-plant tests to be used to define the air-clearing loads for either quencher device. (The bases for these test requirements are described in detail in Section 3.10.2.)

### 3.10.1 SRV Discharge Line Pressure Transient

Following SRV actuation, high-pressure steam released from the primary system will compress the air initially contained in the SRV discharge line (SRVDL) and force the water slug in the submerged pipe out into the suppression pool. During this transient, the line pressures are significantly higher than the quasi-steady values that prevail following water clearing. The methods proposed in the LDR to define these transient pressure loads and the associated reaction loads on pipe segments are based on an analytical model which has been derived from first principles (Ref. 49). This model simulates the transient flow of gas and water in the SRVDL, using appropriate conservation equations together with conservative assumptions regarding plant-operation conditions. A properly formulated sub-model accounts for steam condensation on the interior pipe walls.

Guidelines for the choice of input parameters for these calculations are provided in Section 5.2.1.3 of the LDR. Substantial conservatism is introduced by the values recommended by these guidelines.

Comparisons of calculated pressure transients with pipe and support stresses from the Monticello test data have been presented to support the adequacy of

the model (Ref. 50). The comparisons are generally favorable, with over-prediction of the loads ranging from 20 percent for initially cold pipe conditions to as much as 85 percent for initially hot pipe cases. These deviations are consistent with the conservatism which is intrinsic to the analytical model.

Based on its review of the analytical bases and the supporting test data, the staff finds the proposed analysis technique acceptable.

### 3.10.2 SRV Air-Clearing Torus Pressure Loads

Following expulsion of the submerged water leg, the air initially contained in the SRVDL is driven through perforations in the quencher arms at high pressure and into the suppression pool. The precise manner in which this occurs is a complex phenomenon, involving spatial variations as more and more holes are cleared, variations in the rate at which the air exits as a result of a decrease in the driving pressure, and break up of the discrete air jets into bubbles and their subsequent coalescence. Ultimately, following the expulsion of essentially all of the air, one or more pockets of a noncondensable gas at elevated pressure (relative to local hydrostatic pressure) are formed in the suppression pool. The subsequent expansion of these "bubbles" accelerates the surrounding water, creating a transient pressure field within the pool, which is transmitted to the submerged boundaries. Because of the inertia of the accelerated water, this transient pressure field exhibits an oscillatory character as the pockets of noncondensable gas first overexpand and then are recompressed as the lowered pressures allow a reversal of the bulk water motion. As the bubbles execute these alternate expansions and compressions, buoyancy also causes them to rise until breakthrough occurs at the pool surface, completing the air-clearing transient and associated pressure loads on the submerged boundaries.

The key element of the load definition procedure proposed in the LDR is a semi-empirical analytical model which predicts the transient characteristics of the bubble in the pool (Ref. 51). Using the water-clearing and air-discharge conditions derived from RVFORCE (Section 3.10.1), this model describes the evolution of the air bubble during the charging phase of the air-clearing process and the subsequent bubble dynamics in terms of the temporal variation of bubble pressure, radius, and vertical position. With

this information, the spatial and temporal variation of the pressures experienced by the submerged boundaries of the suppression pool are also derived. Procedures for combining the loads as a result of several bubbles (associated with multiple-valve actuations) have also been developed.

The equation which describes the bubble dynamics is a modified form of the classic "Rayleigh Bubble" solution. The modifications include a mass addition term to represent the initial air-charging phase, gravitational forces to represent the buoyancy, and appropriate thermodynamics to account for energy conservation. The latter two modifications are modeled using reasonable first principle assumptions. Representation of the mass addition term is strictly empirical and is derived by employing both Monticello and subscale parametric test data. An additional assumption is that the air temperature is equal to the pool temperature during the charging phase.

The spatial variation at the submerged boundaries for quenchers located along the vertical axis of the torus has been determined empirically using attenuation rules derived from the test data (Ref. 51). Attenuation rules for quenchers located off the vertical axis of the torus have also been developed from the subscale test data (Ref. 45).

The analysis technique in the LDR has further proposed the use of the "square-root-of-the-sum-of-the-squares" (SRSS) rule for the superposition of pressure loads as a result of multiple bubbles caused by multiple SRV actuations.

Solution of the bubble dynamics equation is accomplished numerically using the computer code QBUBBS. Output from this code includes the pressure loads at the boundaries for the given plant-unique geometry. A multiplier of 1.65 is applied to the predicted value to define the wall-pressure loads. This multiplier is used to bound experimentally observed loads, as will be discussed below. The program also supplies information relative to the bubble characteristics needed to perform submerged-structure drag loads (see Section 3.11.6). In this case, a conservative multiplier of 2.5 is applied to the mass addition term to bound observed bubble pressures. Guidelines for the specification of conservative inputs are also provided in the LDR.



The basis for calibration, benchmarking, and verification of the model described above consists of the in-plant tests performed in the Monticello plant and a series of one-quarter-scale parametric tests (as described in Section 3.10). The Monticello tests involved a total of 46 SRV actuations and were conducted at essentially fixed values of discharge line volume, discharge line steam-flow rate, pool temperature, water-leg length, submergence, and torus airspace pressure. Table 3.10-1 shows the specific value of these parameters during the Monticello tests and provides a comparison with the overall range of Mark I plants. The only effects examined during these tests were those of subsequent actuation and multiple-valve actuations, although the data do provide information on spatial distribution of boundary loads and bubble pressure attenuation. During the one-quarter-scale parametric tests, which involved 107 simulated SRV first actuations, the effects of the other variables were examined, as was the effect of submerged SRVDL geometry and pressure differential between SRVDL and torus. Table 3.10-1 also includes the range of these parameters, scaled up to prototypical plant conditions.

An examination of Table 3.10-1 shows that there is significant variance of Mark I plant parameters from the conditions tested in the Monticello plant. Thus, the one-quarter-scale tests play a crucial role in the SRV air-clearing load definition, in that they provide the sole basis for development of the requisite trend information for extrapolation to the differing plant-unique conditions. In view of their importance, the applicability of the subscale test results in terms of dynamic similitude, relative to the prototype, requires justification via rigorous scaling laws (Ref. 52).

In summary, the basis for the proposed load definition involves four key elements:

- (1) an in-plant test series from which load levels at one representative set of plant conditions were determined;
- (2) a semi-empirical analytical model to be used for extrapolation to other plant conditions;
- (3) subscale tests from which the trends needed for (2), above, are derived;  
and

Table 3.10-1 Comparison of Mark I SRV Parameters

| Characteristic                       | Mark I Plant Range | Monticello Tests | 1/4-Scale Tests* |
|--------------------------------------|--------------------|------------------|------------------|
| SRVDL volume (ft <sup>3</sup> )      | 25 - 106           | 49               | 24 - 98          |
| SRV flow rate (lb <sub>m</sub> /sec) | 180 - 270          | ~200             | 100 - 320        |
| Pool temperature (F)                 | 120 max            | 50 - 84          | Not varied       |
| Water-leg length (ft)                | 3 - 22             | 13.5             | 6.6 - 26.0       |
| Submergence (ft)                     | 3 - 11             | 6.5              | 4 - 13.5         |
| Torus pressure (atm)                 | 1 - 2.8            | 1.0              | 1 - 3            |
| Subsequent actuations                | Yes                | Yes              | No               |
| Multiple actuations                  | Yes                | Yes              | No               |
| Torus shell diameter/thickness       | 300 - 900          | ~600             | N/A              |

\*Full-scale equivalent conditions.

- (4) a scaling analysis which demonstrates the applicability of the results obtained from (3), above.

The staff and consultants have reviewed this basis in detail and find that the proposed methods are not acceptable in all respects. Accordingly, they have developed a set of acceptance criteria which represent modification of, and impose restrictions on, the proposed methods (see Appendix A, Section 2.13.3).

The unacceptability of the analysis techniques relates primarily to the scaling laws used to select the geometry and test conditions used in the one-quarter-scale parametric tests. The staff has concluded that the proposed scaling relationships do not ensure dynamic similitude of the tested subscale device with the prototype. The deficiency arises as a result of improper modeling, in the scaling analysis, of dissipative mechanisms which are known to exist in full-scale conditions. In view of this conclusion, the credibility of the analytical model in terms of its ability to predict trends correctly is seriously compromised. This determination has been reached because the analysis employs empirical constants derived directly from the subscale parametric tests to complete the mathematical formulations and has been structured so as to reproduce the trends observed in those tests.

The approach adopted by the staff to resolve these uncertainties and to expedite the development of a conservative load specification consisted of comparisons of the design-load trends predicted by the LDR methods, with both in-plant and full-scale load data obtained using other quencher-type devices, and other load definition techniques accepted by the staff. In those cases where the comparisons indicate similar or conservative trends, the proposed procedures have been found acceptable. In those cases where the proposed procedures exhibit nonconservative trends, the staff has imposed restrictions to ensure that all experimentally observed load trends are bounded. In the judgment of the staff, sufficient similarity exists between these other devices (Mark II T-quencher, Mark III cross-quencher) and the Mark I T-quencher design to ensure similar performance with respect to trends to justify this approach. Table 3.10-2 presents a comparison of the geometric features which characterize the various quenchers. Also included in the table are the range of test conditions at which the performance of the various devices has been evaluated experimentally.

Table 3.10-2 Comparison of Quencher Geometries and Test Conditions

| Characteristic                    | Mark I<br>T-Quencher | Mark II<br>T-Quencher     | GE<br>Cross-Quencher | KWU<br>Cross-Quencher |
|-----------------------------------|----------------------|---------------------------|----------------------|-----------------------|
| Hole diameter                     | Same                 | Same                      | Same                 | Same                  |
| Arm length (ft)/number<br>of arms | 9.5/2                | 4.8/2                     | 4.8/2                | 4.8/4                 |
| Arm diameter (ft)                 | 1.06                 | 1.33                      | 1.06                 | 1.33                  |
| Total hole area<br>(normalized)   | 1.0                  | 0.70                      | 0.94                 | 1.40                  |
| Hole pitch                        | Same                 | Same                      | Same                 | Same                  |
| SRVDL volume (ft <sup>3</sup> )   | 49                   | 73 and 104                | 65                   | 50                    |
| Steam flow (lbm/sec)              | 200                  | 63 - 225                  | 210 - 245            | 28 - 306              |
| Pool temperature (°F)             | 50 - 84              | 74 - 179                  | 76 - 95              | 90 - 170              |
| Water-leg length (ft)             | 13.5                 | 20                        | 17.7                 | 14                    |
| Subsequent actuation              | Yes                  | Yes                       | Yes                  | Yes                   |
| Multiple actuations               | Yes                  | N/A                       | Yes                  | Yes                   |
| Facility                          | In-plant             | Single-cell<br>Full-scale | In-plant             | In-plant              |

The following sections discuss the results of the staff evaluation of each of the pressure-load and frequency trends predicted by the LDR analysis techniques as they compare to other available information. This information is summarized in Table 3.10-3.

#### 3.10.2.1 Trend with Discharge Line Volume

The LDR procedure predicts an increase of SRV pressure loads with an increase of SRV discharge-line air volume to the maximum line volume of interest (106 cubic feet). Comparison with all available data indicates that this prediction represents a conservative trend for SRV loads, particularly for line volumes greater than about 65 cubic feet, where the data exhibit a distinctly decreasing trend. The LDR procedure is also very conservative relative to the Mark III analysis technique (Ref. 53), which predicts no increase in the load magnitude for line volumes greater than 65 cubic feet. Based on these comparisons, the staff finds the proposed load trend with discharge-line volume acceptable and concludes that no increase in load magnitude is necessary for line volumes greater than 65 cubic feet. This conclusion is reflected in the acceptance criteria (Appendix A, Section 2.13.3.1).

With regard to the frequency of oscillations during first actuations, the LDR method has been found to predict accurately the trends exhibited by all of the data. Specifically, a distinct inverse dependence of frequency on the cube root of the discharge-line volume is apparent in both the data and the LDR method. The staff has concluded that the proposed method will provide a "best-estimate" of the variation of the bubble frequency with discharge-line volume and is, therefore, acceptable.

#### 3.10.2.2 Trend with Discharge-Line Steam Flow Rate

For steam flows greater than the rate at which the Monticello tests were performed (200 pounds per second), the LDR procedure predicts a more rapid increase in first-actuation peak-pressure amplitude than that observed experimentally and that predicted by the Mark III analysis technique. At lower values, the LDR trend is somewhat nonconservative (i.e., decreases faster relative to the Mark III trend). The staff does not consider this a serious

Table 3.10-3 Comparison of Mark I T-Quencher Load Trends

| Influencing Parameter        | Pressure Amplitude Trends  | Bubble Frequency Trends           | Staff Evaluation                                     |
|------------------------------|--|-----------------------------------|--|
| SRVDL volume                 | Conservative relative to other information                                       | Consistent with other information | Acceptable   |
| SRV steam flow rate          | Conservative for MS > 200 lb/sec<br>Slightly nonconservative for MS < 200 lb/sec | Consistent with other information | Acceptable   |
| Suppression pool temperature | Conservative relative to other information                                       | Consistent with other information | Acceptable   |
| Water-leg length             | Conservative for LW < 13.5'<br>Nonconservative for LW > 13.5'                    | Consistent with other information | Acceptable for LW < 13.5'<br>Criterion 2.13.3.1.1    |
| Submergence                  | Consistent with other information  | Consistent with other information | Acceptable   |
| Torus pressure               | Consistent relative to other information   | Consistent with other information | Acceptable   |
| Subsequent actuations        | Nonconservative relative to other information                                    | Consistent with other information | Not Acceptable<br>Criteria 2.13.3.1.2 and 2.13.3.4.2 |

deficiency since design loads are based on conservatively high values of steam flow (i.e., 122.5 percent rated flow); these values are, in all cases, in excess of 200 pounds per second. The staff also finds that the experiments and both load definition techniques indicate that the frequency of the forcing function is essentially independent of steam flow. Accordingly, the staff finds the Mark I procedures acceptable for the prediction of single-valve first-actuation trends with steam flow.

#### 3.10.2.3 Trend with Pool Temperature

Predictions of the LDR procedures for first-actuation peak-pressure amplitudes compare favorably with both the experiments and the Mark III analysis technique. Conservative trends prevail throughout the pool temperature range of interest, with the greatest conservatism exhibited at the higher values (>100° F). Trends for frequency are in satisfactory agreement. Consequently, the staff finds the methods acceptable for predicting single-valve first-actuation trends with pool temperature.

#### 3.10.2.4 Trend with Water-Leg Length

The LDR procedures predict a decreasing trend of peak-pressure amplitude with increasing water leg. This is in direct contradiction with behavior suggested by available experiments (exclusive of the subscale parametric tests) and the Mark III analysis technique. For water legs less than that tested at Monticello (13.5 feet), the LDR method is conservative relative to other information, since it predicts increasing loads. For water legs greater than 13.5 feet, the staff considers the proposed analysis technique to be nonconservative, yielding as much as a 30-percent under-prediction in loads at the maximum water leg of interest (22 feet). A detailed examination of the other available data and the Mark III analysis technique indicates that load levels are relatively insensitive for water legs greater than 13.5 feet. Accordingly, the staff requires that for Mark I plants with a water leg greater than 13.5 feet, it shall be assumed that the load is equal to that determined by the LDR method at 13.5 feet. No significant trends of the load frequency with water-leg length are exhibited by experiment or implied by either load definition technique.

Accordingly, the proposed procedures are acceptable with regard to water-leg trends, subject to the restriction cited above.

#### 3.10.2.5 Trend with Submergence

All available information suggests that there is no explicit dependence of first-actuation peak-pressure loads on submergence beyond that accounted for by the water-leg dependence. A frequency dependence on submergence is apparent, however. The LDR method correctly predicts the observed trends. Accordingly, the staff finds the analysis technique acceptable with respect to submergence trends.

#### 3.10.2.6 Trend with Torus Airspace Pressure

The LDR procedure predicts significant increases in first-actuation peak-pressure loads at elevated torus pressure. This result is consistent with the trends observed with the subscale parametric test results. No in-plant or full-scale data exist to verify this effect.

The staff has, however, reviewed the subscale tested conditions in comparison with the expected conditions during events which would result in an increase in torus pressure. In the event of a small-line break in the primary system, the drywell would be pressurized by the blowdown from the break. Carryover of the drywell air/steam mixture to the torus through the vent system will also pressurize the torus airspace. The same mixture will also be forced into the SRV lines via the vacuum breakers on the lines which are located inside the drywell. Bounding estimates indicate that, as a result, the SRV line will contain a mixture of air and steam at a high pressure (relative to that at normal conditions) but with a lower air volume. These initial conditions, however, were not simulated during the subscale tests, which were performed with essentially pure air. The air mass in the one-quarter-scale tests is much greater than that expected in a prototypical condition and is, in fact, greater than that for normal actuations. Because air mass in the SRV line is a dominant factor controlling the SRV loads, the subscale tests are conservative. The Mark I analysis technique also predicts a strong influence of torus pressure on bubble frequency. In this case, the staff finds that the predicted trend



is consistent with the underlying physics of the phenomena; i.e., the trend correlates well with the square root of the local hydrostatic pressure, which is anticipated on physical grounds. The predicted trend is also in agreement with other analyses (Ref. 54).

Based on these considerations, the staff finds the proposed procedures acceptable for the prediction of load trends with torus airspace pressure.

#### 3.10.2.7 Trend with Subsequent Actuation

The effect of repeated SRV actuations on the magnitude and frequency of SRV air-clearing loads is derived solely from the in-plant Monticello tests. In general, the loads observed were lower than first-actuation values. Using "best-estimate" values to characterize the pipe conditions prevailing prior to subsequent actuations, the LDR method conservatively predicted these lower loads. The predicted frequencies agreed reasonably well with the observed means which were, in general, substantially higher than first-actuation values (by as much as a factor of 2). Using design values to characterize initial pipe conditions leads to predictions of loads comparable to first-actuation values and, therefore, considerably in excess of the measured loads.

All other available test results indicate that subsequent-actuation loads can be higher than first-actuation loads. The increases observed (in mean value) ranged from a minimum of 31 percent with the Mark II T-quencher to a maximum of 58 percent with a cross-quencher. For the first-actuation load observed in the Monticello tests, the Mark III analysis technique would apply a multiplier of 1.75 to define corresponding subsequent-actuation loads. These multipliers were developed to provide a substantial margin, corresponding to a 95-95 tolerance level, in recognition of the very stochastic behavior of observed loads and the considerable uncertainty regarding the physical mechanisms which give rise to the randomness.

In the judgment of the staff, there is insufficient understanding of the phenomenon to warrant the use of a purely mechanistic approach to subsequent-actuation load definition. The staff has examined the performance of the LDR method in detail and has concluded that the use of design first-actuation

loads for definition of subsequent-actuation loads provides such a bounding approach.

Staff studies indicate that the use of these design first-actuation loads will bound all experimentally observed values. Accordingly, the staff requires that the design first-actuation values of peak-pressure amplitudes be used to define suppression-pool SRV air-clearing loads for subsequent-actuation event cases (as described in Appendix A, Section 2.13.3.1).

With regard to the frequency of subsequent-actuation loads, the proposed methods predict a significant increase over first-actuation values. This is qualitatively consistent with most experimental observations in general and with the behavior observed in the Monticello tests in particular. Quantitatively, the predicted trends are in reasonable agreement with the trends of the observed means, although considerable data scatter does exist.

The staff finds that this scatter can be bounded adequately by application of a margin of  $\pm 40$  percent to the frequency predicted by the LDR methods. This margin will also provide an adequate bound of subsequent-actuation bubble frequencies observed during all full-scale experiments for which information is currently available to the staff. Accordingly, the staff requires that structural, piping, and equipment evaluations during SRV events involving subsequent actuations be carried out with the forcing function frequency varied over the entire range implied by the  $\pm 40$  percent margin applied to the predicted values (as described in Appendix A, Section 2.13.3.4).

In addition to the concerns that are identified in Table 3.10-3, the staff has addressed a number of other issues which have bearing on the adequacy of the proposed analysis techniques, but which are not explicitly related to load trends. These include: (1) the adequacy of the load predicted for first actuation of a single valve (SVA) in an absolute sense (i.e., does the method provide a conservative specification for the conditions tested at Monticello?); (2) the adequacy of the method relative to the spatial distribution and bubble-pressure attenuation; (3) the acceptability of the proposed method of superposition of multiple valve loads (MVA); and (4) the impact of any potential fluid-structure interaction (FSI) present during the Monticello test program. The

staff's comments, evaluation, and conclusions for each of these areas are presented below.

#### 3.10.2.8 Single-Valve Actuation

Comparisons between the "best-estimate" predictions of the proposed method and the Monticello SVA test results (Ref. 47) show reasonable agreement with observed mean values of peak bubble pressure and torus shell pressure. A multiplier of 1.65 applied to the predicted peak shell pressures provides a bound of all observed values. Bubble pressures are bounded by increasing the theoretical air-flow rate through the perforations by a factor of 2.5. This approach for bounding bubble pressures is adopted to ensure that appropriate conservatism is also introduced in the "source" terms needed to define submerged structure loads (see Section 3.11.6).

The design-pressure loads that would actually be specified for the Monticello plant are, of course, substantially higher than the best-estimate values. Design torus pressures are approximately 12 psid compared to best-estimate values of 7 psid. The increase results primarily from the use of conservative design values for steam flow and pool temperatures, both of which are well above the corresponding Monticello test values and somewhat above conditions that are likely to prevail during an actual SRV first-actuation event. Based on the trend data available, the staff estimates that the use of these conservative design values provides a margin of approximately 40 percent. Additional conservatism is provided by the analysis techniques via the spatial variation which is employed (to be discussed later). The frequency prediction is also in reasonable agreement with the observed mean frequencies in the Monticello data. Data scatter in this case is substantially less than that observed with subsequent actuation, which is consistent with other experimental observations. A margin of  $\pm 25$  percent is sufficient to bound conservatively the observed data spread. The staff also has made a detailed comparison of representative measured pressure wave forms with those predicted by the analysis. A typical predicted wave form is shown in Figure 3.10-2. The predicted wave form is characterized by an essentially constant frequency of oscillation, so that the total power is concentrated at a single frequency. The experimentally observed wave forms, on the other hand, consistently exhibit a spreading of the frequency

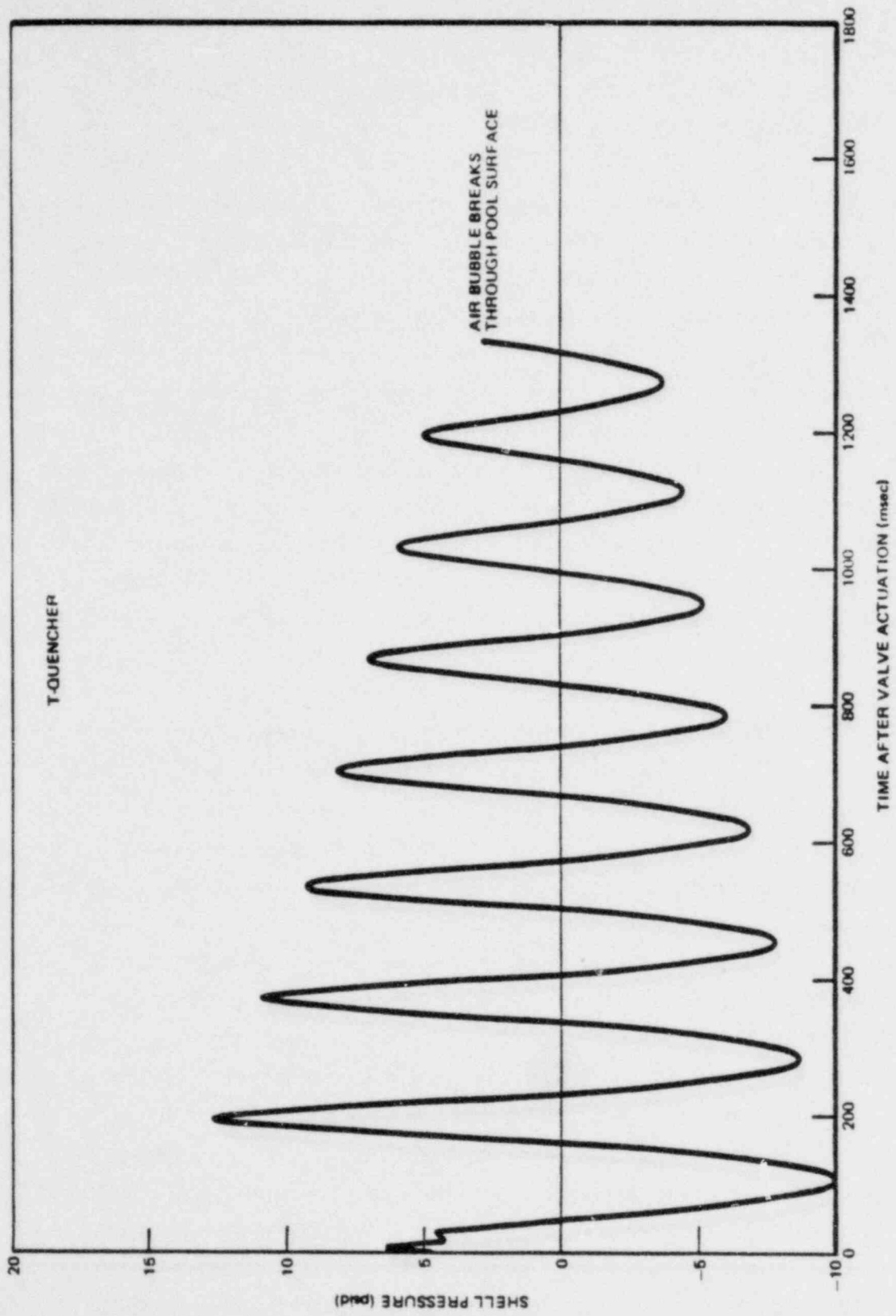


Figure 3.10-2 Typical T-quencher shell pressure transient.

with time. Thus, the proposed wave form represents a conservative forcing function for the structural response when the natural frequencies of the structures and/or components are within or close to the frequency band which has been established by the  $\pm 25$ -percent margin applied to the predicted frequency. Accordingly, the staff finds the proposed method, together with the  $\pm 25$ -percent frequency margin (Appendix A, Section 2.13.3.4), acceptable for defining the peak torus shell pressure loads that result from the first actuation of a single SRV.

#### 3.10.2.9 Spatial Distribution and Pressure Attenuation

As indicated above, the spatial distribution and pressure attenuation predicted by the LDR procedures are developed empirically, drawing directly on the experimental behavior observed during the Monticello and subscale tests. The staff considers the subscale tests to be correctly scaled for developing these features of the analysis. The data suggest that significant bubble attenuation occurs, in the sense that pressures recorded in the vicinity of the quencher centerline are significantly higher (by about 40 percent) than the peak values seen at the torus shell.

Data from both the Monticello and subscale tests show a very distinct lateral asymmetry with both peak bubble and torus shell pressures on the reactor side of the quencher consistently 30 percent to 50 percent higher than those recorded on the outboard side. A possible mechanism for this effect is the presence of an inclined submerged segment of the SRV discharge line. The lateral component of momentum that this arrangement imparts to the water slug in the discharge line may result in preferential clearing of the perforations on the reactor side of the quencher. This, in turn, allows venting of most of the high-pressure air in that direction. In addition to this lateral asymmetry, the data from the Monticello tests also exhibit a marked asymmetry in the axial direction. In this case, pressure differences as great as 50 percent were recorded between equidistant points on opposite sides of the quencher centerline. The axial asymmetry is probably the result of a slight offset in the installation of the quencher relative to the torus bay centerline. Some confirmation of this speculation is provided by the subscale tests, where no axial asymmetry was observed, presumably because the quencher was located symmetrically in the simulated torus.

A prediction of peak torus shell pressure for the point located directly below the quencher center is developed in terms of a 1/R attenuation from the predicted bubble pressure, using the experimentally observed variation. Two bubbles of equal strength are assumed to be formed at each side of the T-quencher arm. Their vertical track is assumed to be at the midpoint of the quencher arm and one (mean) bubble radius away from the torus centerline. This peak value is conservatively applied uniformly over a segment of the torus which extends longitudinally to 70 percent of the quencher arm length. In the direction perpendicular to the quencher arm, the pressure is attenuated to zero at the pool surface by means of a multiplier which is a function of the cosine of the local angle from the vertical. As indicated earlier, a multiplier of 1.65 is applied to the peak value. The uniform application of this peak pressure provides a large margin in terms of the global (spatially integrated) vertical loads experienced by the torus. The staff estimates this margin to be at least 20 percent. Beyond this region of uniform peak-pressure application, a 1/R attenuation is applied in the circumferential direction. Extensive comparisons of these spatial distributions have been presented for both the Monticello and subscale tests. In all cases, the data are conservatively bounded. Accordingly, the staff finds the proposed methods acceptable for prediction of spatial variation of the local peak-pressure loads. However, for the evaluation of global pressure loads on the torus (for the support structures assessment), the staff believes that the 1.65 bounding multiplier would be overly conservative because it was derived from peak-pressure measurements. Therefore, the staff's requirements (Appendix A, Section 2.13.3.2) permit a separate bounding multiplier to be specified from the Monticello data, based on the net vertical-pressure loads.

#### 3.10.2.10 Multiple Valve Actuations

For MVA event cases, the LDR procedure develops a peak-pressure amplitude at any particular point on the torus shell by combining the peak-pressure amplitudes that result from individual valves by the SRSS method. For a plant similar to the Monticello plant (8 quenchers equally spaced around a 98-foot major diameter torus), this method of superposition would imply that peak pressures directly below the quencher centerline for the all-valve case would be only 4 percent higher than those for a single-valve case. The Mark I

Owners Group has proposed that this method is justified on the basis of several MVA tests (three valves) conducted in the Monticello plant. These tests indicated that peak pressures were less than those observed during single-valve tests. This result can be qualitatively explained as being the result of slight variations in bubble entry times, bubble phasing, and individual bubble frequencies. However, the test report does not provide sufficient information to quantify any of these effects, beyond acknowledging that the delay time between actuation of the first and last valve was approximately "2/3 second" (Ref. 47).

It is the judgment of the staff that the loads experienced by submerged boundaries that result from several bubbles oscillating in phase with the same frequency would be that corresponding to algebraic summation of the individual contributions from each valve. The staff acknowledges that such synchronous behavior is highly unlikely. Nevertheless, it has concluded that there is not sufficient justification currently available to permit the use of the SRSS method to account for this effect in all cases. In particular, the staff does not consider the MVA tests performed at Monticello to be relevant to the potential synchronization of the bubbles in the pool as a result of the potentially large delay time between individual valve actuations.

Another deficiency in the proposed method relative to MVA event cases is that it does not take into account the free-pool-area-per-quencher effect which is implicit in both the Mark II and Mark III load specifications. For example, peak pressures for the all-valve case in the Mark III are taken to be 40 percent higher than single-valve loads to account for this effect (Ref. 53). In the case of Mark II, this effect is included indirectly by virtue of the fact that the peak loads which are specified bound those observed in a single cell (Ref. 54), which is the smallest expected to be encountered in the Mark II lead plant designs (in terms of pool area per quencher).

Based on these considerations, the staff finds the proposed method of superposition unacceptable and requires that the algebraic sum method (ABSS) be employed to define peak-pressure amplitudes for MVA event cases, provided that these do not exceed the predicted peak bubble pressures for the SVA analysis by a factor greater than used to bound either the local or global pressure load. This

upper bound reflects our recognition that peak torus pressures are not expected to exceed maximum local values of bubble pressure. The multiplier is applied to the predicted bubble pressures to be consistent with the observed attenuation from the quencher-centerline-to-torus-shell pressures, as discussed above.

Changes in the pool-area-per-quencher will affect the bubble frequency for MVA events because of variations in the virtual mass associated with each discharge device. The LDR method does not account for this effect. However, the staff has examined this issue in some detail and estimates that for Mark I plants the maximum adjustment to the mean bubble frequency for an all-valve discharge would be on the order of a 10-percent reduction (the adjustment for other MVA events would be substantially less). In view of the margins specified for the frequency uncertainty (Appendix A, Section 2.13.3.4), the staff concludes that a further adjustment to account for multiple-valve effects on bubble frequency is not necessary.

#### 3.10.2.11 Fluid-Structure Interaction

The concern regarding FSI effects relates to the applicability of the data base obtained from the Monticello in-plant tests to plants with differing FSI characteristics.

FSI is an effect caused by the motion of the torus shell (boundary) relative to the oscillatory pressure source that drives that motion. The motion of the torus shell will change the pressure measured on the torus shell and, if the motion is strong enough, will feed back to affect the source pressure as well.

Analytical studies have demonstrated that increased wall flexibility will tend to reduce the measured shell pressure for dynamic loads with higher frequencies than the structural natural frequency. The Monticello SRV discharge tests indicate that the measured bubble pressure frequency was less than the predominant shell response frequency. Therefore, the staff does not expect that there was a significant reduction in the shell pressures in the Monticello data as a result of FSI.



On this basis, the staff has concluded that no corrections to the methods previously described are required to account for any FSI effects which may have been present during the Monticello tests.

#### 3.10.2.13 Plant-Specific SRV In-Plant Tests

The analysis techniques described previously in this section were developed to define T-quencher air-clearing loads on the torus generically. However, two of the Mark I licensees have indicated that they plan to install Y-quenchers, and a number of other Mark I licensees have indicated that the generic load definition procedures are overly conservative for their plant design, especially when the procedures are coupled with conservative structural analysis techniques. To allow for these special cases, the staff has stipulated requirements (Appendix A, Section 2.13.9) whereby in-plant tests could be used to derive the plant-specific structural response to the SRV air-clearing loads on the torus.

Because of the preponderance of phenomena associated with the air-clearing phase of SRV discharge, some form of analysis procedure is necessary to extrapolate from test conditions to the event cases under consideration. This is especially true for subsequent actuations, multiple-valve actuations, and structural-response characteristics. Therefore, the staff's requirements are predicated on formulating a coupled load-structure analysis technique which is calibrated to the plant-specific conditions for the simplest form of SRV discharge (i.e., single-valve first actuation) and then applied to the design-basis event conditions. The minimum of four tests was selected to provide sufficient statistical significance. The discharge line expected to produce the highest loads would be used in the tests.

To reflect the plant-specific SRV discharge, the staff requirements permit the coupled load-structure model to be adjusted to match conservatively the measured first-actuation peak pressures and structural response. The subsequent-actuation peak pressures, however, cannot be adjusted because the analytical model was developed on a bounding basis (as described in Section 3.10.2(g)). In addition, because the analytical attenuation characteristics were developed specifically for the Monticello T-quencher geometry, attenuation characteristics for the Y-quencher geometry must be established from the in-plant tests.

One of the dominant aspects of the air-clearing, relative to the structural response, is the frequency content of the forcing function. However, the frequency content is affected by a variety of conditions. Therefore, instead of using the maximum structural amplification which would result from a resonant-frequency sinusoidal function, the staff's requirements permit the actual measured pressure wave forms in all of the tests (Monticello and in-plant) to be used to develop a maximum structural amplification for resonant conditions. In order to reflect the uncertainty between the tested conditions and to reflect the observed variability in the existing test data, the staff requires that the maximum amplification be applied to the calculated structural response over the range of predicted frequencies (established by the mean frequency and the frequency margins). The staff considers, however, that because of the basic differences in the phenomena, first- and subsequent-actuation data should be analyzed separately.

The staff concludes that the analysis techniques described above and in Appendix A, Section 2.13.9 will ensure a conservative assessment of the air-clearing loads resulting from an SRV discharge through a quencher device.

### 3.10.3 SRV Reflood Transient

Following closure of an SRV, the pressure in the SRVDL decreases rapidly because of the outflow of the remaining steam. At a sufficiently low pressure, cool water will reenter the line through the quencher perforations; this results in a further decrease in line pressure as the remaining steam is condensed by the inflowing water. The reduced pressures also activate the SRVDL vacuum breaker, allowing drywell air/steam to enter the line. Experiments indicate that these events occur in a very transitory fashion before a new state of equilibrium is achieved. Specifically, the water column within the SRVDL has been observed to overshoot the original water level, followed by several oscillations about a new equilibrium level, which is generally below the normal value. Pressure fluctuations and corresponding actuations of the vacuum breaker accompany these excursions in water-column elevation.

In order to establish the pipe conditions prevailing prior to a potential subsequent SRV actuation during this transient period, the LDR has proposed a

method which employs a first principles analytical model of the reflood phenomenon (Ref. 55). As with the line-pressure transient model (Section 3.10.1), appropriate conservation equations, coupled to submodels for vacuum breaker inflow and steam condensation at the pipe walls and water-steam interface, are solved numerically. Empirical constants are employed to characterize condensation rates for the latter two submodels. An important conservatism incorporated in the model involves maximizing the air inflow to the SRVDL via assumptions related to vacuum breaker performance. The analysis predicts the transient variation of water-leg elevation, SRVDL pipe pressures, air and steam partial pressure, and related parameters from the onset of reflood. Plant-unique values of the time interval from SRV closure to the onset of reflood (reflood delay time) are determined from an empirical relation given in Section 5.2.3.3 of the LDR.

Plant-unique determination of these transient histories is obtained via the computer code RVRIZ. Guidelines for selection of input parameters are provided in Section 5.2.3.3 of the LDR.

Comparison of the predictive capability of the proposed method with in-plant test results (Ref. 55) exhibits good agreement for the initial upward water-leg excursion and the frequency of oscillation, but tends to overpredict the subsequent water-leg elevations and equilibrium positions. This effect is probably the result of the vaporization of the water film left on the inside of the hot pipe as the water level drops after the first upward excursion; it is not accounted for by the analysis. Because this implies higher-than-actual air partial pressures and longer-than-actual water legs, these results are deemed conservative.

The staff has made a detailed review of this analysis and the supporting data base and has concluded that they provide either a best-estimate or conservative description of the transient reflood phenomenon following the onset of reflood. With regard to the reflood delay time, the staff does not find that any evidence has been presented to support the relatively rudimentary method proposed to extrapolate test observations in the Monticello plant to differing plant-unique conditions. The staff concurs that, to first order, the suggested dependence

on SRVDL line volume is appropriate. It has, however, examined other potential influences and concludes that some dependence on T-quencher submergence (more specifically, hydrostatic pressure at the quencher centerline) can also be deduced. However, for the range of variation of submergence and depressurization rates following SRV closure, the staff concludes that the overall effect on delay time will be negligible.

For the reasons presented in the previous section relative to subsequent actuations, the results of the proposed reflood analysis will have a very small influence on the final specification of torus shell pressure loads. Accordingly, on the basis of the discussion presented above, the staff has found the proposed method acceptable for the purpose of facilitating the computational procedures needed to define SRV air-clearing loads on the torus shell.

#### 3.10.4 SRV Quencher Thrust Loads -

During the water-clearing phase of an SRV actuation, expulsion of water through the perforations in the T-quencher arms induces thrust loads on the individual arms as well as a global thrust load on the T-quencher, in the event the water clearing does not occur with biaxial asymmetry. Axial asymmetry arises in those cases where the T-quencher is equipped with end cap holes, resulting in a net differential of water flow rate in the two arms. Asymmetry perpendicular to the quencher arms has been inferred from test observations which indicate that most of the water clears from the outboard (relative to the drywell) perforations.

This effect is probably due to the presence of an inclined submerged SRVDL segment upstream of the quencher hub.

To estimate the magnitude of these loads, the LDR has proposed a method which has been developed by applying classical momentum balance considerations together with conservative and, in some cases, bounding assumptions regarding the distribution of the expelled water. The requisite information to define water velocities and acceleration is obtained from the RVFORCE computer code

(discussed in Section 3.10.1). The calculation is continued following total water expulsion into the steady-state steam flux phase of the blowdown by assuming choked flow at the perforations.

No direct experimental verification of this analysis technique is available. However, the favorable comparison of predicted stress levels with measurements from the Monticello test (Ref. 47) throughout the entire clearing phase of the blowdown supports the adequacy of the proposed method. Based on these considerations and the inherent conservatism of the assumptions, the proposed analysis technique is acceptable.

### 3.10.5 SRV Temperature Transients

During SRV actuation, the SRVDL and discharge device (T-quencher) are subjected to thermal expansion loads as a result of the sustained flow of high-temperature-and-pressure steam. To define these loads, a method is proposed in the LDR to provide an estimate of the temperature of the pipe wall and T-quencher. In this method, the local SRVDL wall temperature is assumed to be the saturation temperature corresponding to the local steady-state pressure predicted by the SRVDL pressure transient model (Section 3.10.1). The temperature of the discharge device is assumed to be equal to the saturation temperature corresponding to a bounding value of steam-stagnation pressure. This bounding value is taken to correspond to the maximum steam flux for all Mark I SRVs, together with the assumption of choked flow at the T-quencher perforations and a conservative choice of exit hole discharge coefficient. A generic value of a maximum T-quencher temperature of 370° F is specified on this basis.

The proposed method is clearly a very conservative model of the physical process of interest. Examination of some limited pipe temperature data obtained during the Monticello tests verifies these conservatisms (Ref. 47). The staff also finds that the thermal loads developed during extended SRV discharges will bound any other thermal loads likely to arise from normal or accident conditions. Accordingly, the proposed method is acceptable.

### 3.10.6 SRV Discharge Event Cases

The SRVs provide protection against overpressure of the primary system. In response to varied transients of the primary system, the SRVs are actuated in accordance with the need for pressure relief of the primary system. Consequently, the number of SRV actuations and sequence of actuation are varied in each transient and will vary with the primary system designs. These SRV operational modes can be grouped into the following four general event cases:

#### (1) Single-Valve Actuation

This load case deals with events such as inadvertent opening of an SRV and actuation of an SRV following small- or intermediate-line breaks in the primary system. A subsequent single SRV actuation may also result to provide pressure relief following a multiple-valve actuation, as described in (4), below. This function, however, involves opening, closing, and reopening a SRV. The SRV loads, therefore, shall be analyzed for both first and subsequent actuations.

#### (2) Asymmetric SRV Discharge

The events involving this load case are similar to those identified in (1), above. Concerns relating to a single failure of a pressure sensor of an SRV may lead to the actuation of additional valve(s). Results of this load case will impose more severe asymmetrical loading conditions than those of the single-valve actuations. The most restrictive loading condition shall be determined from a plant-specific primary system analysis, in conjunction with the consideration of plant arrangement of the SRV system.

#### (3) Automatic Depressurization System (ADS)

A group of SRVs is designated to function for the ADS, as described in Section 2.3. These valves open automatically as part of the emergency core-cooling system in the event of a small-line break in the primary system. Although the ADS will remain open until the primary system is depressurized to a sufficiently low pressure, the potential for subsequent actuations of the ADS must be determined on the basis of a plant-specific primary system analysis and the plant-specific operational procedures.

#### (4) Multiple-Valve Actuation

Events that are expected to actuate more than one SRV include generator load rejection, loss of main condenser, turbine trip, closure of all main steam isolation valves, and some less severe transients such as loss of auxiliary power and pressure regulator failure. Some of these anticipated transients may result in actuation of all relief valves. However, the pressurization rate of the primary system following these anticipated transients may not reach the spring setpoint for the valves designed solely for safety functions, because the pressure relief systems for plants using the Mark I containment are designed in various ways. In light of this consideration, the number of SRV actuations following these anticipated transients must be determined from plant-unique primary system analysis in conjunction with the plant-unique SRV arrangement.

These general considerations led to the specific criteria presented in Appendix A, Section 2.13.7. For the most part, the SRV event cases will be established from the plant-specific primary system configuration. The SRV event cases are also presented in the event combinations in Section 4.3.

#### 3.10.7 Suppression Pool Temperature Limit

As described in Section 2.3, SRV actuation at elevated pool temperatures could result in severe vibratory pressure loads. To eliminate this concern, the current practice is to limit the pool temperature so that the "threshold" temperature for severe vibrations will not be achieved during operational and upset modes; e.g., a stuck-open SRV event. In this section, the results of the staff evaluation of the pool temperature limit for the quencher devices will be discussed.

##### 3.10.7.1 Local and Bulk Temperature Difference

Local temperature denotes an average water temperature in the vicinity of the discharge device and represents the relevant temperature which controls the behavior of the condensation process occurring at the pipe exit. In general, this temperature will differ from both the temperature of water in contact with the steam and the bulk temperature of the entire suppression pool. The

latter, of course, is a calculated value based on the total energy and mass release into the pool, assuming it acts as a uniform heat sink. Because bulk temperature is used in plant transient analyses, the difference between the bulk and local value must be specified so that the analysis can demonstrate operation within the prescribed limits.

In a test facility, the volume of water associated with a single discharge device is only a small fraction of the volume which would exist under prototypical conditions. In such a confined pool, differences between local and bulk conditions are minimal. Tests indicate that temperature distributions in a confined pool are relatively uniform, with generally no more than a 2° F to 3° F variation. Thus, under test conditions, the measured temperature can generally be interpreted as local temperature.

To determine the difference between bulk and local conditions for the quencher device, the Mark I Owners Group relied on the in-plant tests at Monticello (Ref. 47). Test results indicated that the difference between bulk and local temperature is 43° F for the test without the residual-heat-removal (RHR) system in operation and 38° F for the tests with RHR operation. The test with RHR was conducted with only one RHR loop operating in the pool recirculation mode.

In late 1978, the Mark I Owners Group conducted an adjunct series of tests at the same facility (Ref. 56). The purpose of the tests was to investigate methods to improve thermal mixing in the suppression pool and reduce the bulk to local pool temperature difference. These methods include modifications of T-quencher design and the RHR discharge configuration. The T-quencher was modified by adding a number of holes on the tips of one of the quencher arms. The RHR system was modified by installing a 90° elbow, with a 10 x 8-inch reducing nozzle at the end of the existing discharge lines. All of these modifications were intended to promote mixing in the suppression pool during SRV discharge. Test results show a substantial improvement in the pool mixing. The difference between bulk and local temperature was reduced to approximately 15° F for the test, with one RHR operating in the pool recirculation mode.



Results of these two series of tests clearly indicate that the quencher design and RHR discharge line configuration influence the difference between bulk and local pool temperature to a great extent. The Mark I Owners Group has not presented a generic method for determining the pool temperature difference. Consequently, the staff requires that each plant establish the pool temperature difference, supported by the appropriate data base and with consideration for the plant-specific SRV discharge and RHR system arrangement.

#### 3.10.7.2 Local Pool Temperature Limit

A local pool temperature limit of 200° F has been established generically for quencher devices based on small-scale and in-plant tests. Small-scale tests on selected quencher devices were performed by Kraftwerk Union AG (KWU) in West Germany. The results of these tests indicate that the hole pattern in a perforated pipe quencher is the controlling parameter for effective steam condensation. Using a quencher device with an optimized hole pattern, KWU conducted tests at elevated pool temperatures. Steam condensation instability did not occur, even as the local pool temperature approached the boiling point.

In-plant tests were also performed in a European BWR plant. The discharge devices tested were four-arm quenchers with an optimized hole pattern. The results of the tests indicate that smooth steam condensation is achieved over a wide range of reactor pressures (100 psia to 1100 psia) and pool temperatures (140° F to 176° F). These tests also showed good pool mixing, which was attributed to the bulk pool motion induced by the air or steam jets discharging through special holes in the end of two adjacent quencher arms. The maximum variation of pool temperature was not more than 10° F.

Based on its evaluation of these test data, the staff finds that:

- (1) The hole (i.e., perforation) pattern is the primary design feature for achieving smooth steam condensation. Therefore, the 200° F local pool temperature limit applies to all quencher devices designed with the same hole pattern as that tested. Based on its review of the available data,

the staff concludes that the 200° F local pool temperature limit also applies to the generic Mark I T-quencher (Ref. 47) and similar devices with an equal hole diameter and an equal or greater hole spacing (as described in Appendix A, Section 2.13.8).

- (2) The small-scale test results showed that steam condensation instability did not occur when the maximum local temperature reached 210° F. In the judgment of the staff, a 200° F temperature limit will provide additional conservatism and will ensure that unstable steam condensation will not occur with a quencher device.
- (3) Plant-unique analyses of the pool temperature response to transients involving SRV operations will be necessary to demonstrate that the suppression pool can be maintained within the limit of a 200° F local temperature.

It must be emphasized that the above limit on maximum suppression pool local temperature was established on the basis of test data that are currently available to the staff. As additional data become available, the staff evaluation will continue.

### 3.11 Submerged Structure Drag Loads

The expulsion of water, air, and, subsequently, steam following a postulated LOCA or an SRV actuation induces a flow velocity and acceleration field within the suppression pool. Structures either initially submerged within the pool or sufficiently close to the pool surface will experience loads as a result of this induced pool motion. These loads can be conveniently divided into three major chronological phases. Water-jet loads arise from the expulsion of the water slug which is initially within the downcomer or SRV discharge line. Bubble-drag loads arise from the induced pool motion created by the expulsion of the air from the drywell through the vent system or from the SRV discharge line. Condensation and chugging loads arise from the unsteady condensation process that occurs during certain time segments of a postulated LOCA. Unsteady condensation is not considered for the SRV quencher device, because the device is designed to avoid such unsteady phenomena within its operating range.

Because of the large number of plant-unique features associated with submerged structures, numerical loading values are not proposed in the LDR. Instead, calculational techniques based on analytical models and empirical data have been developed. The following subsections present the staff's evaluation of the load definition procedures for each of the loads described above.

### 3.11.1 LOCA Water-Jet Loads

During the downcomer-clearing phase of a LOCA (except with a full differential pressure between the drywell and torus), water is discharged rapidly from the downcomers into the suppression pool. The LDR-proposed method for computing water-jet loads is based on an analytical quasi-one-dimensional model (Ref. 57) which uses plant-unique downcomer-clearing information based on QSTF data (Ref. 58). This analytical model is referred to here and in the acceptance criteria (Appendix A, Section 2.14.1) as the "Moody Jet Model," after the author of the report. Loads are based only on a standard drag calculation for those structures either wholly or partially intercepted by the jet computed on the basis of the Moody model. The LDR method circumvents the infinite jet front area inherent in the one-dimensional model by considering the jet front to be located one-downcomer diameter behind the "Moody Jet Model" front. However, this method does not consider induced velocity or acceleration fields outside this modified jet.

Experimental data from the QSTF facility (Ref. 58) and EPRI tests (Ref. 20) suggest that the actual jet is much more three-dimensional in character than the Moody model. Furthermore, a substantial interaction occurs between the water initially in the downcomer and the water in the pool that has to be pushed out of the way by the jet front, inducing a velocity-and-acceleration field outside the boundaries of the actual jet. Accordingly, it is apparent that the Moody model does not accurately represent the water-clearing phenomenon at the downcomer exit. Nevertheless, the results of that model can be used to conservatively bound loads on structures totally or partially engulfed by the model jet. Neglecting the momentum exchange between the jet and the pool will produce conservative estimates of both jet penetration distance and fluid velocities within the jet. The procedures of the LDR are, therefore, acceptable for those structures that are intercepted by the model jet.

The LDR method, however, predicts zero loads during the water-jet phase for all structures that are not directly intercepted by the jet. This does not agree with experimental observations (Ref. 58), nor with the conclusion that an induced-flow field must exist in the pool. A conservative estimate of the acceleration and standard drag loads for structures outside the jet has been made by considering the flow field induced by a slightly modified Moody jet. A model that utilizes the conservative penetration and velocity predictions of the Moody jet, but introduces an induced three-dimensional flow field that incorporates the momentum transmitted to the pool, is present in the acceptance criteria, Section 2.14.1, along with the specific formulas for the flow field and their derivations.

### 3.11.2 LOCA Pool Swell Bubble-Drag Loads

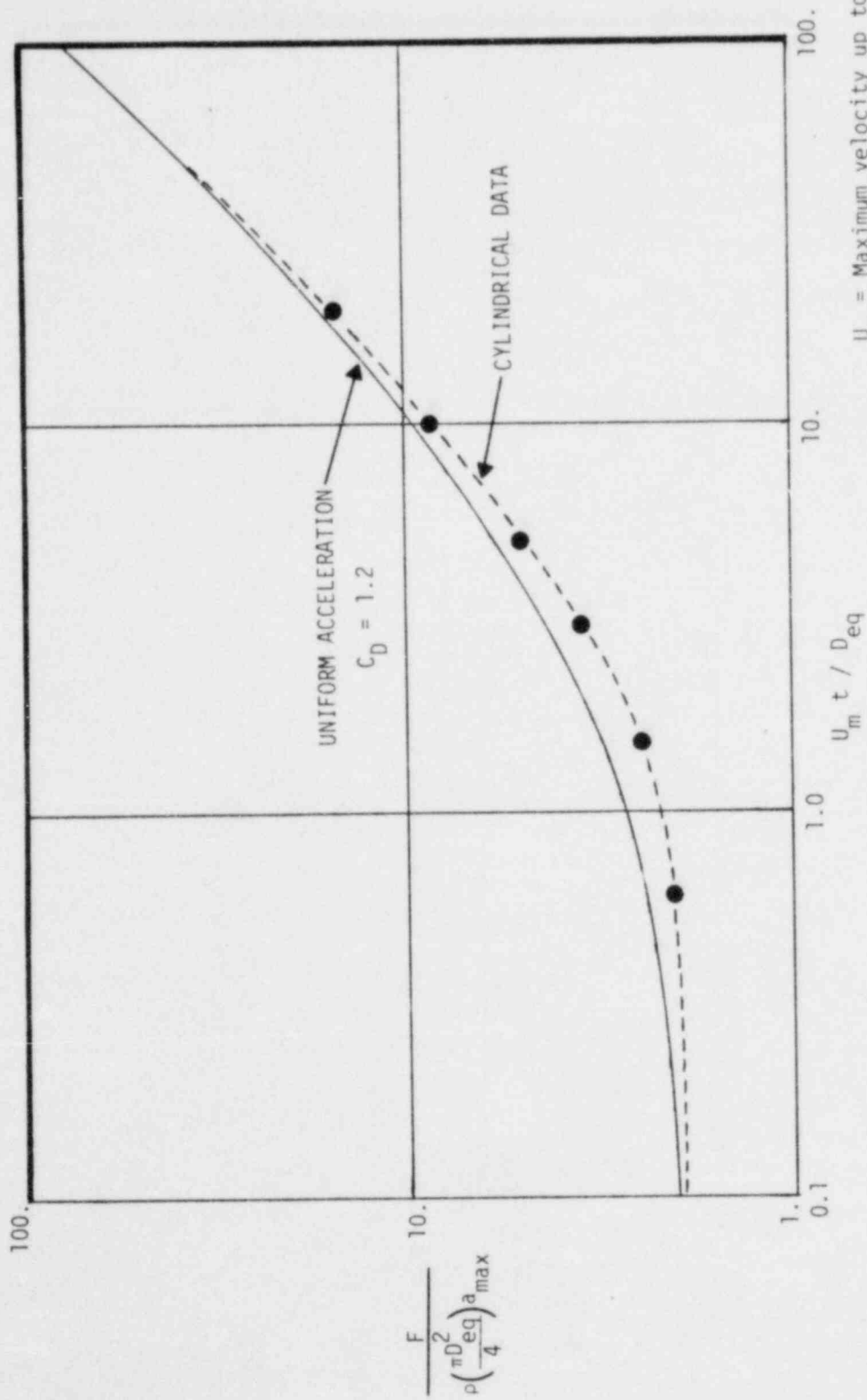
After the water leg in the downcomer clears, the pressurized drywell air is forced into the pool, forming a single bubble at the end of each downcomer. During the bubble growth, possible bubble coalescence, and bubble breakthrough, unsteady fluid accelerations and velocities in the pool produce loads on submerged structures.

The LDR has proposed that the plant-unique QSTF data for the drywell pressure history be used as an input to the classic Rayleigh bubble equation to compute the source strengths at each downcomer. The flow field is computed on the basis of potential flow theory, using the method of images to represent an approximate rectangular cross-section for the pool geometry. The loads on the structures would then be computed using a sum of the acceleration drag and standard drag components, based on an equivalent local uniform flow. The acceleration drag coefficient (hydrodynamic mass) is based on potential theory, while the standard drag comes from steady-flow experimental data generally available. Some confirmation of this technique is provided by the comparison of results to experimental measurements in QSTF (Ref. 59). The staff considers the basic approach sound and, thus, acceptable, subject to certain modifications and/or constraints in the details of the procedure (as described in Appendix A, Section 2.14.2).

To ensure conservatism in the acceleration and velocity fields, conservatism in the input data for the drywell pressure and in the method of images modeling must be preserved. The scaled QSTF drywell pressure history and a specific rectangular equivalent cell model (Model E) for the method of images are, in the judgment of the staff, adequate to provide such conservatism. After the bubbles have grown to the point that they coalesce or almost coalesce, the flow field in the slug of water above the bubbles is not expected to be predicted accurately by the superimposed source model. The staff, therefore, requires that loads for structures in that region of the flow field be computed after coalescence, using the pool surface velocities and accelerations obtained from the plant-unique QSTF tests (as described in Appendix A, Section 2.14.2.1(c)).

After the flow field is established, the loads on individual segments of the structure must be computed by taking the appropriate local acceleration and velocity square and multiplying by the appropriate coefficients. To ensure conservatism in the implementation of this procedure, the staff has listed a number of constraints in the acceptance criteria.

Substantial evidence exists in the literature that the standard drag coefficient in unsteady flow is not generally equal to its value for steady flow (Refs. 60-65). For the LOCA bubble, the most relevant data come from experiments on cylinders in a uniformly accelerating flow. Figure 3.11-1 shows a comparison of the data with the LDR method using the steady flow drag coefficient,  $C_D = 1.2$ , which is appropriate for the Reynolds number range of the experiment. Unfortunately, no other data for different geometries and/or higher Reynolds numbers with uniform acceleration exist. Other data for oscillating flow (shown in Figure 3.11-2) suggest that the Reynolds number has an effect on the relationship of unsteady drag coefficient to the steady-flow value. The data also suggest that a sharp-edged geometry can have a dramatic effect on both the hydrodynamic mass and unsteady drag coefficient. In order to ensure conservatism in the application of the LDR method, the maximum value of drag coefficient ( $C_D = 1.2$ ) must be used for cylindrical objects, and sharp-edged structures must be approximated by equivalent cylinders which are large enough to bound the limited data for such structures. (These constraints are also listed in the acceptance criteria, Appendix A, Sections 2.14.2-2(a) and 2.14.2-2(b).)



$U_m$  = Maximum velocity up to time  $t$ .  
 $t$  = Time from start of motion.  
 $D_{eq}$  = Effective diameter.

Figure 3.11-1 Comparison of drag forces in accelerating flows.

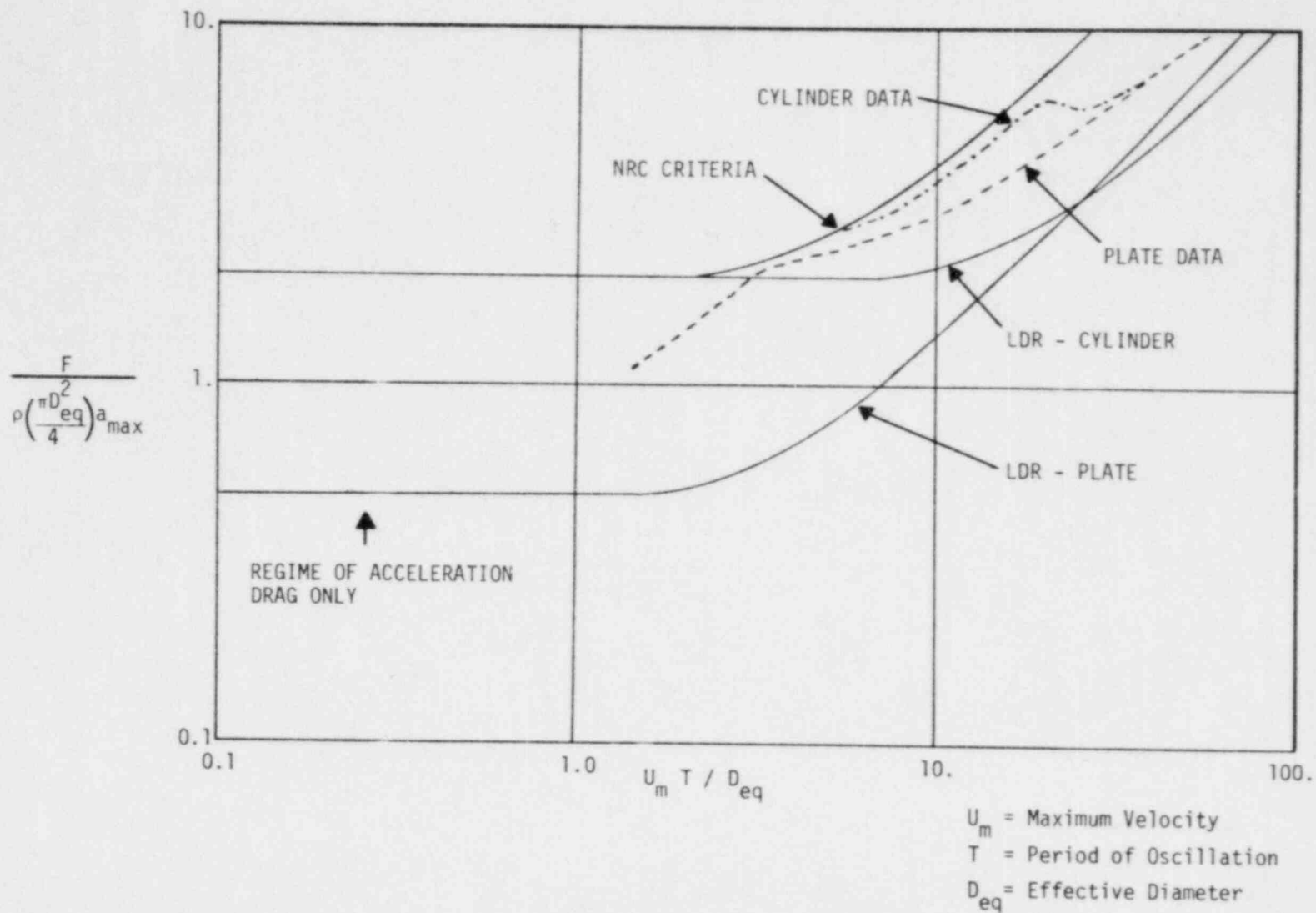


Figure 3.11-2 Comparison of drag forces in oscillating flows.

The use of the equivalent uniform flow approximation is clearly accurate only if the structure is small compared to the scale of variation of the flow field. To ensure conservatism in this application, a limit on the segmentation of long slender structures is provided in the acceptance criteria (Appendix A, Section 2.14.2-2(c)). The basis for the criterion on segment length was obtained from numerical studies performed for the Mark II program (Ref. 39).

The LDR makes no mention of possible interference effects between neighboring structures, although there is substantial literature to indicate that both acceleration and standard drag can be altered by the proximity of other structures and/or walls. While the effects are small for structures separated by several diameters, experimental and theoretical results suggest that the effects are not negligible for structures closer than 1.5 diameters to a wall or 3 average diameters from each other. The acceptance criteria (Appendix A, Section 2.14.2-2(d)), therefore, require the inclusion of such effects for all structures that fall within this range. Explicit formulas are provided for structures near walls or approximately parallel to each other, based on bounding curves deduced from experimental and theoretical results in the open literature (Refs. 66-71). For structures outside the range of the applicability of these formulas, the applicable experimental or analytical results must be used to determine the effects of interference. The staff concludes that the method proposed in the LDR, as modified by the acceptance criteria, will ensure conservative estimates of the submerged structure drag loads as a result of LOCA bubble expansion in the pool.

### 3.11.3 LOCA Condensation Oscillation Drag Loads

After an initial high mass flow and high-air-content phase of steam flow through the downcomers following a postulated LOCA, the mass flow decreases because of the dropping drywell pressure, and the steam purity increases because of the drywell air urging. It is during this phase that the condensation becomes unsteady, resulting in induced oscillatory fluid accelerations and velocities within the suppression pool (as described in Section 3.8). The LDR treats the loads on submerged structures as a result of these condensation oscillations by the same method used for LOCA bubble loads, except that the



oscillatory source strengths at the downcomer exits are inferred from boundary pressures measured in the FSTF facility (Refs. 42,72).

The acceleration and velocity flow fields, as computed in the LDR, are based on the assumption of equal source strengths at all of the downcomers. While this is supported qualitatively by the FSTF data, the possible sensitivity of some structures to asymmetric loading requires the consideration of alternative nonuniform source strengths. Therefore, the staff requires that the loads be computed on the basis of both the average and maximum source strengths derived from FSTF data (as described in Appendix A, Section 2.14.5.1(a)).

The LDR does not explicitly discuss the possible alteration of the flow field as a result of fluid-structure interaction (FSI) in the FSTF facility. Because the FSI effects are significant with respect to inferring the source strengths, it is prudent to include these effects on the flow field (especially near boundaries). Therefore, the staff requires that a conservative estimate of this effect be included by adding the calculated plant-unique boundary acceleration to the computed fluid acceleration (as described in Appendix A, Section 2.14.5.1(b)).

The drag-load assessment procedure proposed in the LDR must be subjected to the same constraints and/or modifications that are applied to the LOCA-bubble loads (Section 3.11.2), except for the value of the unsteady standard drag coefficient. Figure 3.11-2 shows data from a selection of oscillating flow experiments for the normalized force as a function of the period parameter ( $U_m T/D_{eq}$ ), where  $U_m$  is the maximum velocity,  $T$  is the period, and  $D_{eq}$  is the diameter of the cylinder or equivalent cylinder representing the body. The total force includes the lift force added vectorially to the drag. Also shown on the graph are the predictions that would result from the LDR-proposed method, as well as the prediction resulting from the staff's criteria (Appendix A, Section 2.14.4.2(a)). Note that the use of  $C_D = 3.6$  and  $D_{eq} = 2\frac{1}{2} L_{max}$  bounds both the cylinder data and the limited data available for flat strips perpendicular to the flow. Therefore, the acceptance criteria require that all structures be approximated by an equivalent cylinder of diameter  $D_{eq}$ .

Because of the frequency content observed in the condensation oscillation source, it is not clear that all structures will be rigid enough to allow application of the load on a quasi-static basis. The staff criteria, therefore, require that the loads be applied dynamically, unless the highest significant source frequency is less than half the lowest structural mode frequency.

The staff has concluded that the proposed method in the LDR, as modified by the acceptance criteria, will ensure conservative estimates of the oscillatory drag loads on submerged structures during condensation oscillations.

#### 3.11.4 LOCA Chugging Drag Loads

Following a postulated LOCA, when the mass flow through the downcomers is low enough, the unsteady condensation is of sufficient amplitude to let water enter the downcomer. This phenomenon, called chugging, is more stochastic in character than the condensation oscillations and less synchronized between the individual downcomers. The induced hydrodynamic flow will produce forces on submerged structures in a fashion analogous to condensation oscillation and LOCA bubble loads, but with a slightly different source strength.

The LDR has proposed a method which makes use of the FSTF chugging data (Ref 72). Because of the almost harmonic character of the prechug pressure traces (see Section 3.9), the LDR treats this portion of the event in a manner identical to that used for condensation oscillations. Because of the less synchronized nature of the postchug signal, the LDR computes the source strength by a more conservative procedure and requires investigation of the phasing between neighboring downcomer sources to maximize the load on any particular structure.

The staff concurs that the prechug analysis can be performed in a manner identical to the condensation oscillation method, subject, of course, to the applicable constraints, because of the similar characteristics of the sources.

For the postchug portion, the staff believes that the highly stochastic and nonsynchronous behavior of the phenomena (as exhibited in the pressure traces) requires that a bounding approach be used in the interpretation of the available data.

Therefore, the acceptance criteria (Appendix A, Section 2.14.6-1(a)) require a procedure for computing source strengths and phasing that will maximize the load. Similarly, the acceptance criteria (Appendix A, Section 2.14.6-2(b)) require that the range in a frequency analysis must be large enough to include adequate modeling of the "spikes" observed in some of the data, in the event that the structure can respond on that time scale. The staff believes that the "spikes" are not necessarily a strictly local structural response, but may represent a possible mode of rapid collapse which must, therefore, be included in the determination of possible postchug source strengths.

The staff has concluded that the method proposed in the LDR, as modified by the acceptance criteria, will ensure a conservative estimate of the potential submerged-structure drag loads that may be created during the chugging regime.

#### 3.11.5 SRV Water-Jet Loads

The clearing of the water leg in the SRV line through a T-quencher device involves a process of small water jets emanating from the quencher holes, coalescing into larger rectangular jets emanating from each side of a quencher arm. Structures within the penetration distance of these jets will be subjected to hydrodynamic loads.

The LDR-proposed method involves a computation of the velocity flow field within the jets through semi-empirical modeling based on visual experimental data of the penetration depth from subscale quencher discharge tests (Ref. 73).

Based on its review, the staff finds that the proposed technique will provide a conservative estimate of the water-jet loads due to quencher discharge and is, therefore, acceptable.

#### 3.11.6 SRV Bubble-Drag Loads

After the water in the SRV line is expelled, air flows through the quencher holes, eventually coalescing into bubbles which separate from the quenchers and rise while oscillating in size. The initial charging and subsequent

oscillation of these bubbles induces pool accelerations and velocities that result in hydrodynamic loads on submerged structures.

The LDR-proposed method uses the same empirically based model for source strengths that is used for predicting torus shell pressures (Ref. 51) to compute the flow field by potential theory with a slightly modified form of the analysis used for LOCA bubble-drag loads (Ref. 74).

The staff finds this procedure fundamentally acceptable, subject to both a conservative estimate of the source strengths with respect to possible asymmetric loads and, of course, subject to the same constraints on drag coefficients, nodalization, and interference effects that apply for LOCA condensation oscillations (Section 3.11.3). These requirements are reflected in Appendix A, Section 2.14.4.

However, loads will occur on the quencher arms and the SRV line itself as a result of asymmetric bubble dynamics. Although the data base for the analytical model does qualitatively support a general synchronization among the bubbles during SRV discharge, there is not sufficient evidence regarding either source strength or phase variation between bubbles. The acceptance criteria, therefore, require either a bounding loading condition based on full asymmetry or a more detailed evaluation of an upper bound of asymmetry deduced from the experimental data (Appendix A, Section 2.14.4.1(b)). Subsequently, the Mark I Owners Group has indicated that the intent of the LDR was to apply two bubbles so as to maximize both the bending and twisting moments on the quencher. The staff finds this approach acceptable, because it is conservative with respect to the Monticello data.

The staff concludes that the proposed method, as modified by the acceptance criteria, will provide a conservative estimate of the oscillatory bubble-drag loads which would be experienced during SRV discharge.

### 3.12 Secondary Loads and Other Considerations

During the course of its review of the LTP, the staff investigated a number of suppression pool hydrodynamic-related phenomena which could affect the loading

conditions or the performance of the containment system. The evaluations of each of these related phenomena are presented in the following sections, along with the staff's conclusion regarding their potential effects.

### 3.12.1 Seismic Slosh

Seismic motion induces suppression pool waves which can impart an oscillatory pressure loading on the torus shell and potentially lead to uncovering the ends of the downcomers, which would result in steam bypass of the suppression pool and potential overpressurization of the torus, should the seismic event occur in conjunction with a LOCA. To assess these effects, the Mark I Owners Group undertook the development of an analytical model which would provide plant-specific seismic wave amplitudes and torus wall pressures. This model was based on 1/30-scale "shake test" data for a Mark I torus geometry (Ref. 75).

Based on the results of the plant-specific analyses using the analytical model, the Mark I Owners Group concluded that the seismic wave pressure loads on any Mark I torus are insignificant in comparison with the other suppression pool dynamic loads, and the seismic wave amplitudes will not lead to uncovering the downcomers for any Mark I plant. These conclusions were based on the maximum calculated pressure loads and the minimum wave trough depth relative to the downcomer exit.

The staff has reviewed comparisons of the analytical predictions with scaled-up test data, the small-scale program, and the seismic spectrum envelope used in the plant-specific analyses. Based on this review, the staff has concluded that the seismic slosh analytical predictions will provide reasonably conservative estimates of both the wall-pressure loading and the wave amplitude for the range of Mark I plant conditions.

Because the maximum local wall pressures were found to be less than 0.8 psi at a 95-percent upper-confidence limit, the Mark I Owners Group has proposed that the seismic slosh loads may be neglected in the structural analysis. The staff agrees that the seismic slosh loads are insignificant by comparison to the other suppression pool loads. On this basis, neglecting seismic slosh loads for the plant-unique analyses is acceptable.

The results of the slosh wave amplitude predictions indicated that within the local area of maximum amplitude and with maximum suppression pool drawdown (resulting from ECCS system flows), the slosh waves will not cause uncovering of the downcomers. The staff has reviewed the assumptions used in these analyses and has concluded that they are sufficiently conservative.

### 3.12.2 Post-Pool Swell Waves

Following the initial pool swell transient, pool wave action will result from continued flow through the vent system. This wave action, in turn, will result in pressure loads on the torus walls.

For the period immediately following the downward and upward vertical pressure transient, the Mark I Owners Group has concluded that this wave action is inherently included in the QSTF (Ref. 14) pressures and is negligible. Although the scaling relationships by which the QSTF was designed are not applicable following bubble breakthrough, the staff agrees that the QSTF results provide a reasonable estimate of the wave loads during this period and that they are negligible.

During the subsequent condensation period, the pool wave action is inherently included in the condensation oscillation and chugging load specifications. These loads were derived from wall pressure measurements from full-scale steam condensation tests; therefore, a separate load specification for the condensation wave loads is unnecessary.

### 3.12.3 Asymmetric Vent System Flow

The effects of asymmetric flow rates in the vent system have been considered with respect to unequal vent flows (e.g., vent blockage) and unequal vent flow composition to evaluate the potential for asymmetric pool hydrodynamic loading conditions.

The three-dimensional pool swell tests conducted by EPRI for the Mark I Owners Group (Ref. 20) and the confirmatory three-dimensional pool swell tests conducted for the NRC by the Lawrence Livermore Laboratory (Ref. 17) included specific

tests to assess the effects of partial and full blockage of one main vent. The results of these tests indicate that the distribution of the pool swell pressure loads is relatively insensitive to the main vent blockage, because the vent header tends to equalize in pressure and, therefore, equalize flow through the downcomers. Because of the configuration of the Mark I vent system, the main vent entrance is the principal location where flow blockage could occur, if at all, and, therefore, flow blockage assumptions for other locations in the vent system have not been considered.

To assess the effects of potential asymmetric vent flow composition, the staff has considered the extreme case of localized steam flow through the vent system, without benefit of any steam-air mixing. For the DBA, the earliest time that a steam front could reach the downcomer exit is shortly before the peak vertical upward pressure load. However, as the steam condenses and begins reducing the bubble growth, the air compression (which is the major contributor to the upward loading phase) would tend to equalize. This would result in a reduced potential for an asymmetric loading condition and would lessen the severity of the pool swell loads.

The staff has also considered this extreme asymmetric flow case for smaller breaks, to assess the potential for localized pool heating which might lead to overpressurization of the torus. For the SBA, the staff has determined that there is insufficient energy released with the break flow to cause overpressurization of the torus, even if all of the flow were confined to one main vent and only the layer of water above the associated downcomer exits were available to absorb that energy. The staff performed a similar analysis for larger break sizes, and concluded that the increased vent flow rates accompanying higher energy deposition in the pool will provide sufficient mixing to prevent overpressurization of the torus. This conclusion was based primarily on the thermal gradients observed in the FSTF test results for IBA conditions. In making this assessment, the staff neglected the mixing effects of SRV discharge and the operation of the RHR system, both of which would occur in conjunction with the smaller breaks.

Based on the results of this evaluation, neglecting asymmetric vent system flow for the purpose of load definition is acceptable.

#### 3.12.4 Downcomer Air-Clearing Loads

During the initial phase of a LOCA, the rapid clearing of air from the vent system causes the downcomer to be subjected to a lateral load as bubbles are being formed in the pool. This is in addition to the thrust loads on the vent system previously discussed. Conservative estimates of the air-clearing lateral loads were obtained from the FSTF data (Ref. 42). The Mark I Owners Group has proposed to neglect the air-clearing lateral load because it is bounded by the repetitive steam condensation loads on the downcomer. The staff concurs with this assessment and, therefore, concludes that neglecting the air-clearing lateral load on the downcomers is acceptable.

#### 3.12.5 Sonic and Compression Wave Loads

Immediately following the postulated instantaneous rupture of a large primary-system pipe, a shock wave is created at the break location and will propagate through the drywell and into the vent system. A compression wave will then propagate into the water leg inside the downcomer and then through the pool, resulting in a differential pressure loading on submerged structures and the torus wall.

These loading conditions were observed in the FSTF data<sup>a</sup> (Ref. 42). The design of FSTF was such that a conservative estimate of the loading condition could be established, because the simulated drywell volume did not allow significant attenuation of the wave front. The maximum observed loads were approximately 20 psid in the drywell and vent system and 10 psid on the torus walls, with a maximum duration of less than 5 milliseconds.

This loading condition precedes all other dynamic loads and is insignificant in comparison to the other dynamic loads. In addition, a more realistic attenuation of the wave, based on the actual configuration of the drywell, would result in even lower loads than those observed in FSTF.

On this basis, neglecting shock and compression wave loads is acceptable.



### 3.12.6 Downcomer Submergence and Pool Thermal Stratification

One method of suppression pool hydrodynamic load mitigation that the Mark I Owners Group has adopted for the LTP is reducing the initial submergence of the downcomer in the suppression pool to a minimum of 3 feet. The pool volume (i.e., thermal capacity) of the original design would be maintained. This approach, however, raises concerns regarding the increased potential for uncovering the downcomers and reducing the steam condensation capability, both of which could lead to torus overpressurization.

The potential for uncovering the downcomer was addressed in the seismic slosh assessment in Section 3.12.1. This assessment was performed at the most extreme conditions that could potentially lead to uncovering the downcomers and was predicated on a minimum of 3-foot downcomer submergence.

Condensation capability of the suppression pool for the spectrum of LOCAs is a function of the local pool temperature in the vicinity of the downcomer exit. FSTF test results (Ref. 42) and foreign test data (Ref. 76) have shown that thermal stratification occurs and becomes more severe as the downcomer submergence is reduced. The most severe thermal stratification has been observed in low-flow tests with a quiescent pool. In actual plant conditions, the residual-heat-removal (RHR) system and SRV discharge will provide sufficient long-term pool mixing to minimize thermal stratification. As discussed in Section 3.12.3, for asymmetric vent system flows, the staff has determined that the increased vent-system flow rates with higher energy deposition will prevent overpressurization. This assessment included consideration for vertical thermal stratification. In addition, the analytical predictions of the torus pressure and bulk temperature response have been found to be conservative by comparison with FSTF test data for the plant-simulated initial conditions. The local temperature variation in the pool which has been observed in the test data is not significant to the structure and, therefore, need not be considered in the structural analysis.

Based on this assessment, the staff has concluded that a minimum initial downcomer submergence of 3 feet is acceptable, and there is sufficient

conservatism in the containment response analysis techniques to accommodate the effects of thermal stratification.

### 3.12.7 Differential Pressure Control

During the course of the short-term program, studies of pool swell phenomena showed that a differential pressure between the drywell and torus would significantly reduce the pool swell-related loads. The drywell-torus differential pressure reduces the length of the water leg inside the downcomer. In the event of a LOCA, the downcomer clearing and subsequent bubble formation will occur earlier at a lower driving (i.e., drywell) pressure. This technique was used in the short-term program to enhance the containment margins of safety.

For the LTP, the Mark I Owners Group proposed the continued use of "differential pressure control" as one load mitigation technique which could be used to restore the intended margins of safety in the containment design. However, because this technique is an operational feature (i.e., the differential pressure must be maintained and controlled and could be lost during plant operation), the staff determined that certain restrictions would have to be imposed for differential pressure control to be considered acceptable for long-term application.

The length of the water leg inside the downcomer is limited by the downcomer submergence. Consequently, the drywell-to-torus differential pressure and the resulting pool swell load mitigation effects are also limited. In addition, in the design assessment for differential pressure control systems (Ref. 77), the Mark I Owners Group concluded that the probability of the occurrence of a large-break LOCA where the differential pressure is reduced or out of service (for reasons described below) is less than  $10^{-7}$  per reactor-year. The staff determined that this probability is sufficiently small to support the use of differential pressure control for the LTP. Nevertheless, the staff concluded that the occurrence of a design-basis accident without the differential pressure control should not result in unacceptable consequences, regardless of the probability of the event. Therefore, each facility for which differential pressure control is proposed for the LTP is required to perform an additional structural assessment to demonstrate that the containment can maintain its

functional capability when the differential pressure control is out of service (as described in Section 4.3.3 and in Appendix A, Section 2.3).

Although the existence of a differential pressure between the drywell and torus is safety related, the system used to develop the differential pressure need not be designed to engineered safeguards criteria because it does not perform a post-accident function. The design requirements for the differential pressure control system (Appendix A, Section 2.16) have been established to ensure that the system will not increase either the probability or the consequences of an accident.

There are certain periods during normal plant operation when the differential pressure control cannot be maintained. Therefore, limiting conditions for operation (LCOs) must be established in the Technical Specifications of the license to ensure that these periods are minimized (Appendix A, Section 2.16). The justification for relaxing the differential pressure during specific periods and the basis for selecting the duration of these periods are discussed in detail below.

During plant startup and shutdown, the drywell atmosphere undergoes significant barometric changes because of the variation in heat loads from the primary and auxiliary systems. In addition, it is during these periods that the drywell is being either inerted with nitrogen gas or deinerted for most of the BWR/Mark I plants. These conditions make establishing or maintaining the drywell-torus differential pressure extremely difficult. To keep the periods during which the differential pressure control is not fully effective as short as possible, the staff has limited the relaxation of the differential pressure control requirements for the startup and shutdown periods to 24 hours following startup and 24 hours prior to shutdown. The postulated design-basis accident for the containment assumes that the primary system is at operating pressure and temperature. During the startup and shutdown transients, the primary system is at operating pressure and temperature for only a part of the transient. These time periods have been shown by previous operating experience to be adequate with respect to the startup and shutdown transients, and at the same time they are sufficiently small in comparison to the duration of the average power run. Because the principal accident event for which differential pressure

control is important to assure containment integrity is a large-break LOCA, the staff has considered whether there is a significantly greater probability of a large-break LOCA during the startup and shutdown transients. The staff has concluded that there is not. Furthermore, the operation of the plant systems are monitored more closely than normal during these periods, and a finite magnitude of differential pressure will be available during the majority of these periods to mitigate the potential consequences of an accident during the startup or shutdown transients.

During normal operation, there are a number of tests which are required to demonstrate the continued functional performance of engineered safety features. The testing of certain systems will require, or result in, a reduction in the drywell-torus differential pressure. The operability testing of the drywell-torus vacuum breakers requires the removal of the differential pressure to permit the vacuum breakers to open. For the testing of high-energy systems (e.g., high-pressure coolant-injection pumps) during normal operation, the discharge flow is routed to the suppression pool. This energy deposition will raise the temperature of the suppression pool, resulting in an increase in torus pressure and a reduction in the differential pressure.

Functional performance testing of engineered safety features is necessary to ensure proper maintenance of these systems throughout the life of the plant. Some of these tests (i.e., pump operability and drywell torus vacuum breakers) may require or result in a reduction in the differential pressure. The staff estimates that each month no more than four tests will be required which will result in a reduction in differential pressure. To keep the periods during which the differential pressure control is not fully effective as short as is reasonable, the staff will permit a relaxation of differential pressure control to conduct these tests. This will be limited to a period of up to 4 hours. Again, the staff has carefully considered whether the probability of a large LOCA is significantly greater during these testing periods than during normal operation and has concluded that it is not. Moreover, only the testing of the drywell-torus vacuum breakers requires complete removal of the differential pressure.

Provisions will also be included in the Technical Specifications for performing maintenance activities on the differential pressure control system and for

resolving operational difficulties which may result in an inadvertent reduction in the differential pressure for a short period of time. In certain circumstances, corrective action can be taken without having to attain a cold-shutdown condition. To avoid repeated and unnecessary partial cooldown cycles, a restoration period will be incorporated into the action requirements of the LCO for differential pressure control; i.e., in the event that the differential pressure cannot be restored in 6 hours, an orderly shutdown shall be initiated and the reactor shall be in a cold-shutdown condition within 24 hours. The 6-hour restoration period was selected on the basis that it represents an adequate minimum period of time during which any short-term malfunctions could be corrected, coupled with the minimum period of time required to conduct a controlled shutdown. The allowable time to conduct a controlled shutdown has been minimized, because the containment transient response is more a function of the primary system pressure than the reactor power level.

The staff has concluded that these limiting conditions for plant operation, coupled with the related structural assessment requirements, provide an adequate basis for application of differential pressure control as an effective long-term mitigation technique.

### 3.12.8 SRV Steam Discharge Loads

Following the initial SRV clearing transient (as described in Sections 2.3 and 3.10) relatively pure steam is discharged into the suppression pool until the valve closes. Data from the Monticello quencher discharge tests (Ref. 47) indicate that the loads produced during this period are small as a result of the inherently stable steam discharge. Limits on the suppression pool temperature (as discussed in Section 3.10.7) further assure the stability of the steam discharge.

Shell pressures during steam discharge in the Monticello quencher tests were approximately  $\pm 0.6$  psid at 75 to 230 Hz, with comparably low shell strain measurements. The staff has concluded that these loads are negligible by comparison to the other suppression pool hydrodynamic loads and need not, therefore, be considered in either the limiting stress or fatigue analyses.

## 4. STRUCTURAL AND MECHANICAL ANALYSES AND ACCEPTANCE CRITERIA

### 4.1 Introduction

This section presents the staff's evaluation of the generic structural and mechanical acceptance criteria and of the general analysis techniques proposed by the Mark I Owners Group for use in the LTP plant-unique analyses (Ref. 8). Because most of the BWR/Mark I facilities were designed and constructed at different times, there are variations in the codes and standards to which they were constructed and subsequently licensed. For this reassessment of the suppression pool hydrodynamic loads, the criteria have been developed to provide a consistent and uniform basis for acceptability. In this evaluation, references to "original design criteria" mean those specific criteria approved by the staff during the operating license review of a plant's FSAR.

The structural and mechanical elements that are to be reassessed in the LTP plant-unique analyses will include the following:

- (1) Pressure Suppression System
  - (a) The torus shell with associated penetrations, reinforcing rings, and support attachments.
  - (b) The torus shell supports to the building structure.
  - (c) The vents between the drywell and the vent-ring header, including penetrations therein.
  - (d) The local region of the drywell at the vent penetrations.
  - (e) The bellows between the vents and the torus shell, internal or external to the torus.

- (f) The vent-ring header and downcomers attached thereto.
- (g) The vent-ring-header supports to the torus shell.
- (h) Vacuum breaker valves attached to vent penetrations within the torus, where applicable.
- (i) Vacuum breaker piping systems, including vacuum breaker valves, attached to torus shell penetrations and to vent penetrations external to the torus, where applicable.

## (2) Internal Structures

- (a) Internal structural elements such as monorails, catwalks, and their supports. Although these elements are not operative in the performance of the containment function, it is important that their failure does not impair that function.
- (b) Vent-header deflectors and associated hardware.

## (3) Attached Piping Systems

- (a) Piping systems, including pumps and valves, internal to the torus, attached to the torus shell, and/or vent penetrations.
- (b) All SRV discharge piping.
- (c) Applicable portions of active containment system piping, such as ECCS suction piping and other piping systems required to maintain core cooling after a LOCA.
- (d) Applicable portions of the piping systems which provide the drywell-torus differential pressure control (as described in Section 3.12.7).
- (e) Applicable portions of other affected piping systems, including vent drains.

(f) Supports for all such piping systems.

## 4.2 Classification of Structures

The structures described above have been categorized in accordance with their functions in order to assign the appropriate service limits (as described in Section 4.3.1). The general components of a Mark I suppression chamber have been classified in accordance with the American Society of Mechanical Engineers (ASME) Boiler and Pressure Vessel Code in the following manner:

### 4.2.1 Pressure Suppression System

The pressure-retaining elements of the suppression chamber system and associated supports are classified in accordance with the ASME Boiler and Pressure Vessel Code criteria for Class MC vessels and Class MC supports.

### 4.2.2 Attached Piping Systems

Piping systems will be classified as Class 2 or Class 3 for ASME Code evaluation. In addition, for each event combination, piping systems will be categorized as either essential or nonessential. Essential piping systems have the additional requirements for operability of active components.

A piping system, or a portion of a piping system, will be considered essential if, during or following the event combination being considered, the system is necessary to ensure:

- (1) The integrity of the reactor coolant pressure boundary.
- (2) The capability to shut down the reactor and maintain it in a safe-shutdown condition.
- (3) The capability to prevent or mitigate the consequences of accidents which could result in potential offsite exposure comparable to the guideline exposures of 10 CFR Part 100.



In addition, essential piping may become nonessential piping in a later portion of an event combination if the piping is no longer required to perform a safety-related role during the event combination being considered or during any subsequent event combination. In all cases, piping shall be considered to be essential if it performs a safety-related role at a later time during the event combination being considered or during any subsequent event combination.

A pump or valve in an essential piping system is considered an active component if it is required to perform a mechanical motion during the course of accomplishing a system safety function. Other pumps and valves are inactive components.

#### 4.2.3 Internal Structures

Internal structures, such as monorails, ladders, catwalks, and vent-header deflectors, are nonsafety-related elements because they do not perform a pressure-retaining function. As such, these elements are not covered by the ASME Code criteria, with the exception of attachment welds to Code structures. These attachment welds are classified in accordance with the Code requirements for the structure to which they are attached.

#### 4.3 Service Limits and Associated Load Combinations

The structural acceptance criteria set forth in the PUAAG (Ref. 8) generally are contained in Section III of the ASME Boiler and Pressure Vessel Code through the Summer 1977 Addenda. These criteria are to be used in the LTP plant-unique analyses to evaluate the acceptability of the existing Mark I containment designs or to provide the basis for any plant modifications necessary to withstand the suppression pool hydrodynamic loading conditions. The staff has concluded that the application of the stress limits associated with these criteria will provide adequate margins of safety to ensure the containment structural integrity for all anticipated loading combinations and will ensure that the containment and attached piping systems will perform their intended functions during those loading conditions expected to occur as a result of a LOCA or SRV discharge.

Additionally, the ratio of the dynamic collapse load to the static collapse load was established by analysis for typical LOCA pool swell pressure loads on the torus shell and typical pool swell impact loads on the vent header. These values, in conjunction with Code Case N-197, were used to establish the allowable stress values for the torus-shell and the vent-header local stresses. Since the ASME Code-allowable stresses were established based on statically applied loads, Code Case N-197 was developed to provide uniform factors of safety to failure for both static and dynamic loads. Specific application of Code Case N-197 is described in more detail in Section 4.3.3.

#### 4.3.1 Service Limits

The service limits which follow are defined in terms of the Winter 1976 Addenda, which introduced Level A, B, C, and D Service Limits. The selection of specific service limits for each load combination is dependent on the functional requirements of the component analyzed and the nature of the applied load. For example, loads associated with normal plant operations are assigned Level A Service Limits, while loads associated with combinations of low-probability events are assigned Level C or D Service Limits. The assignments of service levels for each load combination are given in Figures 4.3-1 to 4.3-3. The consequences associated with each of the service levels specified in the ASME Boiler and Pressure Vessel Code are discussed below.

##### 4.3.1.1 Level A Service Limit

This level provides for complete evaluation of all possible failure modes, including fatigue, and applied factors of safety consistent with the expectation that the events to which this level is assigned will actually occur. That is, they represent the performance of normal service functions.

For example, the design-basis accident condition for the plant is considered the normal service function for torus shell design.

| EVENT COMBINATIONS  | SRV             |   |   | SRV + EQ |   | SBA IBA |   | SBA + EQ IBA + EQ |   |    |    | SBA + SRV IBA + SRV |    | SBA + SRV + EQ IBA + SRV + EQ |    |    |    | DBA |    | DBA + EQ |    |    |    | DBA + SRV |    | DBA + EQ + SRV |    |        |        |
|---|-----------------|---|---|----------|---|---------|---|-------------------|---|----|----|---------------------|----|-------------------------------|----|----|----|-----|----|----------|----|----|----|-----------|----|----------------|----|--------|--------|
|   | 1               | 2 | 3 | 4        | 5 | 6       | 7 | 8                 | 9 | 10 | 11 | 12                  | 13 | 14                            | 15 | 16 | 17 | 18  | 19 | 20       | 21 | 22 | 23 | 24        | 25 | 26             | 27 |        |        |
|   |                 |   |   |          |   |         |   |                   |   |    |    |                     |    |                               |    |    |    |     |    |          |    |    |    |           |    |                |    | CO, CH | CO, CH |
| TYPE OF EARTHQUAKE  |                 | O | S |          |   | O       | S | O                 | S |    |    | O                   | S  | O                             | S  |    |    | O   | S  | O        | S  |    |    | O         | S  | O              | S  |        |        |
| COMBINATION NUMBER  | 1               | 2 | 3 | 4        | 5 | 6       | 7 | 8                 | 9 | 10 | 11 | 12                  | 13 | 14                            | 15 | 16 | 17 | 18  | 19 | 20       | 21 | 22 | 23 | 24        | 25 | 26             | 27 |        |        |
| LOADS   |                 |   |   |          |   |         |   |                   |   |    |    |                     |    |                               |    |    |    |     |    |          |    |    |    |           |    |                |    |        |        |
| Normal (2)  | N               | X | X | X        | X | X       | X | X                 | X | X  | X  | X                   | X  | X                             | X  | X  | X  | X   | X  | X        | X  | X  | X  | X         | X  | X              | X  |        |        |
| Earthquake  | EQ              |   | X | X        |   |         | X | X                 | X | X  |    |                     | X  | X                             | X  | X  |    | X   | X  | X        | X  |    |    | X         | X  | X              | X  |        |        |
| SRV Discharge   | SRV             | X | X | X        |   |         |   |                   |   | X  | X  | X                   | X  | X                             | X  |    |    |     |    |          |    | X  | X  | X         | X  | X              | X  |        |        |
| LOCA Thermal  | T <sub>A</sub>  |   |   |          | X | X       | X | X                 | X | X  | X  | X                   | X  | X                             | X  | X  | X  | X   | X  | X        | X  | X  | X  | X         | X  | X              | X  |        |        |
| LOCA Reactions  | R <sub>A</sub>  |   |   |          | X | X       | X | X                 | X | X  | X  | X                   | X  | X                             | X  | X  | X  | X   | X  | X        | X  | X  | X  | X         | X  | X              | X  |        |        |
| LOCA Quasi-Static Pressure  | P <sub>A</sub>  |   |   |          | X | X       | X | X                 | X | X  | X  | X                   | X  | X                             | X  | X  | X  | X   | X  | X        | X  | X  | X  | X         | X  | X              | X  |        |        |
| LOC. Pool Swell   | P <sub>PS</sub> |   |   |          |   |         |   |                   |   |    |    |                     |    |                               |    | X  |    | X   | X  |          |    | X  |    | X         | X  |                |    |        |        |
| LOCA Condensation Oscillation   | P <sub>CO</sub> |   |   |          | X |         |   | X                 | X |    | X  |                     |    | X                             | X  |    |    | X   |    | X        | X  |    |    |           |    | X              | X  |        |        |
| LOCA Chugging   | P <sub>CH</sub> |   |   |          | X |         |   | X                 | X |    | X  |                     |    | X                             | X  |    |    | X   |    | X        | X  |    |    |           |    | X              | X  |        |        |
| <b>STRUCTURAL ELEMENT</b>   | <b>ROW</b>      |   |   |          |   |         |   |                   |   |    |    |                     |    |                               |    |    |    |     |    |          |    |    |    |           |    |                |    |        |        |
| <u>External Class MC</u>  |                 |   |   |          |   |         |   |                   |   |    |    |                     |    |                               |    |    |    |     |    |          |    |    |    |           |    |                |    |        |        |
| Torus, External Vent Pipe, Bellows, Drywell (at Vent), Attachment Welds, Torus Supports, Seismic Restraints | 1               | A | B | C        | A | A       | B | C                 | B | C  | A  | A                   | B  | C                             | B  | C  | A  | A   | B  | C        | B  | C  | C  | C         | C  | C              | C  |        |        |
| <u>Internal Vent Pipe</u>   |                 |   |   |          |   |         |   |                   |   |    |    |                     |    |                               |    |    |    |     |    |          |    |    |    |           |    |                |    |        |        |
| General and Attachment Welds  | 2               | A | B | C        | A | A       | B | C                 | B | C  | A  | A                   | B  | C                             | B  | C  | A  | A   | B  | C        | B  | C  | C  | C         | C  | C              | C  |        |        |
| At Penetrations (e.g., Header)  | 3               | A | B | C        | A | A       | B | C                 | B | C  | A  | A                   | B  | C                             | B  | C  | A  | A   | B  | C        | B  | C  | C  | C         | C  | C              | C  |        |        |
| <u>Vent Header</u>  |                 |   |   |          |   |         |   |                   |   |    |    |                     |    |                               |    |    |    |     |    |          |    |    |    |           |    |                |    |        |        |
| General and Attachment Welds  | 4               | A | B | C        | A | A       | B | C                 | B | C  | A  | A                   | B  | C                             | B  | C  | A  | A   | B  | C        | B  | C  | C  | C         | C  | C              | C  |        |        |
| At Penetrations (e.g., Downcomers)  | 5               | A | B | C        | A | A       | B | C                 | B | C  | A  | A                   | B  | C                             | B  | C  | A  | A   | B  | C        | B  | C  | C  | C         | C  | C              | C  |        |        |
| <u>Downcomers</u>   |                 |   |   |          |   |         |   |                   |   |    |    |                     |    |                               |    |    |    |     |    |          |    |    |    |           |    |                |    |        |        |
| General and Attachment Welds  | 6               | A | B | C        | A | A       | B | C                 | B | C  | A  | A                   | B  | C                             | B  | C  | A  | A   | B  | C        | B  | C  | C  | C         | C  | C              | C  |        |        |
| <u>Internal Supports</u>  | 7               | A | B | C        | A | A       | B | C                 | B | C  | A  | A                   | B  | C                             | B  | C  | A  | A   | B  | C        | B  | C  | C  | C         | C  | C              | C  |        |        |
| <u>Internal Structures</u>  |                 |   |   |          |   |         |   |                   |   |    |    |                     |    |                               |    |    |    |     |    |          |    |    |    |           |    |                |    |        |        |
| General   | 8               | A | B | C        | A | A       | C | D                 | C | D  | C  | C                   | D  | E                             | D  | E  | E  | E   | E  | E        | E  | E  | E  | E         | E  | E              | E  |        |        |
| Vent Deflector  | 9               | A | B | C        | A | A       | C | D                 | C | D  | C  | C                   | D  | D                             | D  | D  | D  | D   | D  | D        | D  | D  | D  | D         | D  | D              | D  |        |        |

Figure 4.3-1 Event combinations and service levels for class MC components and internal structures.



| EVENT COMBINATIONS             | SRI               | SRI + EQ |      |        |      | SRA + EQ |     |        |     | SRA + SRV |      |        |     | SRA + SRV + EQ  |        |      |        | DRA  |     | DRA + EQ |     |        |     | DRA + SRV |     | DRA + EQ + SRV |     |  |  |
|--------------------------------|-------------------|----------|------|--------|------|----------|-----|--------|-----|-----------|------|--------|-----|-----------------|--------|------|--------|------|-----|----------|-----|--------|-----|-----------|-----|----------------|-----|--|--|
|                                |                   | CO, CH   |      | CO, CH |      | CO, CH   |     | CO, CH |     | CO, CH    |      | CO, CH |     | PS (1)          | CO, CH | PS   | CO, CS |      | PS  | CO, CH   | PS  | CO, CH | PS  | CO, CH    |     |                |     |  |  |
|                                |                   | 0        | S    | 0      | S    | 0        | S   | 0      | S   | 0         | S    | 0      | S   | 0               | S      | 0    | S      | 0    | S   | 0        | S   | 0      | S   | 0         | S   | 0              | S   |  |  |
| COMBINATION NUMBER             | 1                 | 2        | 3    | 4      | 5    | 6        | 7   | 8      | 9   | 10        | 11   | 12     | 13  | 14              | 15     | 16   | 17     | 18   | 19  | 20       | 21  | 22     | 23  | 24        | 25  | 26             | 27  |  |  |
| LOADS                          |                   |          |      |        |      |          |     |        |     |           |      |        |     |                 |        |      |        |      |     |          |     |        |     |           |     |                |     |  |  |
| Normal                         | N                 | X        | X    | X      | X    | X        | X   | X      | X   | X         | X    | X      | X   | X               | X      | X    | X      | X    | X   | X        | X   | X      | X   | X         | X   | X              | X   |  |  |
| Earthquake                     | EQ                |          | X    | X      |      | X        | X   | X      | X   |           |      | X      | X   | X               | X      |      |        | X    | X   | X        | X   |        |     | X         | X   | X              | X   |  |  |
| SRV Discharge                  | SRV               | X        | X    | X      |      |          |     |        |     | X         | X    | X      | X   | X               |        |      |        |      |     |          |     | X      | X   | X         | X   | X              | X   |  |  |
| LOCA Thermal                   | T <sub>A</sub>    |          |      |        | X    | X        | X   | X      | X   | X         | X    | X      | X   | X               | X      | X    | X      | X    | X   | X        | X   | X      | X   | X         | X   | X              | X   |  |  |
| LOCA Reactions                 | R <sub>A</sub>    |          |      |        | X    | X        | X   | X      | X   | X         | X    | X      | X   | X               | X      | X    | X      | X    | X   | X        | X   | X      | X   | X         | X   | X              | X   |  |  |
| LOCA Q-S Press                 | P <sub>A</sub>    |          |      |        | X    | X        | X   | X      | X   | X         | X    | X      | X   | X               | X      | X    | X      | X    | X   | X        | X   | X      | X   | X         | X   | X              | X   |  |  |
| LOCA Pool Swell                | P <sub>PS</sub>   |          |      |        |      |          |     |        |     |           |      |        |     |                 |        |      | X      |      | X   | X        |     |        | X   |           | X   | X              |     |  |  |
| LOCA Condensation Oscillation  | F <sub>(C)</sub>  |          |      |        |      | X        |     |        | X   | X         |      | X      |     | X               | X      |      |        |      | X   | X        |     | X      |     |           | X   | X              |     |  |  |
| LOCA Chugging                  | F <sub>(CH)</sub> |          |      |        |      | X        |     |        | X   | X         |      | X      |     | X               | X      |      |        |      | X   | X        |     | X      |     |           | X   | X              |     |  |  |
| LOAD                           |                   |          |      |        |      |          |     |        |     |           |      |        |     | LOAD FACTOR (2) |        |      |        |      |     |          |     |        |     |           |     |                |     |  |  |
| Normal                         |                   |          |      |        |      |          |     |        |     |           |      |        |     |                 |        |      |        |      |     |          |     |        |     |           |     |                |     |  |  |
| Dead                           | D                 | 1.4      | 1.0  | 1.0    | 1.0  | 1.0      | 1.0 | 1.0    | 1.0 | 1.0       | 1.0  | 1.0    | 1.0 | 1.0             | 1.0    | 1.0  | 1.0    | 1.0  | 1.0 | 1.0      | 1.0 | 1.0    | 1.0 | 1.0       | 1.0 | 1.0            | 1.0 |  |  |
| Live                           | L                 | 1.7      | 1.0  | 1.0    | 1.0  | 1.0      | 1.0 | 1.0    | 1.0 | 1.0       | 1.0  | 1.0    | 1.0 | 1.0             | 1.0    | 1.0  | 1.0    | 1.0  | 1.0 | 1.0      | 1.0 | 1.0    | 1.0 | 1.0       | 1.0 | 1.0            | 1.0 |  |  |
| Operating Temperature          | T <sub>0</sub>    |          | 1.0  | 1.0    |      |          |     |        |     |           |      |        |     |                 |        |      |        |      |     |          |     |        |     |           |     |                |     |  |  |
| Operating Reactivity           | R <sub>0</sub>    |          | 1.0  | 1.0    |      |          |     |        |     |           |      |        |     |                 |        |      |        |      |     |          |     |        |     |           |     |                |     |  |  |
| Earthquake                     |                   |          |      |        |      |          |     |        |     |           |      |        |     |                 |        |      |        |      |     |          |     |        |     |           |     |                |     |  |  |
| Operating                      | O                 |          | 1.25 |        |      | 1.1      | 1.1 |        |     |           | 1.1  | 1.1    |     |                 |        |      |        | 1.1  | 1.1 |          |     |        |     | 1.0       | 1.0 |                |     |  |  |
| Shutdown                       | S                 |          |      | 1.0    |      |          | 1.0 | 1.0    |     |           |      | 1.0    | 1.0 | 1.0             |        |      |        | 1.0  | 1.0 | 1.0      |     |        |     | 1.0       | 1.0 | 1.0            | 1.0 |  |  |
| SRV                            | SRV               | 1.5      | 1.25 | 1.0    |      |          |     |        |     | 1.25      | 1.25 | 1.1    | 1.0 | 1.1             | 1.0    |      |        |      |     |          |     | 1.0    | 1.0 | 1.0       | 1.0 | 1.0            | 1.0 |  |  |
| LOCA                           |                   |          |      |        |      |          |     |        |     |           |      |        |     |                 |        |      |        |      |     |          |     |        |     |           |     |                |     |  |  |
| Thermal                        | T <sub>A</sub>    |          |      |        | 1.0  | 1.0      | 1.0 | 1.0    | 1.0 | 1.0       | 1.0  | 1.0    | 1.0 | 1.0             | 1.0    | 1.0  | 1.0    | 1.0  | 1.0 | 1.0      | 1.0 | 1.0    | 1.0 | 1.0       | 1.0 | 1.0            | 1.0 |  |  |
| Reactions                      | R <sub>A</sub>    |          |      |        | 1.0  | 1.0      | 1.0 | 1.0    | 1.0 | 1.0       | 1.0  | 1.0    | 1.0 | 1.0             | 1.0    | 1.0  | 1.0    | 1.0  | 1.0 | 1.0      | 1.0 | 1.0    | 1.0 | 1.0       | 1.0 | 1.0            | 1.0 |  |  |
| Q-S Press                      | P <sub>A</sub>    |          |      |        | 1.25 | 1.25     | 1.1 | 1.0    | 1.1 | 1.0       | 1.25 | 1.25   | 1.1 | 1.0             | 1.1    | 1.0  | 1.25   | 1.25 | 1.1 | 1.0      | 1.1 | 1.0    | 1.0 | 1.0       | 1.0 | 1.0            | 1.0 |  |  |
| Pool Swell                     | P <sub>PS</sub>   |          |      |        |      |          |     |        |     |           |      |        |     |                 |        | 1.25 |        | 1.1  | 1.0 |          |     | 1.0    |     | 1.0       | 1.0 |                |     |  |  |
| Cond OSC                       | F <sub>(C)</sub>  |          |      |        |      | 1.25     |     |        | 1.1 | 1.0       |      | 1.25   |     | 1.1             | 1.0    |      | 1.25   |      | 1.1 | 1.0      |     | 1.0    |     |           | 1.0 | 1.0            |     |  |  |
| Chugging                       | F <sub>(CH)</sub> |          |      |        |      | 1.25     |     |        | 1.1 | 1.0       |      | 1.25   |     | 1.1             | 1.0    |      | 1.25   |      | 1.1 | 1.0      |     | 1.0    |     |           | 1.0 | 1.0            |     |  |  |
| Category                       |                   |          |      |        |      |          |     |        |     |           |      |        |     |                 |        |      |        |      |     |          |     |        |     |           |     |                |     |  |  |
| Normal                         | X                 |          |      |        |      |          |     |        |     |           |      |        |     |                 |        |      |        |      |     |          |     |        |     |           |     |                |     |  |  |
| Normal/Severe Environmental    |                   | X        |      |        |      |          |     |        |     |           |      |        |     |                 |        |      |        |      |     |          |     |        |     |           |     |                |     |  |  |
| Normal/Extreme Environmental   |                   |          | X    |        |      |          |     |        |     |           |      |        |     |                 |        |      |        |      |     |          |     |        |     |           |     |                |     |  |  |
| Abnormal                       |                   |          |      | X      | X    |          |     |        |     | X         | X    |        |     |                 |        | X    | X      |      |     |          | X   | X      |     |           |     |                |     |  |  |
| Abnormal/Severe Environmental  |                   |          |      |        |      | X        | X   |        |     |           | X    | X      |     |                 |        |      | X      | X    |     |          |     | X      | X   |           |     | X              | X   |  |  |
| Abnormal/Extreme Environmental |                   |          |      |        |      |          | X   | X      |     |           | X    | X      |     |                 |        |      | X      | X    |     |          |     | X      | X   |           |     | X              | X   |  |  |

Figure 4.3-3 Event combinations and load factors for concrete structures.

#### 4.3.1.2 Level B Service Limits

For Class MC vessels and component supports, Level B Service Limits are the same as Level A Service Limits. For other components, Level B Service Limits are the same as those applied to Level A, except that the primary stress allowable is increased to account for possible pressure accumulation when relief valves are actuated. For such components, the design pressure does not include this 10-percent accumulation, so that the higher allowable stress essentially permits acceptance of this condition without further analysis.

#### 4.3.1.3 Level C Service Limits

For containment and other components, the basic allowable stress value applicable to the Level A Service Limits is replaced by a higher value when the Level C Service Limit is imposed. Level C Service Limits are applied for combinations of low-probability events that may occur simultaneously. For example, for containment design, the combination of design-basis accident and safe-shutdown earthquake is evaluated to Level C Service Limits. Level C Service Limits have less safety margin than Levels A or B Service Limits; however, pressure-retaining integrity is ensured by these limits.

#### 4.3.1.4 Level D Service Limits

The Level D Service Limits are the least restrictive limits in Section III of the ASME Code. Level D Service Limits are used for combinations of low-probability events to preclude structural failure. These service limits still ensure pressure-retaining integrity.

#### 4.3.1.5 Level E Service Limits

Special non-Code limits are associated with Level E and are applicable only to nonsafety-related structural elements where element failure may be acceptable, if such failure does not result in significant damage to safety-related items. For this purpose, failure shall be considered to occur at any point at which the Level D Service Limit is exceeded. Therefore, demonstrating that Level D Service Limits are satisfied shall be an objective. When this cannot be done,

and the limit is exceeded at any one point on the element, the analysis must continue with a break at that point and the consequences evaluated. If the limit is exceeded at another point, the structure between the two points shall be considered to be unrestrained and the consequences must be considered in evaluation of other elements to their respective limits.

#### 4.3.2 Applicable Code Sections

The design requirements of the following ASME Code sections and the associated addenda are applicable to the listed component groups and must be satisfied for the long-term program:

##### Class MC Containment Vessels

Article NE-3000, covering the design of Class MC vessels, is completely revised by the Summer 1977 Addenda, and these rules will be used.

##### Class 2 and 3 Piping

The design rules through the Summer 1977 Addenda to the Code will be used.

##### Pumps and Valves

The design rules for Class 2 and 3 pumps and valves through the Summer 1977 Addenda will be used.

##### Linear-Type Component Supports

The design rules for Class 2, 3, and MC linear-type supports through the Summer 1977 Addenda will be used, except as modified by the following:

- (1) For bolted connections, the requirements of Level A and B Service Limits are applicable where Level C and D Service Limits are permitted without increase in the allowable stresses above those applicable to Levels A and B.

- (2) The increased stress level for the combined effects of mechanical loads and constraint of free-end displacements permitted by the last sentence of NF-3231.1(a) is for the primary-plus-secondary stress range.
- (3) All increases in allowable stress permitted by Subsection NF (i.e., those allowed by NF-3231.1(a), XVII-2100(a), and F-1370(a)) are limited by XVII-2110(b) when buckling is a consideration.

#### Other Component Supports

The design rules through the Summer 1977 Addenda will be used for component supports other than the linear type.

#### Internal Structures

The design rules for Class 2, 3, and MC supports will be used for internal structures.

#### Concrete Vessels

The Brunswick plant is the only steel-lined concrete containment, and it will satisfy the requirements of ACI-318-63, Part IV.B. Additional requirements are specified in the Brunswick CSAR regarding the capacity-reduction factors and the necessity that steel reinforcing remain elastic. If additional criteria are necessary, Article CC-3000, Section III, Division 2, will be used.

#### 4.3.3 Service Level Assignments

The component-loading service level assignments for each of the component groups discussed below are shown in Figures 4.3-1 through 4.3-3. The symbols used in these figures are defined in Table 4.3-1.

The service levels for steel structures and piping and the load factors for concrete structures have been assigned in accordance with the general requirements described in Sections 4.3.1 and 4.3.2. Additional requirements and



Table 4.3-1 Structural Criteria Symbol Definition

| Symbol          | Definition  |
|-----------------|---|
| N               | Normal loads  |
| D               | Dead loads<br>(includes hydrostatic)  |
| L               | Live loads  |
| T <sub>O</sub>  | Thermal effects during operation  |
| T <sub>A</sub>  | Thermal effects as a result of<br>a LOCA  |
| R <sub>O</sub>  | Pipe reactions during operation   |
| R <sub>A</sub>  | Pipe reactions as a result of<br>a LOCA   |
| EQ (O)          | Operating-basis earthquake loads  |
| EQ (S)          | Safe-shutdown earthquake loads  |
| SRV             | SRV discharge loads   |
| P <sub>A</sub>  | LOCA quasi-static loads<br>SBA = small-break accident<br>IBA = intermediate-break accident<br>DBA = design-Basis Accident |
| P <sub>PS</sub> | Design-basis pool swell loads<br>(pressure, impact, drag, etc.)   |
| P <sub>CO</sub> | LOCA condensation oscillation Loads   |
| P <sub>CH</sub> | LOCA chugging loads   |

clarifications of the general Code requirements for specific application to the Mark I hydrodynamic load evaluation are identified as footnotes on Figures 4.3-1 through 4.3-3. These specific requirements which were proposed by the Mark I Owners Group in the PUAAG are explained in the following sections, along with the staff evaluation of the proposed requirements.

#### 4.3.3.1 Class MC Components and Internal Structures

The component-loading service level assignments for the Class MC components and internal structures are given in Figure 4.3-1. The following notes apply:

- (1) "Where the drywell to wetwell pressure differential is normally utilized as a load mitigator, an additional evaluation will be performed without SRV loadings but assuming loss of the pressure differential. In the additional evaluation, Level D Service Limits will apply for all structural elements except Row 8 internal structures, which need not be evaluated. If drywell to wetwell pressure differential is not employed as a load mitigator, the listed service limits shall be applicable."

This additional analysis is intended to demonstrate the functional capability of the suppression chamber to withstand LOCA pool swell loads when the drywell-torus differential pressure is out of service (as described in Section 3.12.7.) The staff has concluded that Level D Service Limits are appropriate for this analysis.

- (2) "Normal loads (N) consist of the combination of dead loads (D), live loads (L), thermal effects during operation ( $T_0$ ), and pipe reactions during operation ( $R_0$ )."

This note is a clarification and is self-explanatory.

- (3) "Evaluation of primary-plus-secondary stress intensity range (NE-3221.4) and of fatigue (NE-3221.5) is not required."

These analyses are not necessary for the short-duration pool swell loading condition and, therefore, their exclusion is acceptable.

- (4) "When considering the limits on local membrane stress intensity (NE-3221.2) and primary-membrane-plus-primary-bending stress intensity (NE-3221.3), the  $S_{mc}$  value may be replaced by  $1.3 S_{mc}$ .

"(NOTE: The modification to the limits does not affect the normal limits on primary-plus-secondary stress intensity range (NE-3221.4 or NE-3221.3) nor the normal limits on fatigue evaluation (NE-3221.5(e) or Appendix II-1500). The modification is that the limits on local membrane stress intensity (NE-3221.2) and on primary-membrane-plus-primary-bending stress intensity (NE-3221.3) have been modified by using  $1.3 S_{mc}$  in place of the normal  $S_{mc}$ .

"This modification is a conservative approximation to results from limit analysis testing as reported in Reference 3 and is consistent with the requirements of NE-3228.2.)"

This requirement was derived from limit analysis testing (Ref. 78), identified as Reference 3, above, for the downcomer-vent header system. This approach is permitted by the ASME Code. The staff has reviewed the application of the test data and has concluded that the specified stress limit is acceptable.

- (5) "Service Level Limits specified apply to the overall structural response of the vent system. An additional evaluation will be performed to demonstrate that shell stresses due to the local pool swell impingement pressures do not exceed Service Level C limits."

This requirement was derived from a limit analysis which established the ratio of the dynamic collapse load to the static collapse load for the vent header (Ref. 79), as permitted by Code Case N-197. The staff has reviewed these analyses and their application and has concluded that the specified service level will provide a margin of safety equivalent to or greater than that intended by the Code.

- (6) "For the torus shell, the  $S_{mc}$  value may be replaced by  $1.0 S_{mc}$  times the dynamic load factor derived from the torus structural model."

This requirement was derived from a limit analysis of the torus shell (Ref. 80) which established the ratio of the dynamic collapse load to the static collapse load, as permitted by Code Case N-197. The staff has reviewed these analyses and considers the application of the results as specified in note (6) acceptable. Because of the sensitivity of the elastic dynamic response to the torus shell natural frequency, note (6) requires a plant-specific elastic dynamic amplification factor derived from the structural analysis to adjust the allowable stress limit.

#### 4.3.3.2 Class 2 and 3 Piping Systems

The component-loading service level assignments for Class 2 and 3 piping systems are given in Figure 4.3-2. Operability and functionality requirements for piping systems are discussed in Section 4.3.4. The following notes apply to Figure 4.3-2:

- (1) "Where drywell to wetwell pressure differential is normally utilized as a load mitigator, an additional evaluation will be performed without SRV loadings but assuming the loss of the pressure differential. Service Level D limits shall apply for all structural elements of the piping system for this evaluation. The analysis need only be accomplished to the extent that integrity of the first pressure boundary isolation valve is demonstrated. If the normal plant operating condition does not employ a drywell to wetwell pressure differential, the listed service level assignments will be applicable."

This additional analysis is required on the same basis as that for the Class MC components and internal structures (discussed in Section 4.3.3.1). The staff has concluded that Level D Service Limits to the first isolation valve are sufficient to ensure the functional performance of the containment and are, therefore, acceptable.

- (2) "Normal loads (N) consist of dead loads (D)."

This note is a clarification and is self-explanatory.

- (3) "As an alternative, the  $1.2 S_h$  limit in Equation (9) of NC-3252.2 may be replaced by  $1.8 S_h$ , provided that all other limits are satisfied and operability of active components is demonstrated. Fatigue requirements are applicable to all columns, with the exception of 16, 18, and 19."
- (4) "Footnote (3) applied except that instead of using  $1.8 S_h$  in Equation (9),  $2.4 S_h$  is used."
- (5) "Equation (1) of NC or ND-3659 will be satisfied, except the fatigue requirements are not applicable to columns 16, 18, and 19 since pool swell loadings occur only once. In addition, if operability of an active component is required to ensure containment integrity, operability of that component must be demonstrated."

Notes 3, 4, and 5 are a clarification of the Code requirements as they apply to the specific service conditions under consideration. The staff has concluded that these requirements will ensure the margins of safety intended by the Code for piping systems and are, therefore, acceptable.

#### 4.3.3.3 Concrete Containment Design Requirements

The load factors associated with the Code requirements for steel-lined concrete structures are given in Figure 4.3-3. These requirements apply only to the torus structure. All other structural elements are covered by the requirements contained in Section 4.3.3.1. The following notes apply to Figure 4.3-3:

- (1) "Where drywell to wetwell pressure differential is normally utilized as a load mitigator, an additional evaluation will be performed without SRV loading but assuming the loss of the pressure differential. All load factors will be taken as unity and the category will be Abnormal/Extreme Environmental. If the normal plant operating condition does not employ a drywell to wetwell pressure differential, the listed load factor and category will be applicable."

This additional analysis is intended to demonstrate the functional capability to withstand LOCA pool swell loads when the drywell-torus differential pressure is out of service (as described in Section 3.12.7).

(2) "An additional evaluation will be performed applying the following load factors and the normal category:

|         |     |     |     |                |                |       |
|---------|-----|-----|-----|----------------|----------------|-------|
| Load:   | D   | L   | F   | T <sub>o</sub> | R <sub>o</sub> | SRV   |
| Factor: | 1.0 | 1.3 | 1.0 | 1.0            | 1.0            | 1.3." |

The purpose of this analysis is to assess the local effects of the concrete prestress load (F) in combination with the normal loads. These loads and load factors are consistent with current design practice for similar containment designs (i.e., Mark II and Mark III).

The liner will be evaluated for the various load combinations defined by Figure 4.3-3, except that all load factors shall be taken as unity. The liner also will be analyzed in regard to the dynamic nature of the load, recognizing that although the concrete wall provides restraint in one direction, only the concrete anchors provide support in the opposite direction. Atmospheric pressure will be considered to act between the liner and the concrete.

Self-limiting and other loads will be considered, and the Section III, Division 2, liner plate allowable stress of Table CC-3720-1 and the anchor allowable stresses of Table CC-3730-1 will be satisfied. In addition, combined mechanical negative pressure loads and self-limiting loads will satisfy the criteria identified by the service level designations of Row 1 of Figure 4.3-3 for the equivalent load combinations.

The staff has concluded that the load factors specified for the steel-lined concrete structures will provide the margins of safety intended by the Code and are consistent with those specified for steel structures. On this basis, the requirements specified for the concrete structures are acceptable.

#### 4.3.4 Operability and Functionality Requirements

Operability is defined as the ability of an active component to perform required mechanical motion. Functionality is defined as the ability of a piping system

to pass rated flow. With reference to Figure 4.3-2, operability of an active component is included in notes (3), (4), and (5), and functionality is included in notes (3) and (4). The specific considerations described below have been made regarding the operability and functionality requirements for this program.

In the criteria proposed by the Mark I Owners Group, active components are to be considered operable if Level A or B Service Limits are met, unless the original component design criteria establish more conservative limits. If the original component design criteria do establish more conservative limits, conformance with these more conservative limits shall be demonstrated, even if Level A or B Service Limits are met. If the original component design criteria are silent with respect to operability limits, satisfaction of Level A or B Service Limits would be sufficient to demonstrate operability.

Active components which do not satisfy Level A or B Service Limits, and, therefore, satisfy either Level C or D Service Limits, require demonstration of operability. If original component design criteria for operability exist, conformance with those criteria shall be demonstrated. If the original component design criteria are silent with respect to operability limits, operability limits shall be established, and conformance with those criteria shall be demonstrated.

The operability requirements are necessary to ensure that the active safety-related components will be able to perform their intended functions. It is the staff's position that loads which are calculated by elastic analysis and which produce stresses in excess of the material yield stress can produce excessive deformation in a component and, therefore, can cause interference of mechanical motion.

The staff recognizes that the designation of Level A and B Service Limits does not, by itself, guarantee the operability of active components. However, the scope of the Mark I containment long-term program is directed toward the effects of the incremental load increase as a result of the definition of suppression pool hydrodynamic loads and toward the restoration of the originally intended design-safety margins. The criteria for operability specify that the original component design criteria must be met where they are more conservative than

the Level A and B Service Limits. The staff believes that these operability criteria are sufficient to accomplish the objectives of the program and are, therefore, acceptable.

In the criteria proposed by the Mark I Owners Group, functionality of piping components is to be addressed in a manner consistent with the original design criteria.

Recently, a general set of functionality criteria was developed for piping designed to Level C and D Service Limits, based on a study performed by Battelle (Ref. 81). In order to cover all piping system arrangements and loading conditions, these criteria were developed using the following conservative assumptions and test data:

- (1) The analytical basis considered the most conservative combination of assumptions possible, i.e., a cantilevered pipe segment, the material yield at the Code-specified minimum yield, no consideration of strain-hardening effects, and a static-type loading.
- (2) The supporting test data are based on slowly applied static loads on cantilevered test specimens, with failure defined at a deflection equal to two times the proportional limit. This failure limit produces very small changes in the piping cross-sectional area and would have a negligible effect on fluid flow.
- (3) The dynamic test data presented in the report show the code equations to be conservative for elbows which, according to the functionality criteria, are the least conservative with respect to Class 2 and 3 Code limits.

For the Mark I containment design, the majority of the piping of concern, in terms of the functionality criteria, is that in the externally attached essential piping systems. These piping systems will be subjected to the dynamic motion of the torus shell, which may result in amplified piping system response. For these analyses, the theoretical basis and test data used to develop the general functionality criteria are not directly applicable to the piping associated with the Mark I evaluation for the following reasons:



- (1) The loadings of concern in the Mark I long-term evaluation are dynamic and are calculated on a linear-elastic basis. In order to significantly reduce the flow area of a piping segment, a large inelastic deformation must occur. The large load amplifications associated with linear-elastic analysis are conservative when inelastic behavior occurs (Ref 82).
- (2) The piping attached to the torus is carbon steel, typically A-106, Grade B. For this material, the Level D Service Limit is approximately equal to the Code-specified minimum yield stress.
- (3) The piping attached externally to the torus shell is continuous from the torus shell to the anchor point which bounds the analysis; therefore, large inelastic deformations will not occur without some degree of load redistribution. For this reason, data developed for cantilevered segments would be overly conservative.

Based on the dynamic nature of the Mark I loadings considered in this evaluation and the type of material and support of the attached piping systems, the staff considers the Service Level assignments for Class 2 and 3 piping adequate for the prevention of significant flow reduction in the attached piping. On this basis, the staff has concluded that the proposed criteria are acceptable with respect to functionality of piping systems.

#### 4.4 Analysis Techniques

##### 4.4.1 General Guidelines

The general structural analysis techniques proposed by the Mark I Owners Group are to be performed with sufficient detail to account for all significant structural response modes and consistent with the methods used to develop the loading functions defined in the LDR. For those loads considered in the original design but not redefined by the LDR, either the results of the original analysis may be used or a new analysis may be performed, based on the methods employed in the original plant design. The staff finds this general approach consistent with the objectives of the program and, therefore, acceptable.

#### 4.4.2 Damping

The damping values used in the analysis of dynamic loading events will be those specified in Regulatory Guide 1.61, "Damping Values for Seismic Design of Nuclear Power Plants." Because these values are specified for seismic analysis of structures and components for OBE and SSE conditions, the values used will be consistent with the stresses expected under hydrodynamic loading conditions.

The staff has investigated the effects of variable damping (Ref. 83), because the type of loading input to piping would produce response levels that vary along the length of the piping system, with higher response levels near the torus attachment. These results indicate that a constant damping, consistent with the higher response level near the torus, would produce approximately the same response as the variable damping.

Based on these results, the staff finds the use of the Regulatory Guide 1.61 damping values acceptable for the Mark I dynamic analyses.

#### 4.4.3 Combination of Structural Responses

In the criteria proposed by the Mark I Owners Group, the structural responses resulting from two dynamic phenomena will be combined by the absolute sum method. Time phasing of the two responses will be such that the combined state of the stress results in the maximum stress intensity. However, as an alternative, the cumulative distribution function (CDF) method may be used if the absolute sum does not satisfy the structural acceptance criteria. The CDF combined stress intensity value corresponding to a nonexceedance probability of 84 percent would be used to compute a reduction factor; this factor would then be applied to the stress intensity computed by the absolute sum method. An 84-percent probability of nonexceedance corresponds to a mean-plus-one standard deviation for two dynamic responses.

The proposed CDF technique is applied on a component-specific basis and, therefore, reflects the nature of each component's response to two dynamic events. In the Mark I evaluation, the CDF technique will not be applied to

more than two dynamic events occurring at any point in time. The staff finds the rationale for the use of the proposed methods similar to that contained in NUREG-0484 (Ref. 84) and, therefore, acceptable.

## 5. CONCLUSIONS

This report describes the NRC staff's evaluation of the generic criteria and analysis techniques proposed by the Mark I Owners Group for the reassessment of the suppression chamber (torus) designs of BWR facilities with the Mark I containment design. The results of this evaluation will be applied by means of a plant-unique analysis for each Mark I configuration. The plant-unique analysis will either demonstrate that the existing design has the intended margins of safety or identify any additional plant modifications that are necessary to restore the intended margins of safety in the containment design. In this manner, the functional performance of the containment system will be assured for both loss-of-coolant accident (LOCA) and safety-relief valve (SRV) discharge suppression pool hydrodynamic loading conditions.

This reassessment of facilities with the Mark I containment system design has been required because, during the large-scale testing of the Mark III containment system, suppression pool hydrodynamic loads associated with a postulated LOCA were identified which had not been considered in the original design of the Mark I systems. These newly identified loads result from the dynamic effects of drywell air and steam being rapidly forced into the suppression pool during a postulated LOCA. Air injection results in a pool swell event of short duration in which a layer or slug of water rises and impacts structural components above the pool. Subsequent steam injection results in oscillatory condensation loads as a result of the rapid formation and collapse of steam bubbles in the pool. SRV discharge to the suppression pool from the primary system results in similar hydrodynamic loading conditions.

The Mark I Owners Group concluded the generic aspects of the long-term program by submitting the Mark I Containment Program Load Definition Report (Ref. 7) and the Mark I Containment Program Structural Acceptance Criteria Plant-Unique Analysis Applications Guide (Ref. 8). These reports describe the generic suppression pool hydrodynamic load definition and assessment procedures proposed

by the Mark I Owners Group for use in plant-unique suppression chamber design analyses. The proposed procedures have been derived from a series of experimental and analytical programs specifically conducted for that purpose.

The staff has reviewed the experimental and analytical programs conducted by the Mark I Owners Group, as well as information produced by related NRC research programs. Based on this review, the staff has concluded that the proposed generic suppression pool hydrodynamic load definition techniques, as modified by the staff's requirements in Appendix A, will provide conservative estimates of the dynamic loading conditions resulting from LOCA and SRV discharge events.

The only exception concerns the lack of an acceptable definition of the downcomer "condensation oscillation" loads. The staff requires (Appendix A, Section 2.11.2.2) that the Mark I Owners Group develop an acceptable load definition procedure for "tied" downcomers, based on FSTF measurements, which will adequately segregate the dynamic loading components in the downcomer-vent header connection and in the tie-bar. This load specification must be developed on a schedule that is compatible with the schedules for implementation. The resolution of this issue will be described in a supplement to this report.

In addition, the staff has identified confirmatory requirements for additional FSTF testing which will establish the uncertainty (i.e., relative error) in the magnitude of the "condensation oscillation" loads, and for analyses which will establish the effects of compressibility on the magnitude of pool swell loads derived from scaled testing facilities. The resolution of these issues will be described in a supplement to this report.

The staff has concluded that the proposed structural acceptance criteria are consistent with the requirements of the applicable codes and standards and, in conjunction with the general structural analysis techniques, will provide an adequate basis for establishing the margins of safety in the containment design.

This evaluation represents the resolution of the staff's "Unresolved Safety Issue," A-7, the "Mark I Containment Long-Term Program." Conformance with the

proposed suppression pool hydrodynamic load definition and assessment procedures, as modified by the staff's requirements, will constitute an acceptable implementation of this program. Schedules for implementation will be established on the basis of the modification schedules that have been submitted by each of the affected licensees.

## 6. REFERENCES

References cited in this report are available as follows:

Those items marked with one asterisk (\*) are available in the NRC Public Document Room for inspection; they may be copied for a fee.

Material marked with two asterisks (\*\*) is not publicly available because it contains proprietary information; however, a nonproprietary version is available in the NRC Public Document Room for inspection and may be copied for a fee.

Those reference items marked with three asterisks (\*\*\*) are available for purchase from the NRC/GPO Sales Program, U.S. Nuclear Regulatory Commission, Washington, DC 20555, and/or the National Technical Information Service, Springfield, Virginia 22161.

All other material referenced is in the open literature and is available through public technical libraries.

- (1) L. L. Myers, T. R. McIntyre, and R. J. Ernst, "Mark III Confirmatory Test Program Phase I - Large-Scale Demonstration Test, Test Series 5701 through 5703," General Electric Proprietary Report NEDM-13377, October 1974.\*\*
- (2) T. Y. Fukushima and others, "Test Results Employed by GE for BWR Containment and Vertical Vent Loads," General Electric Proprietary Report NEDE-21078-P, October 1975.\*\*
- (3) General Electric Company, "Mark I Containment Program, Program Action Plan," General Electric Topical Report EW7610.09, Revision 0, October 29, 1975.\*
- (4) General Electric Company, "Mark I Containment Program, Program Action Plan," General Electric Topical Report EW7610.09, Revision 1, February 11, 1977.\*
- (5) General Electric Company, "Mark I Containment Program, Program Action Plan," General Electric Topical Report EW7610.09, Revision 2, August 1, 1977.\*
- (6) General Electric Company, "Mark I Containment Program, Program Action Plan," General Electric Topical Report EW7610.09, Revision 3, February 15, 1978.\*
- (7) General Electric Company, "Mark I Containment Program Load Definition Report," General Electric Topical Report NEDO-21888, Revision 0, December 1978.\*
- (8) Mark I Owners Group, "Mark I Containment Program Structural Acceptance Criteria Plant-Unique Analysis Applications Guide, Task Number 3.1.3," General Electric Topical Report NEDO-24583, Revision 1, July 1979.\*

- (9) General Electric Company, "The General Electric Pressure Suppression Containment Analytical Model," General Electric Topical Report NEDO-10320, April 1971; Supplement 1, May 1971; Supplement 2, January 1973.\*
- (10) F. J. Moody, Maximum Discharge Rate of Liquid-Vapor Mixtures from Vessels," General Electric Topical Report NEDO-21052, September 1975.\*
- (11) W. J. Bilanin, "The General Electric Mark III Pressure Suppression Containment System Analytical Model," General Electric Topical Report NEDO-20533, Section 2.0, June 1974.\*
- (12) Letter from D. G. Eisenhut, NRC, to L. J. Sobon, General Electric, Subject: Review of General Electric Topical Report NEDO-21052, "Maximum Discharge Rate of Liquid-Vapor Mixtures from Vessels," December 27, 1978.\*
- (13) F. J. Moody, "Maximum Discharge Rate of Liquid-Vapor Mixtures from Vessels," General Electric Topical Report NEDO-21052-A, May 1979.\*
- (14) General Electric Company, "Mark I Containment Program Quarter-Scale Plant-Unique Tests, Task Number 5.5.3, Series 2," General Electric Proprietary Report NEDE-21944-P, Vols. 1-4, April 1979.\*\*
- (15) D. L. Galyardt, C. G. Hayes, and S. L. Kushman, "Mark I Containment Program Quarter-Scale Pressure Suppression Pool Swell Test Program: Scaling Evaluation, Task Number 5.5.1," General Electric Proprietary Report NEDE-21627-P, January 1978.\*\*
- (16) W. G. Anderson, P. W. Huber, and A. A. Sonin, Massachusetts Institute of Technology, "Small-Scale Modeling of Hydrodynamic Forces in Pressure Suppression Systems," USNRC Report NUREG/CR-003, March 1978.\*\*\*
- (17) Lawrence Livermore Laboratory, "Final Air Test Results for the One-Fifth-Scale Mark I Boiling Water Reactor Pressure Suppression Experiment," USNRC Report NUREG/CR-0151, October 1977.\*\*\*
- (18) C. K. Chan and others, University of California, Los Angeles, "Suppression Pool Dynamics," USNRC Report NUREG/CR-0264-3, February 1978.\*\*\*
- (19) S. J. Finch, J. Strazzer, and T. Oguri, "Variability of Upward and Downward Vertical Pressure Loads in a Mark I Containment," prepared for NRC by the State University of New York, Stony Brook, September 1979.\*
- (20) R. L. Kiang and B. J. Grossi, "Three-Dimensional Pool Swell Modeling of a Mark I Suppression System," Electric Power Research Institute Report EPRI NP-906, October 1978.\*
- (21) Nuclear Services Corporation, "Mark I Containment Program Comparison of GE and EPRI Torus Load Test Results, Task Number 5.10," General Electric Proprietary Report NEDE-21973-P, February 1979.\*\*
- (22) General Electric Company, "Mark I Containment Program Quarter-Scale Pressure Suppression Pool Swell Test Program: LDR Load Tests - Generic Sensitivity, Task Number 5.5.3, Series 1," General Electric Proprietary Report NEDE-23545-P, December 1973.\*\*



- (23) D. L. Galyardt, "Mark I 1/12-Scale Pressure Suppression Pool Swell Test Program: Phase IV Tests," General Electric Proprietary Report NEDE-21492-P, March 1977.\*\*
- (24) General Electric Company, "Mark I Containment Program Quarter-Scale Pressure Suppression Pool Swell Test Program - ~~Download~~ Oscillation, Task Number 5.5.2," General Electric Proprietary Report NEDE-21943-P, September 1978.\*\*
- (25) K. Souter and H. Krachman, "Water Impact Tests of Rigid and Flexible Cylinders," Electric Power Research Institute Report EPRI NP-798, May 1978.\*
- (26) W. Kennedy and V. Kulkarni, "Mark I Containment Program Vent Header Deflector Load Definition, Task 7.3.3," General Electric Topical Report NEDO-24612, April 1979.\*
- (27) H. Wagner, "Über Stoss und Gleitvorgänge an der Oberfläche von Flüssigkeiten" (Translation: "Phenomena Associated with Impacts and Sliding on Liquid Surfaces"), Zeitschrift für Angewandte Mathematik und Mechanik, 12, 193-215, 1932. National Advisory Committee for Aeronautics Report 1366, 1932.
- (28) S. F. Hoerner, Fluid-Dynamic Drag, Hoerner Fluid Dynamics, Brick Town, New Jersey, 1965.
- (29) Th. von Karman, "The Impact on Seaplane Floats During Landing," National Advisory Committee for Aeronautics Report TN 321, 1929.
- (30) H. Wagner, Zeitschrift für Flugtechnik und Motor Luft Schifffahrt (Translation: Landing of Seaplanes), 22, 1-8, 1931. National Advisory Committee for Aeronautics Technical Memorandum No. 622, May 1931.
- (31) W. L. Mayo, "Analysis and Modification of Theory for Impact of Seaplanes on Water," National Advisory Committee for Aeronautics Report TN 1008, December 1945.
- (32) M. A. Monaghan, "Theoretical Examination of Effect of Dead-Rise in Seaplane-Water Impacts," Royal Aircraft Establishment TN Aero. 1989, 1949.
- (33) J. D. Pierson, "The Penetration of a Fluid Surface by a Wedge," Experimental Towing Tank, Stevens Institute of Technology Report No. 381, July 1950.
- (34) S. Chuang, "Slamming of Rigid Wedge-Shaped Bodies with Various Dead-Rise Angles," David Taylor Model Basin Report 2268, October 1966.
- (35) S. Chuang, "Investigation of Impact of Rigid and Elastic Bodies with Water," U.S. Naval Ship Research and Development Center Report 3248, February 1970.
- (36) W. Kennedy and others, "Rigid and Flexible Vent Header Testing in the Quarter-Scale Test Facility, Mark I Containment Program, Task 5.5.3," General Electric Proprietary Report NEDE-24520-P, March 1978.\*\*

- (37) T. R. McIntyre and others, "Mark III Confirmatory Test Program One-Third Scale Pool Swell Impact Tests, Test Series 5805," General Electric Proprietary Report NEDE-13426-P, August 1975.\*\*
- (38) D. Gilbarg, "Jets and Cavities," Handbuch der Physik, Vol. 9, Springer Verlag, Berlin, 1960.
- (39) U.S. Nuclear Regulatory Commission, "Mark II Lead Plant Program Load Evaluation and Acceptance Criteria," USNRC Report NUREG-0487, October 1978.\*\*\*
- (40) J. M. Biggs, Introduction to Structural Dynamics, McGraw-Hill, New York, 1964.
- (41) C. W. Hirt and B. D. Nichols, "Numerical Simulation of Hydrodynamic Impact Loads on Cylinders," in Hydrodynamic Impact Analysis, Electric Power Research Institute Interim Report EPRI NP-824, June 1978.\*
- (42) G. W. Fitzsimmons and other, "Mark I Containment Program Full-Scale Test Program Final Report, Task Number 5.11," General Electric Proprietary Report NEDE-24539-P, April 1979.\*\*
- (43) Letter from D. G. Eisenhut, NRC, to all boiling water reactor licensees (except Dresden 1, Humboldt Bay, Big Rock Point, and LaCrosse), Subject: Confirmatory Requirements Relating to Condensation Oscillation Loads for the Mark I Containment Long-Term Program, October 2, 1979.\*
- (44) Bechtel Power Corporation, "Mark I Containment Program Analysis of Full-Scale Test Facility for Condensation Oscillation Loading, Task 5.17.3," General Electric Proprietary Report NEDE-24645-P, July 1979.\*\*
- (45) Letter from L. J. Sobon, General Electric Company, to D. G. Eisenhut, NRC, Subject: Mark I Containment Program Additional Information on NEDO-21888, "Mark I Containment Program Load Definition Report," September 7, 1979.\*\*
- (46) EDS Nuclear Inc., "Mark I Containment Long-Term Program - Development of Downcomer Lateral Loads from Full-Scale Test Facility Data, Task Number 7.3.2," General Electric Proprietary Report NEDE-24537-P, May 1979.\*\*
- (47) R. A. Asia and others, "Mark I Containment Program Final Report, Monticello T-Quencher Test," General Electric Proprietary Report NEDE-21864-P, July 1978.\*\*
- (48) C. T. Sawyer and others, "Mark I Containment Program Final Report - Quarter-Scale T-Quencher Test," General Electric Proprietary Report NEDE-24549-P, December 1978.\*\*
- (49) A. J. Wheeler, "Mark I Containment Program Analytical Model for Computing Transient Pressures and Forces in the Safety-Relief Valve Discharge Line," General Electric Proprietary Report NEDE-23749-P, February 1978.\*\*

- (50) A. J. Wheeler and D. A. Dougherty, "Mark I Containment Program Comparison of Analytical Model for Computing S/RVLD Transient Pressures and Forces to Monticello Data," General Electric Proprietary Report NEDE-23749-1-P, February 1979.\*\*
- (51) P. Valandani and W. T. Hsiao, "Mark I Containment Program Analytical Model for Computing Air Bubble and Boundary Pressures Resulting from an S/RV Discharge Through a T-Quencher Device," General Electric Proprietary Report NEDE-21878-P, January 1979.\*\*
- (52) R. Schrim, "Mark I Containment Program Scaling Analysis for Modeling Initial Air-Clearing Caused by Reactor Safety-Relief Valve Discharge," General Electric Proprietary Report NEDE-23713-P, February 1978.\*\*
- (53) General Electric Company, "Interim Containment Loads Report (ICLR) - Mark III Containment," General Electric Topical Report E2A4365, Revision 2, October 1978.\*
- (54) Letter from N. W. Curtis, Pennsylvania Power and Light Company, to O. D. Parr, NRC, Revisions to Susquehanna Steam Electric Station Final Safety Analysis Report, Docket Number 50-387/388, April 14, 1979, Chapter 8, "SSES Quencher Verification Test" (Proprietary).\*\*
- (55) A. J. Wheeler and D. A. Dougherty, "Mark I Containment Program Analytical Model for Computing Water Rise in a Safety-Relief Discharge Line Following Valve Closure," General Electric Proprietary Report NEDE-23898-P, October 1978.\*\*
- (56) B. J. Patterson, "Monticello T-Quencher Thermal Mixing Test Final Report," General Electric Proprietary Report NEDE-24542-P, April 1979.\*\*
- (57) F. J. Moody, "Analytical Model for Liquid Jet Properties for Predicting Forces on Rigid Submerged Structures," General Electric Proprietary Report NEDE-21472, September 1977.\*\*
- (58) Nuclear Services Corporation, "Mark I Containment Program Quarter-Scale Test Report Loads on Submerged Structures Due to LOCA Air Bubbles and Water Jets," General Electric Proprietary Report NEDE-23817-P, September 1978.\*\*
- (59) S. L. Liu and L. E. Lasher, "Mark I Containment Program Submerged Structures Model Main Vent Air Discharges Evaluation Report, Task Number 5.14.1," General Electric Proprietary Report NEDE-21983-P, March 1979.\*\*
- (60) T. Sarpkaya and C. J. Garrison, "Vortex Formation and Resistance in Unsteady Flow," in Transactions of the ASME, Journal of Applied Mechanics, Vol. 30, pp. 16-24, 1963.
- (61) T. Sarpkaya, "Evolution of the Wake in Unsteady Flow and Transverse Forces," Unpublished Memorandum, 1979.\*
- (62) T. Sarpkaya, "Forces on Cylinders and Spheres in a Sinusoidal Oscillating Fluid," in Transactions of the ASME, Journal of Applied Mechanics, pp. 32-37, 1975.

- (63) G. H. Keulegan and L. H. Carpenter, "Forces on Cylinders and Plates in an Oscillating Fluid," Journal of Research of the National Bureau of Standards, Vol. 60, pp. 423-440, 1958.
- (64) T. Sarpkaya, "In-Line and Transverse Forces on Cylinders in Oscillating Flow at High Reynolds Numbers," Journal of Ship Research, Vol. 21, pp. 200-216, 1977.
- (65) T. Sarpkaya, "Vortex Shedding and Resistance in Harmonic Flow About Smooth and Rough Circular Cylinders at High Reynolds Numbers," U.S. Naval Postgraduate School Report NPS-59SL76021, February 1976.
- (66) T. Yamamoto, "Forces on Many Cylinders Near a Plate Boundary," Oregon State University Report ORESU-R-76-003, 1976.
- (67) T. Yamamoto, "Hydrodynamic Forces on Multiple Circular Cylinders," Journal of the Hydraulics Division ASCE, Vol. 102, pp. 1193-1210, 1976.
- (68) C. Dalton and R. A. Helfinstein, "Potential Flow Past a Group of Circular Cylinders," in Transactions of the ASME, Journal of Basic Engineering, pp. 636-642, 1971.
- (69) T. Sarpkaya, "Forces on Cylinders Near a Plate Boundary in Sinusoidal Oscillating Fluid," in Transactions of the ASME, Journal of Fluids Engineering, pp. 499-505, 1976.
- (70) C. Dalton and J. M. Szabo, "Drag on a Group of Cylinders," in Transactions of the ASME, Journal of Pressure Vessel Technology, pp. 152-157, 1977.
- (71) M. M. Zdravkovich, "Review of Flow Interference Between Two Circular Cylinders in Various Arrangements," in Transactions of the ASME, Journal of Fluids Engineering, pp. 618-633, 1977.
- (72) L. E. Lasher, "Analytical Model for Estimating Drag Forces on Rigid Submerged Structures Caused by Condensation Oscillations and Chugging - Mark I Containments," General Electric Topical Report NEDO-25070, April 1979.\*
- (73) F. T. Dodge, "Analytical Model for T-Quencher Water-Jet Loads on Submerged Structures, Task 5.14.2," General Electric Proprietary Report NEDE-25090-P, May 1979.\*\*
- (74) L. E. Lasher, "Analytical Model for Estimating Drag Forces on Rigid Submerged Structures Caused by LOCA and Safety-Relief Valve Ramshead Air Discharges," General Electric Topical Report NEDO-21471-2, April 1979.\*
- (75) S. M. Arian, "Mark I Containment Program Seismic Slosh Evaluation, Task Number 5.4," General Electric Proprietary Report NEDC-23702-P, March 1978.\*\*
- (76) K. W. Wong, "Mark I Containment Program Downcomer Reduced Submergence Functional Assessment Report, Task Number 6.6," General Electric Proprietary Report NEDE-21885-P, June 1978.\*\*

- (77) L. D. Steinart, "Long-Term Application of Drywell/Wetwell Differential Pressure Control," General Electric Topical Report NEDM-24527, March 1978.\*
- (78) Bechtel Power Corporation, "Limit Analysis of Downcomer-Ring Header Intersection," General Electric Proprietary Report, NEDE-21887-P, July 1978.\*\*
- (79) Engineering Decision Analysis Company, "Analysis to Justify Increased Allowable Stresses for the Mark I Vent Header when Subjected to Pool Swell Impact Loading," General Electric Topical Report NEDO-24529, May 1978.\*
- (80) Bechtel Power Corporation, "Basic Torus Shell Analysis," General Electric Topical Report NEDO-21991, January 1979.\*
- (81) E. C. Rodabaugh, Battelle Columbus Laboratory/Oak Ridge National Laboratory, "Evaluation of the Plastic Characteristics of Piping Products in Relation to ASME Code Criteria," USNRC Report NUREG/CR-0261, July 1978.\*\*\*
- (82) S. J. Scott and others, University of California, "Dynamic Excitation of a Single-Degree-of-Freedom Hysteretic System," USNRC Report NUREG/CR-0362, September 1978.\*\*\*
- (83) R. L. Grubb, EG&G Idaho, Inc., "Piping System Stress-Dependent Damping Study," U.S. Department of Energy Interim Report EGG-EA-5038, October 1979.\*
- (84) R. L. Cudlin and others, "Methodology for Combining Dynamic Responses," USNRC Report NUREG-0484, September 1978.\*\*\*

NRC ACCEPTANCE CRITERIA  
FOR THE  
MARK I CONTAINMENT  
LONG TERM PROGRAM

Revision 1  
February 1980

## TABLE OF CONTENTS

|  | <u>PAGE</u> |
|--|-------------|
| 1. INTRODUCTION.....   | 1           |
| 2. SUPPRESSION POOL HYDRODYNAMIC LOADS.....                      | 2           |
| 2.1 Containment Pressure and Temperature.....                    | 2           |
| 2.2 Vent System Pressurization and Thrust Loads.....             | 2           |
| 2.3 Net Torus Vertical Pressure Loads.....                       | 3           |
| 2.4 Torus Pool Swell Shell Pressures.....                        | 4           |
| 2.5 Compressible Flow Effects in Scaled Pool Swell Tests.....    | 5           |
| 2.6 Vent System Impact and Drag Loads.....                       | 6           |
| 2.7 Pool Swell Impact and Drag on Other Internal Structures..... | 9           |
| 2.8 Froth Impingement and Fallback Loads.....                    | 19          |
| 2.9 Pool Fallback Loads.....                                     | 22          |
| 2.10 Vent Header Deflector Loads.....                            | 23          |
| 2.11 Condensation Oscillation Loads.....                         | 30          |
| 2.11.1 Torus Shell Loads.....                                    | 30          |
| 2.11.2 Downcomer Loads.....                                      | 31          |
| 2.11.3 Vent System Pressures.....                                | 32          |
| 2.12 Chugging Loads.....   | 32          |
| 2.12.1 Torus Shell Loads.....                                    | 32          |
| 2.12.2 Downcomer Loads.....                                      | 33          |
| 2.12.3 Vent System Pressures.....                                | 34          |
| 2.13 Safety-Relief Valve Discharge Loads.....                    | 34          |
| 2.13.1 SRV Discharge Device.....                                 | 34          |
| 2.13.2 Discharge Line Clearing Transient.....                    | 34          |
| 2.13.3 Air-Clearing Quencher Discharge Shell Pressures.....      | 34          |
| 2.13.4 SRV Discharge Line Reflood Transient.....                 | 37          |
| 2.13.5 SRV Air and Water Clearing Thrust Loads.....              | 37          |
| 2.13.6 SRV Discharge Line Temperature Transient.....             | 37          |
| 2.13.7 SRV Discharge Event Cases.....                            | 37          |
| 2.13.8 Suppression Pool Temperature Limits.....                  | 38          |
| 2.13.9 SRV Load Assessment by In-Plant Tests.....                | 41          |
| 2.14 Submerged Structure Drag Loads.....                         | 43          |
| 2.14.1 LOCA Water Jet Loads.....                                 | 43          |
| 2.14.2 LOCA Bubble Drag Loads.....                               | 45          |
| 2.14.3 Quencher Water Jet Loads.....                             | 48          |
| 2.14.4 Quencher Bubble Drag Loads.....                           | 48          |
| 2.14.5 LOCA Condensation Oscillation Drag Loads.....             | 49          |
| 2.14.6 LOCA Chugging Drag Loads.....                             | 50          |

TABLE OF CONTENTS (Continued)

|  | <u>PAGE</u> |
|--|-------------|
| 2.15 Secondary Loads.....                            | 51          |
| 2.16 Differential Pressure Control Requirements..... | 51          |
| 3. STRUCTURAL ANALYSES AND ACCEPTANCE CRITERIA.....  | 53          |
| 4. REFERENCES.....                                   | 53          |



## 1. INTRODUCTION

The purpose of the Mark I Containment Long Term Program is to perform a complete reassessment of the suppression chamber (torus) design to include suppression pool hydrodynamic loads which were neglected in the original design, and to restore the original intended design safety margins of the structure. This reassessment will be accomplished by a Plant-Unique Analysis (PUA) for each BWR plant with a Mark I containment, using load specifications and structural acceptance criteria that are appropriate for the life of the plant.

The following acceptance criteria have been developed from the staff's review of the Long Term Program Load Definition Report (LDR), the Plant Unique Analysis Applications Guide (PUAAG), and the supporting analytical and experimental programs conducted by the Mark I Owners Group. These criteria specifically address the dynamic loading conditions. Unless otherwise specified, all other loading conditions and structural analysis techniques (e.g., dead loads and seismic loads) will be in accordance with the plant's approved Final Safety Analysis Report (FSAR). Similarly, references to original design criteria or original loading conditions shall be defined as those criteria or loading conditions which were found acceptable by the staff during the operating license review of the FSAR.

For ease of reference, LDR refers to "Mark I Containment Program Load Definition Report," NEDO-21888, PUAAG refers to "Mark I Containment Program structural Acceptance Criteria Plant Unique Analysis Applications Guide," NEDO-24583, and other supporting topical reports are referred to by their report numbers. A complete set of the references used in these criteria, listed in numerical order, is presented in Section 4.

## 2. SUPPRESSION POOL HYDRODYNAMIC LOADS

### 2.1 CONTAINMENT PRESSURE AND TEMPERATURE RESPONSE

The pressure and temperature transients for the drywell and wetwell shall be determined by the use of the analytical models and assumptions set forth in Section 4.1 of the LDR. These techniques have, in the past, been found to provide conservative estimates of the containment response to a LOCA, by comparison to the staff's CONTEMP-LT computer code. | 1

The timing and duration of specific loads are based primarily on the plant-specific containment response analysis for the pool swell-related loads, while the condensation periods are non-mechanistically maximized. However, the duration of the generic SBA condensation loads are assumed to be limited by manual operation of the Automatic Depressurization System (ADS) at 10 minutes into the accident. Therefore, as part of the PUA, each licensee shall specify procedures (including the primary system parameters monitored) by which the operator will identify the SBA, to assure manual operation of the ADS within the specified time period. Longer time periods may be assumed for the SBA in any specific PUA, provided (1) the chugging load duration is correspondingly increased, (2) the procedures to assure manual operation within the assumed time period are specified, and (3) the potential for thermal stratification and asymmetry effects are addressed in the PUA. | 1

### 2.2 VENT SYSTEM PRESSURIZATION AND THRUST LOADS

The vent system pressurization and thrust loads shall be defined in accordance with the procedures set forth in Section 4.2 of the LDR, with the following exception. In order to assure the proper transition between vent clearing and bubble breakthrough for those plants that propose operation with a differential pressure control, the vent clearing time shall be derived from a containment analysis assuming no drywell/wetwell differential pressure and this time shall be applied to the vent system transients calculated from a

containment response with the proposed drywell/wetwell differential pressure. In addition, for clarification, in the equation for F2V in Section 4.2.1c of the LDR, P3 shall be replaced by P2.

### 2.3 NET TORUS VERTICAL PRESSURE LOADS

The downward and upward net vertical pressure loads on the torus shall be derived from the series of plant-specific QSTF (Quarter Scale Test Facility) tests, in accordance with Section 4.3.1 of the LDR. However, based on our review of the pool swell tests conducted by the Mark I Owners Group and confirmatory tests performed for the NRC by the Lawrence Livermore Laboratory, we will require that the following margins be applied to each loading phase:

$$\begin{aligned} \text{UP} &= \text{UP}_{\text{mean}} + 0.215 (\text{UP}_{\text{mean}}) \\ \text{DOWN} &= \text{DOWN}_{\text{mean}} + 2 \times 10^{-5} (\text{DOWN}_{\text{mean}})^2 \end{aligned}$$

where "mean" refers to the average of the QSTF plant-specific test results ( $\text{lb}_f$ ). These margins shall be applied to the QSTF "mean" load function prior to scaling the load function to full-scale equivalent conditions. The margin for the downward loading function shall be derived in terms of a fraction of the load at the time of the peak downward load, and that fraction shall be applied to the entire downward loading phase.

The margins specified above may be reduced or omitted where minimum conservatisms (i.e., smallest parameter deviation from the nominal plant condition over the range of tested conditions) in the QSTF tested conditions for a specific plant can be demonstrated by the application of the QSTF sensitivity test series (NEDE-23545-P). The sensitivity tests may not be used to adjust the mean torus vertical pressure loads. If the plant configuration is changed to the extent that the QSTF test series no longer represents a conservative configuration of the plant, then a new series of QSTF tests shall be performed.

For those plants that use drywell/wetwell differential pressure control as a load mitigation feature, an additional structural analysis shall be performed assuming a loss of the differential pressure control to demonstrate the capability of the containment to withstand this extreme condition, as specified in Sections 5.3, 5.4, and 5.6 of the PUAAG. For this analysis, a single plant-specific QSTF test run may be used to define the loading function; however, the downward and upward loading phases shall be increased by the margins specified above for the base analysis.

#### 2.4 TORUS POOL SWELL SHELL PRESSURES

The spatial distribution of the torus shell pressures during pool swell shall be defined from the plant-specific QSTF test results and the azimuthal and longitudinal distribution factors defined in Section 4.3.2 of the LDR.

However, the QSTF results shall be adjusted to incorporate the margins specified for the net torus vertical pressure loading function as follows:

1. During the downward loading phase, the average pool pressure shall be increased by the equivalent differential pressure, as a function of time, corresponding to the margin for the downward load.
2. During the upward loading phase, the torus airspace pressure shall be increased by the equivalent differential pressure, as a function of time, corresponding to the margin for the upward load.
3. The pressure distributions shall be maintained such that the integral of the torus shell pressures will equal the net vertical pressure function with the margins included.

## 2.5 COMPRESSIBLE FLOW EFFECTS IN SCALED POOL SWELL TESTS

The QSTF plant-unique test series are based primarily on a "split-orifice" vent flow scaling relationship. Preliminary calculations performed by EPRI and GE indicate that compressibility effects, which could not be accurately scaled in the testing program, could result in a higher loading condition at full-scale conditions than that derived from "scaled-up" test data. The original intent of these analyses was to provide justification for the scaled flow distribution in the EPRI 1/12-scale, three-dimensional pool swell test program.

The loading functions predominantly affected by this finding are the torus downward and upward vertical pressure loads, the torus pool swell pressure distribution, the vent header pool swell impact timing, and the vent header deflector impact timing. Based on our review of the preliminary analyses performed by EPRI and GE, which were presented to the staff in a meeting on July 24, 1979, we concluded that there is sufficient margin in the loading functions to justify proceeding with implementation of the Mark I LTP, while this assessment continues. We will require, however, that the Mark I Owners Group complete the assessment of compressible flow effects and justify the adequacy of these load specifications. In the event that the adequacy of the load specifications cannot be demonstrated, these loading conditions will have to be reassessed.

The vent header and vent header deflector impact timing do not, however, appear to be sufficiently conservative. Based on our review of the material presented thus far concerning the EPRI 1/12-scale three-dimensional pool swell tests and the compressible flow effects analyses, we conclude that the downcomer orificing used for the "split-orifice" tests do not provide a prototypical pool swell response. Therefore, the vent header and vent header deflector impact timing shall be derived from the "main vent orifice" tests (using the same longitudinal load distribution methodology in the LDR), until a flow distribution analysis, acceptable to the staff, can justify some less severe loading conditions.

## 2.6 VENT SYSTEM IMPACT AND DRAG LOADS

### 2.6.1 Vent Header Impact and Drag Loads

The load definition procedures set forth in Section 4.3.3 of the LDR are acceptable, subject to the following clarifications:

1. The experimental data of local vent header pressure in each of the Mark I plants shall be obtained from the QSTF plant-unique tests.

2. The specification, for each Mark I plant, of the pressure inside the vent header relative to that in the torus airspace at the time of water impact on the vent header shall be determined from the QSTF plant-unique tests.

3. The plant-unique header impact timing (i.e., longitudinal time delay) shall be based on the EPRI "main vent orifice" tests as described in Section 2.5.

### 2.6.2 Downcomer Impact and Drag Loads

The load definition procedures set forth in Section 4.3.3 of the LDR are acceptable, subject to the following clarifications. A pressure of 8 psid is to be applied uniformly over the bottom 50° of the angled portion of the downcomer, starting from the time at which the rising pool reaches the lower end of the angled section and ending at the time of maximum pool swell height. The pressure is to be applied perpendicular to the local downcomer surface. The structural analysis for the downcomer impact shall either be dynamic, accounting for the approximate virtual mass of water near the submerged parts of the downcomer, or a dynamic load factor of two shall be applied.

### 2.6.3 Main Vent Impact and Drag Loads

The impact and drag loads on the main vent shall be evaluated in the following manner:

1. Subdivide the submerged portion of the main vent pipe into six equally wide segments (see Figure 2.6-1). If this subdivision results in  $\Delta L < 0.3D$  fewer segments may be used such that  $\Delta L \sim 0.3D$ .
2. Determine the velocity and acceleration histories at Points 1 through 7 in Figure 2.6-1 from the QSTF data and appropriate corrections for longitudinal variations along the torus (at Point 7, only the initial impact velocity is required).
3. Using the velocity components normal to the vent pipe, calculate the impact and "steady" drag pressure using the method in Section 2.7.1 (Cylindrical Structures). At Point 7, only impact force is to be considered.

Using the acceleration components normal to the vent pipe, calculate the acceleration drag pressure using the equation

$$P_a = \frac{\rho}{2g_c} \left( \frac{\pi D}{144} \right) \cdot V + \frac{F_{\text{static buoyancy}}}{144 DL}$$

Where  $P_a$  = the acceleration pressure averaged over the projected area (psi),

$\rho$  = the density of water (lbm/ft<sup>3</sup>),

$D$  = the diameter in feet,

$V$  = the cross flow acceleration (ft/sec<sup>2</sup>),

$g_c$  = gravitational constant (ft - lbm/lbf - sec<sup>2</sup>), and

$L$  = submerged length of main vent

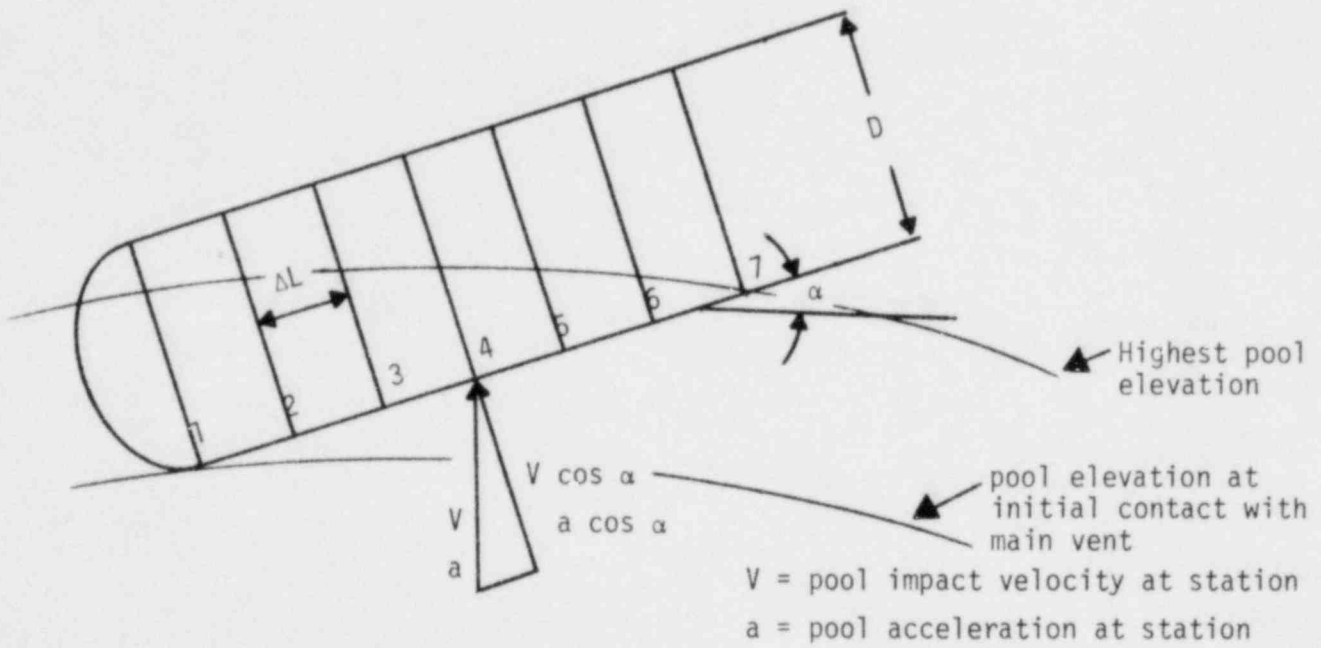


Figure 2.6-1 Schematic Diagram Illustrating the Methodology for Main Vent Impact and Drag



4. Sum the pressures due to impact, viscous drag and acceleration drag and multiply by D to obtain force per unit length at Stations 1 through 7.

5. To obtain a smooth loading history for the main vent as a whole, the linear interpolation method suggested for the vent header deflector in Section 3.5 of NEDO-24612 may be used.

## 2.7 POOL SWELL IMPACT AND DRAG ON OTHER INTERNAL STRUCTURES

The impact and drag loads for internal structures above the suppression pool (except the vent header, downcomers, and vent header deflectors), as specified in Section 4.3.4 of the LDR, shall be modified such that the structures are classified as either cylindrical (e.g., pipes), exposed flat surfaces (e.g., "I" beams), or gratings. The following load specifications for each of the three structural classifications shall be used to replace the methodology in the LDR. Non-cylindrical structures can be conservatively defined as equivalent flat-surfaced structures. However, if such an approach is too conservative, a similar technique may be used with an impact data base which is appropriate for the structural configuration of interest. The longitudinal velocity distribution shall be based on the "main vent" EPRI pool swell tests, as discussed in Section 2.5.

### 2.7.1 Cylindrical Structures

For cylindrical structures, the pressure transient which occurs upon water impact and subsequent drag is depicted in Figure 2.7-1. The parameters in Figure 2.7-1 shall be defined as follows:

1. The maximum pressure of impact  $P_{\max}$  will be determined by

$$P_{\max} = 7.0 \times \frac{1}{2} \left( \frac{\rho}{144} \frac{V^2}{g_c} \right)$$

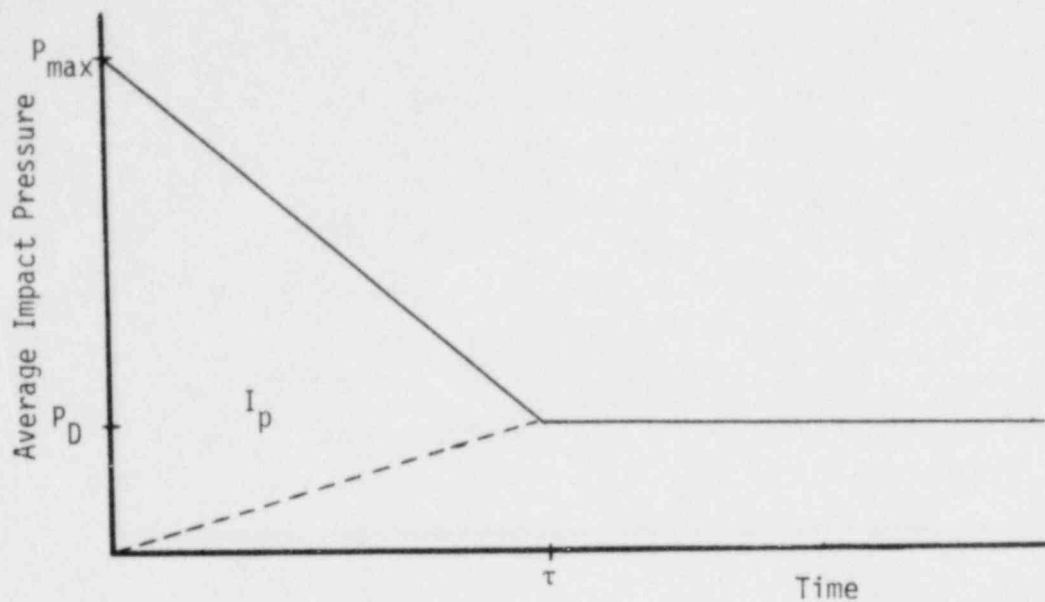


Figure 2.7-1 Pulse Shape for Water Impact on Cylindrical Targets

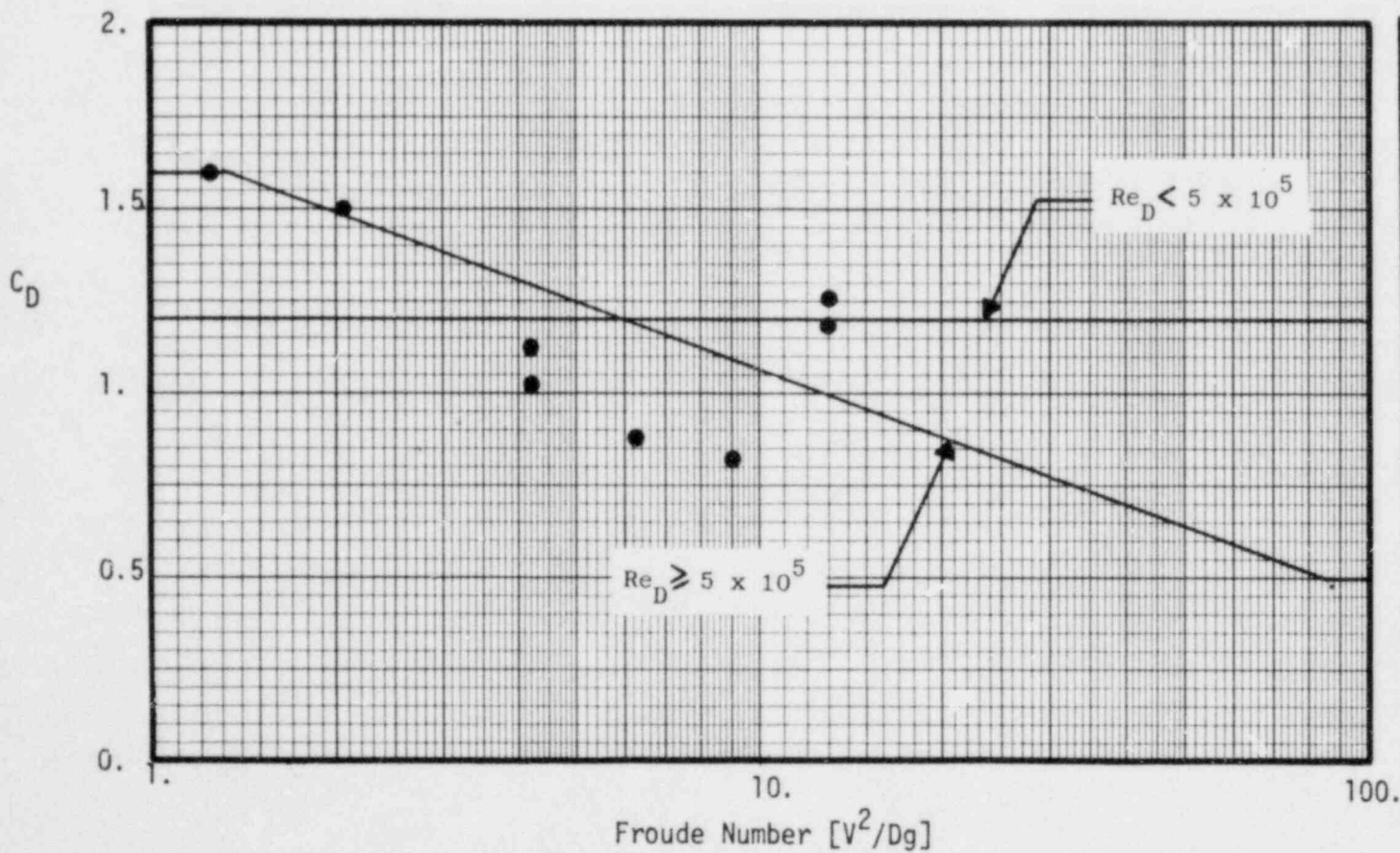


Figure 2.7-2 Drag Coefficient for Cylinders Following Impact

where  $P_{\max}$  = the maximum pressure averaged over the projected area (psi),

$\rho$  = the density of water (lbm/ft<sup>3</sup>),

$V$  = the impact velocity (ft/sec), and

$g_c$  = gravitational constant (ft - lbm/lbf - sec<sup>2</sup>).

2. The hydrodynamic mass per unit area for impact loading shall be obtained from the correlation (cylindrical target) depicted by Figure 6-8 in NEDE-13426-P. A margin of 35% will be added to this value to account for data scatter.

3. The impulse of impact per unit area shall be determined by:

$$I_p = \frac{M_H}{A} \left( \frac{V}{144 g_c} \right)$$

where  $I_p$  = the impulse per unit area (psi-sec),

$M_H/A$  = the hydrodynamic mass per unit area (lbm/ft<sup>2</sup>), and

$V$  = the impact velocity (ft/sec).

4. The pulse duration will be determined from the following equation:

$$\tau = 2I_p/P_{\max}$$

5. The pressure due to drag following impact shall be determined by:

$$P_D = \frac{C_D}{2} \left[ \frac{\rho V_{\max}^2}{144 g_c} \right]$$

where  $P_D$  = the average drag pressure acting on the projected area of the target (psi),

$C_D$  = the drag coefficient as defined by Figure 2.7-2,

$\rho$  = the density of water (lbm/ft<sup>3</sup>), and

$V_{\max}$  = the maximum vertical velocity attained by the pool (ft/sec).

(Note that different velocities are used for the determination of impact and drag loads.)

### 2.7.2 Flat-Surface Structures

For flat-surface structures, the pressure transient which occurs upon water impact and subsequent drag is depicted in Figure 2.7-3. The parameters in Figure 2.7-3 shall be defined as follows:

1. The pulse duration ( $\tau$ ) is specified as a function of the impact velocity:

$$\begin{aligned} \tau &= 0.0016W && \text{for } V \leq 7 \text{ ft/sec} \\ \tau &= \frac{0.011 W}{V} && \text{for } V > 7 \text{ ft/sec} \end{aligned}$$

where  $W$  = the width of the flat surface (feet) and  
 $V$  = the impact velocity (ft/sec).

2. The pressure due to drag following impact shall be determined by:

$$P_D = \frac{C_D}{2} \left[ \frac{\rho V_{\max}^2}{144 g_c} \right]$$

where  $P_D$  = the average drag pressure acting on the frontal area of the structure (psi),

$C_D$  = the drag coefficient ( $C_D = 2$ , flat strips normal to flow, independent of Reynolds number),

$\rho$  = the density of water (lbm/ft<sup>3</sup>), and

$V_{\max}$  = the maximum vertical velocity attained by the pool (ft/sec).

3. The hydrodynamic mass per unit area for impact loading shall be obtained from the correlation (flat targets) in Figure 6-8 in NEDE-13426-P. A margin of 35% shall be added to this value to account for data scatter.

4. The impulse of impact per unit area shall be determined by:

$$I_P = \frac{M_H}{A} \left( \frac{V}{144 g_C} \right)$$

where  $I_P$  = the impulse per unit area (psi-sec),

$M_H/A$  = the hydrodynamic mass per unit area (lbm/ft<sup>2</sup>), and

$V$  = the impact velocity (ft/sec).

5. The maximum pressure ( $P_{max}$ ) shall be calculated from the impulse per unit area and the drag pressure as follows:

$$P_{max} = \frac{2I_P}{\tau} + P_D$$

### 2.7.3 Gratings

The static drag load on gratings in the pool swell zone of the wetwell shall be calculated for gratings with open areas greater than or equal to 60% by forming the product of the pressure differential (Figure 2.7-4) and the total grating area (not only the area of the metal bars). The pressure differential curve in Figure 2.7-4 is based on a velocity of 40 ft/sec. If the maximum pool velocity in the area where gratings are located differs from 40 ft/sec, the force on the grating will be calculated as follows:

$$D = \Delta P \times A_{grating} \left( \frac{V_{max}}{40} \right)^2$$

To account for the dynamic nature of the initial loading, the load shall be increased by a multiplier given by:

$$F_{SE}/D = 1 + [1 + (0.0064 Wf)^2]^{1/2}; \text{ for } Wf < 2000 \text{ in/sec.}$$

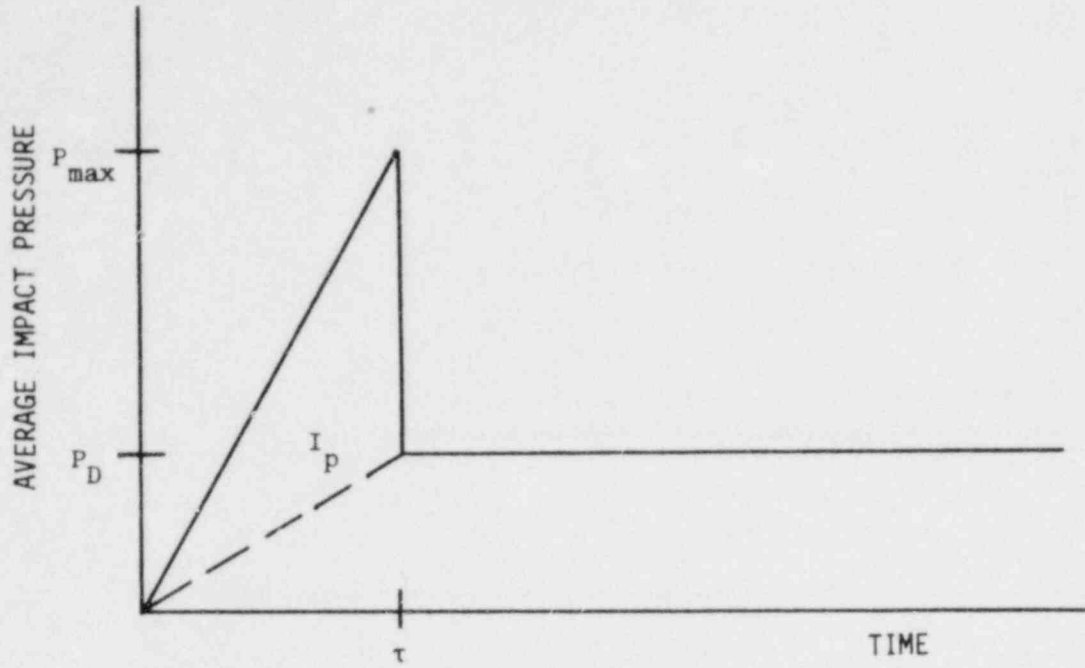


Figure 2.7-3 Pulse Shape for Water Impact on Flat Targets

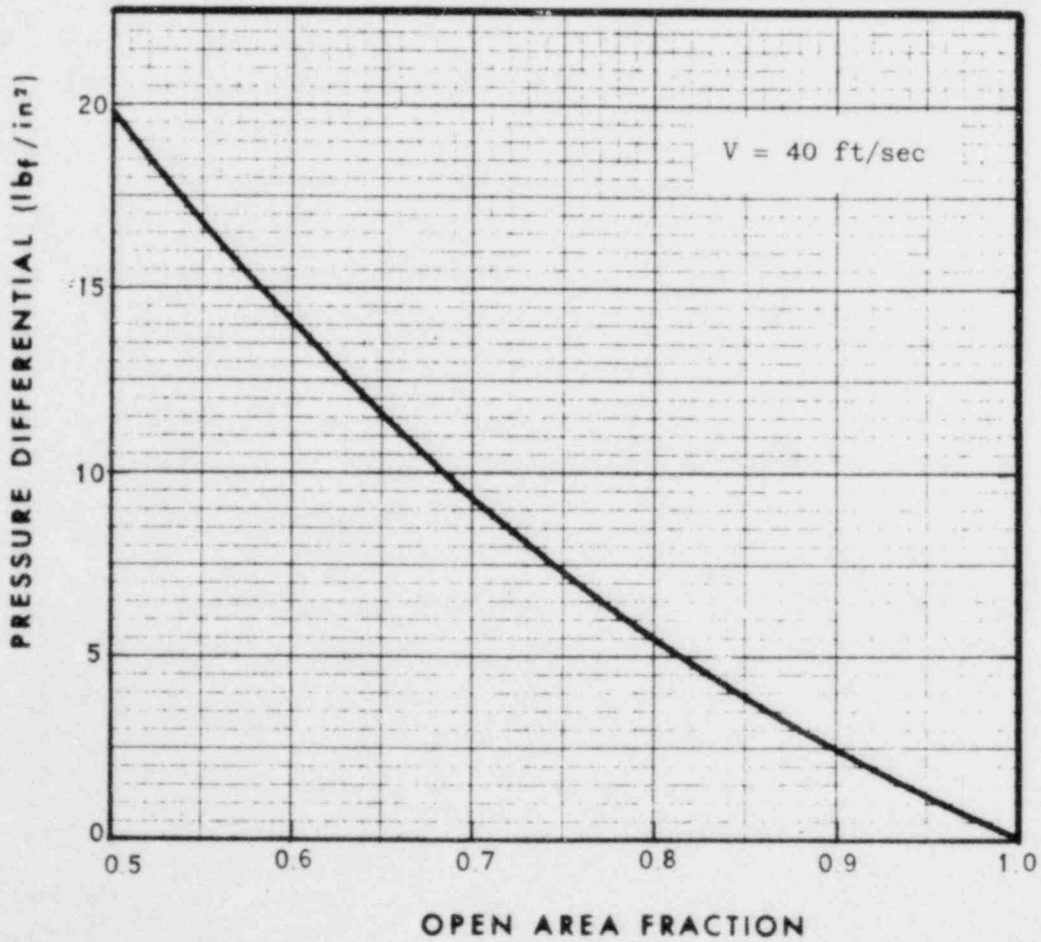


Figure 2.7-4 Pressure Drop Due to Flow Across Gratings

where  $F_{SE}$  = static equivalent load

$W$  = width of grating bars, in.

$f$  = natural frequency of lowest mode, Hz and

$D$  = static drag load

If  $Wf > 2000$  in/sec (not expected for gratings) the force on the bars of the gratings will be calculated by the method outlined above for flat-surfaced structures.

#### 2.7.4 Load Application

These load specifications correspond to impact on "rigid" structure;. When performing the structural dynamic analysis, the "rigid body" impact loads shall be applied; however, the mass of the impacted structure shall be adjusted by adding the hydrodynamic mass of impact, except for the gratings. The value of the hydrodynamic mass shall be obtained from the appropriate correlation in Figure 6-8 in NEDE-13426-P.

In performing the structural dynamic analysis, the drag following impact (as shown in Figures 2.7-1 and 2.7-3) shall be included in the forcing function. The transient calculation shall be continued until the maximum stress in the structure has been identified. | 1

When the impact loading is primarily impulsive and calculations have already been performed in accordance with the LDR methodology, (using the impulse equation on page 4.3.4-5 of the LDR with  $K_h = 0.2$  for cylinders and  $K_H = 0.62$  for flat structures) simple adjustments may be made to the LDR analyses. Under these conditions, a parabolic pulse shape, as proposed in LDR, is acceptable provided corrections are made to account for the 35% margin in the impulse and with additional corrections for the drag force immediately following impact. | 1

For structures with a natural frequency less than 30 Hz, loading can be treated impulsively (i.e., independent of pulse shape) when the conditions fall into the region above the straight line shown in Figure 2.7-5.

The following corrections must be applied to the previously calculated stresses:

1. The calculated stresses will first be multiplied by a factor of 1.35 to account for the data scatter in the impulse data.

2. The calculated stresses will then be multiplied by an additional factor to account for the presence of drag following the impact. This factor is determined as follows:

a. Calculate the drag pressure, ( $P_{\text{drag}}$ ) as described in Sections 2.7.1 or 2.7.2.

b. Form the ratio:

$$P_{\text{drag}}/P_{\text{max}}$$

where  $P_{\text{max}}$  is the amplitude of the parabolic pulse used in the original stress analysis multiplied by 1.35.

c. Determine the dynamic load factor (DLF) from Figure 2.7-6, corresponding to the two cases: (1) parabolic pulse without drag and (2) parabolic pulse followed by drag.

d. Multiply the calculated stress by the factor

$$DLF_{\text{with drag}}/DLF_{\text{w/o drag}}$$



## TYPICAL IMPACT STRUCTURES:

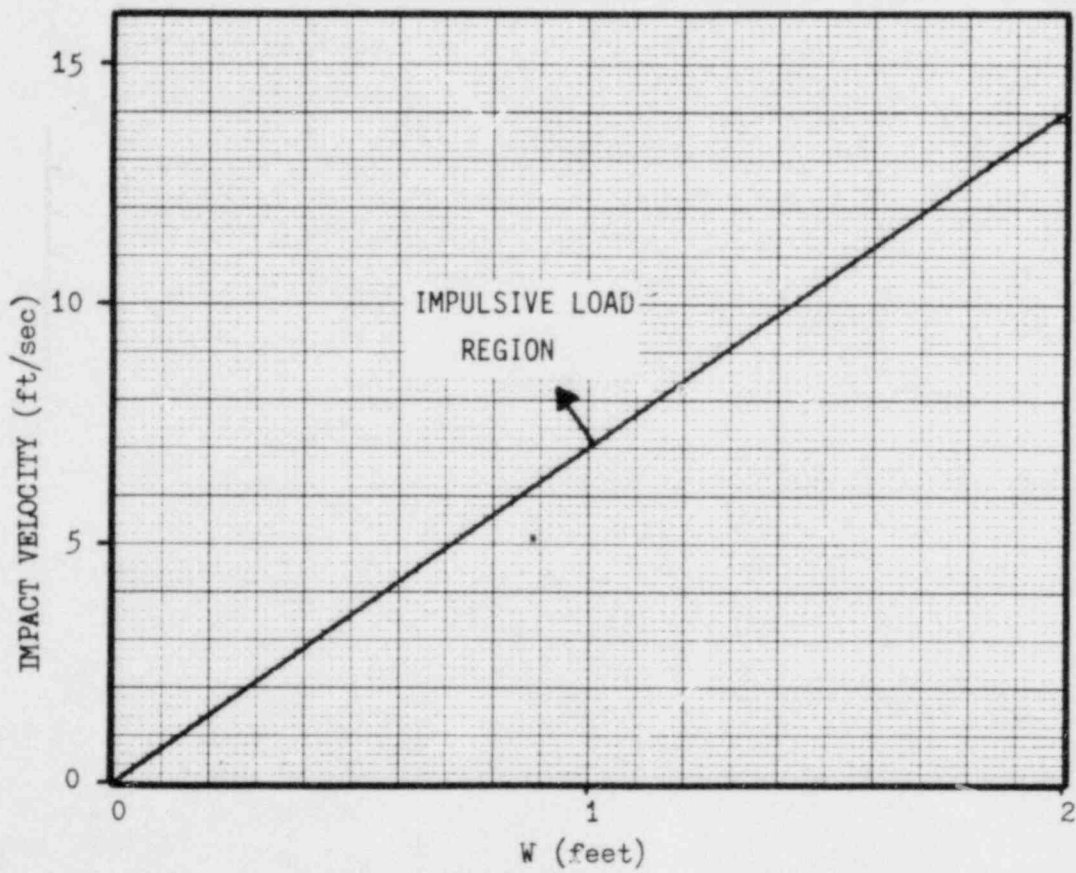


Figure 2.7-5 Impulsive Impact Loading Region for Structures with a Natural Frequency Less Than 30 Hz

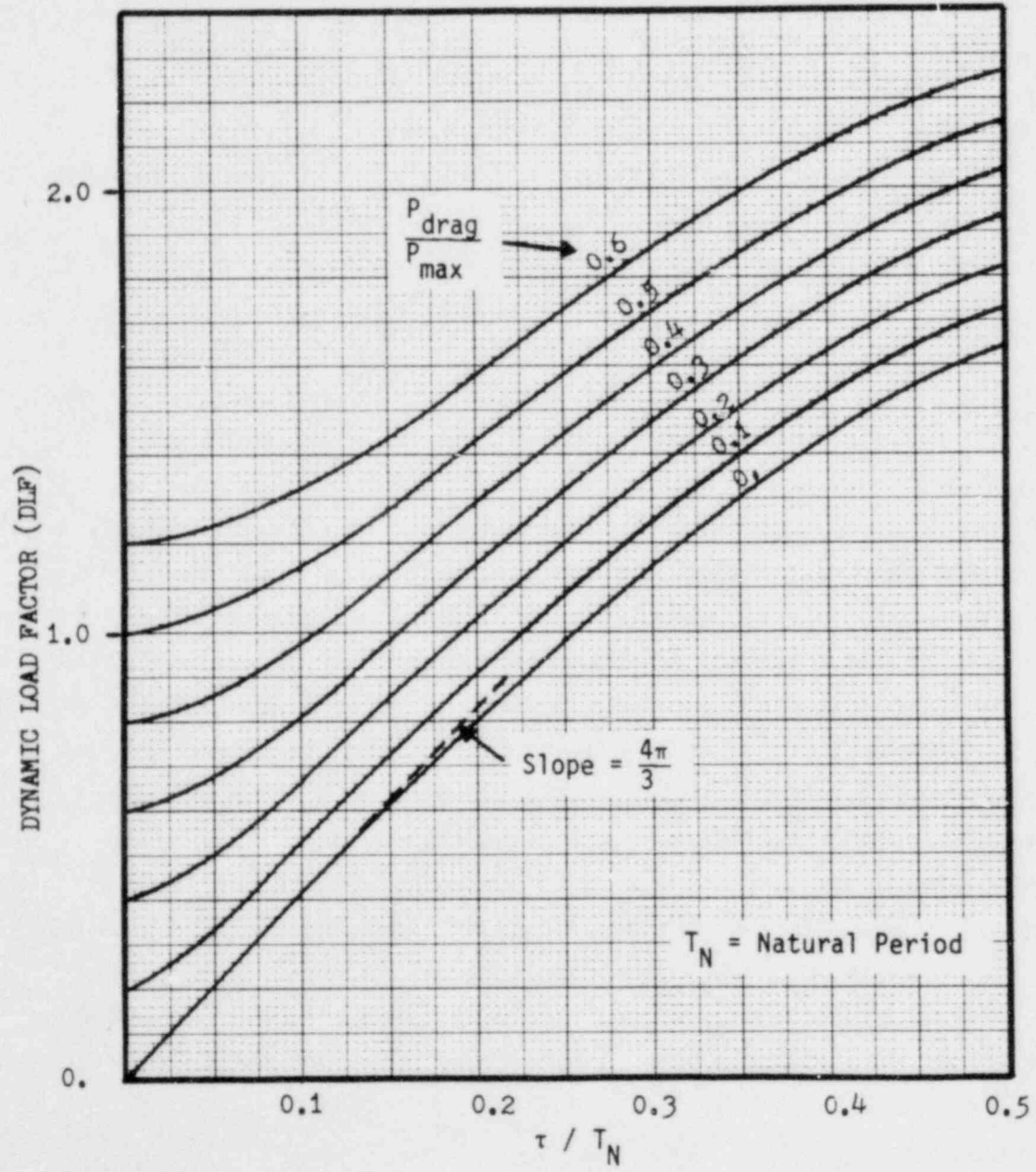
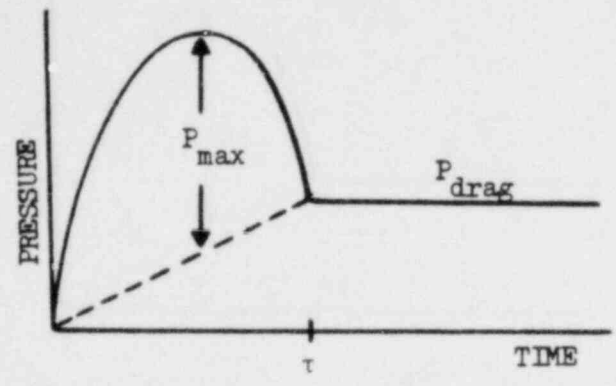


Figure 2.7-6 Effect of Drag Following a Parabolic Impact Pulse

## 2.8 FROTH IMPINGEMENT AND FALLBACK LOADS

Froth is generated by (1) impact of the rising pool surface on the vent header and (2) bubble breakthrough, as described in Section 4.3.5 of the LDR. The following load specification was derived from the high-speed film records of various pool swell tests and an analysis of pool acceleration following vent header impact. The impingement loads for Region I and Region II and the froth fallback loads, as described in Section 4.3.5, shall be defined as follows:

$$P_f = \frac{\rho_f V^2}{144 g_c}$$

where  $P_f$  = froth impingement pressure (psi)

$\rho_f$  = froth density ( $\text{lb}_m/\text{ft}^3$ )

$V$  = froth impingement velocity (ft/sec)

$g_c$  = gravitational constant (ft -  $\text{lb}_m/\text{lb}_f$  -  $\text{sec}^2$ )

Region I: The froth velocity shall be based on a source velocity equal to 2.5 times the maximum pool surface velocity prior to vent header impact, which is corrected for subsequent deceleration due to gravity starting at the 45° tangent on the bottom of the vent header, as shown in Figure 4.3.5-1 of the LDR. The source vector shall be assumed to be on a line between the 45° tangent on the header and the target structure. The froth density shall be assumed to be 20% water density for structures or sections of structures with a maximum cross-sectional dimension of less than or equal to one foot, and a proportionately lower density for structures greater than one foot; i.e.,  $\rho = (0.2/x) \rho_w$ , where  $x$  is the dimension in feet. The load shall be applied in the direction most critical to the structure within the 90° sector bounded by the horizontal opposite the vent header to the vertical upward as shown in Figure 2.8-1. The load shall be assumed to be a rectangular pulse with a duration of 80 milliseconds.

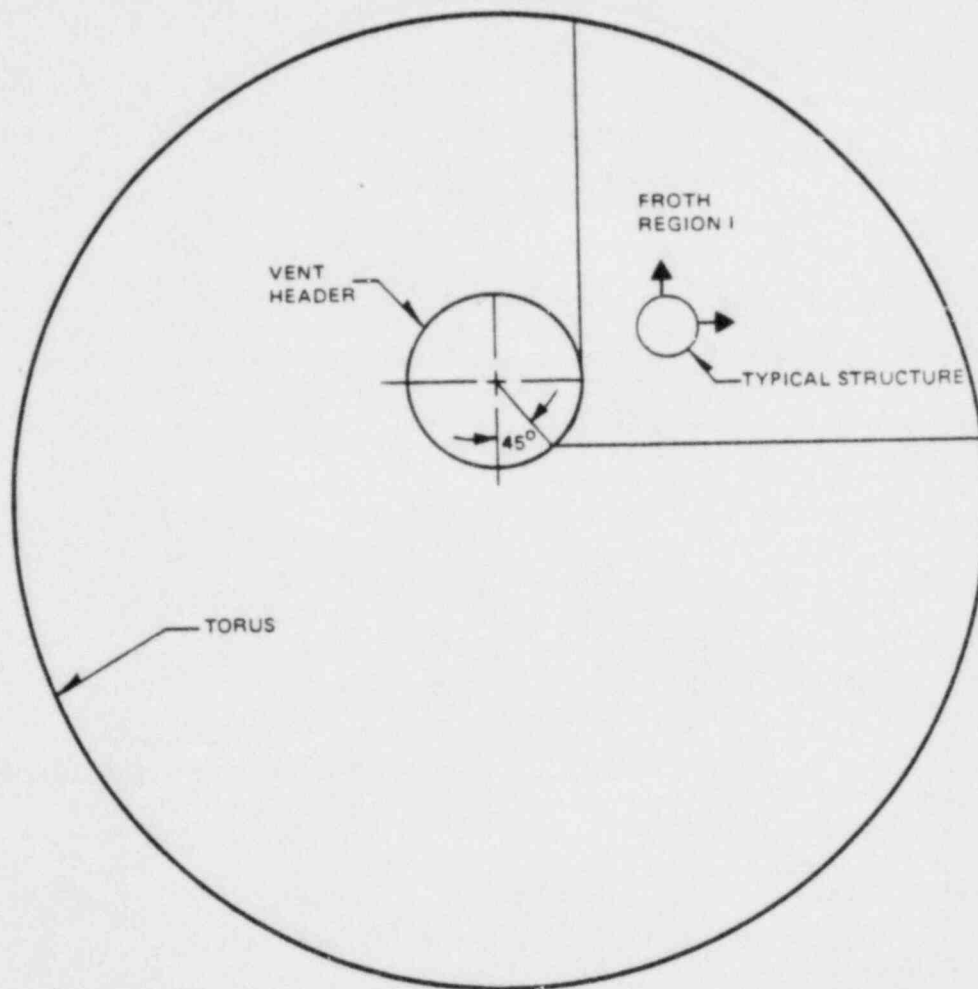


Figure 2.8-1 Direction of Load Application for Froth Region I

Alternately, the froth source velocity, mean jet angle, and froth density in Region I may be derived from a detailed analysis of the QSTF plant-specific high-speed films. Individual movie frames shall be analyzed to determine the mean value and uncertainty limits for the source velocity, wave jet width ( $w_f$ ), the angle of the wave jet relative to the horizontal ( $\theta$ ), and the impingement pulse time ( $\tau$ ). The mass of the froth jet is then given by:

$$m_f = \frac{m_h / 2}{\left[ \left( \frac{V_f}{V_i} \right)^2 - \left( \frac{V_f}{V_i} \right) \sin \theta \right]}$$

where  $m_f$  = the mass of the wave jet,

$m_h$  = the hydrodynamic mass associated with the combined vent header deflector and vent header impact,

$V_f$  = the froth source velocity, and

$V_i$  = the pool velocity just prior to vent header impact.

The froth density ( $\rho_f$ ) at any point in Region I is then given by:

$$\rho_f = \frac{m_f / L}{w_f V_f \tau}$$

where  $L$  is the length of the vent header and  $w_f$  varies to account for spreading of the froth jet with increasing distance from the source.

As before, the vertical component of the source velocity shall be decelerated to the elevation of the target structure to obtain the froth impingement velocity. The load shall be applied in the direction most critical to the structure within the  $90^\circ$  sector defined in Figure 2.8-1.

Uncertainty limits for each parameter shall be applied to assure a conservative load specification. In applying the uncertainty limits, it must be noted that the source velocity derived from the leading edge of the wave jet will be higher than the spatial and temporal mean froth velocity, and could

lead to a non-conservative estimate of the froth density. Consequently, a separate, lower-bound froth source velocity must be used to determine the froth density.

Region II: The froth velocity shall be based on a source velocity equal to the maximum pool surface velocity, directly beneath the structure under consideration, which is corrected for subsequent deceleration from the elevation of the maximum velocity. The froth density shall be assumed to be 100% water density for structures or sections of structures with a maximum cross-sectional dimension less than or equal to one foot, 25% water density for structures greater than one foot, and 10% water density for structures located within the projected region directly above the vent header. The load shall be applied in the direction most critical to the structure within the  $\pm 45^\circ$  sector of the upward vertical. The load shall be assumed to be a rectangular pulse with a duration of 100 milliseconds.

Fallback: The froth fallback velocity shall be based on the freefall velocity from the upper surface of the torus shell directly above the subject structure. The froth density shall be assumed to be 25% water density, with the exception of the projected region directly above the vent header which is 10% water density. The load shall be assumed to directly follow the froth impingement load, with a duration of one second.

## 2.9 POOL FALLBACK LOADS

The proposed load definition procedures set forth in Section 4.3.6 of the LDR for suppression pool fallback loads on internal structures following pool swell are acceptable. The drag load for pool fallback shall be assessed in a manner consistent with the LOCA bubble submerged structure drag loads (Criterion 2.14.2). In addition, structures which may be enveloped by the LOCA pool swell bubbles shall be investigated to determine if bubble collapse causes a higher stress than the submerged structure drag loads.

## 2.10 VENT HEADER DEFLECTOR LOADS

The load definition procedures set forth in Section 4.3.9 of the LDR are applicable only to the four deflector types shown in Figure 4.3.9-2 of the LDR, and are generally acceptable, subject to the following constraints and/or modifications:

### 2.10.1 QSTF Deflector Load

An individual plant may choose to use deflector load data taken directly from the QSTF plant-unique tests. This technique is subject to the following requirements:

1. If the QSTF deflector load measurement does not have a sufficiently fast response time to resolve the initial impact pressure spike for the deflector types 1-3, inclusive, the loading transient shall be adjusted to include the empirical vertical force history of the spike shown in Figure 2.10-1. This impulse need not be applied for the type 4 deflector.

2. The QSTF plant-unique loads shall be adjusted to account for the effects of (a) impact time delays and (b) pool swell velocity and acceleration differences which result from uneven spacing of downcomer pairs. The longitudinal load variation shall be evaluated at the instant when the undisturbed pool surface would have reached the local elevation of the center (half-height elevation) of the deflector. The three-dimensional load variation shall be based on the EPRI "main vent orifice" tests, as discussed in Section 2.5.

3. In applying the load to the deflector, the inertia due to the added mass of water below the deflector shall be accounted for. The added mass per unit length of deflector may be estimated by:

$$M_H = I \frac{g_C}{V}$$

1

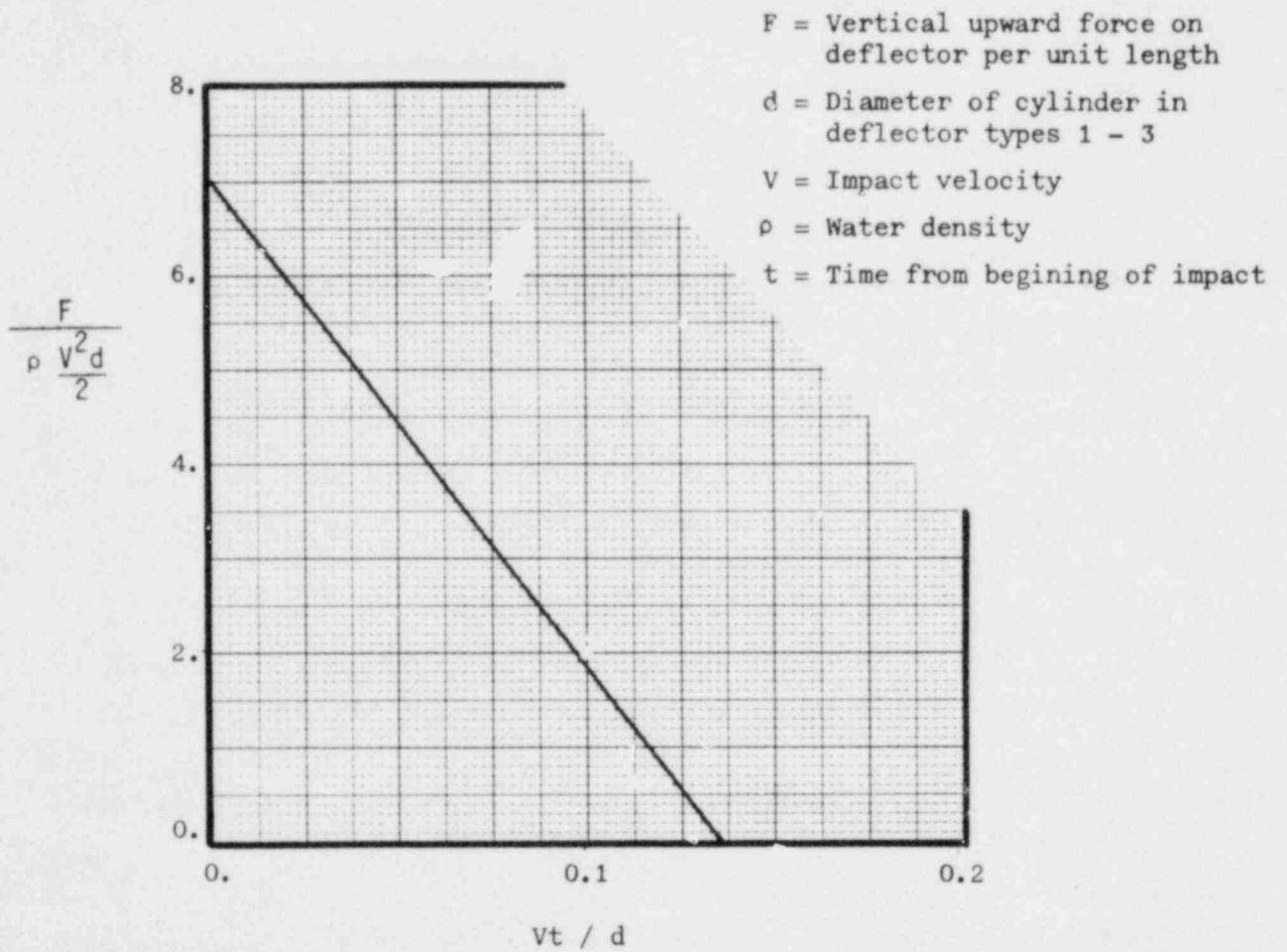


Figure 2.10-1 Impact Force Transient for Addition to the Empirical Data for Deflector Types 1 - 3.



where  $M_H$  = hydrodynamic mass per unit length (lbm/ft),

$I$  = total impulse per unit length associated with the impact transient (lbf-sec/ft),

$V$  = impact velocity (ft/sec),

$g_C$  = gravitational constant (ft - lbm/lbf - sec<sup>2</sup>)

### 2.10.2 Analytic Deflector Loads

The deflector load definition which is based on empirical expressions for impact and drag forces together with plant-specific definition of the pool swell velocity and acceleration transients, as described in Sections 4.3.9.1, 4.3.9.3, and 4.3.9.4 of the LDR, is acceptable, with the following modifications:

1. The impact transient and "steady drag" contributions to the load shall be computed from the correlations shown on Figures 2.10-2 through 2.10-5, for the deflector types 1-4, respectively. For times past the periods shown, the last value shall be extended for the duration of the transient. Slight variations in the wedge angle or ratio w/d should be corrected using Wagner's correlation (National Advisory Committee for Aeronautics Report #1366) for wedges and the final steady drag value.
2. The three-dimensional load variation and timing shall be based on the EPRI "main vent orifice" tests, as discussed in Section 2.5.
3. The gravitational component of the acceleration drag shall be included in  $F_A$ , as defined in NEDO-24612.
4. In computing the deflector response to the load, the added mass of the water shall be accounted for, as described in Section 2.10.1.3 above.

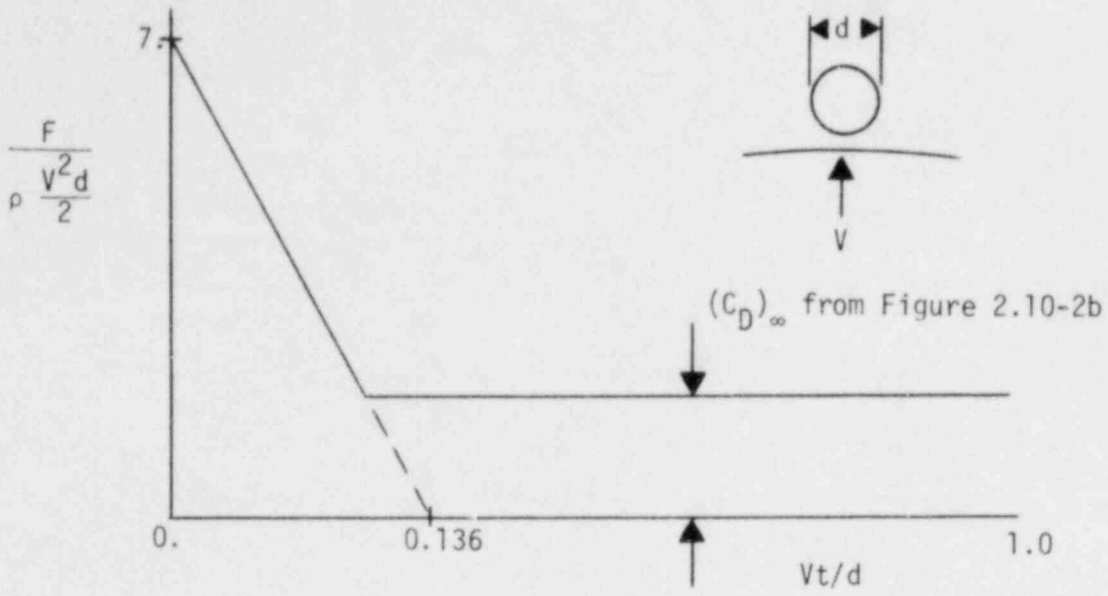


Figure 2.10-2 Impact and Steady Drag Force Correlation for Type 1 Deflector

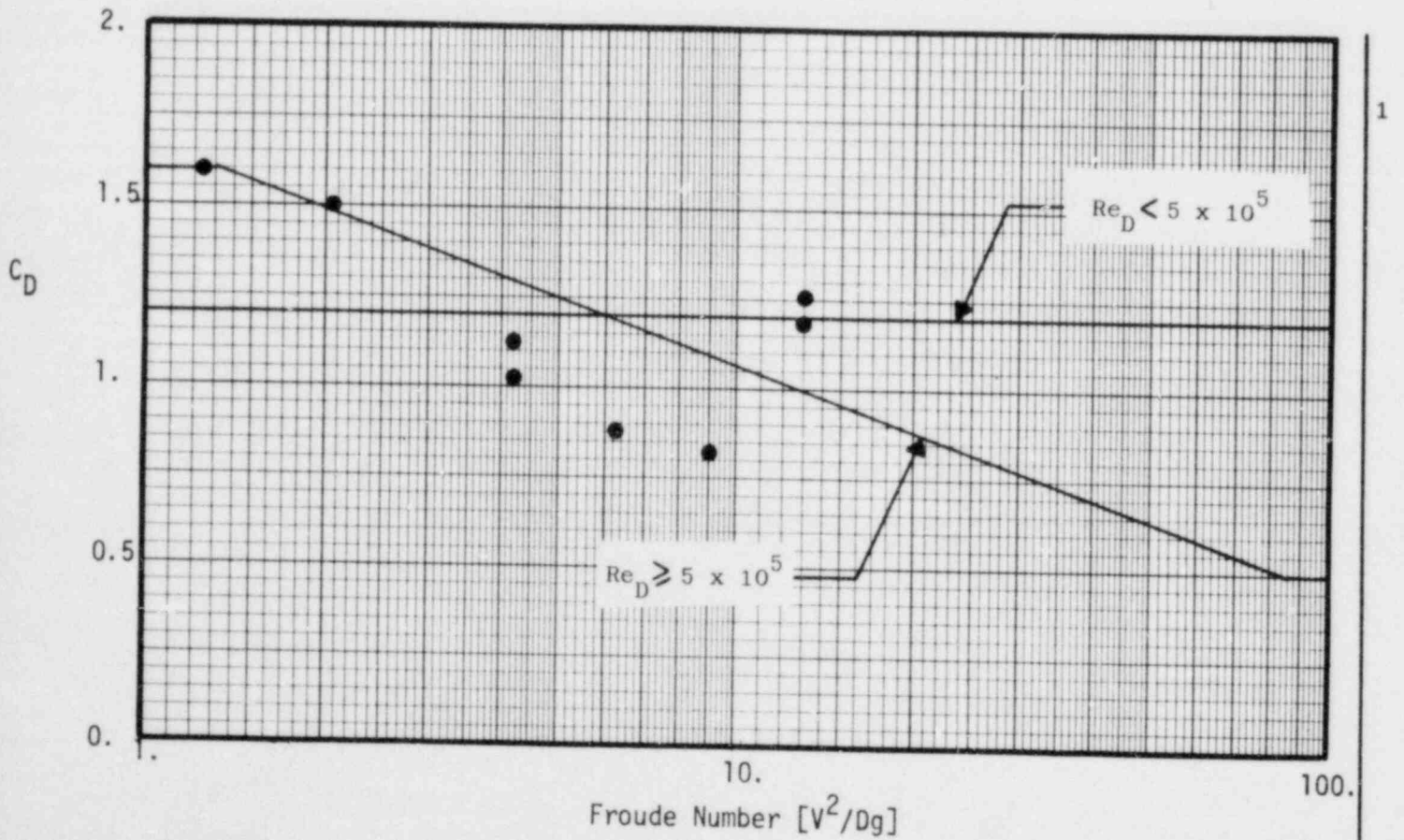


Figure 2.10-2b  $(C_D)_\infty$  for Type 1 Deflector

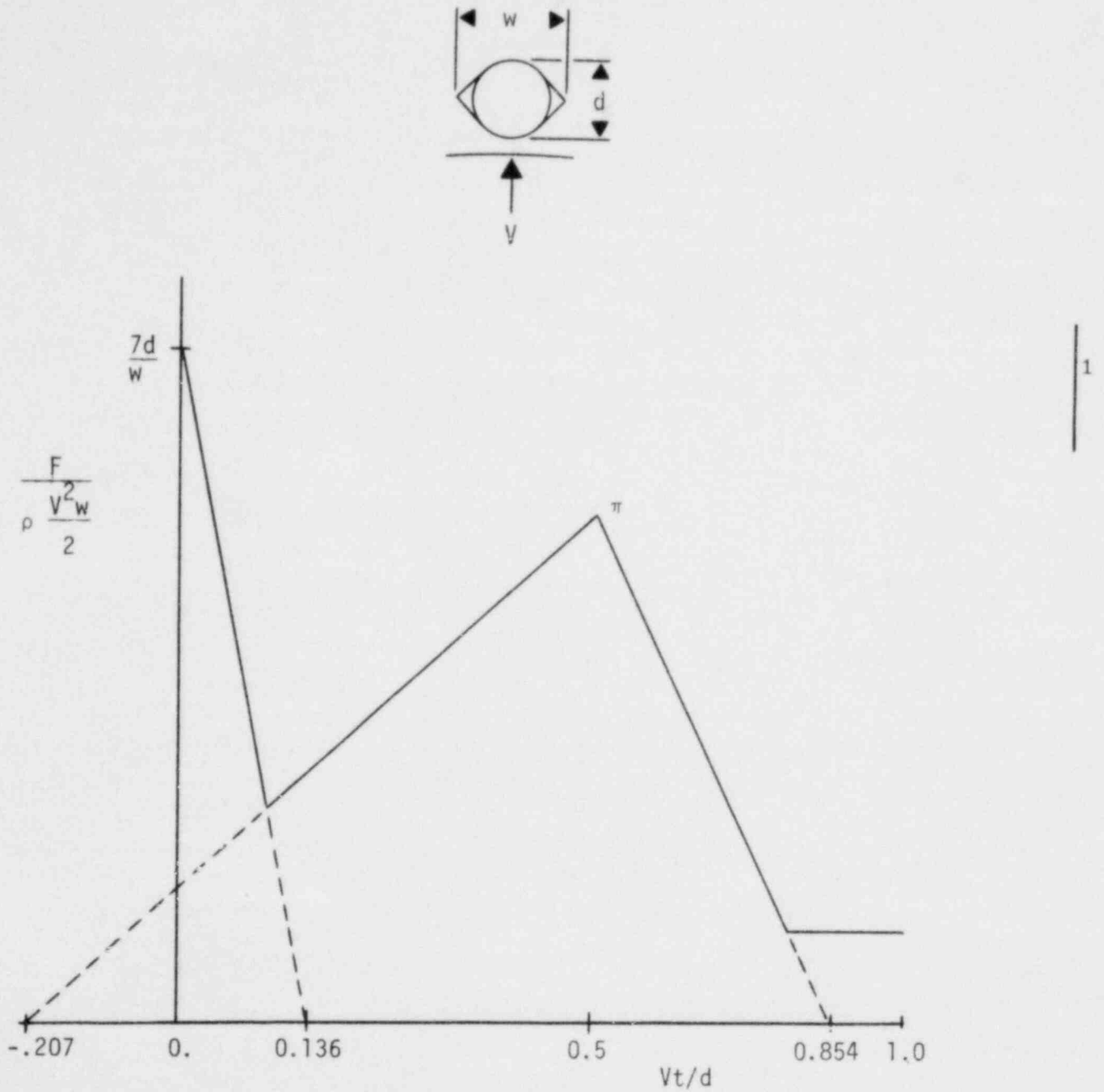


Figure 2.10-3 Impact and Steady Drag Force Correlation for Type 2 Deflector

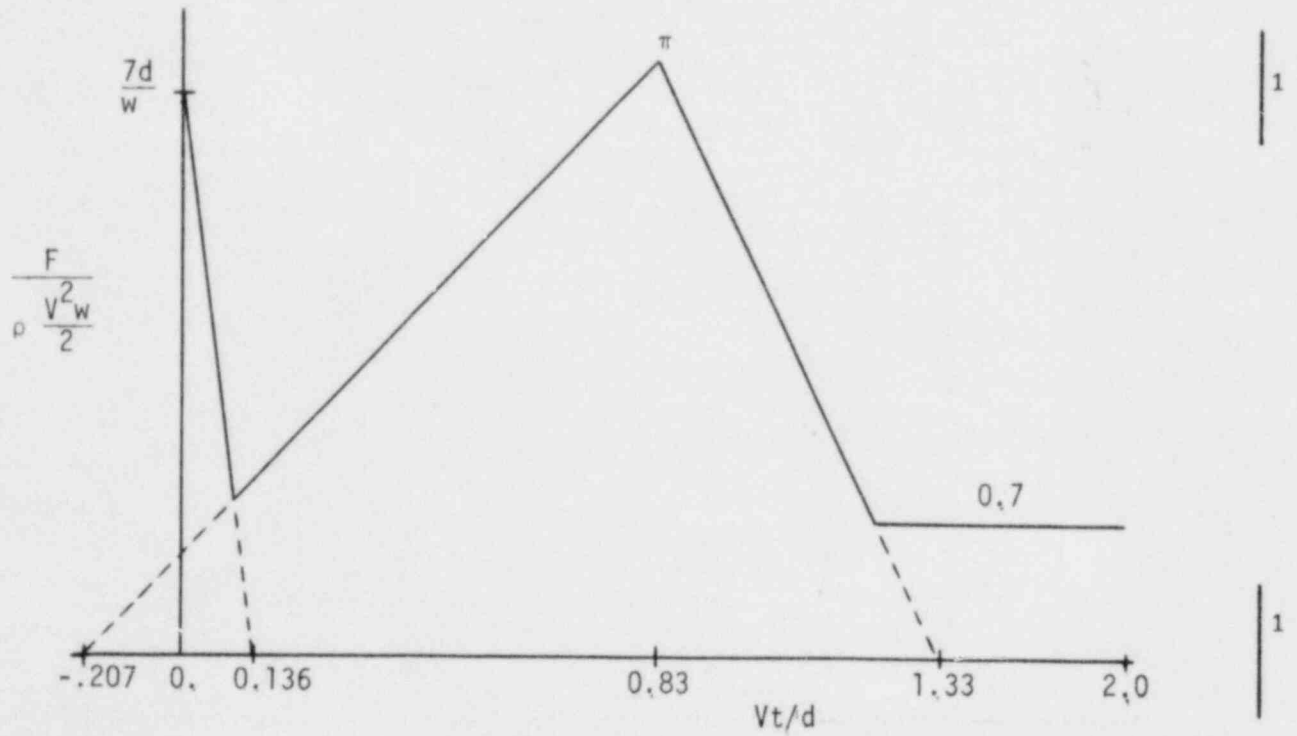
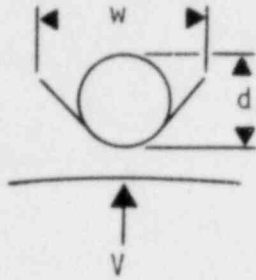


Figure 2.10-4 Impact and Steady Drag Force Correlation for Type 3 Deflector

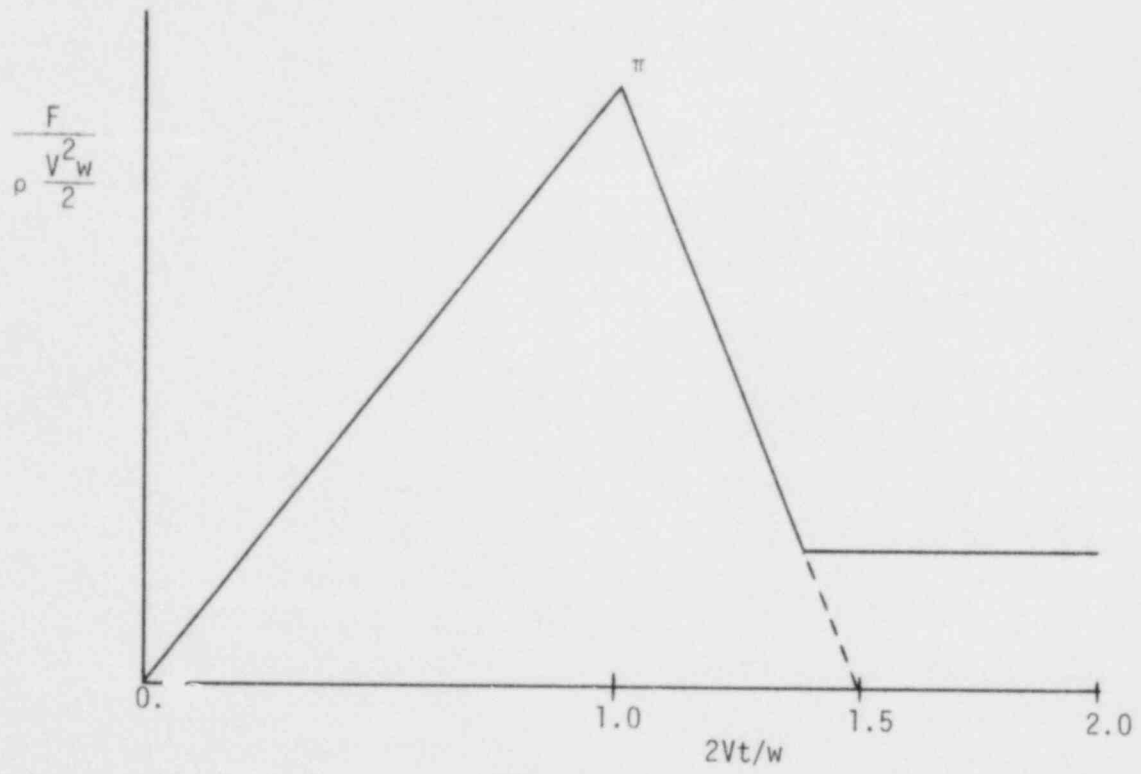
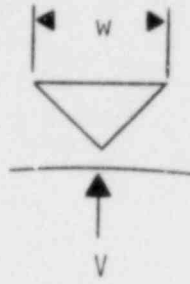


Figure 2.10-5 Impact and Steady Drag Force Correlation for Type 4 Deflector

## 2.11 CONDENSATION OSCILLATION LOADS

The following criteria have been developed in consideration of the fact that the "condensation oscillation" loads (i.e., high vent flow rate with low air content) have been derived from a single FSTF test run (M8). The condensation oscillation regime is a harmonic phenomena and, therefore, statistical variance or load magnitude uncertainty cannot be established from one test run. Although we conclude that the M8 tested conditions are conservative and prototypical for the Mark I design, a reasonable measure of the uncertainty in the loading function is necessary to assure the margins of safety in the containment structure. However, based on our assessment of the phenomenological studies conducted by the industry and the NRC Office of Nuclear Regulatory Research, we believe that the following load specifications are probably conservative and form a sufficient basis to proceed with implementation of the Mark I Long Term Program. We will require that the Mark I Owners Group confirm the condensation oscillation loads (i.e., torus shell loads, downcomer lateral loads, vent system pressure, and submerged drag source) by performing a sufficient number of additional large break, liquid blowdown tests in FSTF to establish the uncertainty in the load magnitudes.

### 2.11.1 Condensation Oscillation Torus Shell Loads

The load definition and assessment procedures set forth in Section 4.4.1 of the LDR for the condensation oscillation loads on the torus shell are acceptable, provided the "rigid wall" load derivation described in NEDE-24645-P and the condensation oscillation coherence (basis for excluding asymmetric loading condition) are confirmed by the additional FSTF tests.

For clarification, the load specification set forth in Section 4.4.1 of the LDR shall be used in conjunction with a coupled fluid-structure analytical model. The condensation oscillation loading for the IBA is a continuous sinusoidal function with a peak amplitude and frequency range of that specified for the "pre-chug" load.

## 2.11.2 Condensation Oscillation Downcomer Loads

### 2.11.2.1 Untied Downcomer Loads

The condensation oscillation downcomer lateral loads for "untied" downcomers shall be defined as described in Section 4.4.3 of the LDR, based on the methodology in NEDE-24537-P. However, in computing the dynamic load factors

$$P_{\max} = P_1 \left( \frac{DLF}{DLF_1} \right)$$

where  $P_{\max}$  = maximum static equivalent lateral load for plant-unique downcomer,

$P_1$  = maximum static equivalent lateral load in FSTF,

DLF = plant unique downcomer dynamic load factor, and

$DLF_1$  = FSTF downcomer dynamic load factor.

the plant-unique loading condition shall be derived as follows. The plant-unique DLF shall be calculated using a damping value consistent with the requirements of Regulatory Guide 1.61, "Damping Values for Seismic Design of Nuclear Power Plants," and a natural frequency determined from the structural analysis of the downcomer-vent header system. The plant-unique driving frequency shall be specified as that frequency in the range 4-8 Hz which produces the maximum structural response. The natural frequency and damping values for the FSTF DLF shall be conservatively established from a "pluck" test of an untied downcomer in FSTF, with a nominal water level of 3 feet 4 inches and an amplitude in the range of the response level. The driving frequency for the FSTF DLF shall be assumed to be 5.5 Hz.

### 2.11.2.2 Tied Downcomer Loads

The condensation oscillation downcomer loads for "tied" downcomers, as described in Section 4.4.3 of the LDR, are unacceptable. We will require that a load specification be derived from the maximum dynamic load components on each downcomer in a tied pair. The load definition and structural analysis technique shall be confirmed by comparisons of the predicted structural responses to the measured strains in the FSTF vent header and tie-bar. The FSTF natural frequency and damping values shall be conservatively established by performing a "pluck" test for a tied downcomer pair in FSTF, with a nominal water level of 3 feet 4 inches and an amplitude in the range of the response level.

### 2.11.3 Condensation Oscillation Vent System Pressure Load

The load definition procedures set forth in Section 4.4.4 of the LDR for the oscillatory pressures in the vent system during the condensation oscillation period, are acceptable subject to confirmation by the additional testing as described above.

## 2.12 CHUGGING LOADS

### 2.12.1 Chugging Torus Shell Loads

The load definition and assessment procedure set forth in Section 4.5.1 of the LDR for the chugging condensation loads on the torus shell are acceptable. For clarification, the load specification for "post-chug" loads set forth in Section 4.5.1 of the LDR shall be used in conjunction with a coupled fluid-structure analytical model.



## 2.12.2 Chugging Downcomer Loads

### 2.12.2.1 Untied Downcomer Loads

The chugging lateral loads on untied downcomers shall be defined as described in Section 4.5.3 of the LDR, which is based on the methodology in NEDE-24537-P, with the following exceptions:

1. The load specification for comparison to the ASME code primary stress limits shall be based on the maximum measured resultant static equivalent load in FSTF.
2. The fatigue usage analysis for each downcomer shall be based on a statistical loading with a 95% probability of non-exceedance.
3. The multiple-downcomer loading to assess statistical directional dependence shall be based on an exceedance probability of  $10^{-4}$  per LOCA.

### 2.12.2.2 Tied Downcomer Loads

For tied downcomers, the strains in the downcomer itself shall be evaluated exactly as in the case of the untied downcomers, using tied downcomer data. The strain in the tie bar shall be evaluated by assuming that one of the two tied downcomers is subjected to a dynamic load of triangular shape, with an amplitude of:

$$F_{\max} = \frac{\text{RSEL}}{\pi f t_d} \quad (\text{RSEL} = \text{Resultant Static Equivalent Load})$$

where RSEL is the maximum measured RSEL for an untied downcomer during chugging,  $f$  is the lowest natural frequency of vibration of an untied downcomer for the specific plant, and the duration of the load,  $t_d$ , shall be assumed to the 3 milliseconds. The load direction shall be taken as that (in the horizontal

plane) which result in the worst loading condition for the tie bar and its attachments to the downcomers.

### 2.12.3 Chugging Vent System Pressure Loads

The load definition procedure set forth in Section 4.5.4 of the LDR for the oscillatory pressures on the vent system during the chugging period are acceptable.

## 2.13 SAFETY-RELIEF VALVE DISCHARGE LOADS

### 2.13.1 Safety-Relief Valve Discharge Device

The acceptance criteria set forth below for analytically derived quencher discharge loads are applicable only to the "T" quencher configuration described in Section 1.1 of NEDE-21864-P. The SRV discharge load assessment procedure for other quencher configurations (e.g., "Y" quencher), or as an alternative method for the T-quencher, using in-plant test data is described in Section 2.13.9.

### 2.13.2 SRV Discharge Line Clearing Transient

The load definition and assessment procedure, described in Section 5.2.1 of the LDR, for the pressure and thrust loads on the SRV discharge line and quencher, which is based on the methodology presented in NEDE-21864-P and NEDE-23749-1-P, is acceptable.

### 2.13.3 SRV Air-Clearing Quencher Discharge Shell Pressure Loads

#### 2.13.3.1 Methodology for Bubble Pressure Prediction

The load definition procedures described in Section 5.2.2 of the LDR and the methodology in NEDE-21878-P for predicting the quencher bubble pressure are acceptable, with the following exceptions:

1. The load definition procedures set forth in Section 5.2.2 of the LDR are acceptable for SRV discharge line water-leg lengths less than or equal to 13.5 feet. In the event that the water-leg length for a particular line exceeds 13.5 feet, the load prediction for a 13.5 foot water-leg shall be used. For discharge line volumes greater than 65 cubic feet, no additional pressure amplitude increase due to the line volume trend is necessary.

2. The proposed methodology for predicting bubble pressures due to SRV subsequent actuations is not acceptable. The pressure amplitude predicted for the SRV first actuation shall be used in conjunction with the bubble frequency range for subsequent actuation, as specified below, for structure, equipment, and piping assessment in response to events containing SRV subsequent actuations.

#### 2.13.3.2 Methodology for Torus Shell Pressure Prediction

Based on the predicted air bubble pressure-time histories, as discussed above, the torus shell pressures at various locations in the suppression pool shall be calculated by the load definition procedures described in Section 5.2.2.3 of the LDR in conjunction with the appropriate pressure attenuation model. For off-center T-quenchers, the pressure attenuation model described in the letter to D. G. Eisenhut, NRC, from L. J. Sobon, GE, Subject: Mark I Containment Program, Additional Information on NEDO-21888, dated September 7, 1979, is acceptable for the quencher location defined therein. For quenchers located on the torus center-line, the pressure attenuation model described in Section 2.4 of NEDE-21878-P in conjunction with the bounding factor presented in Section 3.2 of NEDE-21878-P shall be used. This factor is 1.65 for local shell pressures. However, for the determination of global pressure loads on the torus (for the torus supports evaluation), this multiplier may be reduced to the value required to bound the global pressure loads on the torus from the Monticello in-plant tests (NEDE-21864-P).

### 2.13.3.3 Multiple Valve Discharge Loads

The torus shell loads due to multiple SRV actuations shall be calculated as follows:

1. The peak values of bubble pressure due to a single valve actuation shall be combined with linear superposition (ABSS method) with the appropriate pressure attenuation model, as discussed above. All bubbles shall be assumed to oscillate in-phase with the frequency ranges specified below for both first and subsequent actuations.

2. In the event that the combined peak torus shell pressure exceeds the local predicted peak bubble pressure at the bottom center of the torus by a factor greater than that defined in Section 2.13.3.2, due to a single valve actuation, the resultant torus shell peak pressure for the design assessment may be taken at the lower value.

1

### 2.13.3.4 Frequency of Pressure Wave Form

The pressure wave form predicted by the methodology described in Section 5.2.2 of the LDR, within the following uncertainty ranges (stretched or compressed time scale) that will produce the maximum structural, equipment, or piping system response, shall be used for the design assessment:

1. First Actuation - the frequency range shall be 0.75 times the minimum predicted frequency to 1.25 times the maximum predicted frequency.

2. Subsequent Actuation - the frequency range shall be 0.60 times the minimum predicted frequency to 1.40 times the maximum predicted frequency.

#### 2.13.4 SRV Discharge Line Reflood Transient

The transient analysis technique to compute the plant-specific reflood heights in the SRV discharge line following valve closure, as described in Section 5.2.3 of the LDR and based on the methodology in NEDE-23898-P and NEDE-21864-P, is acceptable.

#### 2.13.5 SRV Air and Water Clearing Thrust Loads

The load definition and assessment procedure for the quencher and quencher support thrust loads, described in Section 5.2.6 of the LDR, is acceptable.

#### 2.13.6 SRV Discharge Line Temperature Transient

The transient analysis technique to compute the maximum temperature loads on the discharge line and quencher device, as described in Section 5.2.7 of the LDR, is acceptable.

#### 2.13.7 SRV Discharge Event Cases

The kind and number of SRV discharge events shall be based on the plant-specific system configuration and a conservative assessment of plant operational history. The following load cases shall be considered for the design assessment:

1. A first actuation, single valve discharge shall be considered for all event combinations involving SRV events. Single valve subsequent actuations shall be considered for the SRV, SBA, and IBA event combinations, as determined from a plant-specific primary system analysis.

2. Asymmetric SRV discharge, both first and subsequent actuations, shall be considered for SRV, SBA, and IBA event combinations. The degree of

asymmetric discharge for each event combination shall be determined from a plant-specific primary system analysis designed to maximize the asymmetric condition.

3. ADS valves discharging on first actuations shall be considered for the SBA and IBA event combinations, followed by subsequent actuations determined from a plant-specific primary system analysis.

4. The maximum number of valves that will actuate for the SRV event combinations shall be determined from a plant-specific primary system analysis for the design basis transients, which assumes that all valves actuate at their set-point pressures. All first and subsequent actuations shall be assumed to occur in phase. The number of subsequent actuations shall be determined from the primary system analysis.

The SRV discharge event cases described above shall be used in the event combinations described in the PUAAG. The plant-unique primary system analysis shall be performed so as to provide a conservative estimate of the number of SRV actuations for both first and subsequent actuation events (e.g., ODYN code modified to account for sensible heat and pressure uncertainties).

1

#### 2.13.8 Suppression Pool Temperature Limits

As part of the PUA, each licensee is required to either demonstrate that previously submitted pool temperature analyses are sufficient or provide plant-specific pool temperature response analyses to assure that SRV discharge transients will not exceed the following pool temperature limits.

##### 1. Local Temperature Limit

The suppression pool local temperature shall not exceed 200°F, throughout all plant transients involving SRV operations, for any quencher device that has (1) the hole diameter equal to, and (2) greater than or equal hole spacing than that of the generic Mark I T-Quencher.

## 2. Local and Bulk Pool Temperature

The local to bulk pool temperature difference shall consider the plant-specific quencher discharge geometry and RHR suction and discharge geometry. The analysis of the plant-specific local to bulk pool temperature difference shall be supported by test data from either the existing Monticello pool temperature data or in-plant tests.

Where in-plant tests are used to establish the bulk to local pool temperature difference, the pool shall be at ambient (i.e., still) conditions prior to opening the SRV and the SRV discharge line selected for testing shall be located away from the RHR discharge nozzle. The duration of the SRV discharge shall be at least ten minutes. RHR flow shall not be initiated sooner than five minutes after the SRV is opened. Temperature monitors shall be located on the reactor side of the torus, downstream with respect to RHR flow, at the same elevation as the quencher, and on the quencher support. The bulk to local pool temperature transient derived from this test may be used directly to determine the local pool temperature transient.

In order to take maximum credit for the effectiveness of the RHR system to mix the pool, an additional in-plant test may be performed where the RHR system is started at the same time the SRV is actuated. The bulk to local pool temperature difference from the previous test shall be assumed up to the time the RHR system started and then linearly decrease in time to the minimum temperature difference from the second test.

The "local" temperature is defined as the temperature in the vicinity of the quencher device during discharge. For practical purposes, the average water temperature observed in the sector containing the discharge device at shell locations on the reactor side of the torus downstream of the quencher centerline at the same elevation as the quencher device and at the quencher support may be considered as the "local" temperature. The "bulk" temperature, on the other hand, is the temperature calculated assuming a uniform distribution of the mass and energy discharged from the SRV.

### 3. Suppression Pool Temperature Monitor System

The suppression pool temperature monitoring system is required to ensure that the suppression pool is within the allowable limits set forth in the plant Technical Specifications. The system shall meet the following design requirements:

a. Each licensee shall demonstrate that there is a sufficient number and distribution of pool temperature sensors to provide a reasonable measure of the bulk temperature. Alternatively, redundant pool temperature monitors may be located at each quencher, either on the quencher support or on the torus shell, to provide a measure of local pool temperature for each quencher device. In such cases, the Technical Specification limits for local pool temperature shall be derived from the calculated bulk pool temperature and the bulk to local pool temperature difference transient. | 1

b. Sensors shall be installed sufficiently below the minimum water level, as specified in the plant Technical Specifications, to assure that the sensor properly monitors pool temperature.

c. Pool temperature shall be indicated and recorded in the control room. Where the suppression pool temperature limits are based on bulk pool temperature, operating procedures or analyzing equipment shall be used to minimize the actions required by the operator to determine the bulk pool temperature. Operating procedures and alarm set points shall consider the relative accuracy of the measurement system. | 1

d. Instrument set points for alarm shall be established, such that the plant will operate within the suppression pool temperature limits discussed above.

e. All sensors shall be designed to seismic Category I, Quality Group B, and energized from onsite emergency power supplies.



### 2.13.9 SRV Load Assessment by In-Plant Tests

The SRV load assessment procedure for plants equipped with quencher devices other than the Monticello T-quencher shall be based on a series of at least four single-valve, "cold" discharge in-plant tests, performed on the SRV discharge line expected to produce the highest loads. This is also an acceptable alternative method for the Monticello-type T-quencher. The pressure wave form and structural response measurements of the in-plant tests shall be used to calibrate a coupled load-structure analytical model. The load prediction portion of the model shall be that described in NEDE-21878-P as modified by the criteria in Sections 2.13.3 and 2.13.4. The model shall be calibrated at test conditions and then applied at design basis conditions.

#### 2.13.9.1 Instrumentation

The following instrumentation shall be used for the SRV in-plant tests, as a minimum.

1. Columns - Uniaxial gages shall be installed on both inner and outer support columns.
2. Shell - Strain gages, accelerometers, and pressure transducers shall be installed on the torus shell. There shall be a sufficient number of gages to characterize both the significant shell vibration modes (6-12) Hz and the pressure waveform. The significant shell vibration modes can be determined from the mode shapes calculated by the analytical model. If necessary, the shell natural frequencies and damping may be derived from the test data.
3. Attached Piping - Where preliminary structural analyses indicate that certain piping systems are expected to have a significant response, instrumenting these lines at the shell attachment with accelerometers and strain gages should be considered, in order to calibrate the analytical

modelling of these structural elements. In such cases, accelerometers or displacement transducers should also be located at points where the maximum piping response is expected. This approach need only be applied where a more realistic piping response analysis is necessary; otherwise, the accepted conservative analysis techniques shall be used.

#### 2.13.9.2 Model Calibration

The analytical modelling used to predict the plant - unique structural response shall be derived from the in-plant test data with the following basic considerations:

1. A general modelling technique should initially be developed using measured pressure waveforms (i.e., actual pressure transients) from the Monticello tests. Adjusting the model to match the measured response from the Monticello tests will identify the significant modelling parameters for the plant-unique analyses.
2. The frequency content of all of the measured pressure waveforms from the Monticello and in-plant tests may be used to determine the maximum amplification of the structural response. Amplification for first actuation and subsequent actuation events should be considered separately. The maximum amplification shall be applied to the structural natural frequencies which occur within the range of predicted frequencies, as defined by the criteria in Section 2.13.3.4.
3. The analysis technique used for the plant-unique analyses shall be verified by comparison to (1) the peak pressure, (2) the longitudinal and circumferential attenuation, and (3) the structural response of the in-plant tests, using tested conditions as inputs. Adjustments to the analytical modelling may be made for first actuation peak pressure and structural response, based on a conservative interpretation of the in-plant test data. Adjustments may not be made for subsequent actuation peak pressure predictions. Attenuation characteristics for quencher devices other than the generic T-quencher

shall be derived from the in-plant test data (longitudinal attenuation may either be defined by using pressure transducers distributed in a manner similar to that used in the Monticello tests or by installing uniaxial gages on the three sets of columns adjacent to the test bay). The response of each structural element shall be determined from design-basis predictions of the corrected analysis technique and the maximum structural amplification.

## 2.14 SUBMERGED STRUCTURE DRAG LOADS

### 2.14.1 LOCA Water Jet Loads

The load definition and assessment procedure described in Section 4.3.7 of the LDR, which is based on the "Moody Jet Model" (NEDE-21472-P), is acceptable subject to the following constraints and/or modifications:

1. The plant-specific jet discharge velocity,  $V_D(t)$ , and acceleration,  $a_D(t) = dV_D/dt(t)$ , from the QSTF plant-specific tests series shall be used as the driving sources for the jet model.

2. Forces due to the pool acceleration and velocity induced by the advancing jet front shall be computed for structures that are within four downcomer diameters below the downcomer exit elevation, even if the structure is not intercepted by the jet. The flow field shall be computed by modelling the moving jet front as a hemispherical cap centered one downcomer diameter (D) behind the "Moody" jet front positions, containing the same amount of water as the "Moody" jet front. The formulas for the hemisphere radius ( $R_S$ ) and the trajectory of the hemisphere center ( $x_C$ ) are:

$$R_S(t) = \frac{D}{2} \left( \frac{3}{2} + 3(x_f(t)/D)^{\frac{1}{2}} \right)^{1/3} \quad \text{for } x_f(t) > D$$

$$R_S(t) = \frac{D}{2} \left( \frac{9x_f(t)}{2D} \right)^{1/3} \quad \text{for } x_f(t) \leq D$$

$$\begin{aligned}
 x_c(t) &= x_f(t) - D && \text{for } x_f(t) > D \\
 x_c(t) &= 0 && \text{for } x_f(t) \leq D
 \end{aligned}$$

where  $x_f(t)$  is the position of the "Moody" jet front as a function of time, as computed in NEDE-21472-P.

Using formulas 1 and 2 in NEDE-21472-P and assuming an average constant acceleration of the particles contained within one downcomer diameter behind the "Moody" jet front, the cross-sectional area in this region can be approximated by:

$$A(x,t) = \frac{\pi D^2}{8} \left(1 + 1/(1 - x/x_f)^{1/2}\right)$$

where  $x_f(t)$  is the "Moody" jet front position as computed in NEDE-21472-P. The volume contained in this portion of the jet can be obtained by integrating  $A(x,t)$  from  $(x_f - D)$  to  $x_f$  for  $x_f$  greater than  $D$ , and from  $x=0$  to  $x = x_f$  for  $x_f$  less than  $D$ . When the jet is modelled by a more realistic hemispherical cap, while conserving the total volume of the fluid, the cap radius and position is given by the equations above.

The equivalent uniform velocity and acceleration at the location of the structure  $(x,y)$  shall be obtained from the time dependent potential  $\phi_j(x,y,t)$  induced by the jet front:

$$\phi_j(x,y,t) = -\left(\frac{R_s}{r}\right)^2 r \left(\frac{dR_s}{dt}\right) - \frac{1}{2} \left(\frac{R_s}{r}\right)^3 (x - x_c) \frac{dx_c}{dt}$$

where  $r = \{(x-x_c)^2 + y^2\}^{1/2}$  and  $y$  is the transverse distance of the structure from the jet axis, and  $(x-x_c)$  is the distance from the structure to the effective jet front center along the jet axis. The potential is the superposition of the expansion and motion of the sphere as given in any standard hydrodynamics

text (e.g., Milne Thompson, Theoretical Hydrodynamics, Fourth Edition, pp. 455-566).

The local uniform flow velocity is

$$U_{\infty}(x,y,t) = \nabla\phi_j$$

as in NEDO-21471, while the acceleration is  $a(x,y,t) = \frac{\partial U_{\infty}}{\partial t}$

This calculation need only be performed for  $r > R_s$  and  $x > x_c$ . If either of these conditions are not satisfied, the methodology in the LDR will bound the load and is, therefore, acceptable.

#### 2.14.2 LOCA Bubble Drag Loads

The load definition and assessment procedures described in Section 4.3.8 of the LDR, which are based on the methodology in NEDO-21471 and experimental confirmation in NEDE-23817-P, are acceptable subject to the following constraints and/or modifications:

1. Flow Field
  - a. QSTF plant-specific test results (NEDE-21994-P) will be used.
  - b. Model E in NEDE-21983-P will be used for the method of images simulation of the torus cross-section.
  - c. After contact between bubbles of adjacent downcomers, the pool swell flow field above the downcomer exit elevation will be derived from the QSTF plant-specific tests.

## 2. Drag Load Assessment

a. Drag forces can be computed for circular cylinders as given in NEDO-21471, but a conservative drag coefficient of  $C_D = 1.2$  must be assumed, independent of the Reynolds number.

b. Drag forces on structures with sharp corners (e.g., rectangles and "I" beams) must be computed by considering forces on an equivalent cylinder of diameter  $D_{eq} = 2^{1/2} L_{max}$ , where  $L_{max}$  is the maximum transverse dimension.  $L_{max}$  is defined as the diameter of a circumscribed cylinder about the cross-section of the structure. For example,  $L_{max}$  equals  $(a^2 + b^2)^{1/2}$  for a rectangular cross-section of sides a and b.

c. Long slender structures must be considered in segments of length (L), which do not exceed the diameter (D or  $D_{eq}$ ). Alternatively longer segments may be used as long as the equivalent uniform flow velocity and acceleration are evaluated conservatively for every point on any such segment.

d. Interference effects due to the proximity of walls shall be considered for each structural segment that has its center less than 1.5 diameters from a boundary. Interference effects between neighboring structures shall be considered whenever the centers of the segments are less than  $3D$ , where  $D = 1/2 (D_1 + D_2)$ , the average diameter of the two structures.

For structures near walls, the multiplier  $(1 + A_w)$  shall be used to increase the acceleration drag and the multiplier  $(1 + D_w)$  shall be used to increase the standard drag.  $A_w$  and  $D_w$  that bound theory and experiments are given below as functions  $x_w$  ( $x_w = r/D - 1/2$ , where r is the distance from the segment center to the boundary).

$$0.05 \leq x_w < 1.0 \quad A_w = 0.05/x_w$$

$$D_w = 0.12/x_w$$

$$x_w < 0.05 \quad A_w = 1.0$$

$$D_w = 2.4$$

For structures with neighbors that are less than 3D away and within 30° of being parallel, the multipliers  $(1 + A_I)$  and  $(1 + D_I)$  shall be applied to the acceleration and standard drag components, respectively. Bounding expressions for  $A_I$  and  $D_I$  are given below as functions of  $x_I$  ( $x_I = r_{12}/D - 1$  where  $r_{12}$  is the distance between segment centers).

$$0.05 \leq x_I < 2 \quad A_I = \frac{0.2}{x_I} \left[ \frac{D_2}{D_1 + D_2} \right]$$

$$D_I = 0.2/x_I$$

where  $D_1$  is the diameter of the structure under consideration and  $D_2$  is the diameter of the neighbor. If more than one neighbor must be considered, the  $A_I$  and  $D_I$  values may be summed over the neighbor structures. For  $x_I$  less than 0.05, the two neighbor structures shall be considered as an effective single structure.

The effects of wall proximity and neighbor structures may be superimposed in order to compute overall multipliers as follows:

$$(1 + A_w + \sum_k A_{Ik})$$

$$(1 + D_w + \sum_k D_{Ik})$$

In situations where interference effects must be considered, but the correction techniques outlined above are not applicable, a detailed interference effects analysis shall be performed.

### 2.14.3 Quencher Water Jet Loads

The load definition procedure described in Section 5.2.4 of the LDR, which is based on the methodology in NEDE-25090-P, is acceptable, subject to the appropriate documentation of the confirmatory tests discussed in NEDE-25090-P.

### 2.14.4 Quencher Bubble Drag Loads

The load definition and assessment procedures described in Section 5.2.5 of the LDR, in NEDE-21878-P, and in NEDO-21471-2, are acceptable subject to the following constraints and/or modifications:

#### 1. Flow Field

a. The determination of the charging, formation, and rise of the oscillating bubbles is subject to the same conservative factors that are used for the quencher torus shell pressure loads, as described in NEDE-21878-P.

b. Drag loads on the quencher arms and the SRV discharge line shall be computed on the basis of asymmetric bubble dynamics. Either a full 180° phase shift shall be considered for full strength bubbles on opposite sides of these structures, or a more detailed assessment of the asymmetry of the bubble source strengths and phasing must be obtained from the experimental information in NEDE-21864-P.

c. Model E in NEDE-21983-P shall be used for the method of images representation of the torus cross-section.



## 2. Drag Load Assessment

a. Drag forces for circular cylinders shall be computed on the basis of acceleration drag alone, under the condition that  $U_m T/D \leq 2.74$ , where  $U_m$  is the maximum velocity,  $T$  is the period of bubble oscillation, and  $D$  is the cylinder diameter. For  $U_m T/D > 2.74$ , the standard drag shall be included with the drag coefficient  $C_D = 3.6$  in order to bound the relevant experimental data.

b. The constraints specified for the LOCA bubble drag load assessment also apply to the quencher bubble drag loads, with the exception of the drag coefficient.

### 2.14.5 LOCA Condensation Oscillation Drag Loads

The load definition and assessment procedures described in Section 4.4.2 of the LDR and the methodology described in NEDO-25070 are acceptable subject to the following constraints and/or modifications:

#### 1. Flow Field

a. An average source strength shall be established by considering equal source strengths at all eight downcomers in equation B-4 in NEDO-25070. A maximum source strength shall be defined as twice the average source strength. For each structure, the loads shall be computed on the basis of both the average source at all downcomers and for the maximum source applied at the nearest downcomer.

b. The fluid-structure interaction effects shall be included for any structural segment for which the local fluid acceleration is less than twice the torus boundary acceleration. This may be accomplished by adding the boundary acceleration to the local fluid acceleration.

## 2. Drag Load Assessment

a. The constraints and modifications specified for the quencher bubble drag loads apply.

b. These loads may be applied quasi-statically to structures, only if the highest significant Fourier components occur at frequencies less than half the lowest structural frequency.

### 2.14.6 LOCA Chugging Drag Loads

The load definition and assessment procedures described in Section 4.5.2 of the LDR and the methodology in NEDO-25070 for the pre-chug drag loads are acceptable subject to the constraints in Section 2.14.5 for the condensation oscillation drag loads. The application for the post-chug drag loads is subject to the following constraints and/or modifications.

#### 1. Flow Field

a. The maximum source strength history shall be obtained by using the maximum measured pressure (not necessarily at the bottom center) in a Type 1 chug in equation B-4 of NEDO-25070, with  $f(r)$  based on the single nearest downcomer. For each structure, the phasing between the two nearest downcomers that maximizes the local acceleration shall then be computed on the basis of the two nearest downcomers chugging at maximum source strengths at the above established phase relation.

b. The fluid-structure interaction effects shall be included for any structural segment for which the local fluid acceleration is less than twice the torus boundary acceleration. This may be accomplished by adding the boundary acceleration to the local fluid acceleration.

## 2. Drag Load Assessment

a. The constraints and modifications specified for the quencher bubble drag loads apply.

b. Unless the lowest structural natural frequency times the duration of the "spike" in the source strength is greater than 3, the loads shall be applied dynamically. Either sufficient Fourier components will be included to bound the "spikes" or the load shall be applied in the time domain using the source time history. The term "spike" refers to the short-duration high overpressure peak, such as that exhibited in Figure 6.2.1-20 of NEDE-24539-P.

### 2.15 SECONDARY LOADS

The following loading conditions may be neglected for the PUA:

- a. seismic slosh pressure loads
- b. post-swell wave loads
- c. asymmetric pool swell pressure loads
- d. sonic and compression wave loads
- e. downcomer air clearing loads

### 2.16 DIFFERENTIAL PRESSURE CONTROL REQUIREMENTS

Those licensees that use differential pressure control ( $\Delta P$ ) as a pool swell load mitigation feature for the LTP, shall demonstrate conformance with the following design criteria as part of the PUA:

1. There shall be no unacceptable change in the radiological consequences of an accident as a result of the inclusion of the  $\Delta P$  system.

2. Steam bypass of the suppression pool via the  $\Delta P$  system shall be eliminated by appropriate system design, or such bypass shall be determined to be acceptable by calculation.

3. Design and installation of the  $\Delta P$  system shall be commensurate with other operational systems in the plant.

4. When the  $\Delta P$  system involves the addition of containment isolation valves, the additional valves shall be included in the plant's Technical Specifications and the valve design and arrangement shall conform to the requirements of General Design Criterion 56 in Appendix A to 10 CFR 50 and the regulatory positions in Standard Review Plan Section 6.2.4.

Subsequent to the PUA, a license amendment shall be submitted to incorporate the following Technical Specification requirements for the  $\Delta P$  system:

a. Differential pressure between the drywell and suppression chamber shall be maintained equal to or greater than "X" (where X is the plant-specific differential pressure and values less than one psid will not be credited for load mitigation), except as specified in b and c below.

b. The differential pressure shall be established within 24 hours after placing the plant in the RUN mode during plant startup. The differential pressure may be reduced below "X" psid 24 hours prior to a scheduled plant shutdown.

c. The differential pressure may be reduced to less than "X" psid for a maximum of four hours during required operability testing of (specify here those safety-related systems for which operability tests either release significant amounts of energy to the suppression pool or cannot be performed with the  $\Delta P$  established).

d. In the event that the specification in a. above cannot be met, and the differential pressure cannot be restored within six hours, an orderly shutdown shall be initiated and the reactor shall be in a cold shutdown condition within the subsequent 24 hours.

e. A minimum of two narrow range instrument channels shall be provided to monitor the differential pressure. Error in the  $\Delta P$  measurement shall be no greater than  $\pm 0.1$  psid or the allowable  $\Delta P$  shall be increased to offset the error in the measurement. The instrument channels shall be calibrated once every six months. In the event that the measurement is reduced to one indication, operation is permissible for the following seven days. If all indication of the differential pressure is lost, and cannot be restored in six hours, an orderly shutdown shall be initiated and the reactor shall be in a cold shutdown condition within the subsequent 24 hours.

### 3. STRUCTURAL ANALYSIS AND ACCEPTANCE CRITERIA

The staff finds the general analysis techniques and proposed structural acceptance criteria set forth in the "Mark I Containment Program Structural Acceptance Criteria Plant Unique Analysis Applications Guide," (PUAAG), NEDO-24583-1, dated October 1979, acceptable. The proposed criteria will provide a sufficient basis for demonstrating the margins of safety required for steel structures and piping in the ASME Boiler and Pressure Vessel Code and for concrete structures in the American Concrete Institute Code.

### 4. REFERENCES (Listed by Report Number)

NEDE-13426-P "Mark III Confirmatory Test Program One-Third Scale Pool Swell Impact Tests, Test Series 5805," General Electric Proprietary Report, August 1975.

- NEDO-21471 "Analytical Model for Estimating Drag Forces on Rigid Submerged Structures due to LOCA and Safety Relief Valve Ramshead Air Discharges," General Electric Topical Report, September 1977.
- NEDE-21472 "Analytical Model for Liquid Jet Properties for Predicting Forces on Rigid Submerged Structures," General Electric Proprietary Report, September 1977.
- NEDE-21864-P "Mark I Containment Program Final Report Monticello T-Quencher Test, Task Number 5.1.2," General Electric Proprietary Report, July 1978.
- NEDE-21878-P "Mark I Containment Program Analytical Model for Computing Air Bubble and Boundary Pressures Resulting from an SRV Discharge Through a T-Quencher Device, Task Number 7.1.1.2," General Electric Proprietary Report, January 1979.
- NEDO-21888 "Mark I Containment Program Load Definition Report," Revision 0, General Electric Topical Report, December 1978.
- NEDE-21944-P "Mark I Containment Program Quarter Scale Plant Unique Tests, Task Number 5.5.3, Series 2," Volumes 1-4, General Electric Proprietary Report, April 1979.
- NEDE-21983-P "Mark I Containment Program Submerged Structures Model Main Vent Air Discharges Evaluation Report, Task Number 5.14.1," General Electric Proprietary Report, March 1979.

- NEDE-23545-P "Mark I Containment Program 1/4 Scale Pressure Suppression Pool Swell Test Program: LDR Load Tests - Generic Sensitivity, Task Number 5.5.3, Series 1," General Electric Proprietary Report, December 1978.
- NEDE-23749-1-P "Mark I Containment Program Comparison of Analytical Model for Computing S/RVDL Transient Pressures and Forces to Monticello Data," General Electric Proprietary Report Addendum, February 1979.
- NEDE-23817-P "Mark I Containment Program 1/4 Scale Test Report Loads on Submerged Structures due to LOCA Air Bubbles and Water Jets, Task Number 5.14," General Electric Proprietary Report, September 1978.
- NEDE-24537-P "Mark I Containment Long Term Program - Development of Downcomer Lateral Loads from Full Scale Test Facility Data - Task Number 7.3.2," General Electric Proprietary Report, May 1979.
- NEDE-24539-P "Mark I Containment Program Full Scale Test Program Final Report, Task Number 5.11," General Electric Proprietary Report, April 1979.
- NEDO-24583 "Mark I Containment Program Structural Acceptance Criteria Plant Unique Analysis Applications Guide, Task Number 3.1.3," General Electric Topical Report, December 1978.
- NEDO-24612 "Mark I Containment Program Vent Header Deflector Load Definition, Task Number 7.3.3," General Electric Topical Report, April 1979.

- NEDE-24645-P "Mark I Containment Program Analysis of Full Scale Test Facility for Condensation Oscillation Loading," General Electric Proprietary Report, May 1979.
- NEDE-25070 "Analytical Model for Estimating Drag Forces on Rigid Submerged Structures Caused by Condensation Oscillation and Chugging Mark I Containments," General Electric Topical Report, April 1979.
- NEDE-25090-P "Analytical Model for T-Quencher Water Jet Loads on Submerged Structures, Task Number 5.14.2," General Electric Proprietary Report, May 1979.





UNITED STATES  
NUCLEAR REGULATORY COMMISSION  
ADVISORY COMMITTEE ON REACTOR SAFEGUARDS  
WASHINGTON, D. C. 20555

February 13, 1980

Honorable John F. Ahearne  
Chairman  
U. S. Nuclear Regulatory Commission  
Washington, D. C. 20555

SUBJECT: NRC ACCEPTANCE CRITERIA FOR THE MARK I CONTAINMENT LONG TERM PROGRAM

Dear Dr. Ahearne:

During its 238th meeting, February 7-9, 1980, the Advisory Committee on Reactor Safeguards reviewed the NRC Acceptance Criteria for the Mark I Containment Long Term Program. This matter was considered at ACRS Fluid Dynamics Subcommittee meetings held on May 23, 1978, November 28-30, 1978, September 13-14, 1979, and November 16, 1979. During its review, the Committee had the benefit of discussions with representatives of the NRC Staff and the Mark I Owners Group.

The NRC Acceptance Criteria for the Mark I Containment Long Term Program are intended to establish design basis loads that are appropriate for the anticipated life of each Mark I BWR facility and to restore the originally intended design safety margins to each Mark I containment system.

The Mark I program was initiated in 1975 in response to loss of coolant accident and safety relief valve (SRV) dynamic loads identified by the General Electric Company during the course of performing large scale testing for the Mark III pressure-suppression containment in 1972-1974. A period of reevaluation resulted in issuance of the Short Term Program Acceptance Criteria in December 1975 which established interim design bases for continued operation of the Mark I BWRs. The Acceptance Criteria for the Long Term Program have been developed from a program of small and full scale tests in two and three dimensional geometries.

The Mark I Owners submitted proposed loads in the "Mark I Containment Program Load Definition Report" in December 1978 and detailed the methods to be used in plant unique analyses in the "Mark I Containment Program Structural Acceptance Criteria Plant Unique Analysis Applications Guide." Following review of the available information, the NRC Staff determined that certain changes and clarifications to the criteria proposed by the Mark I Owners were necessary. The NRC Staff technical requirements were delineated in the "NRC Acceptance Criteria for the Mark I Containment Long Term Program" issued in October 1979 and also in several additions to the acceptance criteria as discussed during the 238th ACRS meeting. The additions to the Acceptance Criteria were intended, in part, to alleviate some of the difficulties the Mark I Owners had in calculating credible structural responses to SRV actuations.

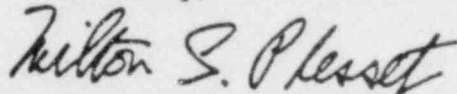
February 13, 1980

The Committee recognizes the thoroughness of the efforts taken by the NRC Staff and the Mark I Owners to resolve the generic Mark I issues and believes that the NRC Acceptance Criteria and additions, as proposed, provide a suitably conservative basis for performing the Long Term Mark I Containment structural response analyses. The Mark I Owners indicated that they continue to have significant difficulty in calculating credible structural responses to some SRV loads and they would like to continue to work with the Staff on a generic basis to resolve these difficulties. The NRC Staff would like to complete the generic Mark I program and resolve any remaining problems as they arise from the plant unique analyses. The Committee believes that the individual Mark I Owners can work with the Staff to resolve any additional difficulties that may arise from the plant unique analyses as modifications are being made to the containment structures.

The Committee believes that the Staff should assure the adequacy of the requirements for verification of the design, fabrication, and inservice inspection of the Mark I containment modifications and, in particular, the SRV discharge piping in the wetwell airspace. Further, in the interim period while the Mark I modifications are being performed, the Staff should investigate the potential for and consequences of a failure in the SRV discharge piping in the wetwell airspace for the existing designs. The Committee wishes to be kept informed on this matter.

The Committee believes that, with due consideration to the above items, the generic Mark I Long Term Program can be concluded and the modifications to the individual Mark I BWRs can be implemented on a reasonable schedule over the next 18 months.

Sincerely,



Milton S. Plesset  
Chairman

References:

1. General Electric Company, "Mark I Containment Program Load Definition Report," Revision 0, NEDO 21888, December 1978.
2. General Electric Company, "Mark I Containment Program Structural Acceptance Criteria Plant Unique Analysis Applications Guide," NEDO 24583, December 1978.
3. U.S. Nuclear Regulatory Commission, "NRC Acceptance Criteria for the Mark I Containment Long Term Program," October 1979, and additions included in the February 8, 1980, transcript of the 238th ACRS Meeting.

|  |  |  |  |  |                         |
|--|--|--|--|--|-------------------------|
| <b>NRC FORM 335</b><br>(7-77)  |  | <b>U.S. NUCLEAR REGULATORY COMMISSION</b><br><b>BIBLIOGRAPHIC DATA SHEET</b> |  | <b>1. REPORT NUMBER (Assigned by DDC)</b><br>NUREG-0661  |                         |
| <b>4. TITLE AND SUBTITLE (Add Volume No., if appropriate)</b><br>MARK I CONTAINMENT LONG TERM PROGRAM SAFETY EVALUATION REPORT, Resolution of Generic Technical Activity A-7   |  |  |  | <b>2. (Leave blank)</b>                                  |                         |
| <b>7. AUTHOR(S)</b><br>C. I. Grimes, USNRC (Task Manager)  |  |  |  | <b>3. RECIPIENT'S ACCESSION NO.</b>                      |                         |
| <b>9. PERFORMING ORGANIZATION NAME AND MAILING ADDRESS (Include Zip Code)</b><br>Office of Nuclear Reactor Regulation<br>U.S. Nuclear Regulatory Commission<br>Washington, D.C. 20555  |  |  |  | <b>5. DATE REPORT COMPLETED</b><br>MONTH March YEAR 1980 |                         |
| <b>12. SPONSORING ORGANIZATION NAME AND MAILING ADDRESS (Include Zip Code)</b><br>Same as 9.   |  |  |  | <b>DATE REPORT ISSUED</b><br>MONTH July YEAR 1980        |                         |
|  |  |  |  | <b>6. (Leave blank)</b>                                  |                         |
|  |  |  |  | <b>8. (Leave blank)</b>                                  |                         |
|  |  |  |  | <b>10. PROJECT/TASK/WORK UNIT NO.</b><br>A-7             |                         |
|  |  |  |  | <b>11. CONTRACT NO.</b>                                  |                         |
| <b>13. TYPE OF REPORT</b><br>NUREG - Generic Safety Evaluation Report  |  |  | <b>PERIOD COVERED (Inclusive dates)</b><br>2/77 to 12/79 |  |                         |
| <b>15. SUPPLEMENTARY NOTES</b>   |  |  |  | <b>14. (Leave blank)</b>                                 |                         |
| <b>16. ABSTRACT (200 words or less)</b><br>During testing for an advanced Boiling Water Reactor (BWR) containment system design (Mark III), suppression pool hydrodynamic loads were identified which had not been considered in the original design of the Mark I containment system. To address this issue, a Mark I Owners Group was formed and the assessment was divided into a short-term and long-term program. The results of the NRC staff's review of the Mark I Containment Short Term Program are described in NUREG-0408. This report describes the results of the NRC staff's review of the generic Mark I Containment Long Term Program (LTP). The LTP was conducted to provide a generic basis to define suppression pool hydrodynamic loads and the related structural acceptance criteria, such that a comprehensive reassessment of each Mark I containment system would be performed. A series of experimental and analytical programs were conducted by the Mark I Owners Group to provide the necessary bases for the generic load definition and structural assessment techniques. The generic methods proposed by the Mark I Owners Group, as modified by the NRC staff's requirements, will be used to perform plant-unique analyses, which will identify the plant modifications, if any, that will be needed to restore the originally intended margin of safety in the Mark I containment designs. |  |  |  |  |                         |
| <b>17. KEY WORDS AND DOCUMENT ANALYSIS</b>   |  |  | <b>17a. DESCRIPTORS</b>                                  |  |                         |
| <b>17b. IDENTIFIERS/OPEN-ENDED TERMS</b>   |  |  |  |  |                         |
| <b>18. AVAILABILITY STATEMENT</b><br>UNLIMITED   |  |  | <b>19. SECURITY CLASS (This report)</b><br>Unclassified  |  | <b>21. NO. OF PAGES</b> |
|  |  |  | <b>20. SECURITY CLASS (This page)</b><br>Unclassified    |  | <b>22. PRICE</b><br>S   |

UNITED STATES  
NUCLEAR REGULATORY COMMISSION  
WASHINGTON, D. C. 20555

OFFICIAL BUSINESS  
PENALTY FOR PRIVATE USE, \$300

POSTAGE AND FEES PAID  
U.S. NUCLEAR REGULATORY  
COMMISSION



\*\*\*\*\*  
120555031837 2 ANXA9A9B  
US NRC  
SECY PUBLIC DOCUMENT ROOM  
BRANCH CHIEF  
HST LOBBY  
WASHINGTON DC 20555